

MIRAI Cruise Report

MR08-06 Leg1

Studies on geophysics and paleoceanography in the South Pacific



Leg.1a: January, 15, 2009-February 3, 2009
(Sekinehama – Papeete)

Leg.1b: February, 4, 2009-March, 14, 2009
(Papeete – Valparaiso)

Preface

Natsue ABE (IFREE, JAMSTEC)

As shown in figure 0-1., a complete trans-Pacific cruise, MR08-06 Leg1, was conducted in January-March 2009 from Sekinehama, Japan to Valparaiso, Chile via Papeete, Tahiti, as a part of SORA 2009 (South Pacific Ocean Research Activity 2009) by JAMSTEC R/V MIRAI, which is a half year cruise in the Pacific Ocean. It was 59 day-long cruise. The main objectives of MR08-06 Leg1 are geological and geophysical surveys in the broad ocean basin, so to say ocean-hemisphere. There are four main themes; (1) studies of magmatism and flux in the area of subduction of mid-ocean ridges, and of formation and evolution of the continental crust, off Chile, (2) seismic and electromagnetic imaging of mantle upwelling in French Polynesia, (3) reconstruction of paleomagnetic intensity in the southern hemisphere during the past 2 million years.

The MR08-06 Leg-1 cruise is an unprecedented opportunity to collect surface geophysical data and bathymetric data in the regions in the Pacific Ocean where is sparsely surveyed using state-of-the-art echo-sounding technology. Gravity field, geomagnetic field, and the echo-sounding data were collected along the ship track. Ocean bottom seismometers (OBEMs) and ocean bottom electro-magnetometers (OBSs) were deployed for a year observation. We conducted geological sampling of hard rocks by dredging and rock-coring, and of sediment by long piston coring. In addition to the geological and geophysical surveys, we also conducted plankton sampling and observations of surface seawater, atmosphere and meteorological data during the cruise with same quality and condition on a research vessel.

The cruise successfully completed without any serious trouble. We could took precious data and samples. I thank all Japanese, French, Kiribati and Chilean authorities on behalf of the scientific party of MR08-06 Leg1. The scientific party deeply appreciates Captain Dr. Akamine, Mr. Inoue (the Chief officer) and MIRAI crew members for their teamwork. We express our appreciation to Chilean national observer Ms. Lucia Alejandra Villar Munoz for her supports and Magellan pilots. NA is finally acknowledge for the cooperation of all marine technicians and participants.

MR08-06 Leg1 Chief Scientist

Natsue Abe

Subseafloor Dynamics Research Team
Institute for Research on Earth Evolution (IFREE),
Independent Administrative Institution/
Japan Agency for Marine-Earth Science and Technology (JAMSTEC)

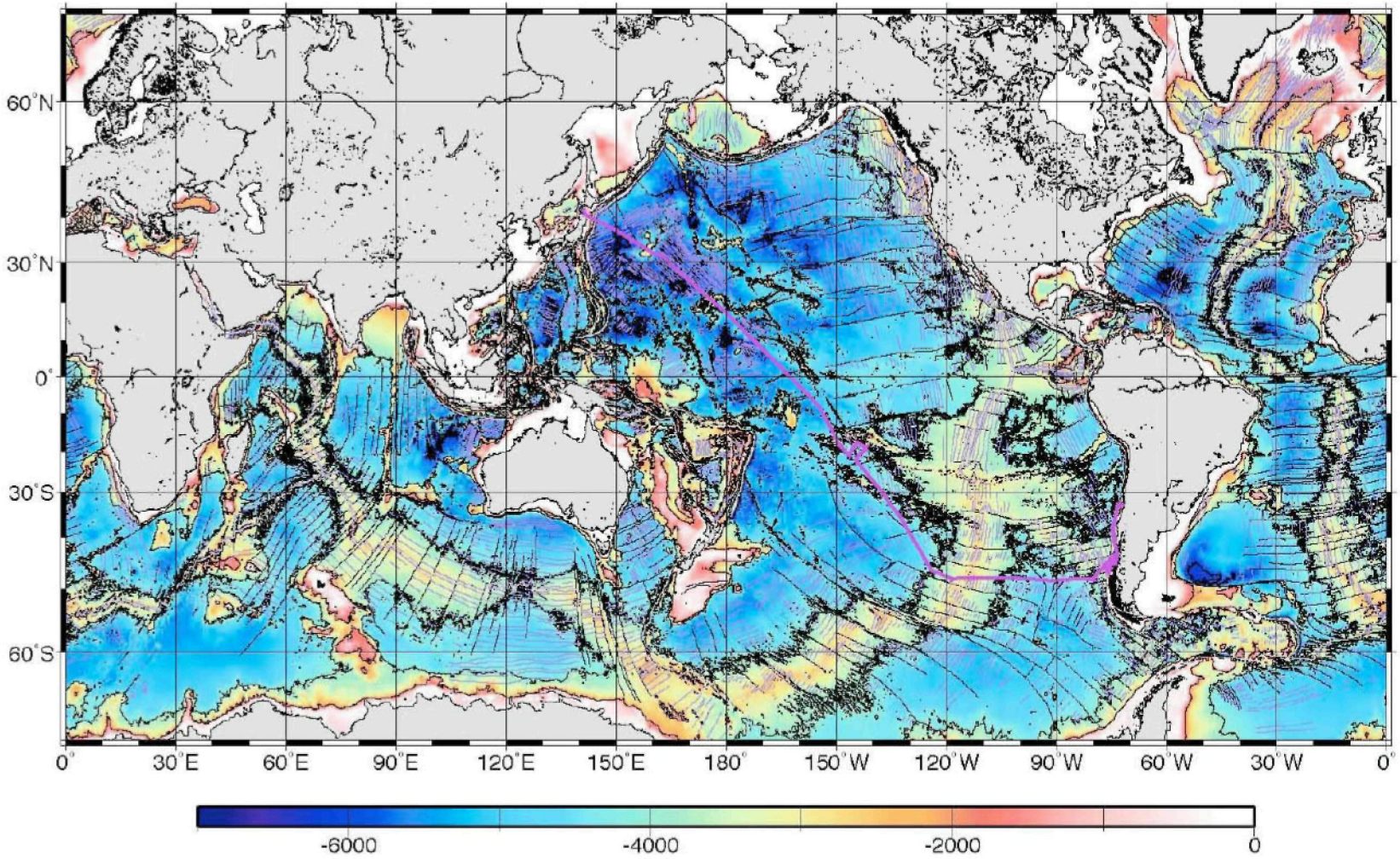


Figure 0-1. Ship Track of MR08-06 Leg1 on the world map with ETOP02, fracture zone, magnetic lineation in the oceanic plate.

Cruise Report Contents

Preface

1 Outline of the MR08-06 Leg.1

1 - 1 Cruise summary

1 - 2 Cruise Log

1 - 3 Cruise track

1 - 4 Survey areas

1 - 5 List of participants

2 Observations

2 - 1 Surface geophysical surveys

2 - 1 - 1 Bathymetry and back scatter intensity

2 - 1 - 2 Descriptions of seamounts

2 - 1 - 3 Gravity field measurements

2 - 1 - 4 Geomagnetic field measurements; three components magnetometer

2 - 1 - 5 Geomagnetic field measurements; Proton magnetometer

2 - 2 French Polynesian superplume observation

2 - 2 - 1 OBEM

2 - 2 - 2 BBOBS

2 - 3 Paleomagnetism in the southeast Pacific

2 - 3 - 1 Objective and strategy

2 - 3 - 2 Site survey: bathymetry and sub-bottom profiling

2 - 3 - 3 Site survey: Single channel seismic survey

2 - 3 - 4 Sediment coring

2 - 4 Chile Triple Junction (continue to Leg2)

2 - 4 - 1 Bathymetry and back scatter intensity

~~2 - 4 - 2 Geophysical underway observations~~

2 - 4 - 3 Ocean bottom seismic observation

2 - 4 - 4 Single channel seismic survey

2 - 4 - 5 Rock sampling

2 - 4 - 6 Sediment sampling

2 - 5 Petit-spot volcanoes

2 - 6 Plankton

2 - 7 Meteorological measurement

2 - 7 - 1 Surface Meteorological observation

2 - 7 - 2 Ceilometer observation

2 - 8 Shipboard ADCP

2 - 9 Satellite observation

3 . Appendix (printed matter)

3 - 1 Operation details of the geological sampling (MWJ)

3 - 2 Single channel seismic survey details (NME)

Notice on Using

This cruise report is a preliminary documentation as of the end of the cruise. It may not be corrected even if changes on content (i.e. taxonomic classifications) are found after publication. It may also be changed without notice. Data on the cruise report may be raw or not processed. Please ask the Chief Scientist for the latest information before using.

1. Cruise summary of MR08-06 Leg. 1

1-1. Cruise summary of MR08-06 Leg. 1

Cruise No./ R/V: MR08-06 Leg.1a,b / MIRAI

Title of the cruise: Studies on geophysics and paleoceanography in the South Pacific: Evolution of climate changes and biogeochemical cycles in the Chilean continental marginal area.

Cruise period:

Leg.1a: January, 15, 2009-February 3, 2009

Leg.1b: February, 4, 2009-March, 14, 2009

Port:

Leg.1a: Sekinehama – Papeete

Leg.1b: Papeete - Valparaiso

Research area:

Leg1a: The Pacific Ocea: 41°N - 17.5°S and 141°E - 149 °W

Leg1b: French Polynesia, Southeast Pacific and Chilean EEZ area: 17.5°S- 49°S, 72°W - 150°W

Backgrounds and Purpose:

The Southeast Pacific in the MR08-06 Leg1b cruise target area is a huge blank area of mass of data on the earth sciences because it is a remote corner with the roughest weather on the earth. Although it is the intriguing place, here are intraplate volcanisms with one of the superplume upwelling possibly from core-mantle boundary, plate divergent boundaries (mid-ocean ridges) and plate convergent boundaries (subduction zone) in the research area. Despite the intriguing place, there are few data available with systematic observations using by research vessels. For example, the precise geomagnetic intensity and the sedimentary rate between South East Pacific Rise and Chile Ridge are unknown. Therefore, the tectonics of the oceanic plate in the area remains obscure.

On the other hand, the Chile Triple Junction area is famous for tectonically unique place. It is one particular area to be able to observe a current subduction of an active ridge system on Earth. There are many evidences that the phenomena occurred in some subduction zones including Japan island arcs in the past. They probably play important role of the continental crust formation on the earth evolution. In addition to this, the research area around Chile Triple Junction is expected as the dead end of the 600km-long rupture of the 1960's Chile Earthquake (Mw = 9.5). The seismicities in the south from this area is very low. The ocean floor investigations seldom take place in the south area of the Chile Triple Junction, though a lot of research, such as high resolution seismic explorations by Germany and French research vessels, have been done in the north of it.

Moreover R/V MIRAI crossed the Pacific Ocean completely from the northwest to the southeast during MR08-06 Leg cruise. The trans-Pacific cruise gives us continuous data with same quality and same process. Therefore, the purpose of the cruise is to do various investigations taking R/V MIRAI's advantage of her stability on the rough weather.

This research cruise is composed of three sub-themes;

- 1) Oceanic and continental crust formation around the Chile Triple Junction (area “c” in Fig.2). To characterize the geological processes of the ridge subduction and to understand the processes of the continental crust growth interacted with ridge subduction systems. To understand the mantle dynamics and mass transfer between the upper and lower mantle around the Society hotspot in Polynesia with determining the seismic structure and conductivity structure.
- 2) Large-scale mantle flow, ‘superplume’ around the Society hotspot in Polynesia (area “a” in Fig.2).
- 3) Paleomagnetic study in the South Pacific (area “b” in Fig.2). To understand geomagnetic inclination anomaly, which would be caused by non-dipole in the South Pacific over the past geological period.

Outline of observation:

- 1) Hard rock sampling using by dredge system, sediment coring will be done around Chile Triple Junction and transform fault. Sub-seafloor structure survey with single channel seismic experiment, Seabeam mapping, surface gravity and magnetic surveys are also planned.
- 2) Eight BBOBS (broadband ocean bottom seismograph) and nine OBEM (ocean bottom electro-magnetometer) will be deployed around the Society hot spot.
- 3) Bathymetric survey using Seabeam system and sediment coring are planned in the South Pacific

Relationships with Other Projects:

- 1) Tectonic, Petrologic and Paleo-environmental Researches in the Chile Triple Junction Area:

In order to conduct all observations in the Chilean water during MR08-06 leg1, we contracted a joint research agreement between Department of Geology Faculty of Physical and Mathematical Sciences of University of Chile and IFREE, JAMSTEC at least for three years on Tectonic, Petrologic and Paleo-environmental Researches in the Chile Triple Junction Area.

The content of the activities is agreed as below: 1) Collecting bathymetrical and geophysical (magnetic, gravimetric, seismic) data of the Chile Triple Junction area to understand geodynamic development of this area. 2) Understanding tectono-magmatic history of the Chile Triple Junction area using rock samples dredged from the area. 3) Reconstructing the magnetic and environmental change with high time resolution in the Chile triple Junction area using sediments recovered by piston cores. 4) Collection of information on modern seasonal, annual and decadal climate conditions of the Chile Triple Junction area and its related land area.

- 2) The Seafloor Geophysical Observation Project, the Society Hot Spot Region, French Polynesia:

With regard to the Research Project of Seafloor Geophysical Observation near the Society Hot Spot Region in French Polynesia (the Seafloor Geophysical Observation Project), IFREE/JAMSTEC, Ocean Hemisphere Research Center, Earthquake Research Institute of the University of Tokyo (OHRC/ERI), Laboratoire Terre Océan de l’Université de la Polynésie Française (UFP), Laboratoire Géosciences de l’Université Montpellier II (MONTPELLIER-II), Commissariat à l’Énergie Atomique de France (CEA),

Laboratoire CNRS Domaines Océaniques de l'Université de Bretagne Occidentale (UBO), and Institut de Physique du Globe de Paris (IPGP), have an implementation agreement on the joint research project.

OHRC/ERI and IFREE/JAMSTEC shall form the Japanese Group. UFP, MONTPELLIER-II, CEA, UBO, and IPGP shall form the French Group. The Japanese Group and the French Group shall consult mutually for the deployment, maintenance, and retrieval of the BBOBS and OBEM near the Society hot spot region in French Polynesia.

3) Integrated Ocean Drilling Program (IODP) proposal 612-Full3 "Paleochlimatic and Orbital Modulation of the Earth's magnetic field: A possible external energy source of the geodynamo:

A IODP proposal was submitted to science advisory structure (SAS) of IODP by T. Yamazaki, T. Kanamatsu, and others, which has been forwarded to the Science Planning Committee (SPC) for ranking. The aim of the IODP proposal is to clarify geomagnetic field variations during the last ca. 10 m.y., and in particular to prove or disprove the hypothesis that the geomagnetic field is modulated by changes of the Earth's orbit. During the cruise, we planed to take piston cores to prove the sediments at the proposed sites having magnetic properties suitable for paleomagnetic studies. We also planned to conduct seismic reflection profiling for fulfilling the minimum requirements of the IODP Site Survey Panel (SSP) for drilling: single-channel seismic reflection lines that cross a proposed site, when proposed penetration depth is less than 400m in an open ocean.

Preliminary results:

Totally 56 days ship time and 25,000km length of the cruise track during MR08-06 Leg1 was successfully done without any serious trouble. All of the underway observations, such as bathymetry, surface ship gravity and geomagnetic data, sea surface seawater and plankton, aerosol, volatile and precipitation samplings, have done from Japan to Chile, that is complete trans-Pacific.

We deployed 9 BBOBSs & 9 OBEMs around the Society Hotspot in French Polynesia (Table 1). The one-year observation on the mantle has been started since early February 2009. The equipments will be recovered in 2010.

While the sediment sampling using 20m-long piston core in the southeast Pacific area was expected 5 stations on the 50°S line, three of them on the 48°S line were taken placed successfully (Table 2). Three cross-line seismic explorations using the single channel streamer system have also done on the same stations.

5 long-term OBSs were deployed with air gun shooting on each of them (Table 1), and SCS explorations on the lines on the 5 OBSs at Chile Triple Junction. These OBSs also started the one-year observation and will be recovered in 2010. 7 times dredges and a rock corer sampling have taken rock samples, and one sedimentary sampling by 10m PC has each time successfully done in this area (Table 3).

1-2 Cruise Log

MR08-06Leg1a

U.T.C.		S.M.T.		Position		Events
Date	Time	Date	Time	Lat.	Lon.	
1/14	00:00	1/14	09:00	41-21.97N	141-14.38E	Departure from Sekinehama
1/16	01:41	1/16	10:41	40-33.24N	141-29.92E	XCTD (#1)
	07:30		16:30	40-35.38N	141-34.04E	Surface sea water sampling pump Start
1/17	01:28	1/17	10:28	38-59.34N	145-50.69E	Proton magnetometer Obs. (#1) Start 8 figure running for magnetometer calibration
	01:50		10:50	38-58.38N	145-53.32E	(#1)
	12:00		22:00	-	-	Time adjustment +1 hours (SMT=UTC+10h)
1/20	00:54	1/20	10:54	31-59.71N	160-15.26E	Proton magnetometer Obs. (#1) End
	23:37	1/21	09:37	30-00.08N	164-27.62E	XCTD (#2)
1/21	11:00		22:00	-	-	Time adjustment +1 hours (SMT=UTC+11h)
1/23	03:29	1/23	14:29	23-00.48N	173-06.19E	(#2) ~ ~
1/24	02:43	1/24A	13:43	20-08.44N	176-37.77E	XCTD (#3)
	10:00		22:00	-	-	Time adjustment +1 hours (SMT=UTC+12h)
1/25	00:06	1/24B	11:06	17-19.18N	179-59.64E	Crosse the Date Line
1/27	03:51	1/26	15:51	10-00.00N	172-23.03W	XCTD (#4)
1/29	09:00	1/28	22:00	-	-	Time adjustment +1 hours (SMT=UTC-11h)
1/30	01:37	1/29	14:37	00-06.11S	162-21.30W	(#3) ~ ~
	02:02		15:02	00-09.63S	162-17.87W	XCTD (#5)
1/31	04:00	1/30	17:00	-	-	EEZ of Kiribati In
2/1	18:52	2/1	07:52	09-59.93S	153-31.34W	XBT (#1)
2/2	08:00	2/1	22:00	-	-	Time adjustment +1 hours (SMT=UTC-10h)
	16:10	2/2	06:10	-	-	EEZ of Kiribati Out
2/3	02:00		16:00	15-12.61S	150-49.72W	Surface sea water sampling pump Stop
	02:28		16:28	15-16.57S	150-47.44W	(#4)
	19:00	2/3	09:00	17-32.02S	149-34.35W	Arrival at Papeete

MR08-06Le g1b

U.T.C.		S.M.T.		Position		Events
Date	Time	Date	Time	Lat.	Lon.	
2/6	19:00	2/6	09:00	17-32.35S	149-34.23W	Departure from Papeete
2/7	02:34		16:34	18-26.48S	149-07.24W	Proton magnetometer Obs. (#2) End
	09:05		23:05	19-20.69S	148-08.57W	XCTD(#6)
	09:36		23:36	19-24.67S	148-03.66W	SBP) Start
	15:20		05:20	19-28.22S	148-02.89W	Station Survey (MBES & SBP) End
	16:02	2/7	06:02	19-28.04S	148-02.89W	OBEM Deployment
	16:07		06:07	19-28.10S	148-02.89W	OBS Deployment
	19:30		09:30	19-28.14S	148-02.36W	from St.1
2/8	03:48		17:48	20-55.42S	146-34.64W	SBP) Start
	07:40		21:40	20-57.44S	146-26.82W	Station Survey (MBES & SBP) End
	07:51		21:51	20-57.65S	146-26.63W	OBEM Deployment
	08:03		22:03	20-57.37S	146-26.43W	OBS Deployment
	12:18	2/8	02:18	20-49.67S	146-24.25W	from St.2
	16:24		06:24	19-54.45S	145-56.47W	SBP) Start
2/9	00:01		14:01	19-56.00S	146-01.37W	Station Survey (MBES & SBP) End
	00:25		14:25	19-55.73S	146-01.50W	OBEM Deployment
	00:33		14:33	19-55.64S	146-01.42W	OBS Deployment
	04:12		18:12	19-55.18S	146-01.47W	from St.3
	10:48	2/9	00:48	18-35.58S	145-03.88W	SBP)
	16:13		06:13	18-25.82S	144-59.25W	Station Survey (MBES & SBP) End
	16:32		06:32	18-25.51S	144-59.17W	OBEM Deployment
	16:39		06:39	18-25.47S	144-59.14W	OBS Deployment
	20:00		10:00	18-25.17S	144-59.14W	from St.4
2/10	00:30		14:30	17-37.10S	144-33.73W	SBP) Start
	06:12		20:12	17-29.98S	144-30.25W	Station Survey (MBES & SBP) End
	06:27		20:27	17-29.91S	144-30.42W	OBEM Deployment
	06:34		20:34	17-29.87S	144-30.38W	OBS Deployment
	09:18		23:18	17-30.06S	144-29.83W	from St.5
	19:00	2/10	09:00	18-44.35S	142-24.18W	SBP) Start
2/11	01:20		15:20	18-48.41S	142-17.61W	Station Survey (MBES & SBP) End
	01:25		15:25	18-48.28S	142-17.61W	Plankton Net (#1)
	02:05		16:05	18-48.31S	142-17.63W	OBEM Deployment
	02:12		16:12	18-48.33S	142-17.56W	OBS Deployment
	05:06		19:06	18-48.88S	142-17.14W	from St.6
	09:06		23:06	19-41.70S	142-44.82W	SBP) Start
	16:13		06:13	19-55.87S	142-41.40W	Station Survey (MBES & SBP) End
	16:29	2/11	06:29	19-56.34S	142-41.19W	OBEM Deployment
	16:36		06:36	19-56.35S	142-41.16W	OBS Deployment
	19:24		09:24	19-56.74S	142-40.72W	from St.7

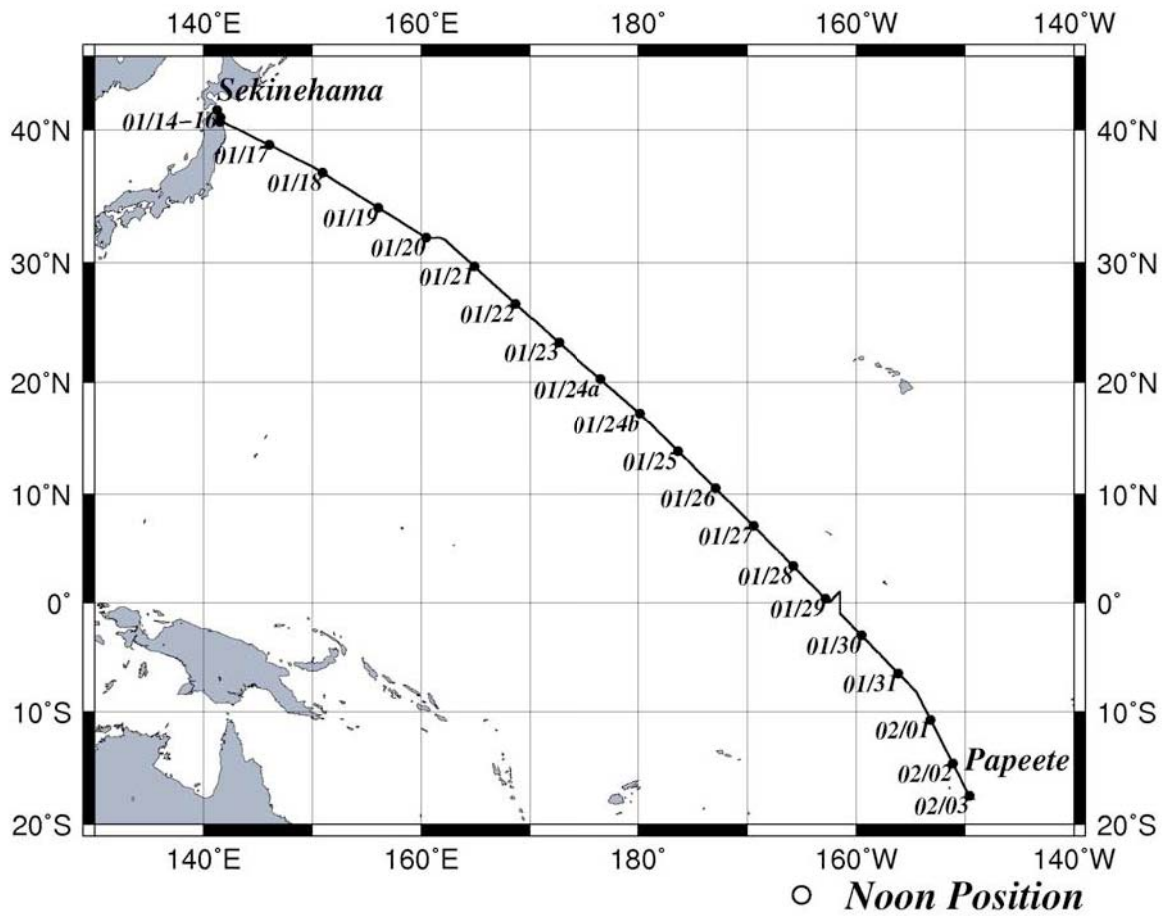
2/12	01:36		15:36	20-43.02S	143-43.13W	SBP) Start
	06:21		20:21	20-57.17S	143-45.39W	Station Survey (MBES & SBP) End
	06:24		20:24	20-57.16S	143-45.35W	OBEM Deployment
	06:31		20:31	20-57.14S	143-45.30W	OBS Deployment
	09:24		23:24	20-57.36S	143-44.84W	from St.8
	15:30	2/12	05:30	22-01.90S	144-36.45W	SBP) Start
	21:10		11:10	22-11.26S	144-42.36W	Station Survey (MBES & SBP) End
	21:23		11:23	22-17.76S	144-46.43W	Plankton Net (#2)
	22:05		12:05	22-10.12S	144-41.87W	OBEM Deployment
	22:11		12:11	22-10.10S	144-41.81W	OBS Deployment
2/13	01:00		15:00	22-10.16S	144-42.42W	OBEM & OBS Fixed position
	01:02		15:02	22-10.20S	144-42.41W	Proton magnetometer Obs. (#3) Start
	01:20		15:20	22-11.59S	144-41.37W	(#5)
	02:00		16:00	22-13.67S	144-39.27W	Departure from St.9
	08:00		22:00	-	-	Time adjustment +1 hours (SMT=UTC-9h)
	17:38	2/13	08:38	25-08.28S	142-02.93W	Proton magnetometer Obs. (#3) End
2/14	06:30		21:30	27-40.08S	139-45.28W	EEZ of French Polynesia Out
	20:25	2/14	11:25	30-22.68S	137-13.07W	Proton magnetometer Obs. (#4) Start
2/15	00:09		15:09	30-51.63S	136-47.79W	Proton magnetometer Obs. (#4) End
	00:17		15:17	30-51.86S	136-47.61W	Proton magnetometer Obs. (#5) Start
	01:41		16:41	31-05.98S	136-36.84W	XBT (#2)
2/16	06:00	2/15	22:00	-	-	Time adjustment +1 hours (SMT=UTC-8h)
	09:12	2/16	01:12	37-18.17S	131-25.70W	Proton magnetometer Obs. (#5) End
2/17	04:06		20:06	40-40.96S	128-53.70W	XCTD (#7)
2/18	08:18	2/18	00:18	46-06.25S	124-32.20W	XBT (#3)
	10:42		02:42	46-32.62S	124-10.35W	SBP) Start
	17:26		09:26	46-50.13S	123-40.28W	Station Survey (MBES & SBP) End
	17:40		09:40	46-50.03S	123-40.17W	Piston Core (#1) Start
	21:52		13:52	46-49.71S	123-39.75W	Piston Core (#1) End
	23:16		15:16	47-02.94S	123-39.64W	SCS Obs. (#1) Start
2/19	14:10	2/19	06:10	46-52.25S	123-19.10W	SCS Obs. (#1) End
	14:29		06:29	46-52.35S	123-19.02W	Plankton Net (#3)
	15:01		07:01	46-52.30S	123-18.27W	Proton magnetometer Obs. (#6) Start
	15:18		07:18	46-52.57S	123-16.65W	Departure from St.10
2/20	05:48		21:48	48-14.19S	118-38.46W	XBT (#4)
	06:00		22:00	48-14.69S	118-36.63W	SBP) Start
	13:55		05:55	48-18.11S	118-14.67W	Station Survey (MBES & SBP) End
	14:06	2/20	06:06	48-17.56S	118-15.21W	Proton magnetometer Obs. (#6) End
	14:32		06:32	48-14.95S	118-18.61W	Piston Core (#2) Start
	18:35		10:35	48-14.76S	118-19.23W	Piston Core (#2) End
	19:31		11:31	48-23.83S	118-18.84W	SCS Obs. (#2) Start
2/21	04:04		20:04	48-14.50S	118-27.02W	SCS Obs. (#2) End
	04:42		20:42	48-09.90S	118-30.51W	Departure from St.11
2/22	05:00	2/21	22:00	-	-	Time adjustment +1 hours (SMT=UTC-7h)

2/22	04:00	2/23	22:00	-	-	Time adjustment +1 hours (SMT=UTC-6h)
2/24	22:19	2/24	16:19	48-29.89S	090-15.27W	(#6)
2/25	03:00		22:00	-	-	Time adjustment +1 hours (SMT=UTC-5h)
	18:05	2/25	13:05	48-13.35S	083-17.14W	Proton magnetometer Obs. (#7) Start
2/26	00:29		19:29	48-14.68S	080-59.87W	XBT (#5)
	01:15		20:15	48-14.96S	080-45.10W	EEZ of Chile In
	02:00		21:00	48-15.01S	080-28.37W	SBP) Start
	10:22		05:22	48-26.25S	080-23.18W	Station Survey (MBES & SBP) End
	10:33	2/26	05:47	48-25.92S	080-25.82W	Proton magnetometer Obs. (#7) End
	11:04		06:04	48-25.04S	080-28.44W	Piston Core (#3) Start
	15:09		10:09	48-25.34S	080-29.11W	Piston Core (#3) End
	15:28		10:28	48-25.65S	080-29.22W	Plankton Net (#4)
	16:55		11:55	48-25.17S	080-15.23W	SCS Obs. (#3) Start
	21:38		16:38	48-23.13S	080-27.78W	SCS Obs. (#3) End
	22:00		17:00	48-21.93S	080-27.17W	Departure from St.14
2/28	02:00	2/27	22:00	-	-	Time adjustment +1 hours (SMT=UTC-4h)
3/1	09:42	3/1	05:42	46-06.10S	075-54.49W	SBP) Start
	10:24		06:24	46-06.91S	075-55.63W	Station Survey (MBES & SBP) End
	10:52		06:52	46-06.97S	075-55.32W	OBS Deployment
	12:12		08:12	46-07.46S	075-55.64W	OBS Fixed position, Departure from St.21
	13:24		09:24	46-18.98S	076-04.96W	Arrival at St.18
	13:55		09:55	46-19.91S	076-05.80W	OBS Deployment
	15:06		11:06	46-20.31S	076-05.56W	OBS Fixed position, Departure from St.18
	16:06		12:06	46-19.81S	075-47.25W	Arrival at St.20
	16:49		12:49	46-20.17S	075-46.01W	OBS Deployment
	17:54		13:54	46-20.52S	075-45.94W	OBS Fixed position, Departure from St.20
	18:17		14:17	46-19.87S	075-42.70W	XCTD (#8)
	19:00		15:00	46-17.63S	075-30.19W	Arrival at St.19
	19:32		15:32	46-17.16S	075-28.26W	OBS Deployment
	20:12		16:12	46-17.06S	075-28.33W	OBS Fixed position, Departure from St.19
	22:54		18:54	46-37.47S	075-54.63W	Arrival at St.17
	23:06		19:06	46-38.22S	075-55.57W	OBS Deployment
3/2	00:24		20:24	46-38.12S	075-55.01W	OBS Fixed position, Departure from St.17
	08:12	3/2	04:12	46-52.95S	075-49.41W	SBP)
	11:46		07:46	46-53.39S	075-47.53W	Dradge (#1) Start
	16:32		12:32	46-53.46S	075-47.48W	Dradge (#1) End
	16:36		12:36	46-53.36S	075-47.51W	Departure from St.26
	17:36		13:36	46-39.73S	075-47.17W	Arrival at St.27
	18:15		14:15	46-37.99S	075-47.07W	Dradge (#2) Start
	22:20		18:20	46-38.42S	075-45.75W	Dradge (#2) End
	22:24		18:24	46-38.51S	075-45.83W	Departure from St.27
	23:06		19:06	46-44.06S	075-56.00W	Arrival at St.26P
	23:10		19:10	46-44.18S	075-56.03W	SCS Obs. (#4) Start
3/3	10:16	3/3	06:16	47-04.46S	075-25.30W	SCS Obs. (#4) End, Arrival at St.27P
	14:32		10:32	46-39.31S	075-54.02W	Piston Core (#4) Start
	17:45		13:45	46-39.30S	075-54.13W	Piston Core (#4) End
	18:00		14:00	46-39.26S	075-54.13W	Survey (MBES & SBP) Start

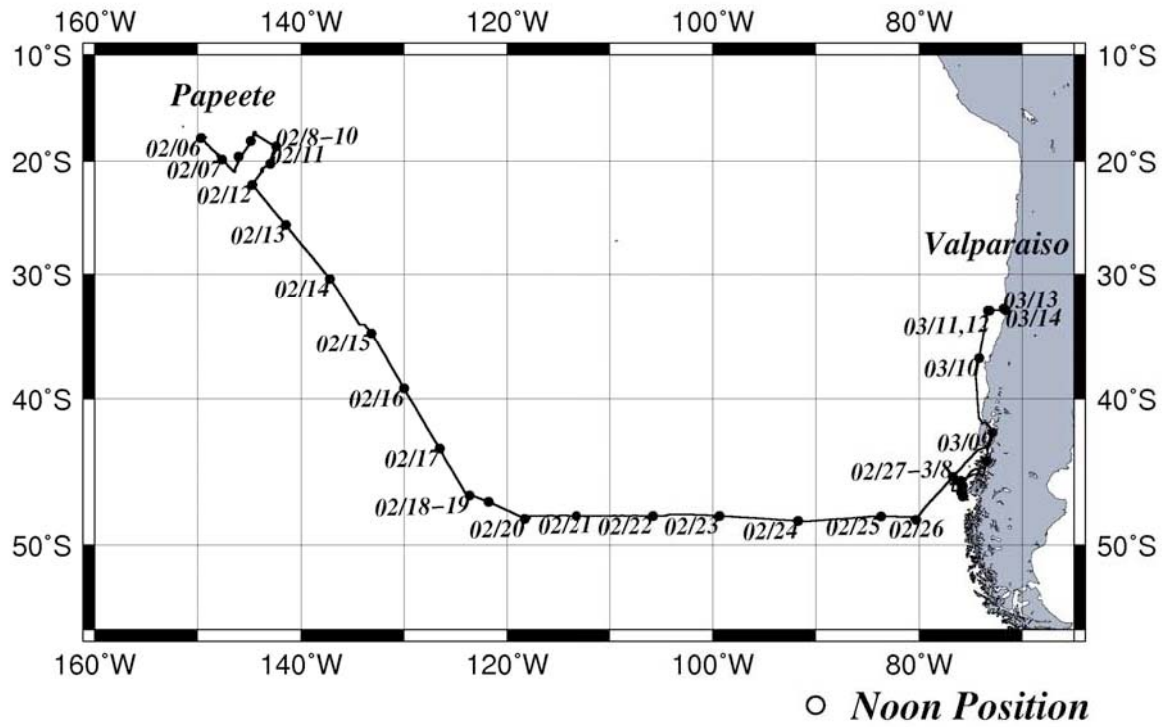
3/4	12:30 15:52 17:20 21:22 22:26	3/4	08:30 11:52 13:20 17:22 18:26	46-03.22S 46-10.28S 46-02.48S 46-02.13S 46-00.15S	076-04.96W 075-46.57W 075-53.73W 075-53.87W 075-49.34W	SCS Obs. (#5) Start End Dradge (#3) Start Dradge (#3) End SCS Obs. (#6) Start
3/6	11:33 12:32 15:52 17:05 20:40 22:00	3/6	07:33 08:32 11:52 13:05 16:40 18:00	46-01.39S 46-04.25S 46-04.14S 46-06.44S 46-06.37S 46-13.49S	075-59.11W 075-54.35W 075-55.07W 075-52.69W 075-53.25W 075-42.20W	SCS Obs. (#6) End Dradge (#4) Start Dradge (#4) End Dradge (#5) Start Dradge (#5) End Survey (MBES & SBP) Start
3/7	11:15 12:17 16:25 17:37 21:22 22:37	3/7	07:15 08:17 12:25 13:37 17:22 18:37	46-29.09S 46-28.41S 46-29.09S 46-33.33S 46-33.21S 46-37.68S	075-49.33W 075-51.91W 075-51.66W 075-57.97W 075-57.08W 075-46.97W	Survey (MBES & SBP) End Dradge (#6) Start Dradge (#6) End Dradge (#7) Start Dradge (#7) End SCS Obs. (#7) Start
3/8	11:53 12:50 15:38 16:30	3/8	07:53 08:50 11:38 12:30	45-47.97S 45-52.49S 45-52.66S 45-50.50S	076-00.59W 075-59.46W 075-59.54W 075-59.11W	SCS Obs. (#7) End Rock Core (#1) Start Rock Core (#1) End Departure from St.30b
3/9	01:00	3/8	22:00	-	-	Time adjustment +1 hours (SMT=UTC-3h)
3/10	22:29	3/10	19:29	35-06.81S	073-46.81W	Proton magnetometer Obs. (#8) Start
3/11	05:06 05:36 11:30 11:48 12:45 17:36 19:16 21:50 22:28	3/11	02:06 02:36 08:30 08:48 09:45 14:36 16:16 18:50 19:28	33-34.84S 33-29.91S 33-00.05S 32-59.79S 33-05.15S 33-05.24S 33-06.99S 33-06.64S 33-03.44S	073-26.55W 073-25.48W 072-59.96W 072-58.79W 073-09.71W 073-10.23W 073-34.33W 072-55.72W 072-59.83W	XBOT (#6) SBP Start Station Survey (MBES & SBP) End Proton magnetometer Obs. (#8) End Dradge (#8) Start Dradge (#8) End Station Survey (MBES & SBP) Start Station Survey (MBES & SBP) End SCS Obs. (#8) Start
3/12	09:58 11:15 14:45 16:04 19:49 19:57	3/12	06:58 08:15 11:45 13:04 16:49 16:57	33-05.49S 33-03.61S 33-03.83S 33-04.67S 33-04.34S 33-04.47S	073-20.93W 073-22.32W 073-21.74W 073-19.24W 073-19.23W 073-19.37W	SCS Obs. (#8) End Dradge (#9) Start Dradge (#9) End Dradge (#10) Start Dradge (#10) End Proton magnetometer Obs. (#9) & Survey (MBES & SBP) Start
3/13	04:27 05:17 06:24	3/13	01:27 02:17 03:24	33-30.19S 33-29.96S 33-29.99S	072-56.19W 072-54.85W 072-40.01W	(#7) Proton magnetometer Obs. (#9) End Survey (MBES & SBP) End
3/14	11:20	3/14	08:20			Arrival at Valparaiso

1-3 Cruise Track

Cruise Track of MR08-06Leg1a



Cruise Track of MR08-06Leg1b



1-4. Survey areas and observation stations

Table 1-4-1 BBOBS and OBEM deployment position list during MR08-06 Leg1b cruise

Date (yymmdd)	Equipment ID	St. ID	Location	Lat. S (SOJ)	Lon. W (SOJ)	Depth (m)	Type of equipment
2009.2.7	SOC1	St. 1	French Polynesia	19-28.197	148-02.923	4398	OBEM/BBOBS
2009.2.7	SOC2	St. 2	French Polynesia	20-57.306	146-26.384	4766	OBEM/BBOBS
22009..8	SOC3	St.3	French Polynesia	19-55.647	146-01.474	4632	OBEM/BBOBS
22009.2.9	SOC4	St.4	French Polynesia	18-25.502	144-56.197	4457	OBEM/BBOBS
2009.2.9	SOC5	St. 5	French Polynesia	17-29.997	144-30.360	4031	OBEM/BBOBS
2009.2.10	SOC6	St. 6	French Polynesia	18-03.099	142-17.629	4484	OBEM/BBOBS
2009.2.11	SOC7	St.7	French Polynesia	19-56.465	142-41.301	4467	OBEM/BBOBS
2009.2.11	SOC8	St. 8	French Polynesia	20-57.202	143-45.380	4779	OBEM/BBOBS
2009.2.12	SOC9	St. 9	French Polynesia	22-10.164	144-41.790	4513	OBEM/BBOBS
2009.3.1	LC4	St.21	Chile TJ	46.116433	75.91919	2841	LTOBS
2009.3.1	LC2	St.18	Chile TJ	46.330797	76.095627	2773	LTOBS
2009.3.1	LC3	St.20	Chile TJ	46.33615	75.76685	2605	LTOBS
2009.3.1	LC5	St.19	Chile TJ	46.286502	75.471313	1106	LTOBS
2009.3.1	LC1	St.17	Chile TJ	46.63808	75.926237	3358	LTOBS

Table 1-4-2 Piston core list during MR08-06 Leg1b cruise

Date (yymmdd)	Core/Dr edge/Rock Corer ID	St. ID	Location	Lat. S (SOJ)	Lon. W (SOJ)	Depth (m)	Tube length (m)	Core length (m)	Corer type
2009.2.18	PC01	St.10a	SE Pacific	46-49.863	123-40.302	3951	20	10.665	Outer
2009.2.20	PC02	St.11	SE Pacific	48-14.949	118-18.640	3358	20	6.255	Outer
2009.2.26	PC03	St.14	SE Pacific	48-25.041	80-28.438	4098	20	19.510	Outer
2009.3.2	PC04	St.27P	Chile TJ (Taitao)	46-39.313	75-54.016	3345	10	8.447	Inner

Table 1-4-3 Dredge and Rock core list during MR08-06 Leg1b cruise

Date (yyymmdd)	Core/ Dredge/ Rock Corer ID	St. ID	Location	Lat. S (SOJ)	Lon. W (SOJ)	Depth (m)	Weight (kg)	note
2009.3.2	D01	St.26D	Chile TJ (Taitao)	46-53.55	75-47.57	2532	299	Sedimentary & volcanic rock
2009.3.2	D02	St.27D	Chile TJ (Taitao)	46-38.056	75-46.657	2808	51.8	Sedimentary, volcanic & plutonic rock
2009.3.4	D03	St.29a	Chile TJ (Chile ridge)	46-02.395	75-53.823	3288	1.5	Mud w/detrital minerals
2009.3.6	D04	St.29a	Chile TJ (Chile ridge)	46-04.200	75-54.39	3000	37.4	basalt
2009.3.6	D05	St.29b	Chile TJ (Chile ridge)	46-06.378	75-52.843	3149	14.0	basalt
2009.3.7	D06	St.28a	Chile TJ (Taitao)	46-29.440	75-51.900	2511	194	Sedimentary rock
2009.3.7	D07	St.28b	Chile TJ (Taitao)	46-33.300	75-58.002	2339	233	Sedimentary & volcanic rock
2009.3.8	RC01	St.30a	Chile TJ (Chile ridge)	45-52.46	75-59.46	3285	0.02	Volcanic rock
2009.3.11	D08	St.36a	Valparaiso	33:05.19	73-09.76	4113	70 pieces	Volcanic rock & mud
2009.3.12	D09	St.36b	Valparaiso	33-03.70	73-22.30	3782	30 pieces	Mn-crust & Volcanic fragment
2009.3.12	D10	St.36c	Valparaiso	33-04.69	73-19.67	3701	50 pieces	Volcanic rock & mud stone

2. Participants:

- (1) Chief Scientist/ Affiliation (Leg.1): Natsue Abe / Institute for Research on Earth Evolution (IFREE), Japan Agency for Marine-Earth Science and Technology (JAMSTEC)
- (2) Principal Investigator/ Affrication: Same as above
- (3) Other participants

Leg.1a

- 1) Atsushi Kurasawa (Hokkaido Univ./JAMSTEC, Plankton)
- 2) Hiroshi Furutani (Univ. of Tokyo, Aerosol)
- 3) Jinyoung Jung (Univ. of Tokyo, Aerosol)
- 4) Ryo Kimura (Global Ocean Development, SeaBeam, SBP, Meteorological measurement)
- 5) Satoshi Okumura (Global Ocean Development, SeaBeam, SBP, Meteorological measurement)
- 6) Asuka Doi (Global Ocean Development, SeaBeam, SBP, Meteorological measurement)
- 7) Minoru Kamata (Marine Works Japan, CTD/hydrocast)
- 8) Seike (Marine Works Japan, CTD/hydrocast)
- 9) Syunsuke Tanaka (Marine Works Japan, CTD/hydrocast)

Leg 1b

- 1) Toshiya Kanamatsu (JAMSTEC, Sediment coring, Earth Magnetics)
- 2) Hiroko Sugioka (JAMSTEC, Seismology)
- 3) Takafumi Kasaya (JAMSTEC, Electromagnetics)
- 4) Noriko Tada (JAMSTEC, Electromagnetics)
- 5) Aki Ito (JAMSTEC, Seismology)
- 6) Shiki Machida (ORI, Univ. Tokyo, Petrology)
- 7) Takehi Isse (ERI, Univ. of Tokyo, Seismology)
- 8) Kiyoshi Baba (ERI, Univ. of Tokyo, Electromagnetics)
- 9) Ryo Anma (Univ. of Tsukuba, Sediment coring, Rock)
- 10) Yuji Orihashi (ERI, Univ. Tokyo, Geochemistry)
- 11) Masatake Aniya (Univ. of Tsukuba, Geomorphology)
- 12) Kiichiro Kawamura (Fukada Geological Institute, Sediment coring)
- 13) Toshitsugu Yamazaki (AIST, Sediment coring, Earth Magnetics)
- 14) Takaya Shimono (Univ. of Tsukuba, Sediment coring, Earth Magnetics)
- 15) Naoto Iirano (Tohoku Univ., Pctrology)
- 16) Atsushi Kurasawa (Hokkaido Univ./JAMSTEC, Plankton)
- 17) Hiroshi Furutani (Univ. of Tokyo, Aerosol)
- 18) Jinyoung Jung (Univ. of Tokyo, Aerosol)
- 19) Sung-Hyun Park (Korea Polar research Institute)
- 20) Eugenio Andres E. Veloso (Universidad de Catolica del Norte)
- 21) Cristina C.A.O. Caurapan (Universidad de Chile)
- 22) Akihisa Motoki (Universidade do Estado do Rio de Janeiro)
- 23) Rodrigo Soares de Souza (Universidade do Estado do Rio de Janeiro)

- 24) Jalowitzki, Tiago L. R. (Universidade do Federal do Rio Grande do Sul)
- 25) Sebastian Martini Salame (Universidad de Chile)
- 26) Ryo Kimura (Global Ocean Development, SeaBeam, Geophysical measurement, SBP, Meteorological measurement)
- 27) Wataru Tokunaga (Global Ocean Development, SeaBeam, , Geophysical measurement SBP, Meteorological measurement)
- 28) Ryo Ooyama (Global Ocean Development, SeaBeam, , Geophysical measurement SBP, Meteorological measurement)
- 29) Asuka Doi (Global Ocean Development, SeaBeam, , Geophysical measurement SBP, Meteorological measurement)
- 30) Satoshi Shimizu (Nippon Marine Enterprises, SCS)
- 31) Shinichi Hosoya (Nippon Marine Enterprises, SCS)
- 32) Syusuke Machida (Nippon Marine Enterprises, SCS)
- 33) Yoshitake Matsuura (Marine Works Japan, Sediment coring, Dredge, Rock coring)
- 34) Kazuhiro Yoshida (Marine Works Japan, Sediment coring, Dredge, Rock coring)
- 35) Syohei Taketomo (Marine Works Japan, Sediment coring, Dredge, Rock coring)
- 36) Yasushi Hashimoto (Marine Works Japan, Sediment coring, Dredge, Rock coring)
- 37) Syugo Oshitani (Marine Works Japan, Sediment coring, Dredge, Rock coring)
- 38) Hideki Yamamoto (Marine Works Japan, CTD/hydrocast)
- 39) Shinichiro Yokogawa (Marine Works Japan, CTD/hydrocast)
- 40) Ayumi Takeuchi (Marine Works Japan, CTD/hydrocast)

2-1 Surface geophysical surveys

2-1-1 Bathymetry and back scatter intensity

Natsue Abe	JAMSTEC: Principal investigator	- Leg1a, b -
Ryo Kimura	Global Ocean Development Inc.	- Leg1a, b -
Asuka Doi	GODI	- Leg1a, b -
Satpshi Okumura	GODI	- Leg1a -
Wataru Tokunaga	GODI	- Leg1b -
Ryo Ohyama	GODI	- Leg1b -

Not on-board;
Takeshi Matsumoto University of the Ryukyus
Masao Nakanishi Chiba University

(1) Introduction

R/V MIRAI equipped a Multi-narrow Beam Echo Sounding system (MBES), SEABEAM 2112.004 (SeaBeam Instruments Inc.). The main system of “SeaBeam 2100”, 12 kHz system, provides swath bathymetry data and back scatter intensity (side scan) data. Sub Bottom Profiler (SBP) subsystem is an add-on option to the “SEABEAM 2100”. SBP collects vertical sub-bottom profile information.

The capital objective of MBES is site survey so that we have gathered necessary bathymetric, back scatter intensity and sub-bottom profiler information around the core sampling, and rock sampling points at the South Pacific and Chile off shore areas. And also, BBOBS and OBEM deployment positions were determined by bathymetry at the French Polynesia area.

The other objective is collecting continuous bathymetry data along ship’s track to make a contribution to geological and geophysical investigations and global datasets.

(2) Data Acquisition

The “SEABEAM 2100” on R/V MIRAI was used for bathymetry mapping during MR08-06 Leg1 cruise from 16 January 2009 to 13 March 2009. For primary data quality management, applying proper sound velocity profile is the most important. Sound velocity profiles were calculated using temperature and salinity data from XBT, XCTD and ARGO floats by the equation in Mackenzie (1981). Variations of sound velocity at transducer face have a large influence on depth, especially side beams, so that this system has Surface Sound Velocimeter, which measuring sound velocity in the surface intake water continuously.

Obvious bad bathymetry data was flagged automatically by real-time data screening function of the system.

Back scatter intensity (Sidescan) data were calculated from echo returned time and amplitude. The resolution was 2000 pixels at each ping. Pixel size were automatically fitted by swath coverage.

System configuration and performance;

SEABEAM 2112.004 (12kHz system);

Frequency:	12 kHz
Transmit beam width:	2 degree
Transmit power:	20 kW
Transmit pulse length:	3 to 20 msec.
Depth range:	100 to 11,000 m
Beam spacing:	1 degree athwart ship
Swath width:	150 degree (max) 120 degree to 4,500 m

	100 degree to 6,000 m
	90 degree to 11,000 m
Depth accuracy:	Within < 0.5% of depth or +/-1m, whichever is greater, over the entire swath. (Nadir beam has greater accuracy; typically within < 0.2% of depth or +/-1m, whichever is greater)
Sidescan data:	Power [dB] = 20.0 * log ₁₀ (Amplitude)

Sub-Bottom Profiler (4kHz system);

Frequency:	4 kHz
Transmit beam width:	5 degree
Sweep:	5 to 100 msec
Depth Penetration:	As much as 75 m (varies with bottom composition)
Resolution of sediments:	Under most condition within < tens-of-centimeters range (Dependent upon depth and sediment type)

(3) Data Archives

Data obtained during this cruise will be submitted to the Marine-Earth Data and Information Department (MEDID) in JAMSTEC, and will be archived there

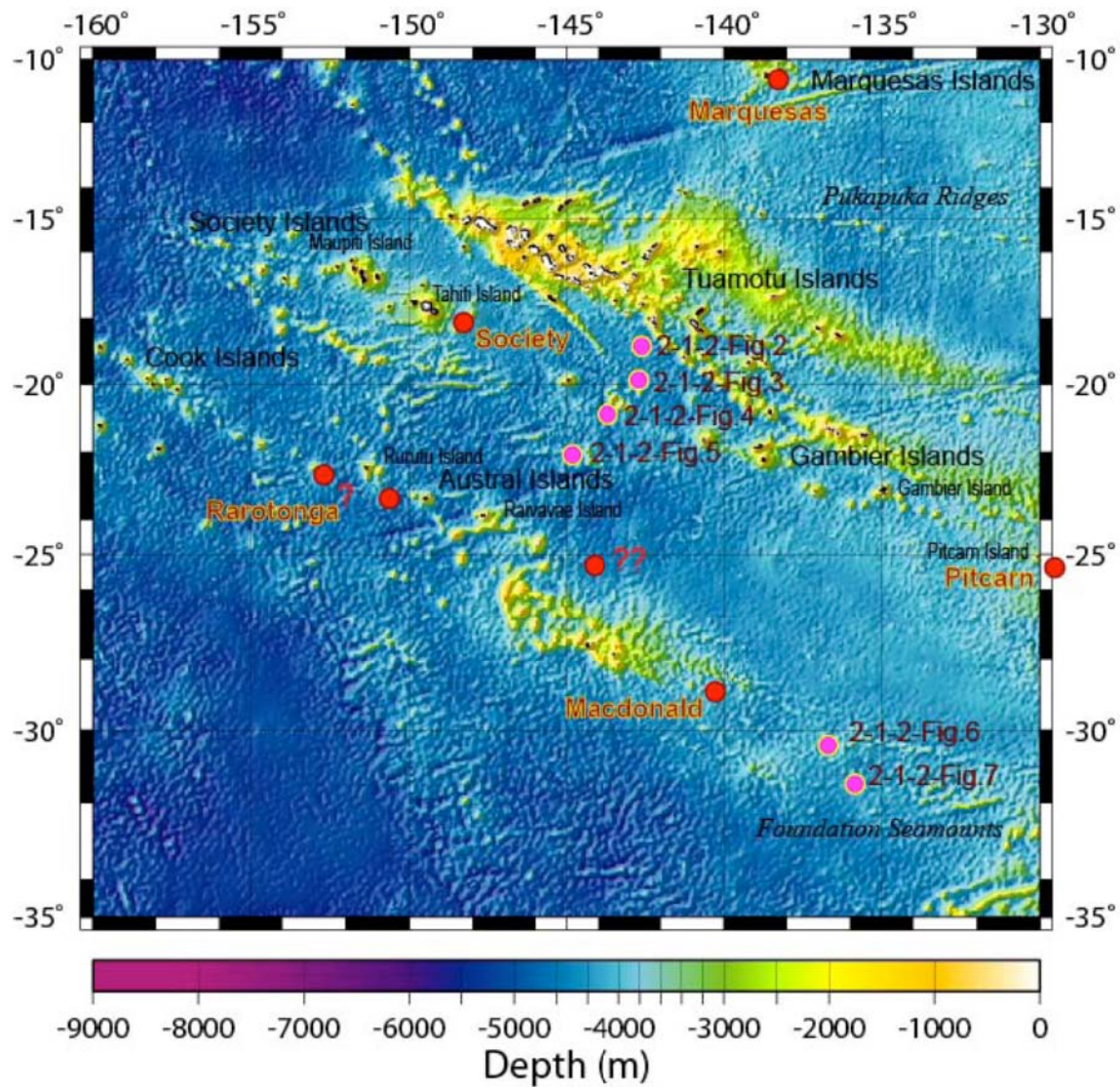
(4) Remarks

1. We stopped underway pinging when the MIRAI navigated in shallow area about less than 100 m depth.
2. GPS data were not effected following the period;
18:56:42 – 18:59:39 UTC, 26 Feb. 2009

2-1-2. Descriptions of seamounts

by N. Hirano & GODI

Hotspots in the French Polynesian Region



2-1-2-Fig. 1: Bathymetrical map around the French Polynesian region using the data of “ETOPO2”. French Polynesian hotspots are shown by red circles. The pink-colored circles are the possible sites showing young volcanoes by the seabeam data on this cruise (2-1-2-Fig. 2 to 7, respectively).

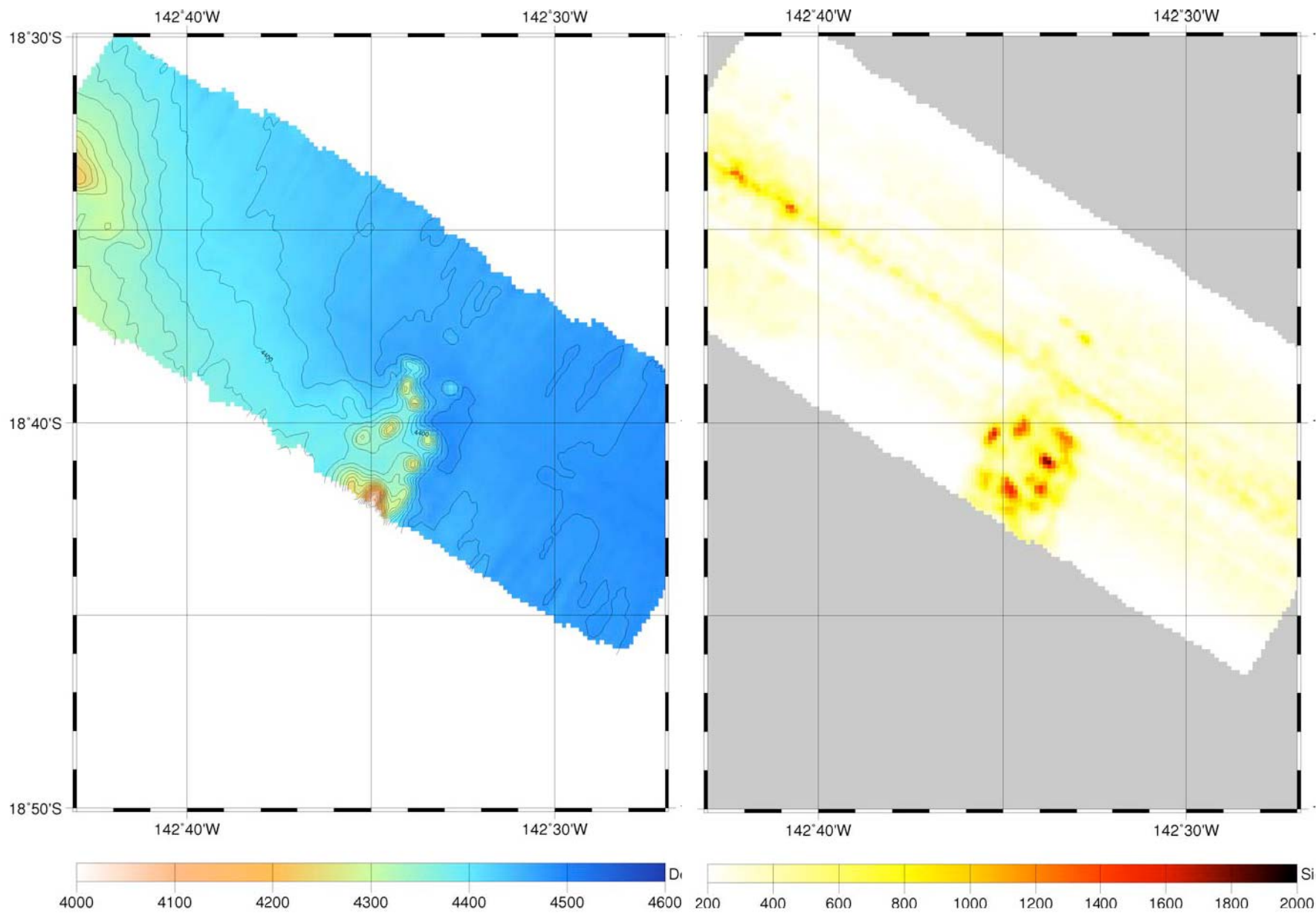
Following Morgan (1972), Earth scientists commonly attribute both types of hotspots to mantle plumes, cylindrical conduits of hot low-viscosity material, which upwell from the deep mantle. Linear seamounts and oceanic-islands of intra-plate volcanoes are built as lithospheric plates move over stationary melt sources (hotspots) from the deeper mantle. The volcanoes, therefore, would be fed by melts formed at different temperatures and pressures during their growth from the initial phase to final phase of volcano growth, because they should be fed by melt formed either at the rim of the plume as it passes beneath previously unaffected lithosphere (Frey *et al.*, 2000) or deep in the plume as the upwelling mantle first crosses the solidus. The initial phases of volcano growth must be complemented by sampling of present-day submarine volcanic activity. The large number of small and active volcanoes suggests that many more volcanic systems are initiated than large or subaerial volcanoes at hotspots. Such sampling has been carried out on Loihi Seamount in the Hawaii chain (e.g. Moore *et al.*, 1979), on the Macdonald Seamount in the Austral Chain (e.g. Johnson, 1970) and on the Vailulu'u Seamount in the Samoan chain (e.g. Konter *et al.*, 2004).

As for the French Polynesian region, we have recognized some hotspots (e.g. Society, Marquesas, Pitcairn, Austral, Cook) (2-1-2-Fig. 1), which might be seated on each hotspot tail from the deep mantle (e.g. McNutt and Fischer, 1987). Although the volcanism along the Cook-Austral seamount chain has occurred repeatedly at loci of magmatism lying thousands of kilometers from reconstructed positions of the presumed hotspot located at the Macdonald Seamount (Johnson, 1970), some seamounts on the chain are rejuvenated or resumed by multiple and overlapping volcanoes erupted at Quaternary time (Dickinson, 1998; Bonneville *et al.*, 2002). It has been difficult to explain the evolution of the Cook-Austral chain with standard models of hotspots. The Society and Pitcairn hotspots, on the other hand, are well known their age progression from Tahiti Island to Maupiti Island and from Pitcairn Island to Gambier Island, respectively (Gripp and Gordon, 2002). But their hotspots are located at each submarine portion on the southeastern-most extension of each chain (e.g. Binard *et al.*, 1991; Cheminee *et al.*, 1989; Hekinian *et al.*, 1991; Hekinian *et al.*, 2003). The detail position of present Society hotspot in the mantle would be fixed by OBS and OBEM team on this cruise (see chapter 2-2), awaiting their scientific results.

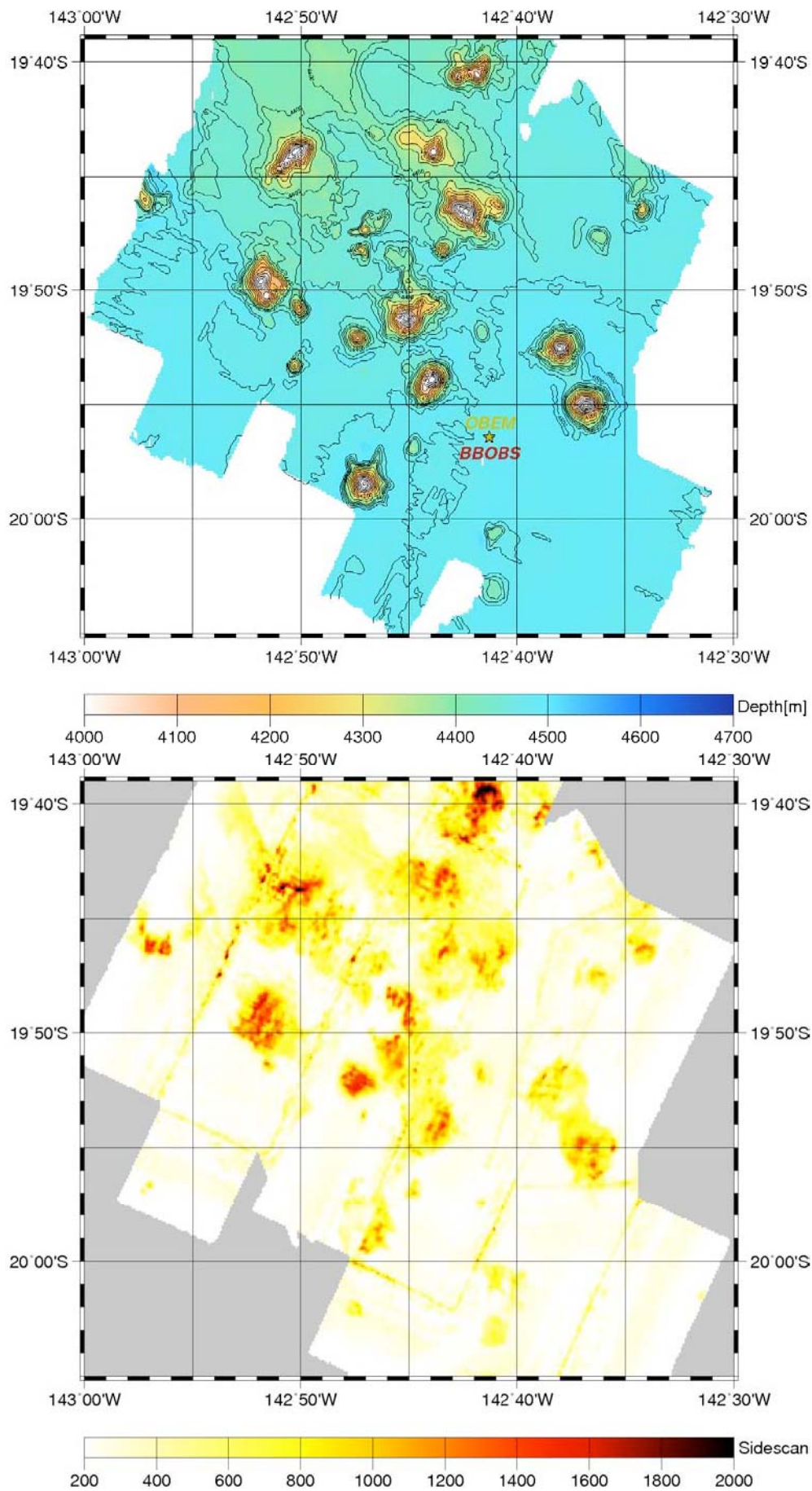
Potential Young Volcanoes at Submarine French Polynesia

Based on our interpretation of the sidescan maps we can possibly conclude some young volcanoes. The sidescan imagery of some volcanic edifices shows high reflectivity because these young lavas are covered with only a thin layer of soft pelagic sediment, much thinner than the surrounding pelagic layer on the Pacific Plate (Hirano *et al.*, 2006). Using their high sidescan intensity as distinguishing characteristics, we were able to identify many young volcanoes at the French Polynesian region (2-1-2-Fig. 2 to 2-1-2-Fig. 7). These data show more than three times as high as the reflective values of surrounding abyssal plain (Hirano *et al.*, 2006). Some of them do not build apparent edifices in spite of showing a high acoustic reflectivity, which possibly is evidence for the exposure of very small-scale flood lavas on the ocean floor, again covered with only a thin pelagic layer. If the top terraces of some knolls and seamounts have low reflectivity with an acoustic reflective intensity analogous to the surrounding pelagic layer of abyssal plain, they are covered with thick pelagic sediments, implying old volcanic edifices.

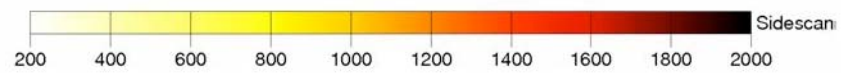
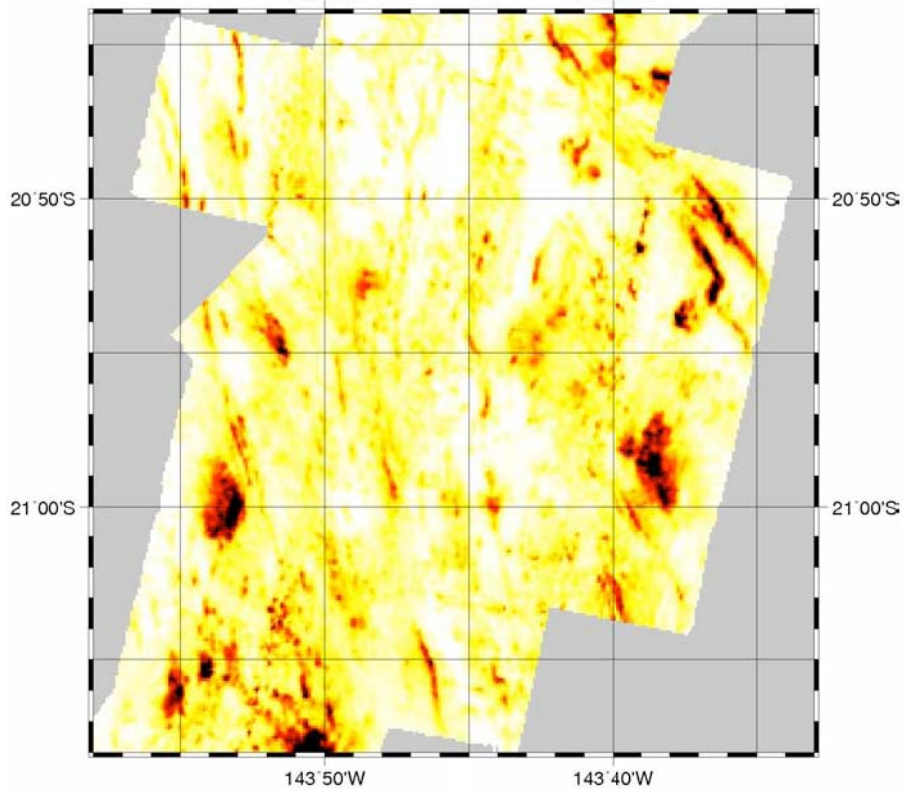
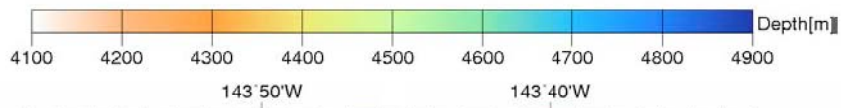
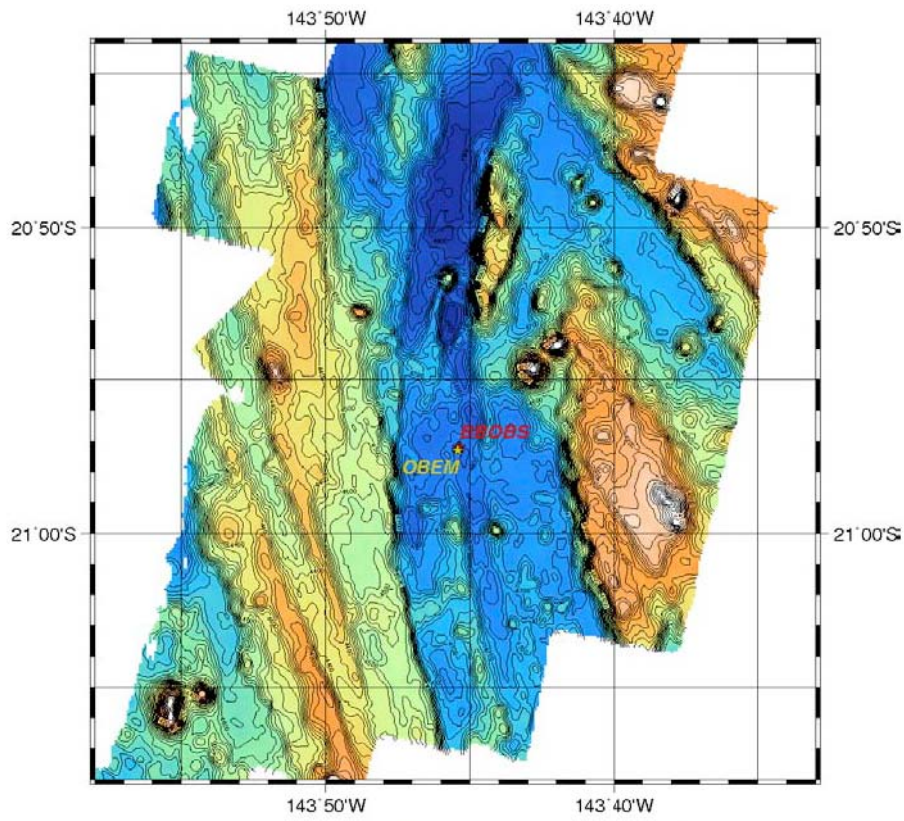
These potential young volcanoes are blown up in 2-1-2-Fig. 2, 2-1-2-Fig. 6 and 2-1-2-Fig. 7. The data of acoustic reflectivity in 2-1-2-Fig. 4 show intensities to be stronger than the high reflectivity patches associated with the fault escarpments, which might be abyssal hills. The center of ship tracks in the sidescan image all is significantly distorted because it coincides with the artificial “high intensity” center beam that always is observed in the middle of a ship track, representing the most direct reflections collected vertically from beneath the ship. The some knoll (e.g. 31 48’S-136 05’W on 2-1-2-Fig. 7), on the other hand, could not be identified as a young volcanoes because the data do not show high reflectivity at the knoll, where only the slope of the knoll seems to have a high reflectivity. The knoll having such reflectivity, therefore, is probably covered with thick pelagic sediments implying an old edifice.



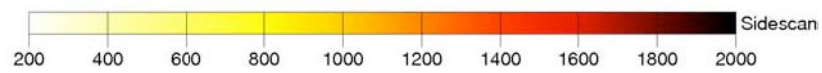
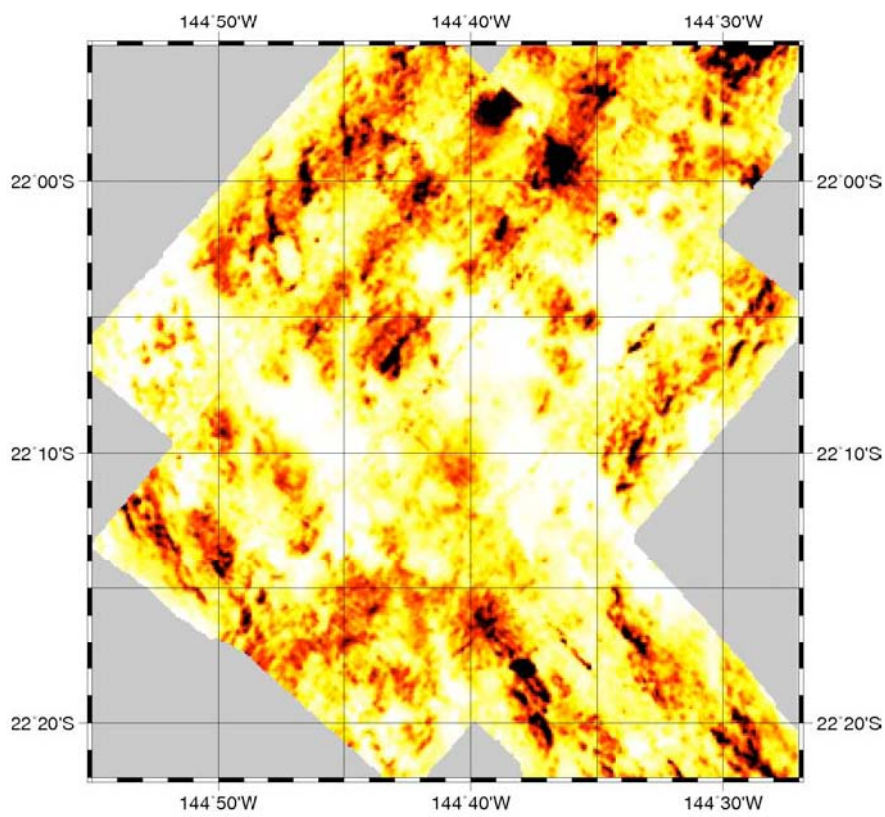
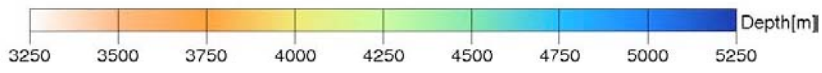
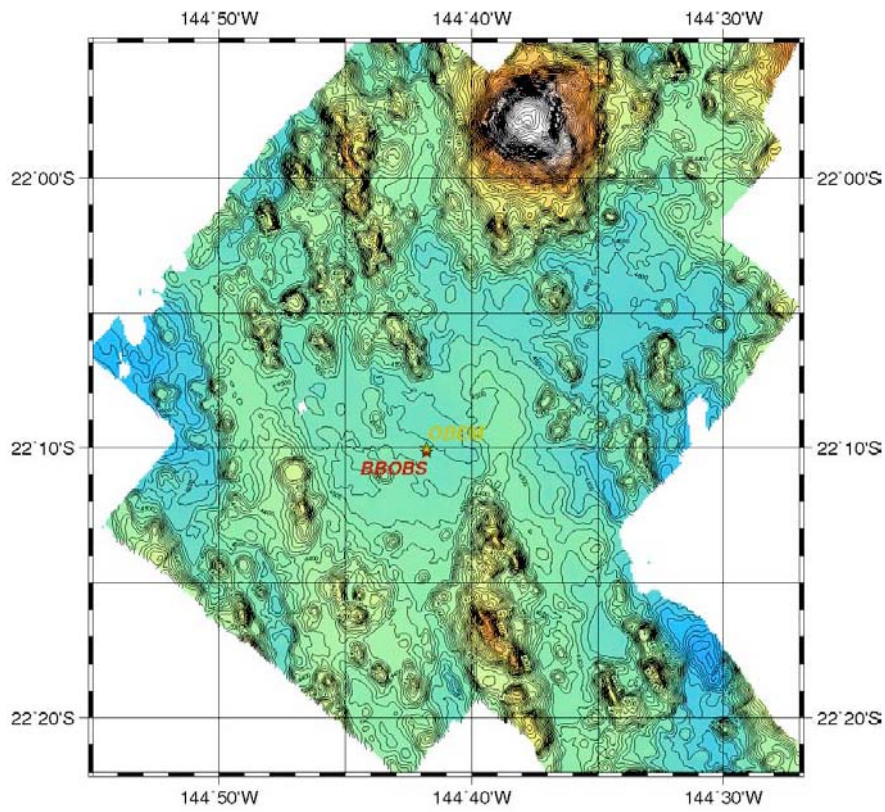
2-1-2-Fig. 2: Bathymetrical and sidescan maps at 18°40'S, 142°35'W.



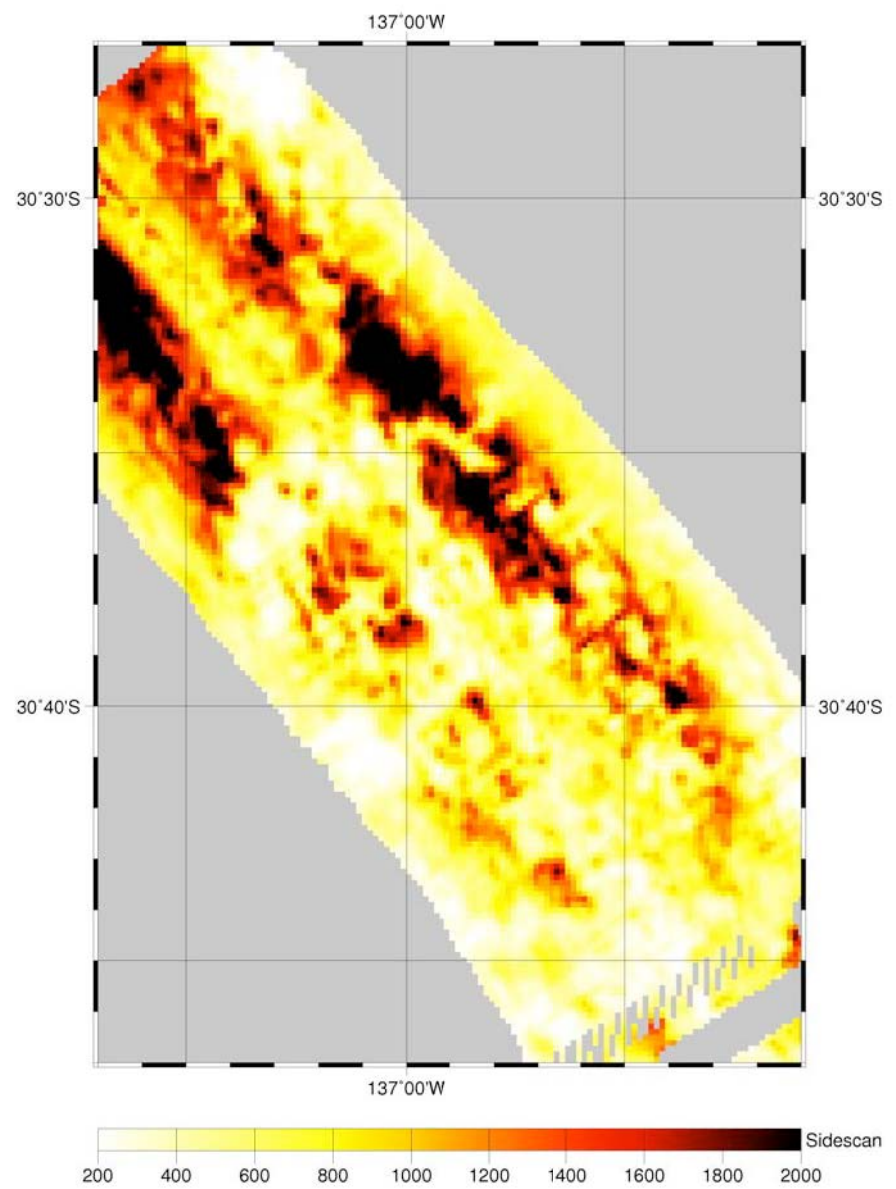
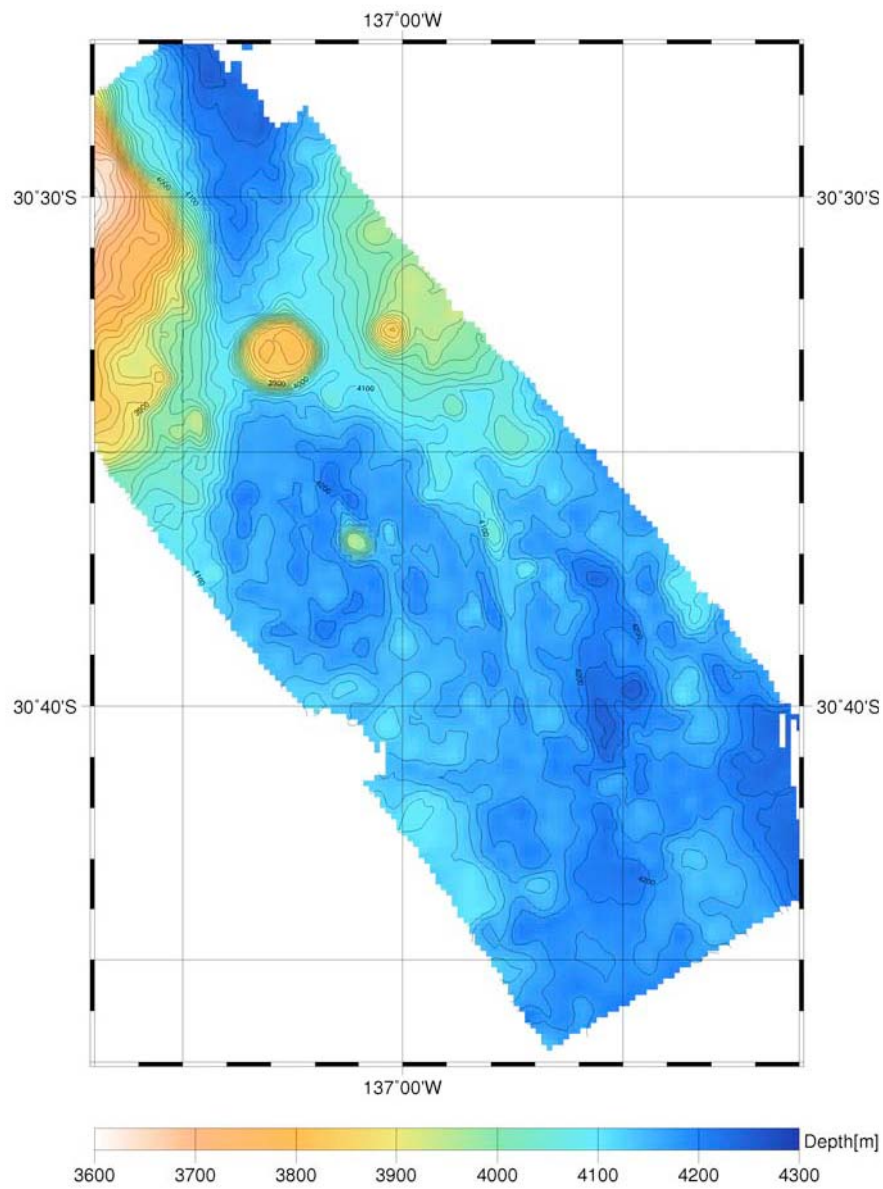
2-1-2-Fig. 3: Bathymetrical and sidescan maps around the Station 7.



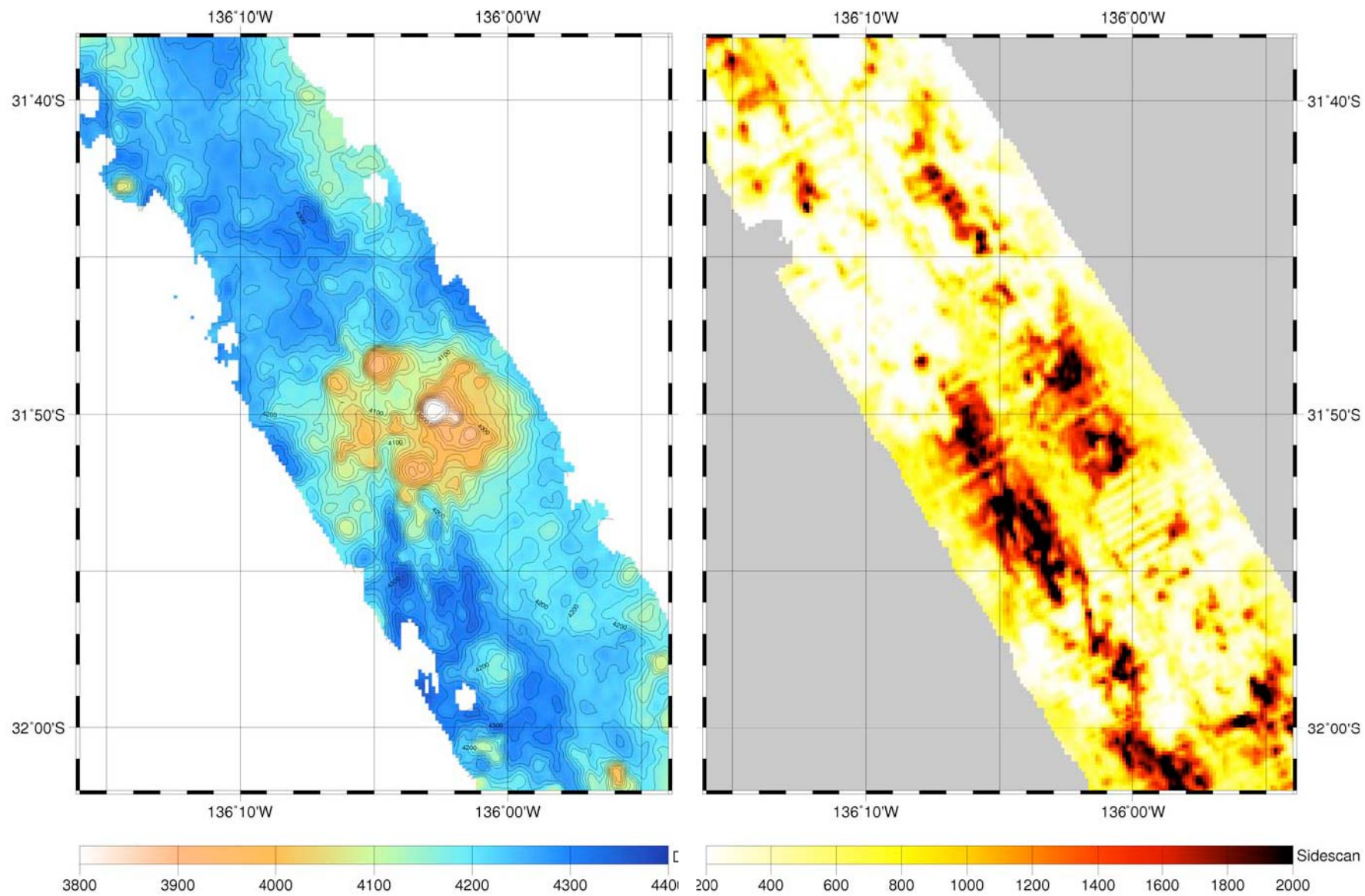
2-1-2-Fig. 4: Bathymetrical and sidescan maps around the Station 8.



2-1-2-Fig. 5: Bathymetrical and sidescan maps around the Station 9.



2-1-2-Fig. 6: Bathymetrical map and sidescan image around 30°37'S, 136°59'W.



2-1-2-Fig. 7: Bathymetrical map and sidescan image around 31°50'S, 136°05'W.

References

- Binard, N., Hekinian, R., Cheminee, J.L., Searle, R.C. & Stoffers, P. (1991) Morphological and structural studies of the Society and Austral hotspot regions in the South Pacific, *Tectonophysics* **186**, 293–312.
- Bonneville, A., Suave, R. L., Audin, L., Clouard, V., Dosso, L., Gillot, P. Y., Jordahl, K., Maamaatuaiahutapu, K. (2002) Arago Seamount: The missing hotspot found in the Austral Islands. *Geology* **30**, 1023-1026.
- Cheminee, J.L., Hekinian, R., Talandier, J., Albarede, F., Devey, C.W., Francheteau, J. & Lancelot, Y. (1989) Geology of an active hotspot: Teahitia-Mehetia region in the South Central Pacific, *Mar. Geophys. Res.* **11**, 27–50.
- Dickinson, W. R. (1998) Geomorphology and geodynamics of the Cook-Austral island-seamount chain in the south Pacific ocean: implications for hotspots and plumes. *International Geology Review* **40**, 1039-1075.
- Frey, F.A., Clague, D., Mahoney, J.J., and Sinton, J.M. (2000) Volcanism at the edge of the Hawaiian plume: Petrogenesis of submarine alkalic lavas from the North Arch volcanic field. *J. Petrol.* **41**, 667–691.
- Gripp, A. E. and Gordon, R. G. (2002) Young tracks of hotspots and current plate velocities. *Geophys. J. Int.* **150**, 321–361.
- Hekinian, R., Bideau, D., Stoffers, P., Cheminee, J. L., Muhe, R., Puteanus, D. & Binard, N. (1991) Submarine intraplate volcanism in the South Pacific: Geological setting and petrology of the Society and Austral regions, *J. Geophys. Res.* **96**, 2109–2138.
- Hekinian R., Cheminee J. L., Dubois J., Stoffers P., Scott S., Guivel C., Garbe-Schönberg D., Devey C., Bourdon B., Lackschewitz K., Mcmurtry G. and Le Drezen E. (2003) The Pitcairn hotspot in the South Pacific: distribution and composition of submarine volcanic sequences. *J. Volcanol. Geotherm. Res.* **121**, 219-245.
- Hirano, N., Koppers, A. A. P., Takahashi, A., Fujiwara, T. and Nakanishi, M. (2008) Seamounts, knolls and petit spot monogenetic volcanoes on the subducting Pacific Plate. *Basin Research* **20**, 543-553
- Johnson, R. H. (1970) Active submarine volcanism in the Austral Islands. *Science* **167**, 977-979.
- Konter, J. G. and Staudigel, H., Hart, S. R. and Shearer, P. M. (2004) Seafloor seismic monitoring of an active submarine volcano: Local seismicity at Vailulu'u Seamount, Samoa. *Geochem. Geophys. Geosyst.*, doi: 10.1029/2004GC000702
- McNutt, M. K. and Fischer, K. M. (1987) The South Pacific Superswell. In: Keating, B.H., Fryer, P., Batiza, R., Boehlert, G.W. (Eds.), *Seamounts, Islands, and Atolls*, Geophysical Monograph Series, **43**. American Geophysical Union, Washington, DC, pp. 25–43.
- Moore J G, Normark W R, Lipman P W (1979) Loihi seamount-a young submarine Hawaiian volcano (abs). Hawaii Symp Intraplate Volc & Submarine Volc, Hilo, Hawaii, Abs, p 127
- Morgan, W. J. (1971) Convection plumes in the lower mantle. *Nature*, **230**, 42–43.
- Morgan, W. J. (1972) Plate motions and deep convection, *Geol. Soc. Am. Mem.* **132**, 7–22.

2-1-3 Gravity field measurements

Natsue Abe	JAMSTEC: Principal investigator	- Leg1a, b -
Ryo Kimura	Global Ocean Development Inc.	- Leg1a, b -
Asuka Doi	GODI	- Leg1a, b -
Satpshi Okumura	GODI	- Leg1a -
Wataru Tokunaga	GODI	- Leg1b -
Ryo Ohyama	GODI	- Leg1b -
Not on-board;		
Takeshi Matsumoto	University of the Ryukyus	
Masao Nakanishi	Chiba University	

(1) Introduction

The difference of local gravity is an important parameter in geophysics and geodesy. We collected gravity data at the sea surface during the MR08-06 Leg1 cruise departure of Sekinehama on 14 January 2009 to arrival of Valparaiso on 14 March 2009, port call Papeete on 3 to 6 February 2009.

(2) Parameters

Relative Gravity [mGal] = Data reading value [CU] * coef.
 Converting Relative Gravity coefficient: coef. = 0.9946

(3) Data Acquisition

We have measured relative gravity using LaCoste and Romberg air-sea gravity meter S-116 (Micro-G LaCosat) during this cruise. To convert the relative gravity to absolute one, we measured gravity, using portable gravity meter (Scintrex gravity meter CG-3M), at Sekinehama, Papeete and Valparaiso as reference points.

(4) Preliminary Results

Absolute gravity shown in 2-1-3-table1

2-1-3-table1

No.	Date	U.T.C.	Port	Absolute Gravity [mGal]	Sea Level [cm]	Draft [cm]	Gravity at Sensor * ¹ [mGal]	L&R * ² Gravity [mGal]
#01	Jan/14	06:04	Sekinehama	980371.94	233	620	980372.70	12634.85
#02	Feb/04	23:43	Papeete	978699.30	53	638	978699.53	10965.51
#03	Mar/14	13:35	Valparaiso	979619.29				

*¹: Gravity at Sensor = Absolute Gravity + Sea Level*0.3086/100 + (Draft-530)/100*0.0431

*²: LaCoste and Romberg air-sea gravity meter S-116

Differential	G at sensor	L&R value
#02 - #01	-1673.18 mGal ---(a)	-1669.34 mGal ---(b)
L&R drift value (b)-(a)	3.8377 mGal	21.7353 days
Daily drift ratio	0.1766 mGal/day	
#03 - #02	???.?? mGal ---(a)	???.? mGal ---(b)
L&R drift value (b)-(a)	???.? mGal	36 days
Daily drift ratio	??.? mGal/day	

#03 - #01	???.?? mGal ---(a)	???.? mGal ---(b)
L&R drift value (b)-(a)	???.? mGal	58 days
Daily drift ratio	?..? mGal/day	

(5) Data Archives

Gravity data obtained during this cruise will be submitted to the Marine-Earth Data and Information Department (MEDID) in JAMSTEC, and will be archived there.

(6) Remarks

GPS data were not effective following the period;
18:56:42 – 18:59:39 UTC, 26 Feb. 2009

2-1-4 Geomagnetic field measurements; three components magnetometer

Natsue Abe	JAMSTEC: Principal investigator	- Leg1a, b -
Ryo Kimura	Global Ocean Development Inc.	- Leg1a, b -
Asuka Doi	GODI	- Leg1a, b -
Satpshi Okumura	GODI	- Leg1a -
Wataru Tokunaga	GODI	- Leg1b -
Ryo Ohyama	GODI	- Leg1b -
Not on-board;		
Takeshi Matsumoto	University of the Ryukyus	
Masao Nakanishi	Chiba University	

(1) Introduction

Measurement of magnetic force on the sea is required for the geophysical investigations of marine magnetic anomaly caused by magnetization in upper crustal structure. We measured geomagnetic field using a three-component magnetometer during the MR08-06Leg1 cruise departure from Sekinehama on 14 January 2009 to arrival of Valparaiso on 14 March, 2009, port call Papeete on 3 to 6 February 2009.

(2) Principle of ship-board geomagnetic vector measurement

The relation between a magnetic-field vector observed on-board, H_{ob} , (in the ship's fixed coordinate system) and the geomagnetic field vector, F , (in the Earth's fixed coordinate system) is expressed as:

$$H_{ob} = \mathbf{A} \mathbf{R} \mathbf{P} \mathbf{Y} \mathbf{F} + \mathbf{H}_p \quad (a)$$

where \mathbf{R} , \mathbf{P} and \mathbf{Y} are the matrices of rotation due to roll, pitch and heading of a ship, respectively. $\tilde{\mathbf{A}}$ is a 3 x 3 matrix which represents magnetic susceptibility of the ship, and \mathbf{H}_p is a magnetic field vector produced by a permanent magnetic moment of the ship's body. Rearrangement of Eq. (a) makes

$$\mathbf{B} H_{ob} + \mathbf{H}_{bp} = \mathbf{R} \mathbf{P} \mathbf{Y} \mathbf{F} \quad (b)$$

where $\mathbf{B} = \mathbf{A}^{-1}$, and $\mathbf{H}_{bp} = -\mathbf{B} \mathbf{H}_p$. The magnetic field, F , can be obtained by measuring \mathbf{R} , \mathbf{P} , \mathbf{Y} and H_{ob} , if \mathbf{B} and \mathbf{H}_{bp} are known. Twelve constants in \mathbf{B} and \mathbf{H}_{bp} can be determined by measuring variation of H_{ob} with \mathbf{R} , \mathbf{P} and \mathbf{Y} at a place where the geomagnetic field, F , is known.

(3) Instruments on R/V MIRAI

A shipboard three-component magnetometer system (Tierra Tecnica SFG1214) is equipped on-board R/V MIRAI. Three-axes flux-gate sensors with ring-cored coils are fixed on the fore mast. Outputs from the sensors are digitized by a 20-bit A/D converter (1 nT/LSB), and sampled at 8 times per second. Ship's heading, pitch, and roll are measured by the Inertial Navigation System (INS) for controlling attitude of a Doppler radar. Ship's position (GPS) and speed data are taken from LAN every second.

(4) Data Archives

These data obtained in this cruise will be submitted to the Marine-Earth Data and Information Department (MEDID) of JAMSTEC.

Remarks

For calibration of the ship's magnetic effect, we made a "figure-eight" turn (a pair of clockwise and anti-clockwise rotation).

01:50 - 02:22 UTC, 17 Jan. about at 38-58N, 145-53E
03:29 - 03:49 UTC, 23 Jan. about at 23-00N, 173-06E
02:37 - 02:56 UTC, 30 Jan. about at 00-06S, 162-21W
02:28 - 02:47 UTC, 03 Feb. about at 15-17S, 150-47W
01:20 - 01:54 UTC, 13 Feb. about at 22-12S, 144-41W
22:19 - 22:42 UTC, 24 Feb. about at 48-30S, 095-15W
04:27 - 04:57 UTC, 13 Mar. about at 33-30S, 072-56W

2-1-5 Geomagnetic field measurements; three components magnetometer

Natsue Abe	JAMSTEC: Principal investigator	- Leg1a, b -
Ryo Kimura	Global Ocean Development Inc.	- Leg1a, b -
Asuka Doi	GODI	- Leg1a, b -
Satpshi Okumura	GODI	- Leg1a -
Wataru Tokunaga	GODI	- Leg1b -
Ryo Ohyama	GODI	- Leg1b -

Not on-board;
Takeshi Matsumoto University of the Ryukyus
Masao Nakanishi Chiba University

(1) Introduction

Measurement of total magnetic force on the sea is required for the geophysical investigations of marine magnetic anomaly. We measured geomagnetic field using a proton magnetometer at the MR08-06Leg1.

(2) Instruments on R/V MIRAI

System : G811 (GEOMETRICS)

Specification:

Setting:

Total Cycle time 10sec (Sensitivity = 0.5nT)

Noise Level:

Ninety percent(90%) of all readings to be within selected sensitivity envelope

Accuracy:

+0.5 gamma or less as determined by the magnetic cleanliness of sensor materials and the known accuracy of the proton gyromagnetic constant.

Dynamic Operating Range:

17,000 to 95,000 gammas

Tuning:

Fully automatic throughout the range with manual selection of ambient field starting point for quick start up.

(3) Data Archives

These data obtained in this cruise will be submitted to the Marine-Earth Data and Information Department (MEDID) of JAMSTEC.

(4) Observed periods

- 1). 01:50UTC, 17 Jan. - 00:54 UTC, 20 Jan.
- 2). 22:00UTC, 06 Feb. - 02:34 UTC, 07 Feb.
- 3). 01:02UTC, 13 Feb. - 17:38 UTC, 13 Feb.
- 4). 20:25UTC, 14 Feb. - 00:09 UTC, 15 Feb.
- 5). 00:17UTC, 15 Feb. - 09:12 UTC, 16 Feb.
- 6). 15:01UTC, 19 Feb. - 14:06 UTC, 20 Feb.
- 7). 18:05UTC, 25 Feb. - 10:33 UTC, 26 Feb.
- 8). 22:29UTC, 10 Mar. - 11:48 UTC, 11 Mar.
- 9). 19:52UTC, 12 Mar. - 05:17 UTC, 13 Mar.

2-2-1 OBEM

N. Tada, T. Kasaya, K. Baba

Instruments

The OBEMs are made by Tierra Tecnica Ltd., which can measure time variations of three components of magnetic field, horizontal electric field, the instrumental tilts, and temperature. The resolutions are 0.01 nT for flux-gate magnetometer, 0.305 μV for voltmeter, 0.00026 degrees for tiltmeter, and 0.01 $^{\circ}\text{C}$ for thermometer. Each OBEM has two pressure-resistant glass spheres; one contains the electromagnetometer and the other contains an acoustic transponder and a Lithium battery pack. The OBEMs have four pipes for attaching five Filloux-type silver-silver chloride electrodes (Filloux, 1987). Those pipes will be folded away when the OBEMs come to the surface during recovery in order to recover them easily. A frame of OBEM can be taken apart (2-2-1-photo1), and it enables us to save keeping space on deck. The OBEMs mount a radio beacon and a flash light.



2-2-1-photo1. OBEM (left) and frame which is taken apart (right).

Deployment of the OBEMs

We first mapped the bathymetry in the vicinity of planned position using SeaBeam system and searched flat seafloor for the final deployment point. The OBEMs were launched from deck using a crane settled on starboard for St1 (TT5) and using A-frame for the other stations, and sunk by their own weights. The operations were quick and smooth. We tracked the OBEMs by acoustic signals and confirmed that the OBEMs were successfully settled on the seafloor. Then, the settled positions were determined by measurements of the slant ranges at least three positions surrounding the launched point for each OBEM. The information that will be needed for the recovery and the data analysis are listed in 2-2-1-table1.

2-2-1-table1. Information of the OBEMs deployed during this cruise.

Site	St1	St2	St3
OBME ID	TT5	ERI13	JM1
Launched position	19° 28.04' S	20° 57.43' S	19° 55.697' S
	148° 02.89' W	146° 26.48' W	146° 01.467' W
Settled position	19° 28.0943' S	20° 57.3671' S	19° 55.7146' S
	148° 02.9869' W	146° 26.5362' W	146° 01.5571' W
Depth	4426.7 m	4772.6 m	4656.2 m
Sampling intervals	60 s	60 s	60 s
Dipole length (N-S)	4.50 m	4.50 m	4.50 m
Dipole length (E-W)	4.50 m	4.50 m	4.50 m
Time for clock reset to GPS (TZ=±0h)	2009-02-07 03:59:21	2009-02-07 19:45:22	2009-02-08 02:16:30
Time for recording start (TZ=±0h)	2009-03-01 00:00:00	2009-03-01 00:00:00	2009-03-01 00:00:00
Acoustic system	Nichiyu Giken	Kaiyo Denshi	Nichiyu Giken
Frequency (Tx, ship side)	9.6 ~ 10.9 kHz	10.000kHz	9.6 ~ 10.9 kHz
Frequency (Rx, ship side)	10.24 kHz	13.500kHz	10.24 kHz
Release command	3-C	3F-1	3-H
Radio beacon	NOVATECH	NOVATECH	NOVATECH
Frequency	159.150MHz	159.200MHz	159.150MHz
Flash light	NOVATECH	NOVATECH	NOVATECH

Site	St4	St5	St6
OBME ID	JM8	JM2	JM7
Launched position	18° 25.51' S	17° 29.91' S	18° 48.31' S
	144° 59.17' W	144° 30.42' W	142° 17.63' W
Settled position	18° 25.6877' S	17° 30.0741' S	18° 48.3272' S
	144° 59.2672' W	144° 30.4126' W	142° 17.7677' W
Depth	4477.6 m	4049.3 m	4507.7 m
Sampling intervals	60 s	60 s	60 s
Dipole length (N-S)	4.50 m	4.50 m	4.50 m
Dipole length (E-W)	4.50 m	4.50 m	4.50 m
Time for clock reset to GPS (TZ=±0h)	2009-02-08 02:58:59	2009-02-09 21:29:20	2009-02-10 02:36:02
Time for recording start (TZ=±0h)	2009-03-01 00:00:00	2009-03-01 00:00:00	2009-03-01 00:00:00
Acoustic system	Nichiyu Giken	Kaiyo Denshi	Kaiyo Denshi
Frequency (Tx, ship side)	9.6 ~ 10.9 kHz	11.029kHz	10.000kHz
Frequency (Rx, ship side)	10.24 kHz	13.501kHz	13.5kHz
Release command	3-B	1C-1	3C-1
Radio beacon	NOVATECH	NOVATECH	NOVATECH
Frequency	159.200MHz	159.150MHz	159.300MHz
Flash light	NOVATECH	NOVATECH	NOVATECH

Site	St7	St8	St9
OBME ID	JM6	ERI11	JM4
Launched position	19° 56.34' S	20° 57.16' S	22° 10.120' S
	142° 41.19' W	143° 45.35' W	144° 41.865' W
Settled position	19° 56.4286' S	20° 57.2894' S	22° 10.0488' S
	142° 41.2916' W	143° 45.4224' W	144° 41.7885' W
Depth	4489.6 m	4805.7 m	4540.0 m
Sampling intervals	60 s	60 s	60 s
Dipole length (N-S)	4.50 m	4.50 m	4.50 m
Dipole length (E-W)	4.50 m	4.50 m	4.50 m
Time for clock reset to GPS (TZ=±0h)	2009-02-11 00:47:30	2009-02-11 01:01:08	2009-02-12 02:18:55
Time for recording start (TZ=±0h)	2009-03-01 00:00:00	2009-03-01 00:00:00	2009-03-01 00:00:00
Acoustic system	Kaiyo Denshi	Kaiyo Denshi	Kaiyo Denshi
Frequency (Tx, ship side)	10.563kHz	10.000kHz	11.029kHz
Frequency (Rx, ship side)	13.500kHz	13.500kHz	13.501kHz
Release command	2C-1	3D-1	1A-1
Radio beacon	NOVATECH	NOVATECH	NOVATECH
Frequency	159.300MHz	159.300MHz	159.200MHz
Flash light	NOVATECH	NOVATECH	NOVATECH

2-2-2. Broadband ocean bottom seismograph (BBOBS)

H. Sugioka, A. Ito, T. Isse

The BBOBS has been developed at the Earthquake Research Institute (ERI) of the University of Tokyo since 1999 based on the OBS with a geophone. A broadband sensor (CMG-3T for OBS, Guralp, UK) is installed on an active leveling unit developed at the ERI. The data is digitized by a 24 bit ADC with 100 Hz, and recorded on 1.8 inch HDDs with the total capacity of 80 GB. The recording period of the BBOBS is 500 days in MR08-06 cruise. These and 70 Li cells (DD size) are fixed inside of a titanium sphere housing ($D = 0.65$ m). Differential Pressure gauge (DPG) is equipped with BBOBS deployed at site2 and site8. The BBOBS is deployed by a free fall from the sea surface and pop up by its buoyancy in the recovery. The anchor is released by a forced electric corrosion of two thin titanium plates after receiving a command of an acoustic transponder from the ship. Appearance of BBOBS is shown in Fig. 1. Principal specifications are described in Table 1.

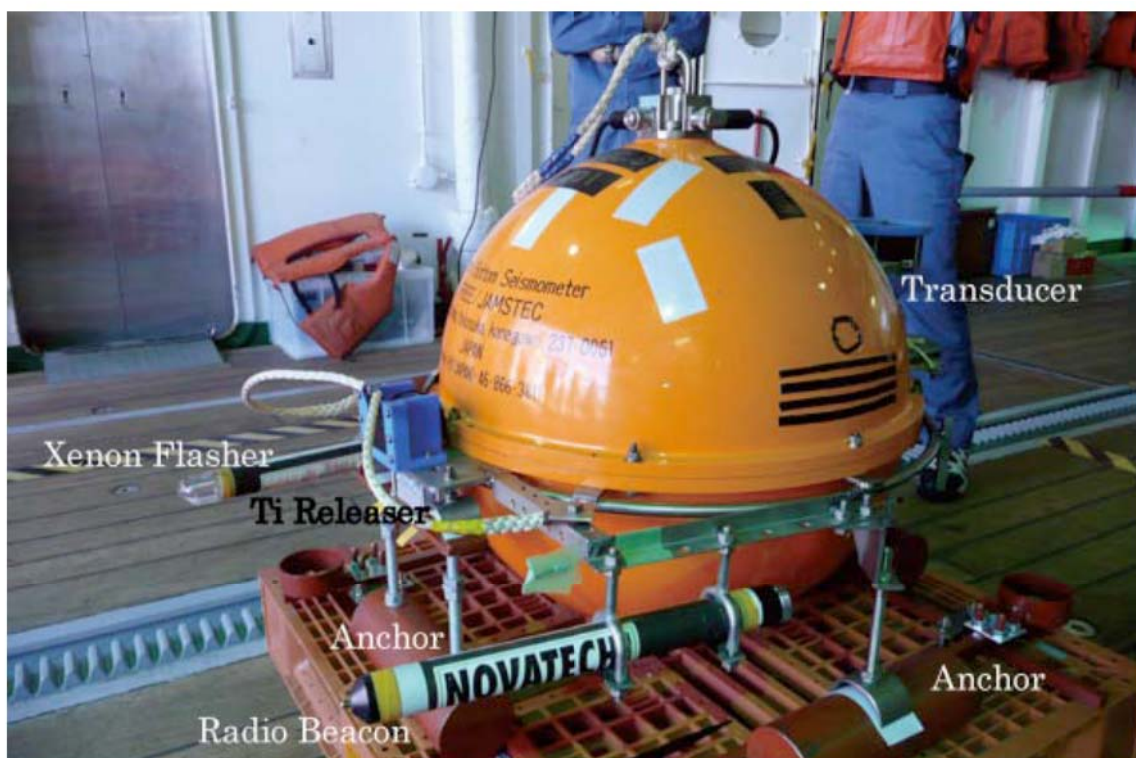
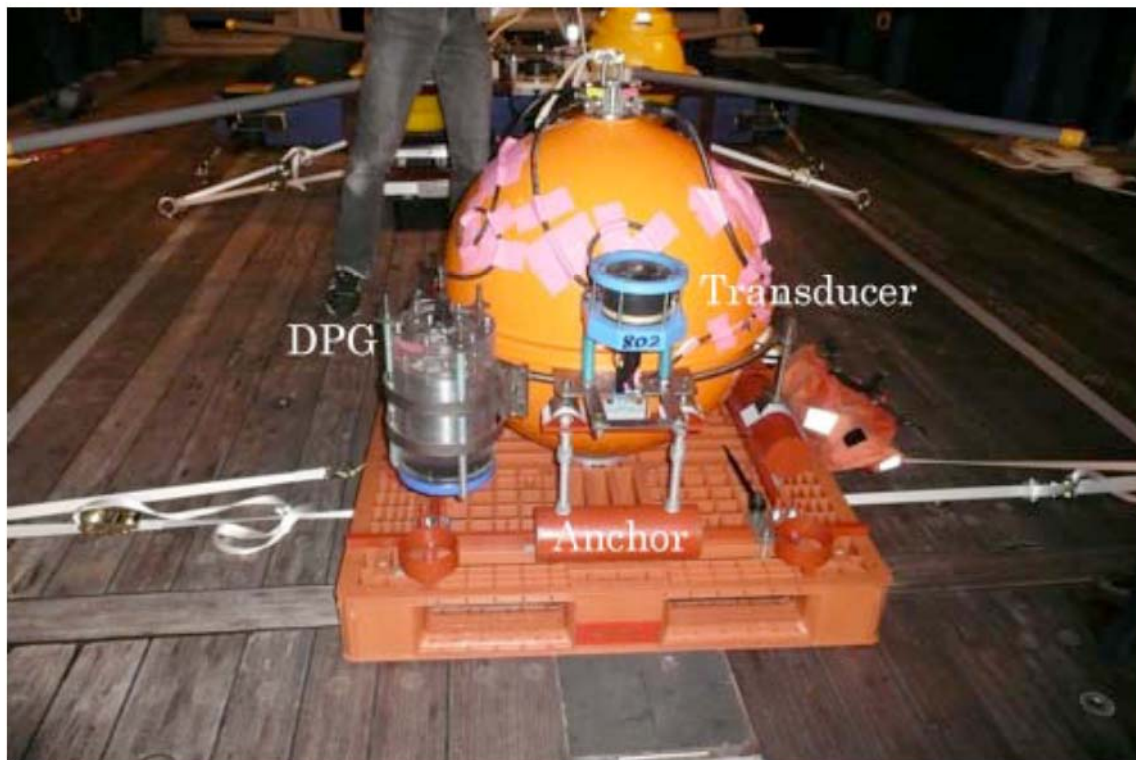
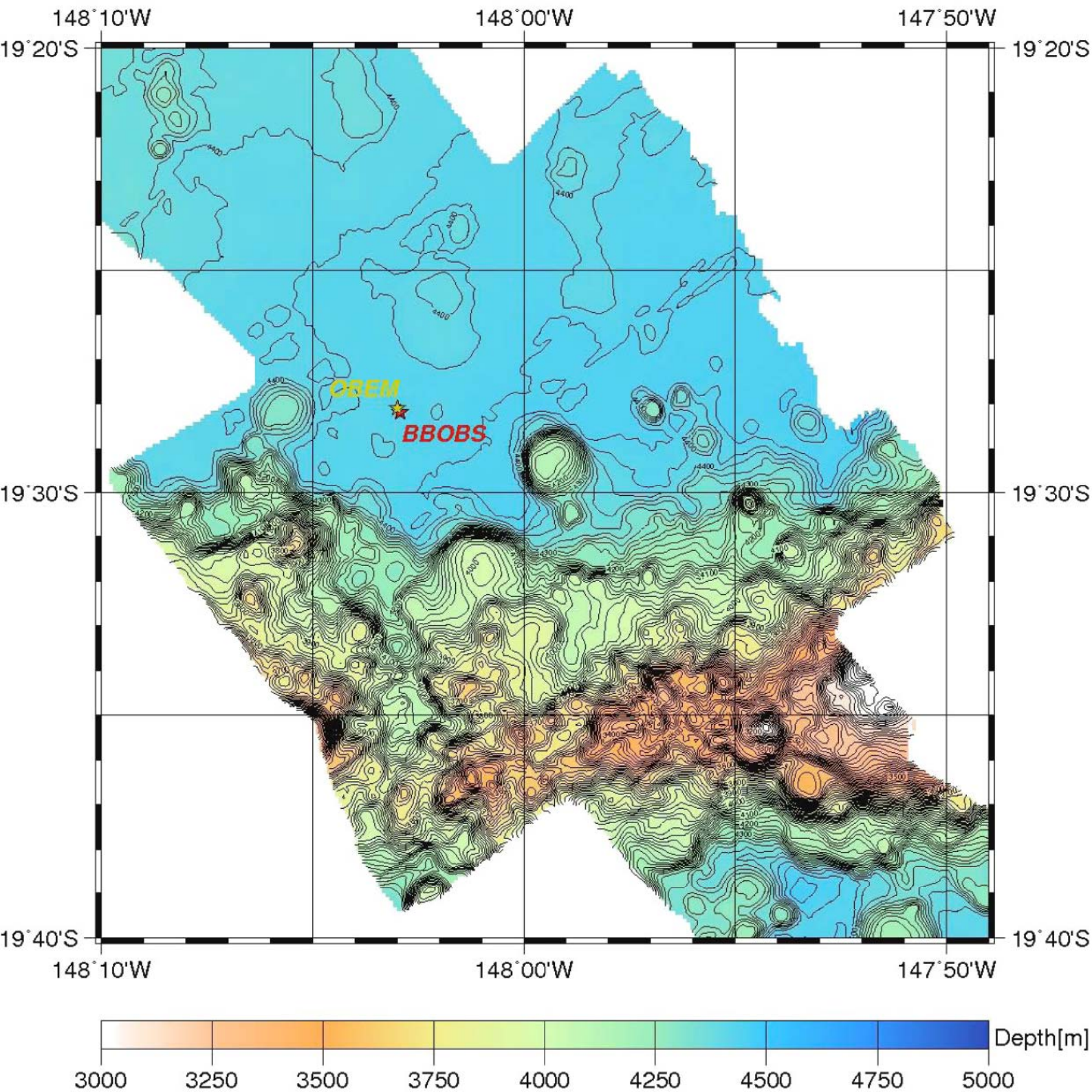


Fig. 1 Appearance of broadband ocean bottom seismometer (BBOBS) deployed at st. 8 (upper) and st. 9 (lower).

Table 1 Principal specifications for BBOBS.

Outside	
Size	1m x 1m x 0.7m (Width x Depth x Height)
Pressure case	Titanium sphere (D=0.65m, Buoyancy=70kg, Made in Russia)
Releasing mechanism	forced electric corrosion of two thin Ti plates (t=0.4~0.6mm)
Recovery control	Acoustic transponder system with recorder communication
Recovery aids	Radio beacon and Xenon flasher with light switch
Inside	
Sensor	CMG-3T for OBS (Guralp, UK) sensor, 360s~50Hz, 1500V/m/s One vertical and two horizontal components
Active leveling unit	leveling works up to 20 deg. tilt
Analog unit	gain: 0 dB, LPF: 32Hz (4th-order Butterworth)
A/D	24bit (0~5V), 100Hz sampling, Win format like compression
Data media	two 1.8inch 40GB SCSI HDDs
Power supply (for 500 days)	Using DD size lithium cells (ElectroChem, 3.9V 30Ah), Leveling unit: 2 (7.2V 30Ah) Sensor: 48 (14.4V 360Ah) Recorder: 39 (10.8V 390Ah) Differential Pressure gauge (DPG): 9 (10.8V 90Ah)

MR08-06 Leg1 Station No.1



2-3. Paleomagnetism in the southeast Pacific

T. Yamazaki, T. Kanamatsu, T. Shimono et al.

2-3-1. Objective and strategy

The purpose of the sediment coring program in this cruise in the southeast Pacific is to conduct a site survey for the Integrated Ocean Drilling Program (IODP) proposal 612-Full3 submitted by T. Yamazaki, T. Kanamatsu, and others, which has been forwarded to the Science Planning Committee (SPC) for ranking. The aim of the IODP proposal is to clarify geomagnetic field variations during the last ca. 10 m.y., and in particular to prove or disprove the hypothesis that the geomagnetic field is modulated by changes of the Earth's orbit (Yamazaki, 1999; Yokoyama and Yamazaki, 2000; Yamazaki and Oda, 2002; Thouveny et al., 2004; Fuller, 2006). In this cruise, we plan to take piston cores to prove the sediments at the proposed sites having magnetic properties suitable for paleomagnetic studies. We also planned to conduct seismic reflection profiling for fulfilling the minimum requirements of the IODP Site Survey Panel (SSP) for drilling: single-channel seismic reflection lines that cross a proposed site, when proposed penetration depth is less than 400m in an open ocean.

The southeast Pacific is one of the three "high priority areas" in our IODP proposal. It is because the southeast Pacific is a particular region for non-dipole components of the geomagnetic field variations. In existing time-averaged field models (e.g., Johnson and Constable, 1997), the southeast Pacific is the only region on the globe that has positive inclination anomaly, which is a manifestation of persistent non-dipole components. The inclination anomaly is defined as observed inclination minus the inclination that is expected from the geocentric axial dipole (GAD). An intriguing correlation between inclination and paleointensity variations, in-phase in Brunhes and anti-phase in Matuyama, was found in the western equatorial Pacific (Yamazaki and Oda, 2002; Yamazaki et al., 2008), where inclination anomaly has large negative values. To explain this observation, a model connecting dipole-field intensity fluctuations and an inclination anomaly caused by a persistent quadrupole component has been proposed by Yamazaki and Oda (2002; 2004). If this model is correct, intensity-inclination correlation opposite in phase to the western equatorial Pacific is expected to be observed in the southeast Pacific. Another reason for conducting a paleomagnetic study in the southeast Pacific is to examine a possibility for lithological contamination to relative paleointensity records. For this purpose, it is necessary to compare paleointensity records from sediments that belong to different oceanographic regimes and have different magnetic properties.

Our strategy for selecting coring sites is as follows. Water depth of at least one site should be much shallower than the carbonate compensation depth (CCD), which is estimated to be 4500 to

5000m in this region, to enable dating of sediments using the oxygen isotope stratigraphy. The age of the seafloor should be older than 10 Ma, because the purpose of the IODP proposal is to clarify geomagnetic field variations during the last ca. 10 m.y. The sediments in a relatively oxidized environment with medium deposition rates of about 10 to 40 m/m.y. are preferable, because sediments covering the last 5 to 20 m.y. can be obtained by the advanced piston corer (APC) of IODP that can penetrate about 200m in general, and time resolution is enough for discussing relation with the Milankovitch orbital parameters. Sediments with a very high deposition rate is not preferable because such sediments usually occur under a high biological productivity area and are anoxic due to a large supply of organic carbon. Dissolution of magnetic minerals may occur in anoxic sediments, which are not suitable for paleomagnetism. The southeast Pacific is the least surveyed region in the world ocean, and thus information available for site selection is scarce. We utilized information on ocean productivity and the sediment thickness map provided by the U.S. National Geophysical Data Center (NGDC).

2-3-2 Site survey: bathymetry and sub-bottom profiling

To find locations suitable for piston coring, bathymetry and sub-bottom profiling was conducted using a SeaBeam 2112 multi-narrow-beam echo-sounder system with sub-bottom profiler of 4 kHz. Bathymetry and sub-bottom profiling were also conducted during single-channel seismic reflection profiling after piston coring. Bathymetric maps and sub-bottom profiles around each coring site are shown in Fig. 2-3-2-1 through 2-3-2-9.

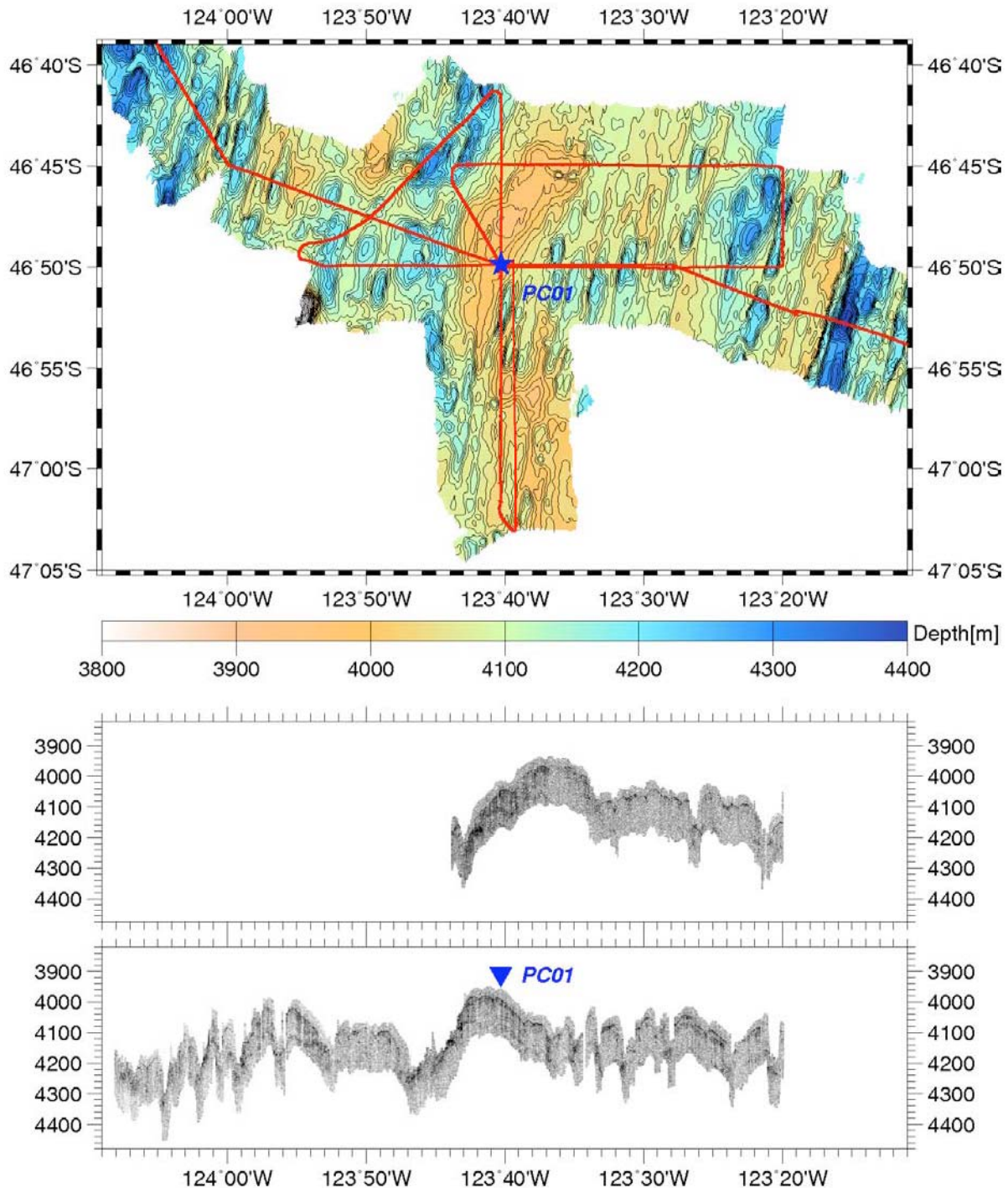


Figure 2-3-2-1. Bathymetric map with survey lines, and sub-bottom profiles around the site PC01.

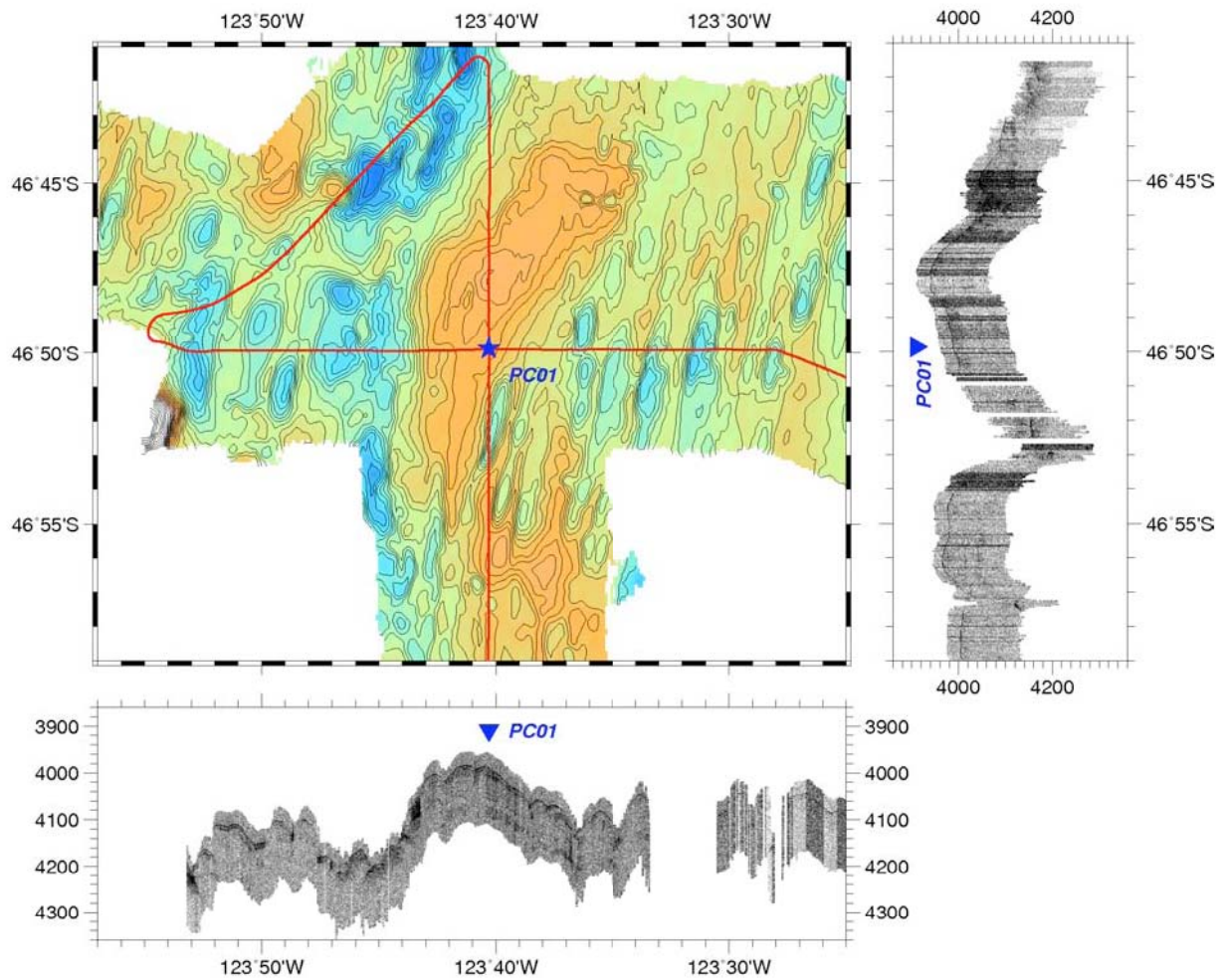


Figure 2-3-2-2. Bathymetric map and sub-bottom profiles crossing site PC01 taken during single-channel seismic reflection survey.

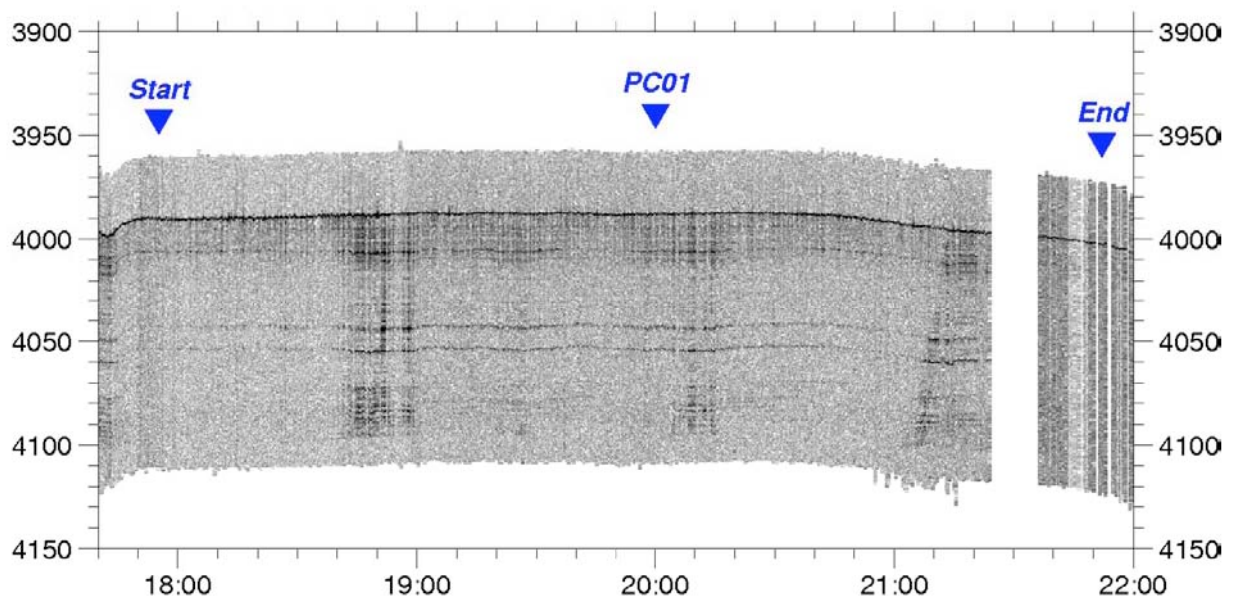


Figure 2-3-2-3. Sub-bottom profile during piston-coring operation.

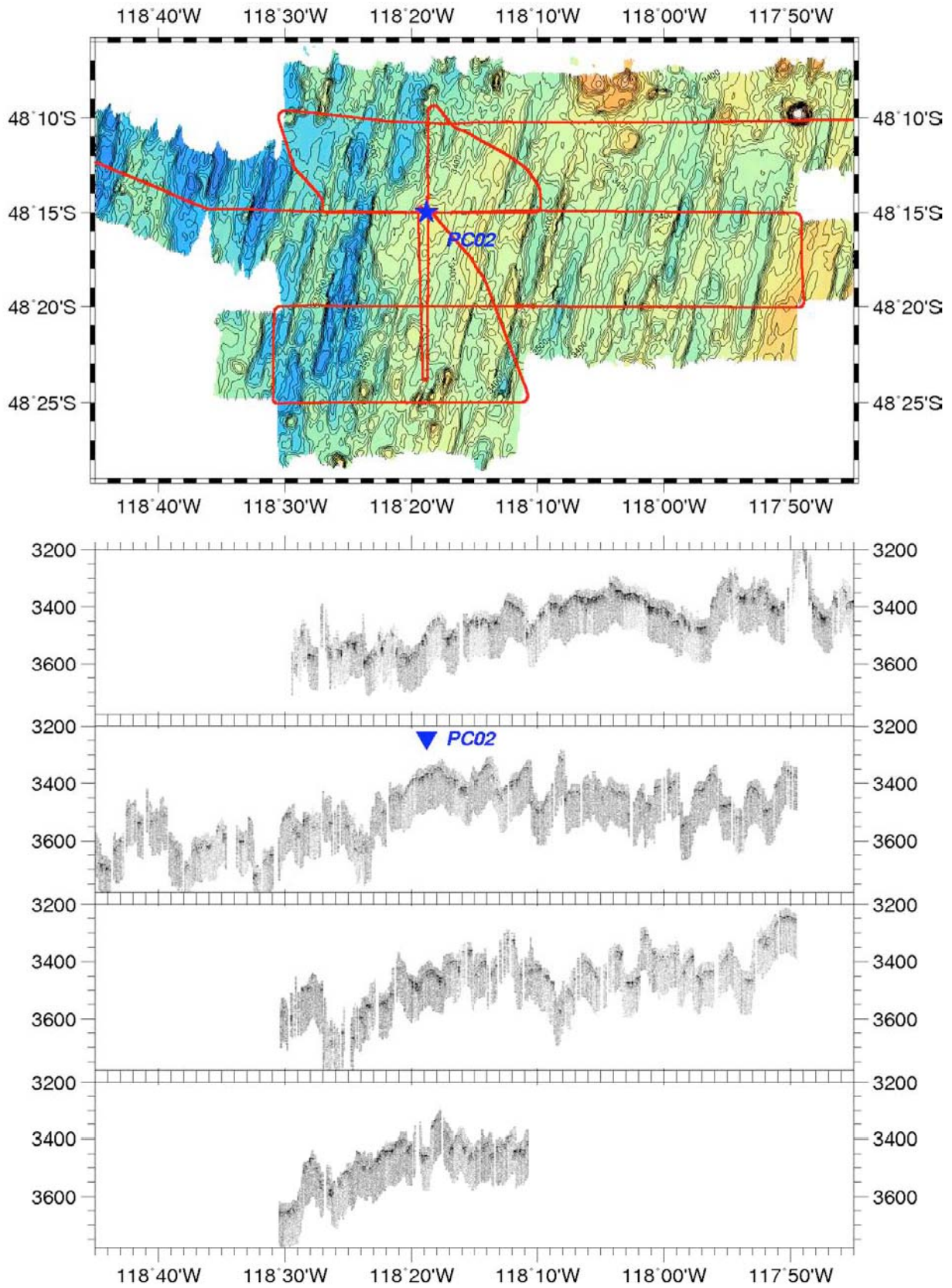


Figure 2-3-2-4. Bathymetric map with survey lines, and sub-bottom profiles around the site PC02.

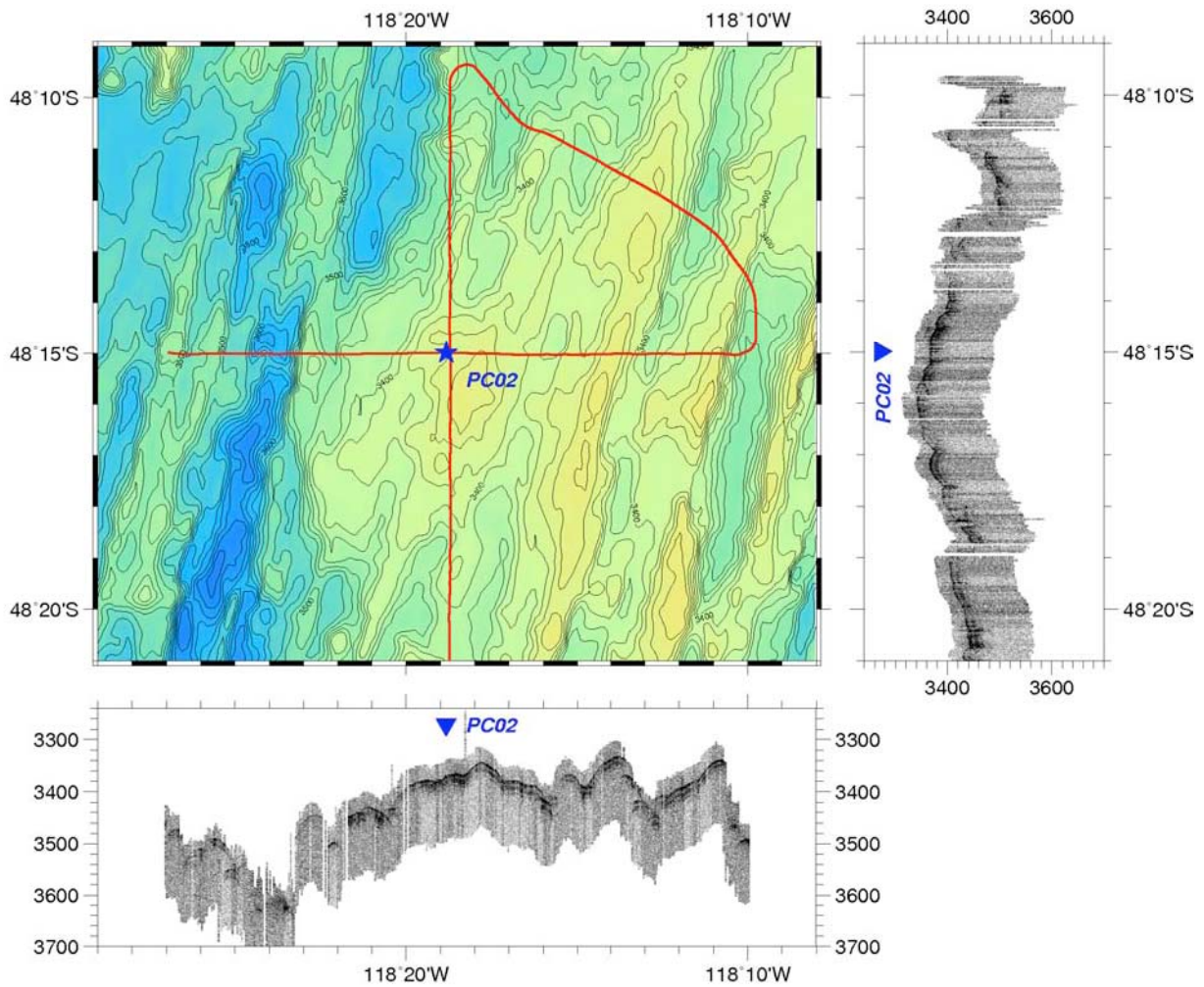


Figure 2-3-2-5. Bathymetric map and sub-bottom profiles crossing site PC02 taken during single-channel seismic reflection survey.

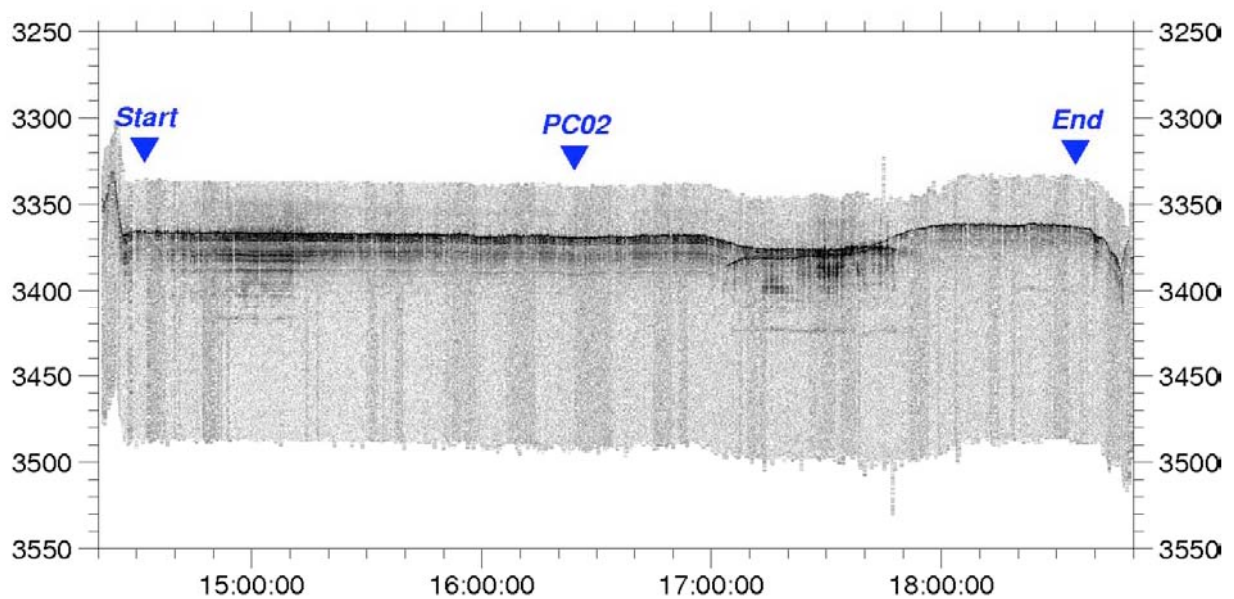


Figure 2-3-2-6. Bathymetric map with survey lines, and sub-bottom profiles around the site PC02.

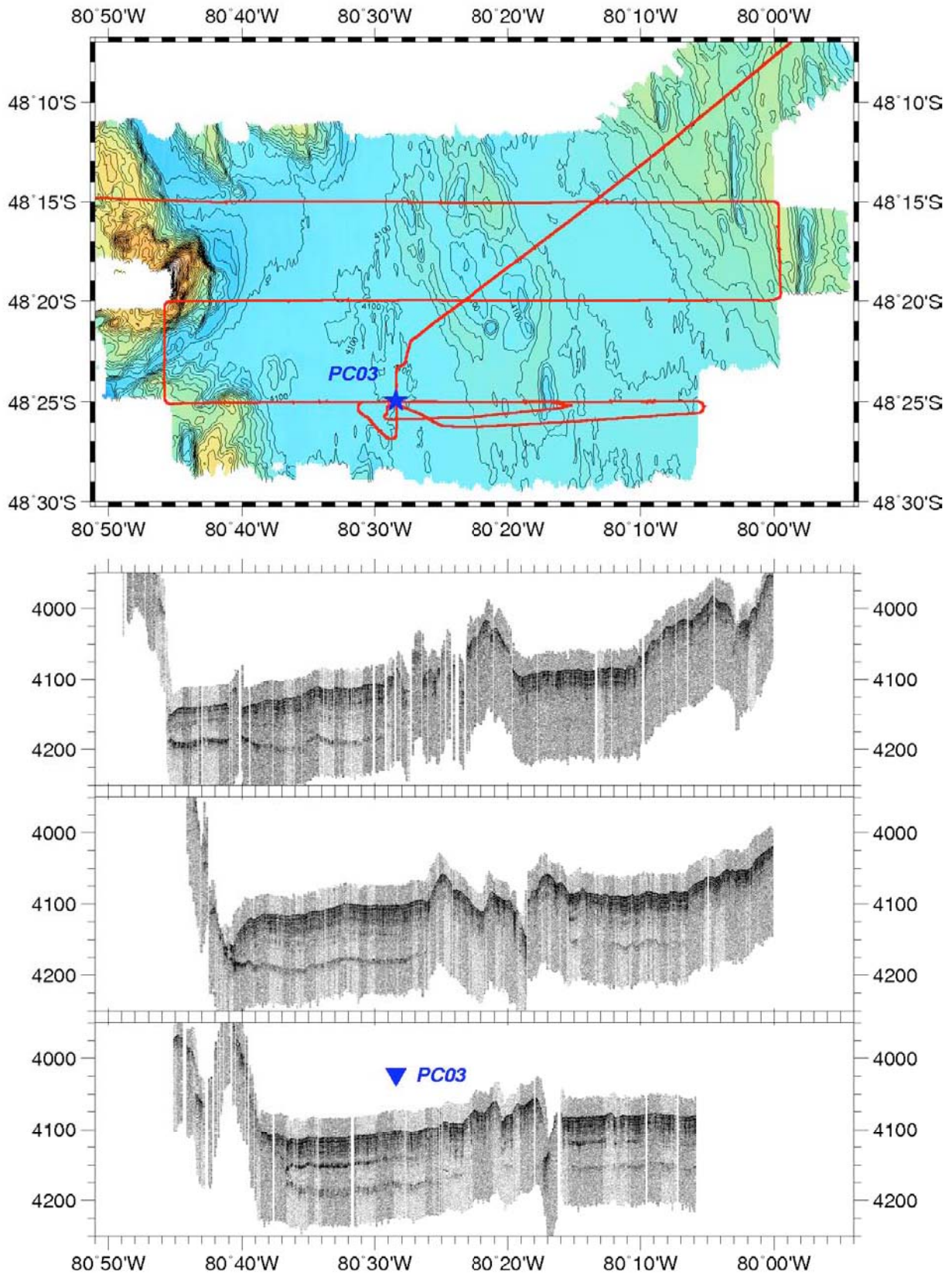


Figure 2-3-2-7. Bathymetric map with survey lines, and sub-bottom profiles around the site PC03.

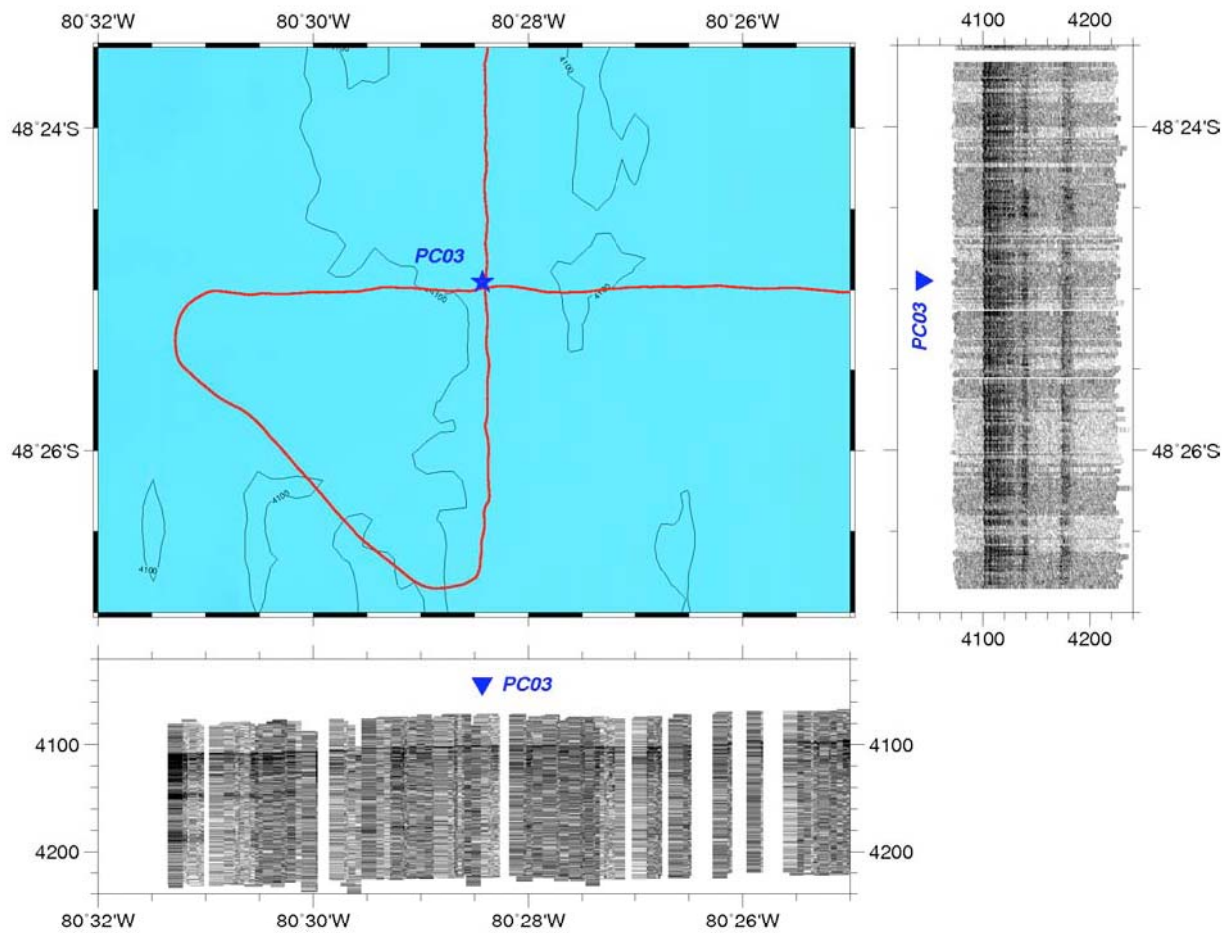


Figure 2-3-2-8. Bathymetric map and sub-bottom profiles crossing site PC03 taken during single-channel seismic reflection survey.

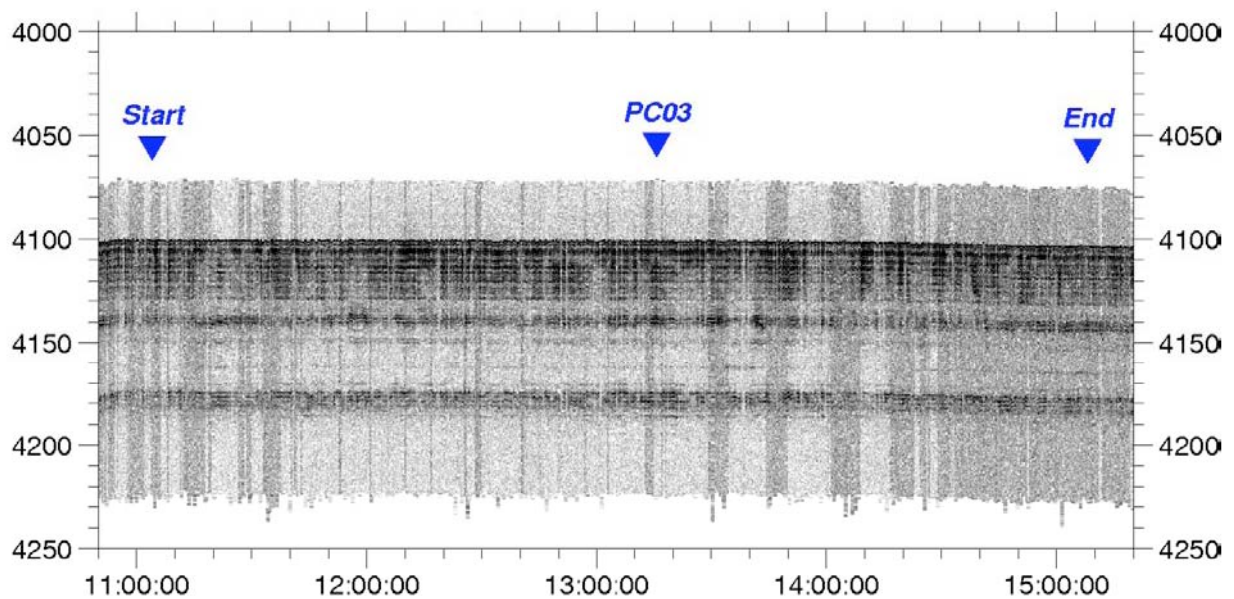
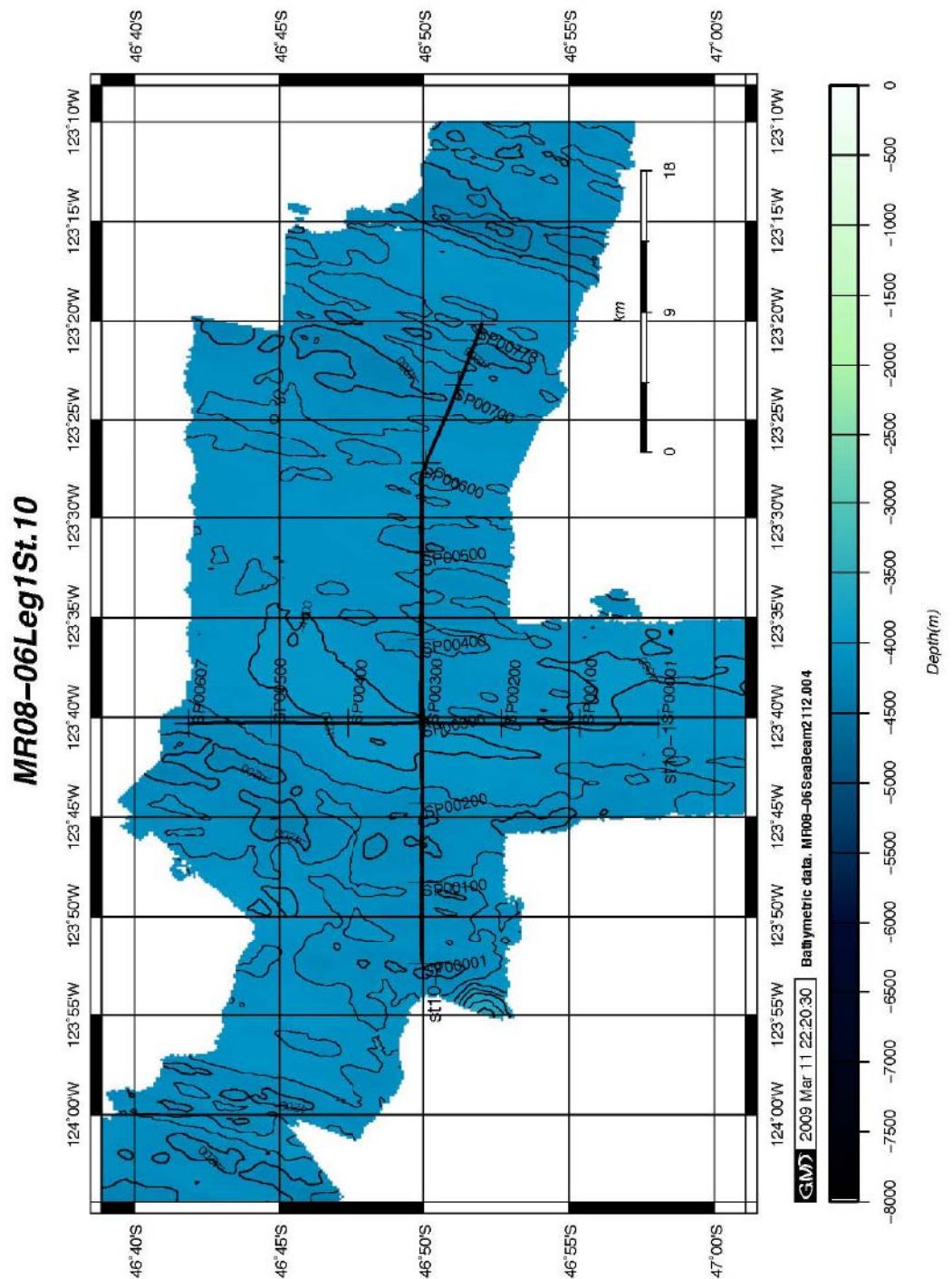


Figure 2-3-2-9. Bathymetric map with survey lines, and sub-bottom profiles around the site PC03.

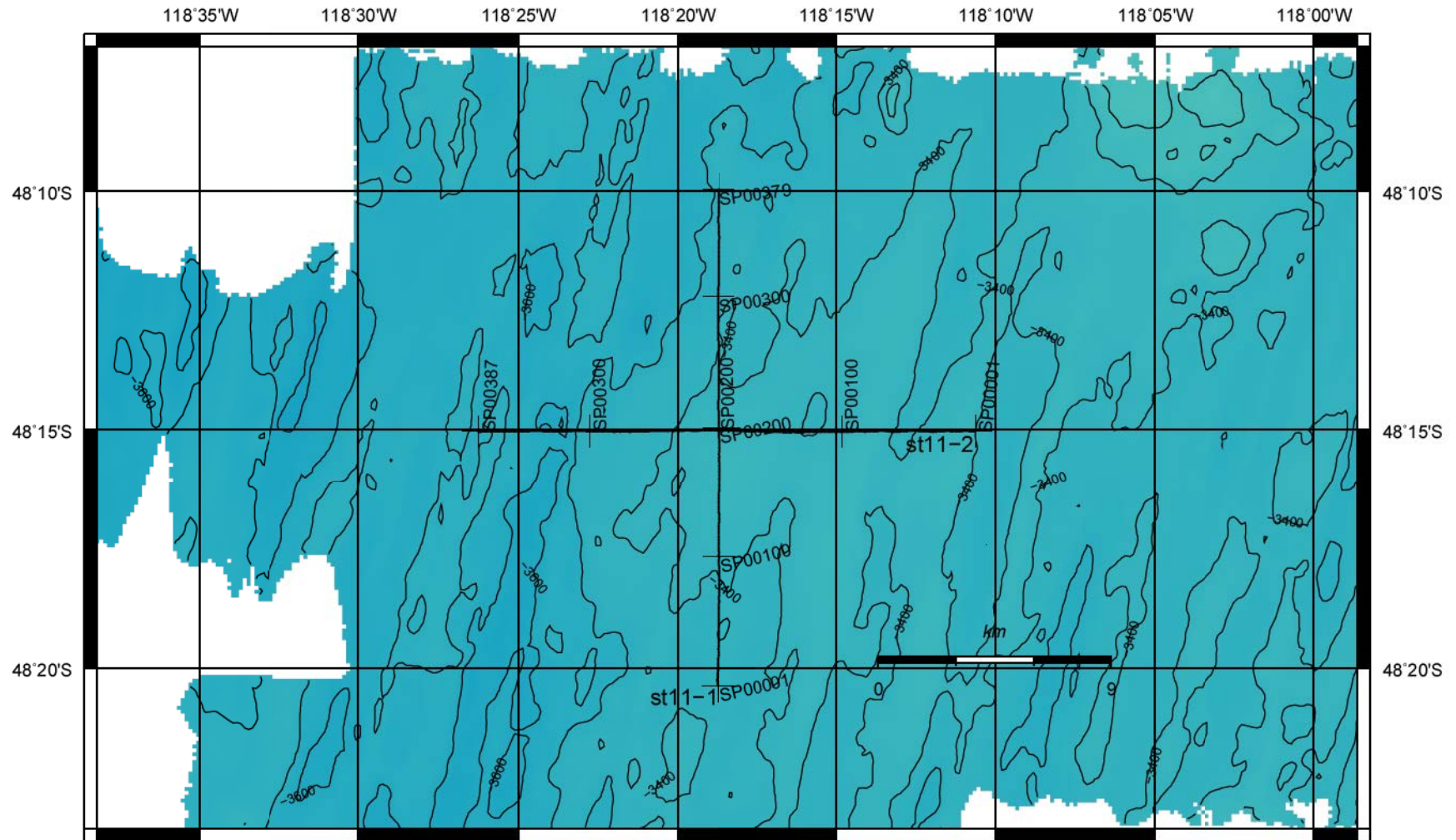
2-3-3. Single channel seismic survey

Next three maps show the cross-shape survey lines on the three PC stations. Stations 10a and 10b are shown as St. 10 and St. 11 on the map titles, respectively. The stations 10a, 10b and 14 correspond to PC 01, PC 02 and PC 03 sites in this section of paleomagnetism in the southeast Pacific.

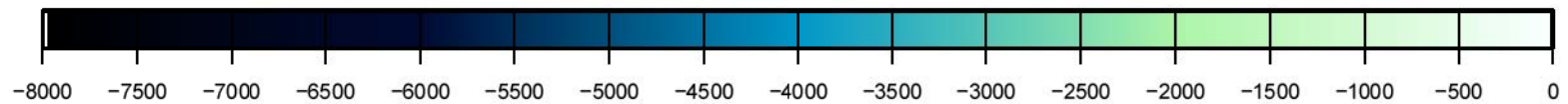
Details of the single channel seismic survey are section 3-2. "Single channel seismic surveys of MR08-06 Leg1b" and Appendix data.



MR08-06Leg1St.11

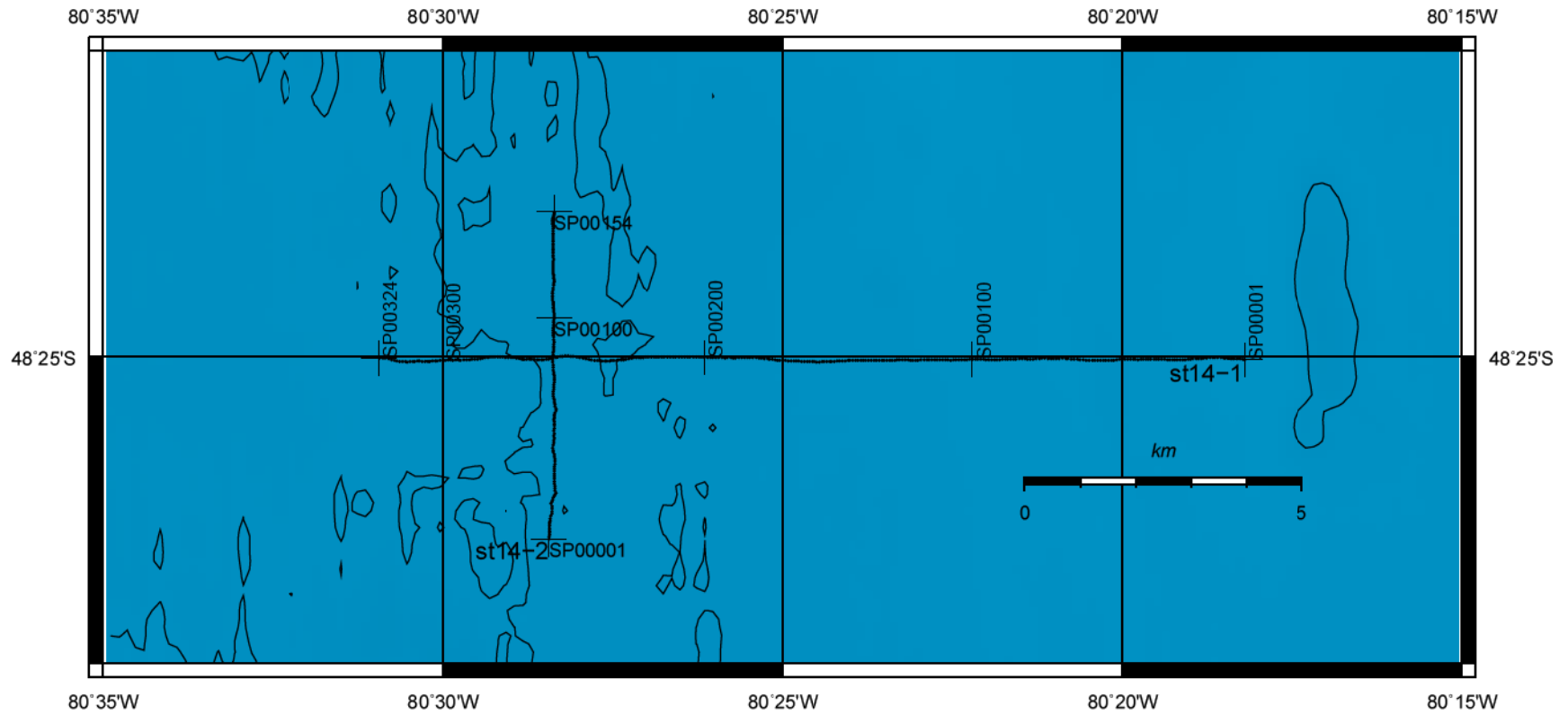


GM 2009 Mar 11 22:19:58 Bathymetric data. MR08-06SeaBeam2112.004

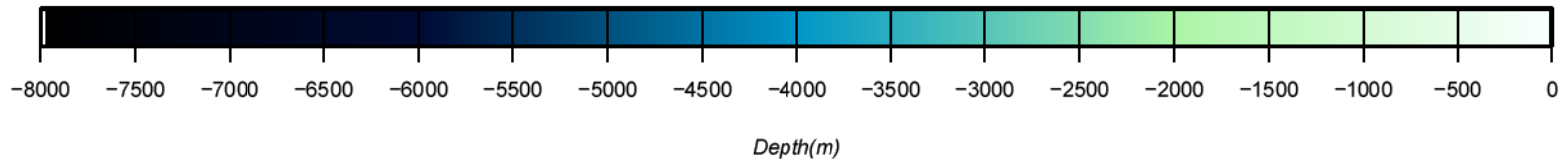


Depth(m)

MR08-06Leg1St.14



GM 2009 Mar 14 09:14:55 Bathymetric data. MR08-06SeaBeam2112.004



2-3-4 Sediment coring

Sediment cores were taken at three sites in the southeast Pacific (Fig. 2-3-4-1). A piston corer having a core barrel of 20m long without core liner was used. Core PC01 (Station 10a) and PC02 (Station 10b) locate on the western flank of the East Pacific Rise, and core PC03 (Station 14) locates west of the outer rise of the Chile trench. Position and water depth of each coring site are summarized in Table 2-3-4-1. The ages of the seafloor at sites of PC01, PC02, and PC03 are about 12, 25, and 15 Ma, respectively.

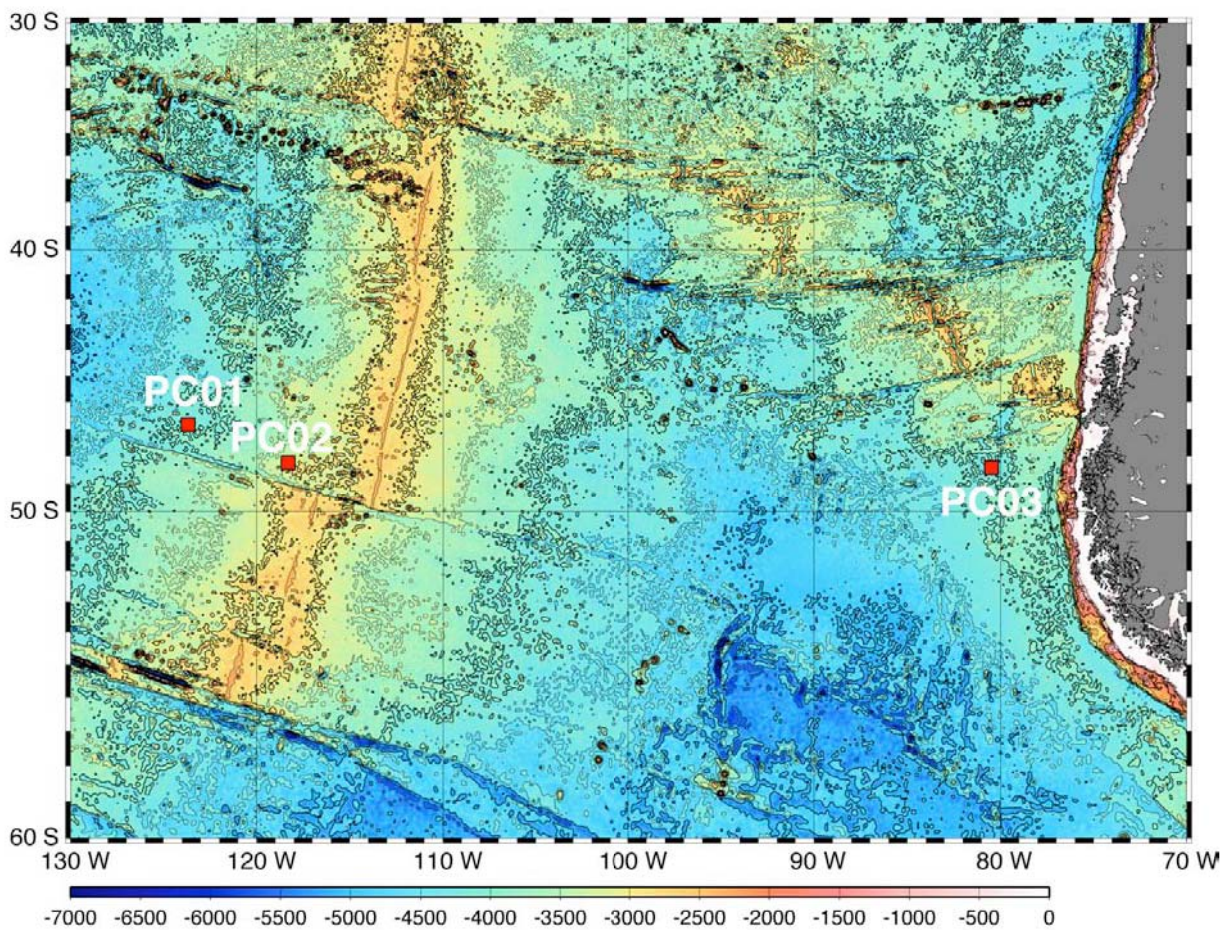


Figure 2-3-4-1. Sites of piston coring.

Table 2-3-4-1. Summary of piston cores.

Core ID	Date	Lat.	Lon.	Depth (m)	Core length (m)
PC01	2009.2.18	46°49.93'S	123°40.30'W	3,983	10.67
PC02	2009.2.20	48°15.02'S	118°18.72'W	3,358	6.26
PC03	2009.2.26	48°24.95'S	80°28.43'W	4,049	19.66

Operation of piston coring

The piston corer consists of the head, barrels, piston, catcher, bit, trigger, and pilot core sampler (Figure 2-3-4-2). Duralumin pipes are used for the barrel to avoid imparting artificial magnetization to sediments. A total of 20m-long duralumin pipe is composed of four 5m segments that are combined one another by stainless joint sleeves. We used a Ewing type corer for a pilot core sampler.

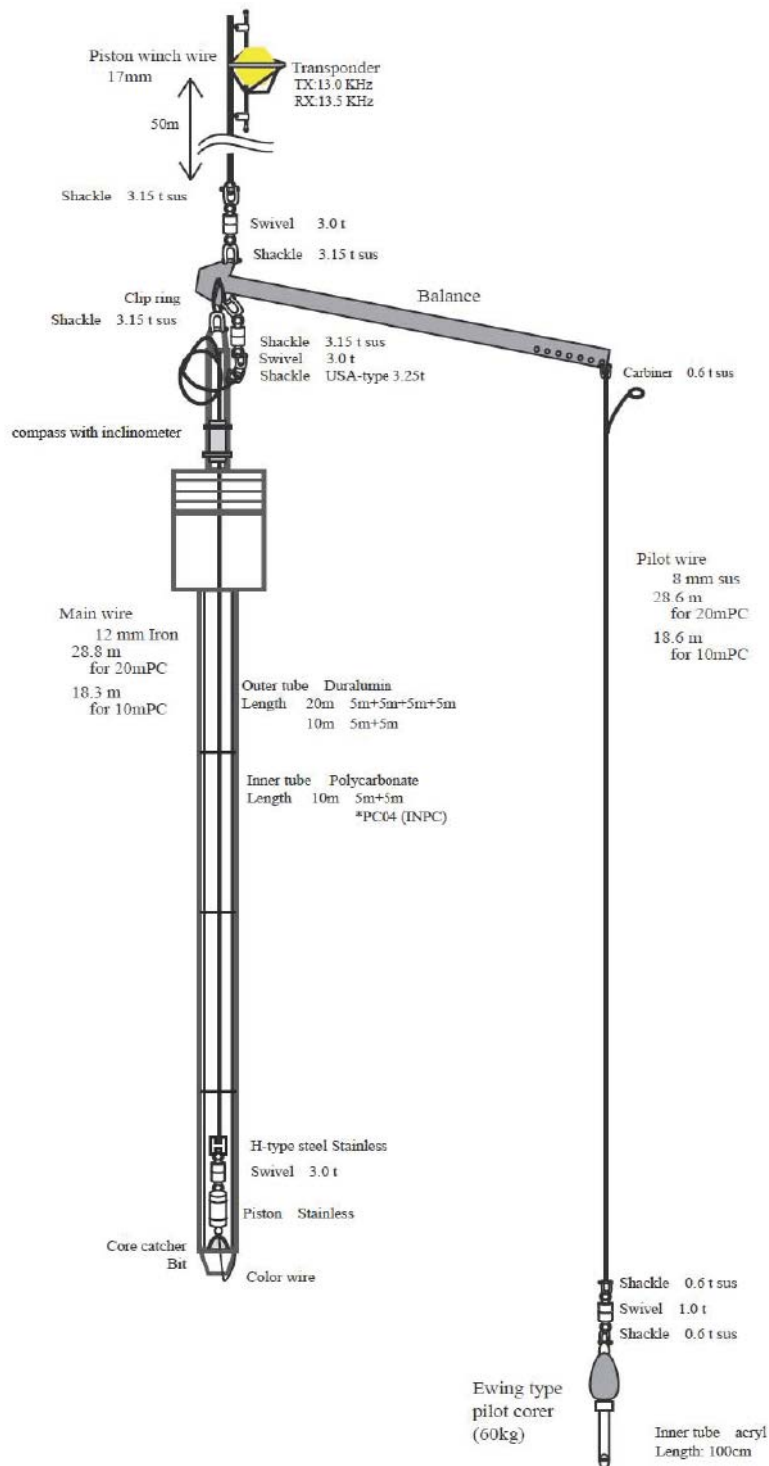


Figure 2-3-4-2. Piston corer system.

When we started lowering the piston corer, a speed of wire out was set to be 0.2 m/s, and then gradually increased to the maximum of 1.0 m/s. The corer was stopped at a depth about 100 m above the sea floor for 3-5 minutes to reduce any pendulum motion of the system. After the corer was stabilized, the wire was stored out at a speed of 0.3 m/s, and we carefully watched a tension meter. When the pilot corer touched the bottom and the trigger was released, wire tension abruptly decreases by the loss of the corer weight. Immediately after confirmation that the corer hit the bottom, wire out was stopped and rewinding of the wire was started at a dead slow speed (~0.3m/s), until the tension gauge indicated that the corer was lifted off the bottom. After leaving the bottom, winch wire was wound in at the maximum speed.

Duralumin pipes were cut into sections of 1 m long each with a band saw, and then sediments were extruded into half round PVC lining using a equipment with a hydraulic piston. Each section was split longitudinally into a working and an archive half by a stainless wire. For both halves, white pins were inserted along the edge of the core surface at intervals of 2cm, and blue pins at interval of 10cm.

Onboard measurements and sampling procedure

For archive halves, we carried out color reflectance measurements and took photographs. Color reflectance was measured using a Minolta Photospectrometer CM-2002. The color was measured at 2 cm intervals through crystal clear polyethylene wrap. The color reflectance data are displayed as the color parameters of L*, a*, and b* (L*: black and white, a*: red and green, b*: yellow and blue). Please refer Appendix 2-3-4-1 for details of the color reflectance measurement method. Photographs were taken using a Nikon single-lens reflex digital camera (Nikon D1x). When using the digital camera, shutter speed was between 1/8 and 1/30, F value was between 8 and 11, exposure value was 0.7, 0 and -0.7, and sensitivity ISO 125 was used. Measurements of magnetic susceptibility, gamma-ray density, and P-wave velocity using a multi-senor core logger (MSCL) will be conducted on shore because the MSCL onboard was out of order. Samples for soft X-ray images will also taken on shore after MSCL measurements.

For working halves, we carried out visual core description and sub-sampling using plastic cubes of 7 cm³ each in two rows (one for paleomagnetism, the other for geochemistry and/or microfossils). For core PC03, remaining sediments were filled into plastic bags at 2 cm intervals for analyses of microfossils.

Onboard results: Visual core description, photograph, and color reflectance

Lithology, photograph, and color reflectance of each core are summarized in Figures 2-3-4-3

through 2-3-4-6. Visual core description sheets and photographs are attached in Appendix 2-3-4-2 and 2-3-4-3. The followings are brief description of each core.

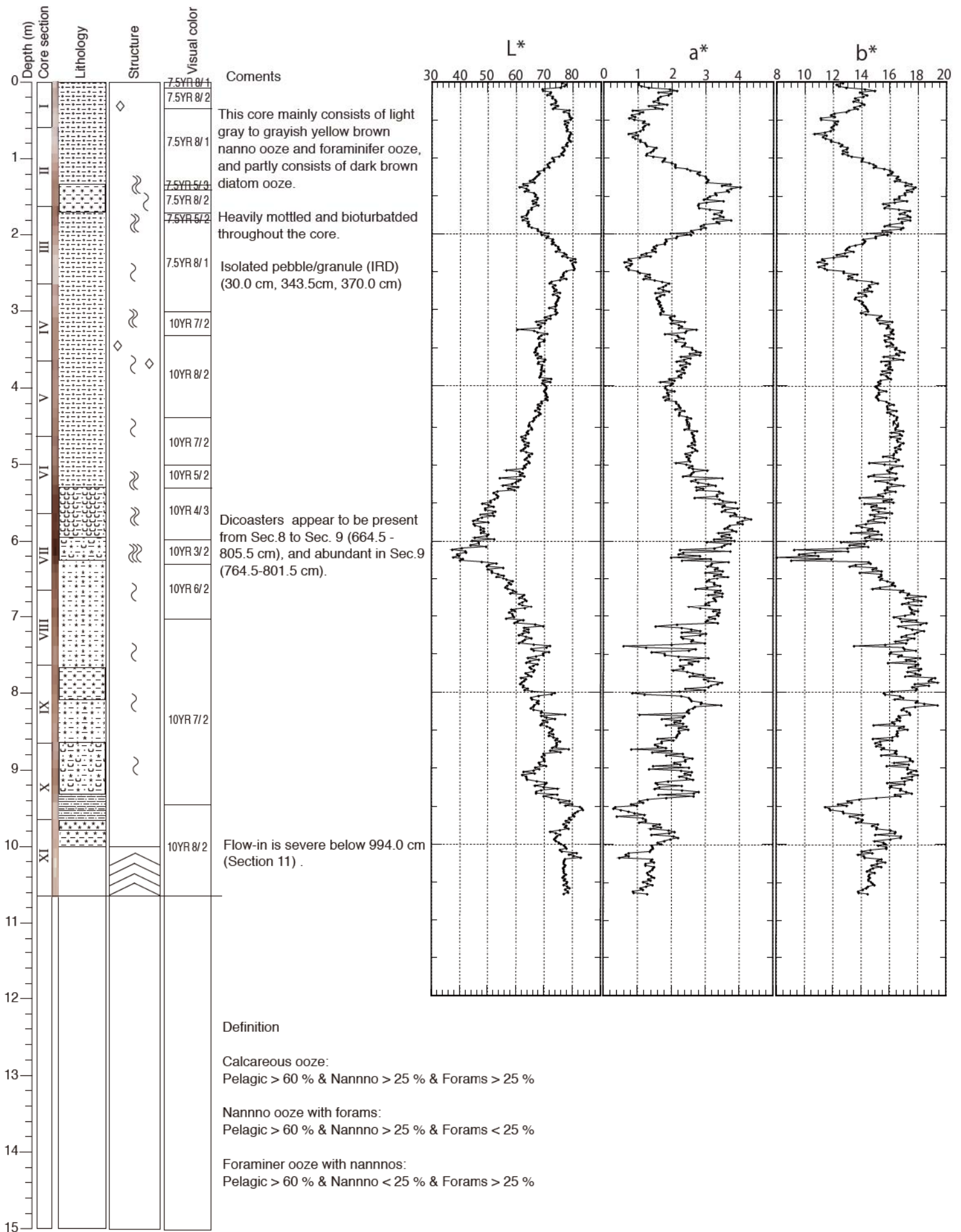
Core PC01 mainly consists of light-gray to grayish-yellow-brown nannofossil ooze and foraminifer ooze, and is partly composed of dark-brown diatom ooze. The sediments are heavily mottled and bioturbated throughout the core. Isolated pebbles and granules of probably IRD in origin occur at 30, 343.5, and 370 cm in depth. Dicoasters appear to be present in sections 8 and 9 (664.5 - 805.5 cm), and abundant in section 9 (764.5 -801.5 cm).

Core PC02 is composed of light-gray nannofossil ooze and foraminifer ooze. Mottles and bioturbation occur throughout the core. The color is lighter in 383-476 cm, which correspond to nannofossil ooze. In this part, foraminifer is relatively rare and/or not preserved well. Isolated pebbles and granules of probably IRD in origin occur at 63.5, 147, and 534.5 cm in depth. Fragments of foraminifer coated with possibly Mn oxides are scattered throughout most of the sections.

Core PC03 consists of silty clay, diatom silty clay, and calcareous silty clay. The color is light gray to grayish olive, and darker in the deeper part of the core in general. Calcareous silty clay tends to have lighter colors. The sediments are lightly to heavily mottled and bioturbated. Concentration of Mn oxides is recognized in parts of the core. Color and extent of bioturbation show cyclic changes. Thin semi-consolidated layers occur in the deeper part of the core.

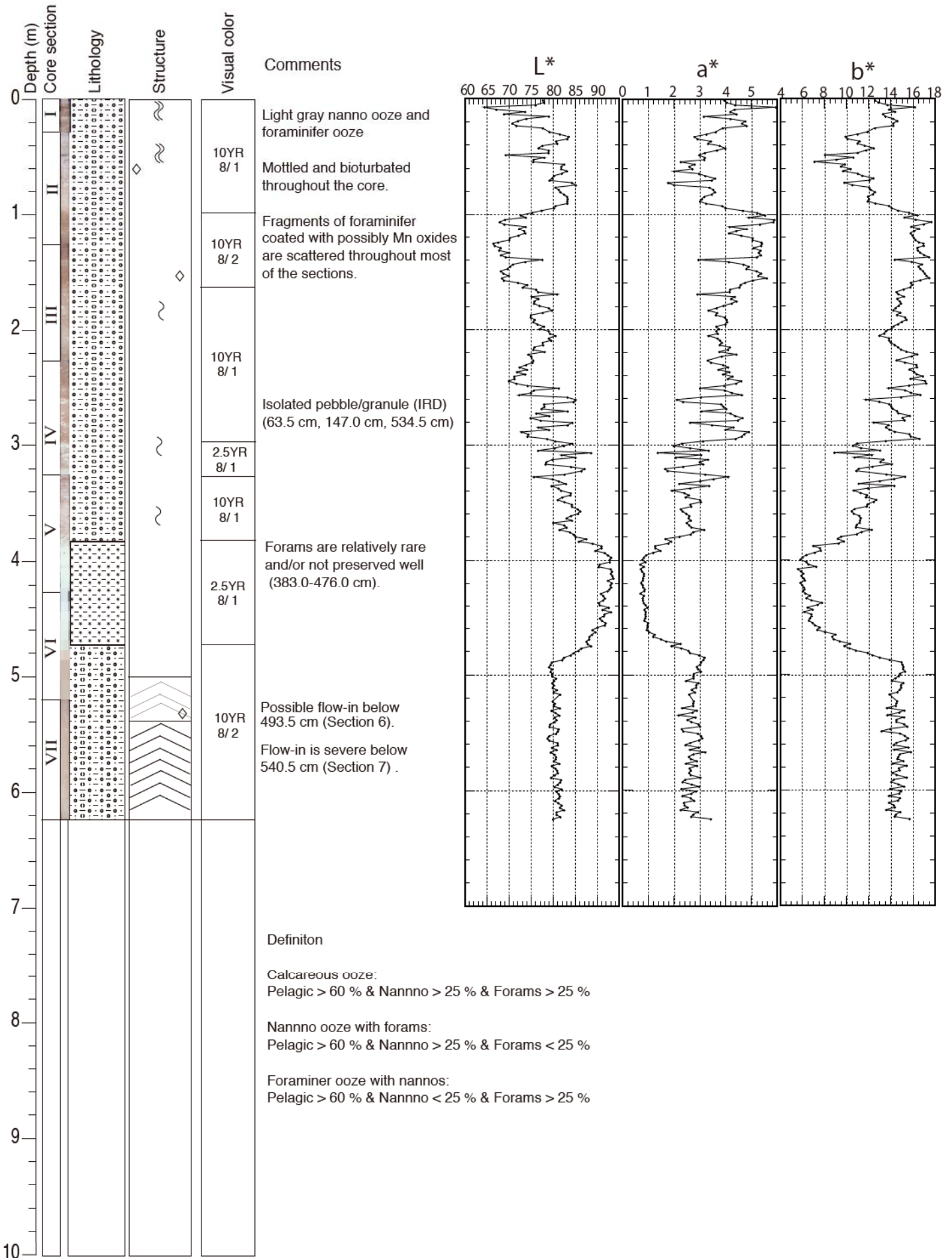
SORA

Core: MR08-06 PC01



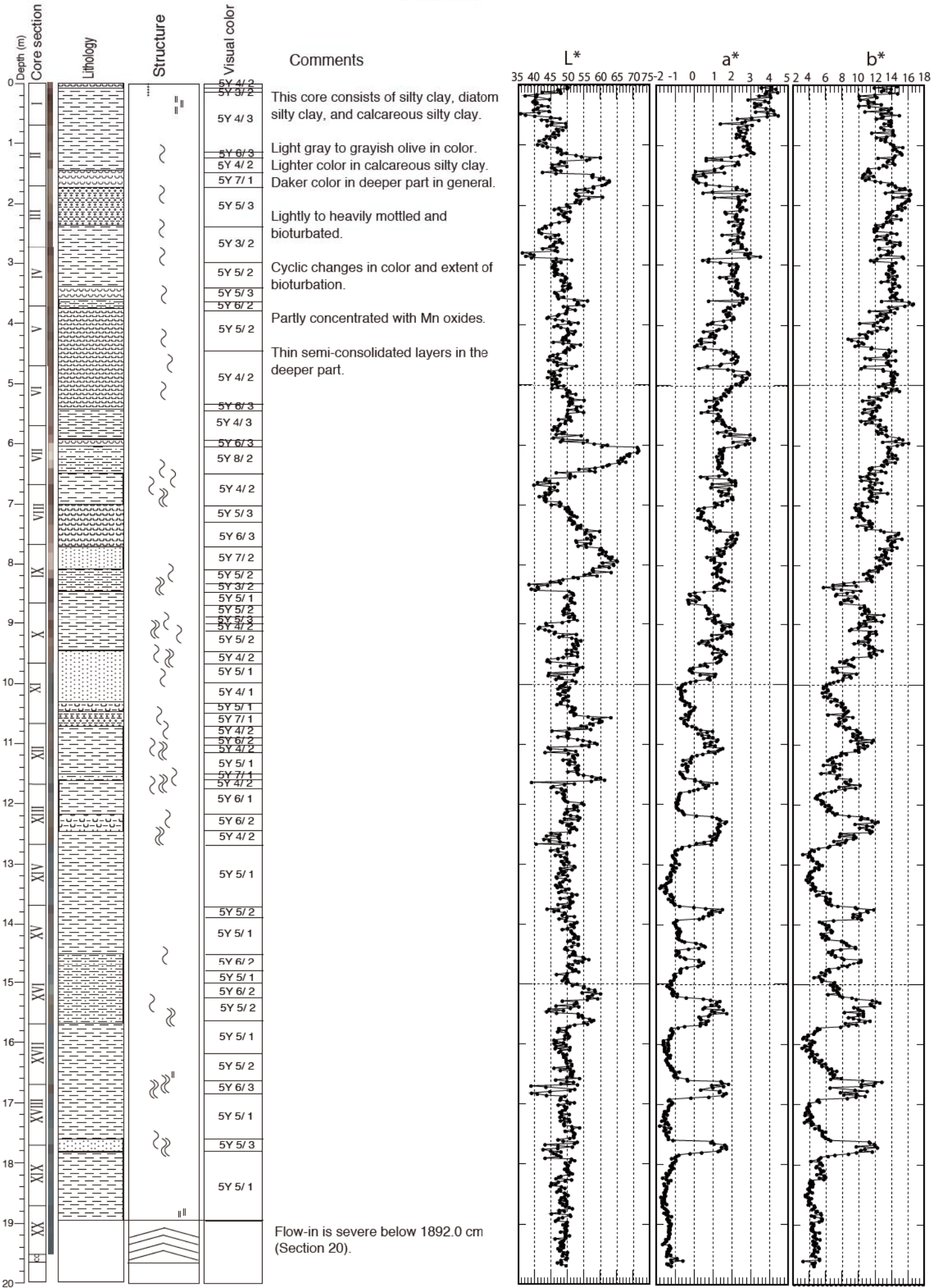
SORA

Core: MR08-06 PC02



SORA

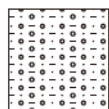
Core: MR08-06 PC03



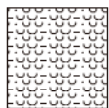
Legend for Core Description

Lithology

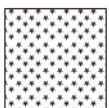
PC01, PC02



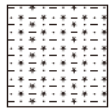
Calcareous ooze



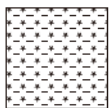
Calcareous ooze with diatoms



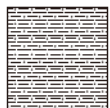
Nannofossil ooze



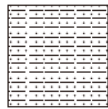
Nannofossil ooze with diatoms



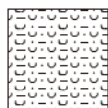
Nannofossil ooze with forams



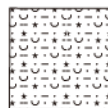
Nannofossil ooze with forams & diatoms



Foraminifer ooze with nannos

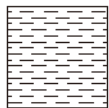


Foraminifer ooze with diatoms

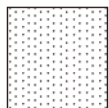


Diatom ooze with forams & nannos

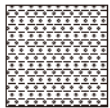
PC03



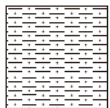
Silty clay



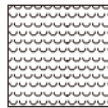
Nannofossil silty clay



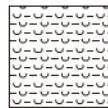
Foraminifer silty clay



Calcareous silty clay



Diatom silty clay



Silicious silty clay

Structure and Drilling Disturbance



Bioturbation



Heavy bioturbation



Disturbed



Isolated pebble/granule



Soupy



Flow-in

2-4. Chile Triple Junction

2-4-1. Bathymetry and observation stations at Chile TJ

N. Abe & GODI

Figs 2-4-1 shows bathymetrical map around Chile triple junction, which taken by our surveys during MR08-06 Leg1b cruise. It is noteworthy that axial valleys on the map are flat on the bottom. The sedimentary rate in this area is assumed quite fast. SCS profiles show the thick sediment layers on the survey lines in this area (See Appendix data).

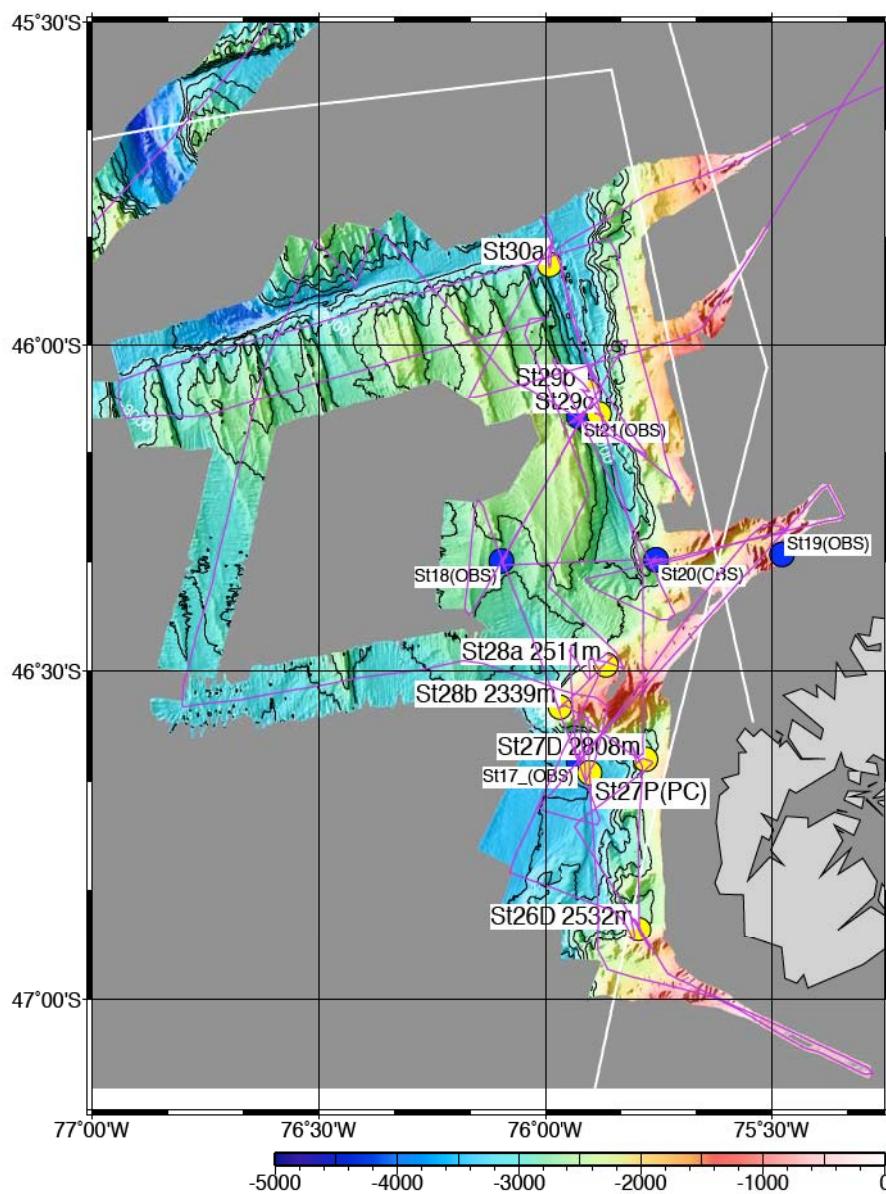


Fig. 2-4-1 Bathymetrical map at Chile Triple Junction with position of observation stations.

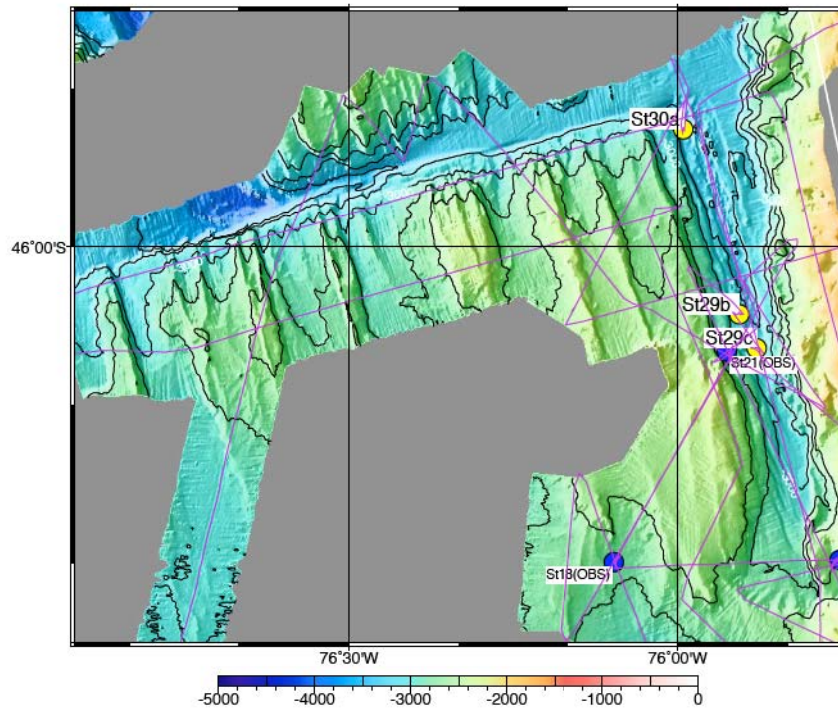


Fig. 2-4-2: Close up bathymetrical map on a fracture zone between segment 1 and 2 of Chile ridge.

2-4-3 Ocean bottom seismic observation

H. Sugioka, A. Ito, T. Isse, H. Iwamori, M. Shinohara

Instruments

The long-term ocean bottom seismometer (LTOBS) was developed at the Earthquake Research Institute (ERI) of the University of Tokyo. A three-component 1-Hz sensor (LE-3Dlite by Lennartz co ltd in German) is installed to the LTOBS. The active-controlled leveling system adjusts the attitude of the 1-Hz sensor. The digital recorder manages on power on/off and samples seismic signals at 100 Hz using a 20-bit ADC and records the digitized data continuously on the hard disks for one year. The sensor with the active-controlled leveling system, the digital recorder, the acoustic transponder and lithium battery cells are contained in a 50-cm diameter sphere that is made of titanium alloy. The acoustic transponder for LTOBS has the functions of data transmission, interrogation and anchor releasing. The acoustic data transmission works very effectively on a long-term seafloor observation to know the status of the function of the seafloor instruments and to change the observation parameters remotely from a surface ship. The LTOBS is deployed by a free fall from the sea surface and pop up by its buoyancy in the recovery. The anchor is released by a forced electric corrosion of two thin titanium plates after receiving a command of an acoustic transponder from the ship. Appearance of LTOBS is shown in 2-4-3-Figure 1.

Deployment

We deployed the five LTOBSs successfully and operated to start the recording by the acoustic transmission between the transponder and the transducer of the ship bottom in this cruise. The deployments were made so that the sites should be as flat as possible on the basis of the bathymetry data obtained on the real time basis by the sea beam. The LTOBSs were launched from MIRAI with the crane. After launching we communicated with the LTOBS using the transponder and made sure they reached down to the sea floor safely. We located the LTOBSs by measuring the slant length at three points around the launched point. The deployment works are shown in 2-4-3-Figure 2. The deployment locations are shown in 2-4-3-Figure 3 for all and 2-4-3-Figure 4 for each and listed in 2-4-3-Table 1.

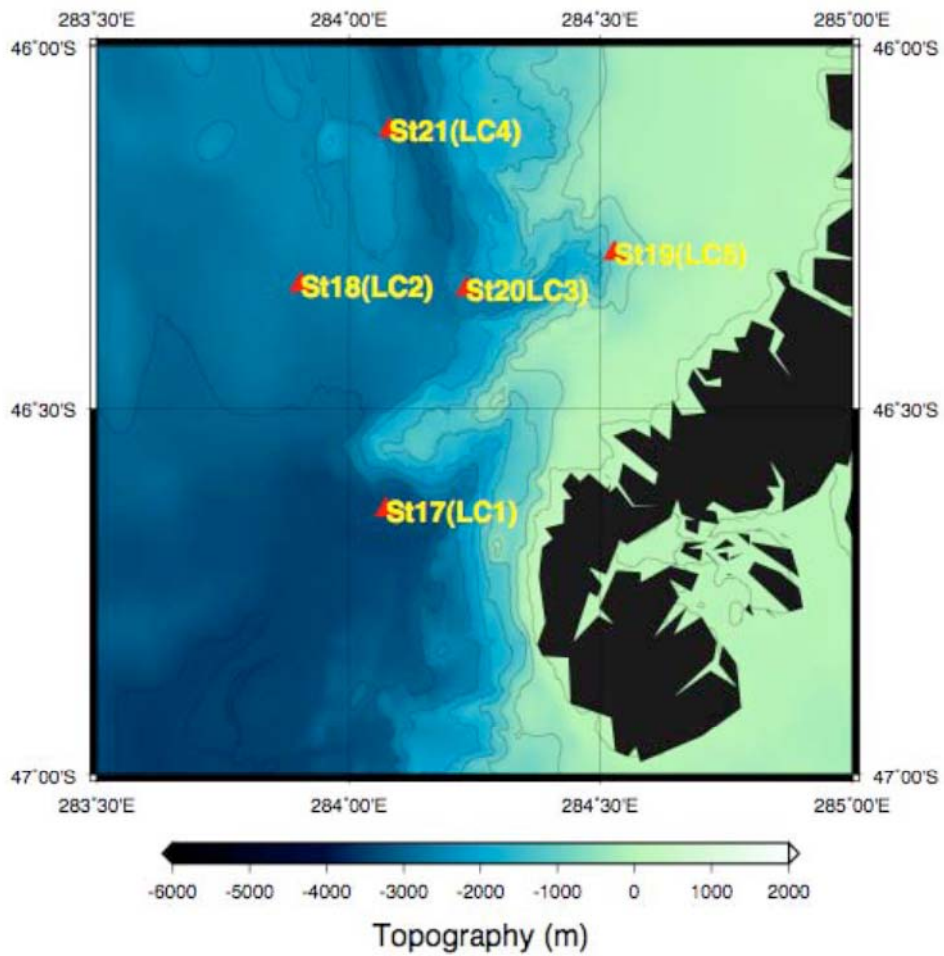
Figures



2-4-3-Fig. 1: Appearance of the LTOBS.

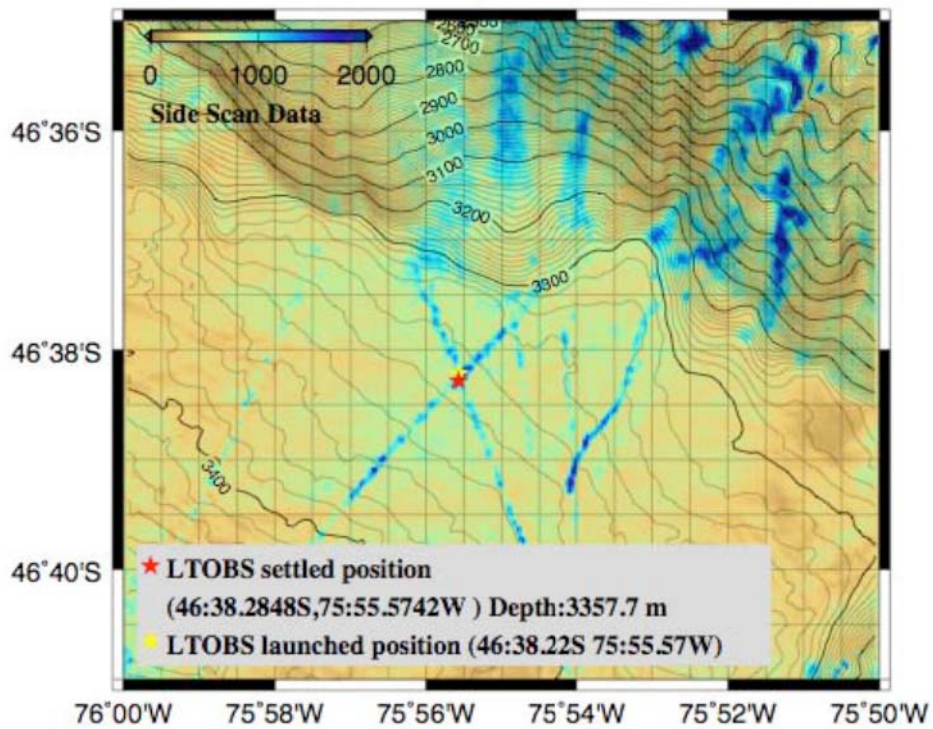


2-4-3-Fig. 2: Deployment work of the LTOBS by the ship crane.

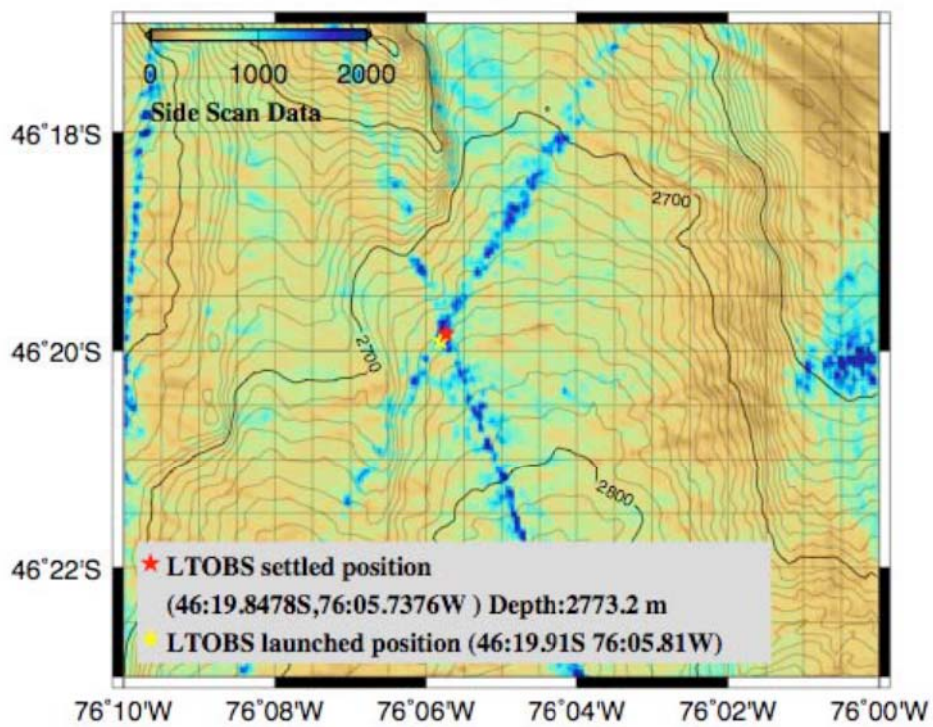


2-4-3-Fig. 3: Distribution of the settled LTOBSs. Background color shows the topography based on the global data of ETOPO2 and the regional data obtained by the Sea Beam survey.

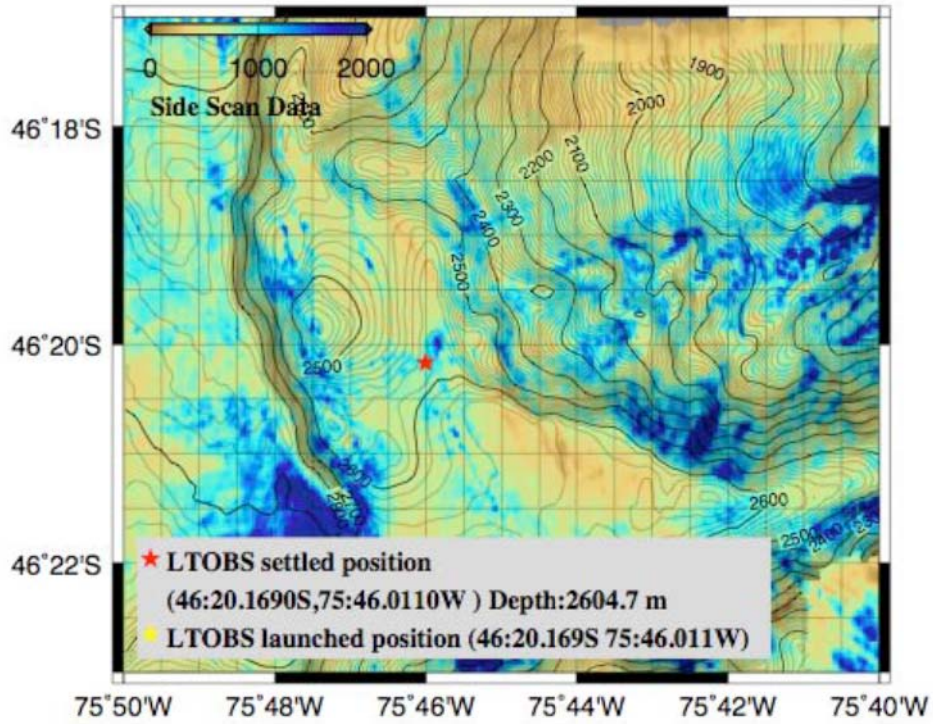
St17 (LC1)



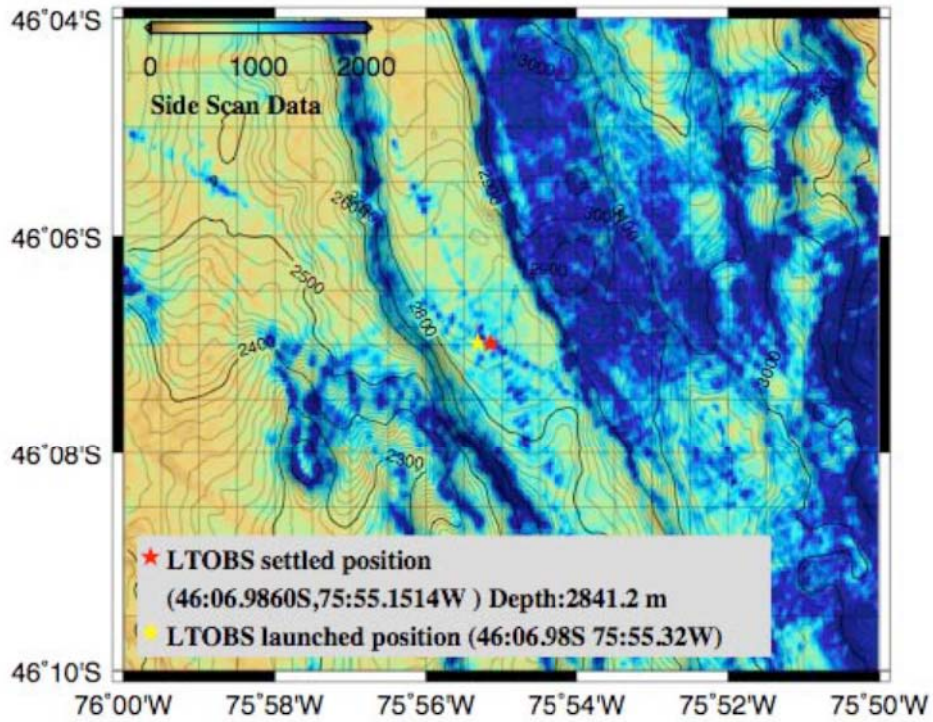
St18 (LC2)

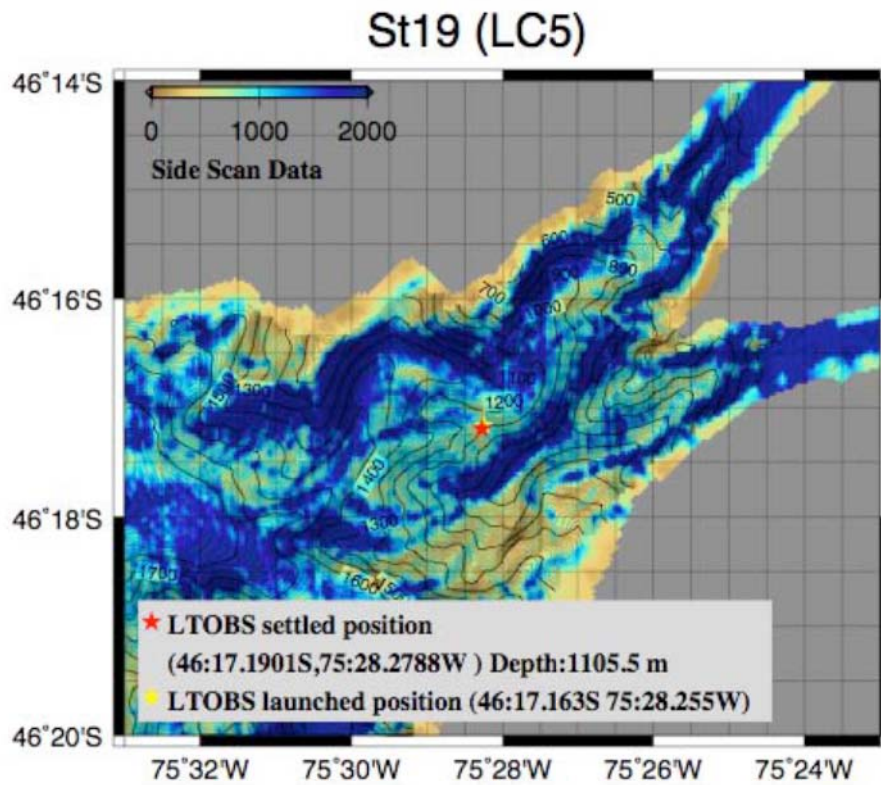


St20 (LC3)



St21 (LC4)





2-4-3-Fig. 4: Locations of the settled LTOBS for St17-21 (LC1-LC5), respectively. Background color shows the intensity of the acoustic reflections from the seafloor by the Side-scan data.

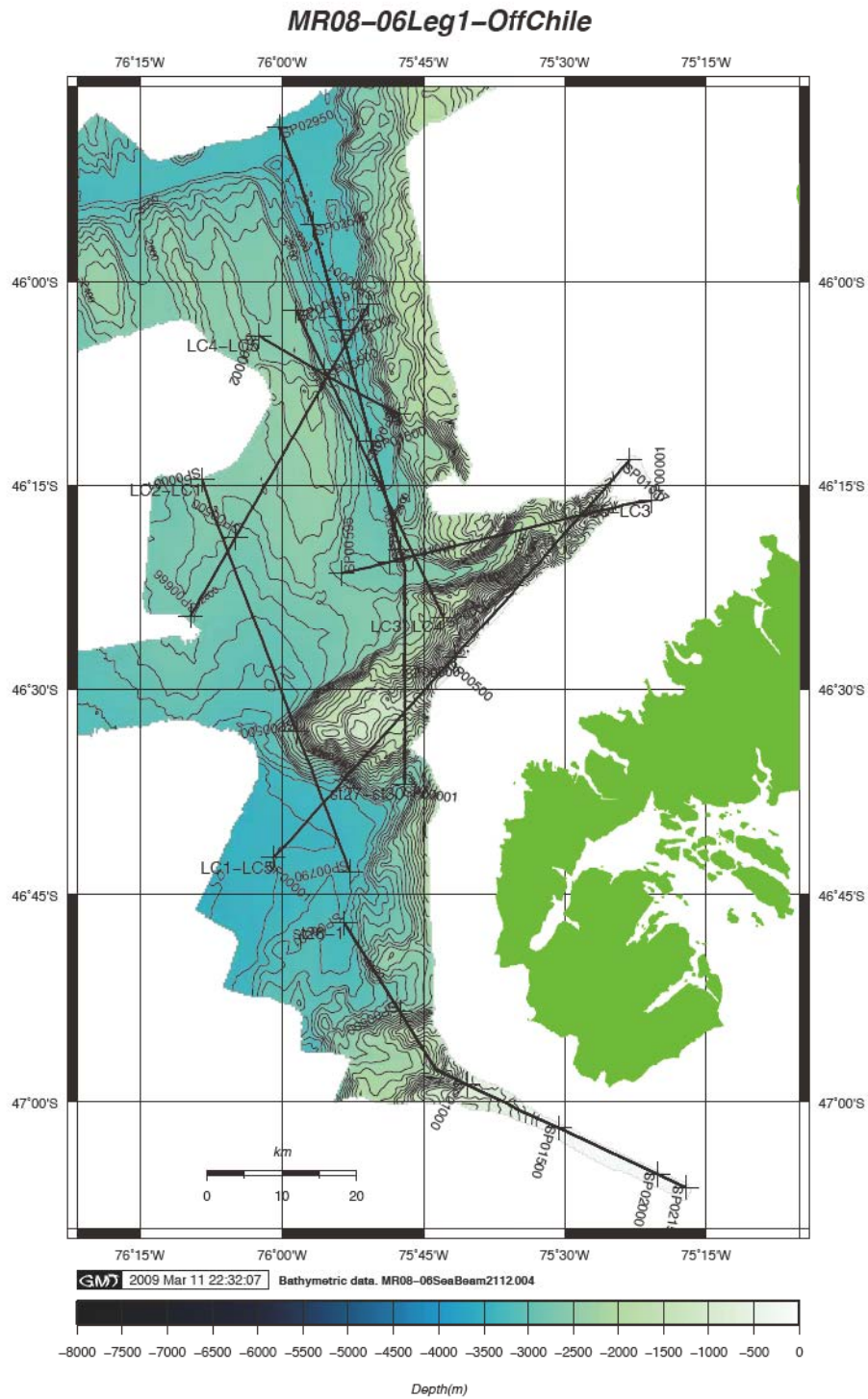
Table

2-4-3-Table 1: List of launching points of the LTOBSs.

Station	Latitude in deg.	Longitude in deg.	Depth in meter
St17	-46.638080	-75.926237	3357.7
St18	-46.330797	-76.095627	2773.2
St19	46.286502	75.471313	1105.5
St20	46.336150	75.766850	2604.7
St21	46.116433	75.919190	2841.2

2-4-4 Single channel seismic survey and air gun shooting in the Chile TJ area

Totally eight survey lines of Single channel seismic were taken in the Chile Triple Junction area. Details of the single channel seismic survey are section 3-2. “Single channel seismic surveys of MR08-06 Leg1b” and Appendix data.



2-4-5 Rock sampling at the Chile Triple Junction (CTJ) area

Chile Triple Junction Study Group (Ryo Anma, Yuji Orihashi, Akihisa Motoki, Natsue Abe, Sung-Hyun Park, Shiki Machida and Andres Veloso)

Objective

The tectonic map around the study area in Figure 2-4-5-1 shows that two oceanic plates, the Nazca plate in the north and Antarctic plate in the south, separated by spreading ridges of the Chile ridge system, subduct beneath the South American plate with convergent rate of 9 cm/yr and 2 cm/yr, respectively. Because NNW-trending central axis of the Chile ridge is oblique to the NS-trending continental margin, three short spreading centers subducted repeatedly almost at the same latitude offshore the Taitao peninsula at 6 ~ 5 Ma, 3 ~ 2.5 Ma and present. At ~6 Ma, emplacement of an ophiolite and contemporaneous granites took place at the western tip of the Taitao Peninsula. Post-Miocene magmatism is widely distributed near the Chile ridge subduction zone, due to partial melting of oceanic crust/subducted sediments. Such partial melting of oceanic crust/subducted sediments may have influence on compositions of the Andean arc volcanism and extra-back arc volcanism widely distributed in Patagonia. The purpose of the dredge sampling in the CTJ area is to collect rocks/sediments that help to understand solid earth recycling processes occurring/occurred due to recent/6 Ma subduction of the Chile Ridge system.

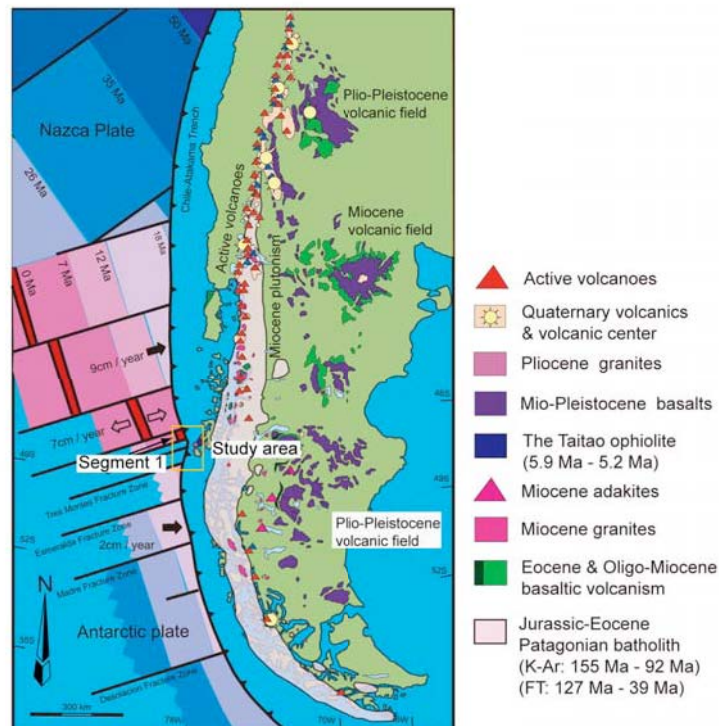


Figure 2-4-5-1: Tectonic map showing distribution of the post-Eocene magmatism around the study area.

The target rocks for dredge operations are 1) MORBs from the Segment 1 of the Chile ridge system, 2) sediments distributed near the ridge subduction zone, and 3) rocks distributed along the western slopes of the tip of the Taitao peninsula (Figure 2-4-5-2).

The dredging of former two aims to obtain compositions of materials that subduct and eventually melt to form arc magmas at deeper part of the ridge subduction zone. Three dredge operations (Table 2-4-5-1) and one rock core operation (Table 2-4-5-2) were conducted for this purpose. Details are described in section 2-4-5-1. MORBs comprise main body of the subducting slab, whereas, though volumetrically small, subducted sediments play an important role in enhancing partial melting of the subducted materials. The CTJ study group will focus on bulk compositions (concentration of major and trace elements, isotopic ratio, etc.) of recovered rocks/sediments to compare with those of the Eocene ~ recent magmatism observed in Patagonia.

The dredges around the Taitao peninsula aim to understand the distribution of submerged extension of the Taitao ophiolite and granites, the products of ~6 Ma ridge subduction event. Four dredge operations were conducted (Table 2-4-5-1). Details are described in section 2-4-5-2.

Visual Rock description

Representative specimens (around 20) were selected from dredged samples for detailed description. We measured size and weight of each selected specimen. The selected specimens were cut into pieces using a rock cutter to expose fresh surface for photographing and for visual rock description. Each selected specimen was sketched and described on a spreadsheet. We followed the IODP-style nomenclature for lithological description of siliciclastic rocks (e.g., Mazzullo et al., 1988). For the description of igneous rocks, we followed terminology recommended by the IUGS (Le Maitre, 2002).

Dredge ID	Date	DB on bottom			DB off bottom			Recovery
		Latitude	Longitude	Depth (m)	Latitude	Longitude	Depth (m)	
D01 (St. 26)	2009.3.2	46°53.46' S	75°47.53' W	2535	46°53.98' S	75°47.07' W	2160	Pyroclastics & sedimentary rocks (299 kg)
D02 (St. 27)	2009.3.2	46°38.05' S	75°46.75' W	2810	46°38.21' S	75°46.00' W	2338	Granite & sedimentary rocks (52 kg)
D03 (St. 29a)	2009.3.4	46°02.46' S	75°53.77' W	3289	46°02.24' S	75°53.84' W	3293	mud (1.5 kg)
D04 (St. 29b)	2009.3.6	46°04.24' S	75°54.36' W	3000	46°04.24' S	75°54.58' W	2968	MORB (37 kg)
D05 (St. 29c)	2009.3.6	46°06.43' S	75°52.81' W	3177	46°06.47' S	75°53.23' W	3047	MORB (14 kg)
D06 (St. 28a)	2009.3.7	46°28.52' S	75°51.92' W	2487	46°28.72' S	75°51.06' W	1857	Sedimentary rocks (194 kg)
D07 (St. 28b)	2009.3.7	46°33.39' S	75°58.00' W	2330	46°33.23' S	75°57.30' W	1783	Pillow breccias & sedimentary rocks (233 kg)

Table 2-4-5-1: Summary of dredge operation.

Core ID	Date	Latitude	Longitude	Depth	Recovery
RC01 (St. 30)	2009.3.8	45°52.52' S	75°59.49' W	3290 m	MORB (ca. 20 g)

Table 2-4-5-2: Summary of rock core RC01 operation.

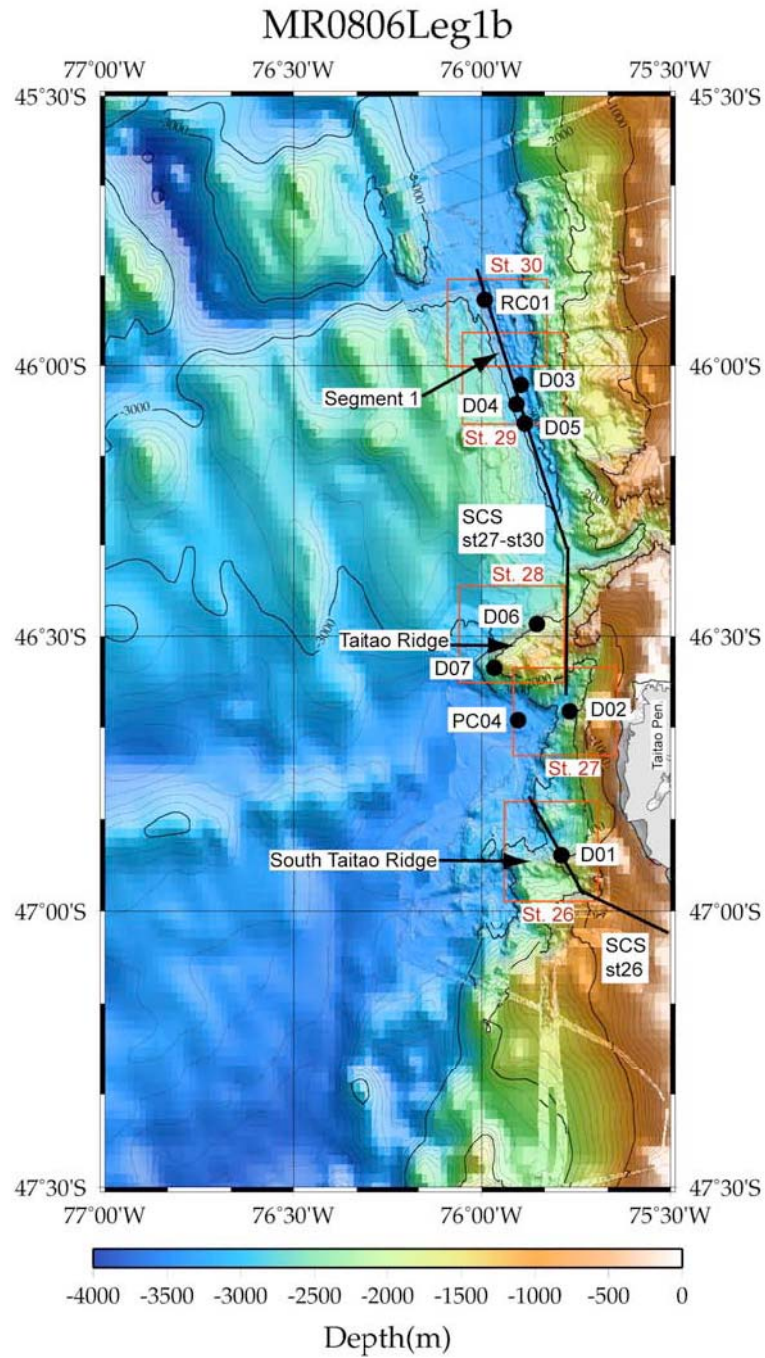


Figure 2-4-5-2: Dredge (D), rock core (RC) and piston core (PC) sites in the Chile Triple Junction area.

2-4-5-1 Rock sampling at the subducting ridge segment (Segment 1)

Yuji Orihashi, Sung-Hyun Park, Shiki Machida, Ryo Anma, Tiago Jalowitzki and Rodrigo de Souza, Akihisa Motoki and Natsue Abe.

Three dredge and one rock-core operations were conducted along the Segment 1 of the Chile ridge system (D03 to D05 and RC01 in Figure 2-4-5-3) to understand along-axis geochemical variation of MORBs in the Segment 1 and to estimate flux compositions derived from the subducting oceanic crust (sediments and altered MORBs) toward the mantle wedge. Locations of the dredge and rock core sites are summarized in Table 2-4-5-1 and Table 2-4-5-2, respectively.

Three dredge operations were conducted in the central part of the NS-trending Segment 1 (Figure 2-4-5-3 and Figure 2-4-5-4). Because only surface sediments (soft grayish mud; ~ 1.5 kg) were recovered at a mound in on-axis ridge of the site D03, sea floor of the on-axis ridge was considered to be covered with a thick soft mud derived from the trench slope. Consequently, following dredge and rock core operations were conducted at off-ridge mounds developed in the western side of the central axis (Figure 2-4-5-4). D04 operation recovered sparsely plagioclase-phyric pillow basalts with rim of 3 – 12 mm thick fresh quenched glass (~ 37 kg). They have no to sporadic Mn-coatings and most are slightly vesicular. D05 operation recovered two types of basaltic rocks (~ 14 kg): plagioclase-phyric pillow basalts with fresh to slightly rusted quenched glass rim of 2 – 12 mm thick (Sample No. 1-13), and aphyric pillow basalts with rim of slightly altered and/or rusted thin quenched glasses (Sample No. 14-17). They are vesicul-free to slightly vesicular and have no or thin film of Mn-coatings. The former ones, however, seems to be younger than the latter ones, based on mesoscopic observation. RC01 operation was conducted at relatively small mound in the northern tip of the Segment 1 (Figure 2-4-5-5) and recovered fresh to slightly rusted quenched basaltic glasses (~ 10 g) with sparsely distributed plagioclase phenocrysts. Minor microfossils and silts were also contained in RC01 samples. For the detailed descriptions, see “Supplementary materials” Chile Ridge RockList.xls file and also photographs in MR0806_D04_RockPhoto.pdf and MR0806_D05_RockPhoto.pdf files. Details of rock core operation are shown in Figure 2-4-5-6.

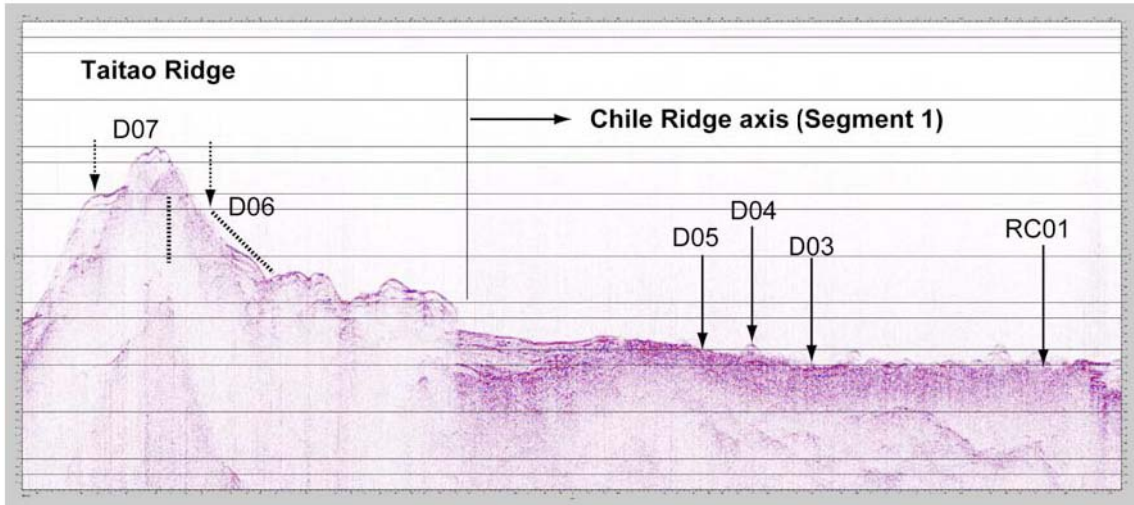


Figure 2-4-5-3: Dredge site indicated on SCS (st27-st30) profile (position is in Figure 2-4-5-2).

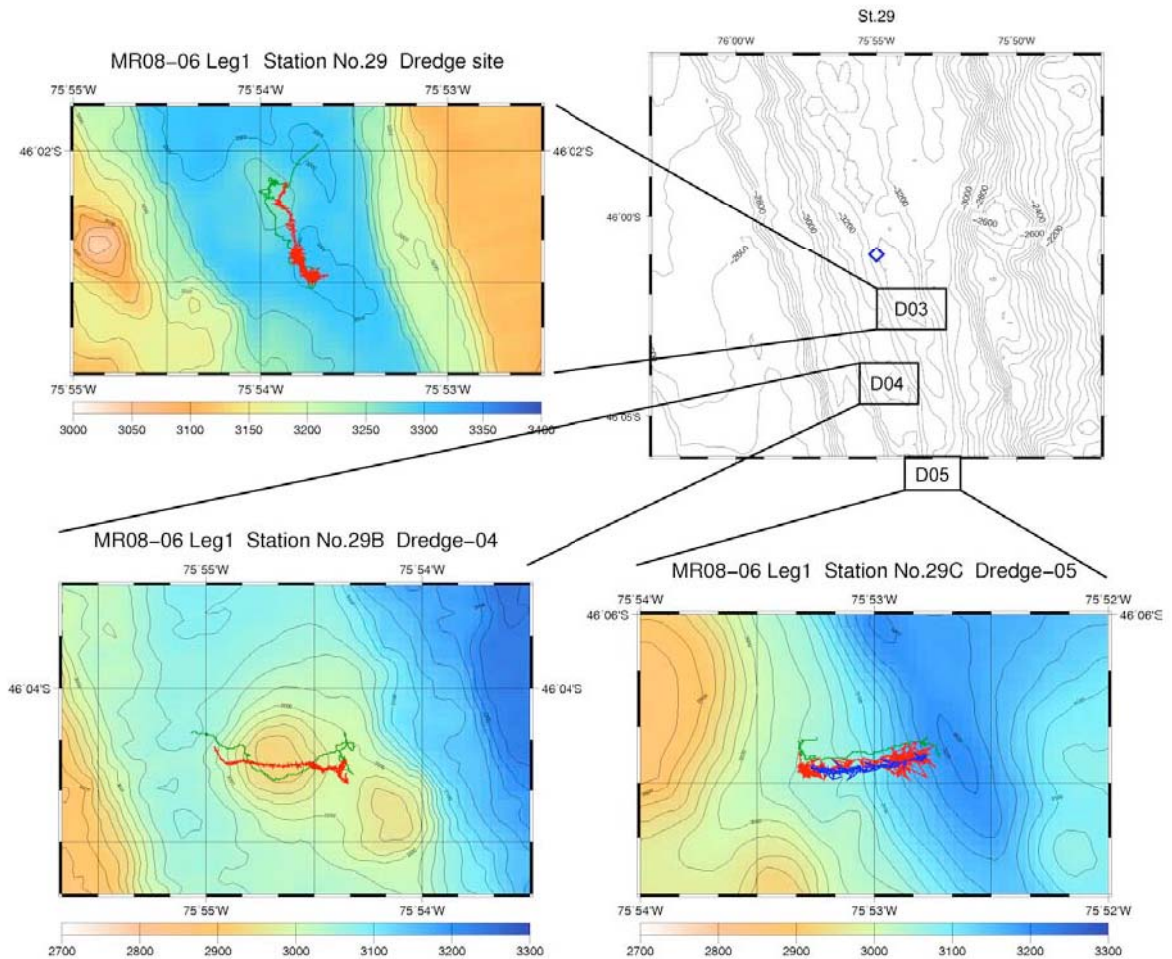


Figure 2-4-5-4: Bathymetric map of the Segment 1 and sites D03 to D05.

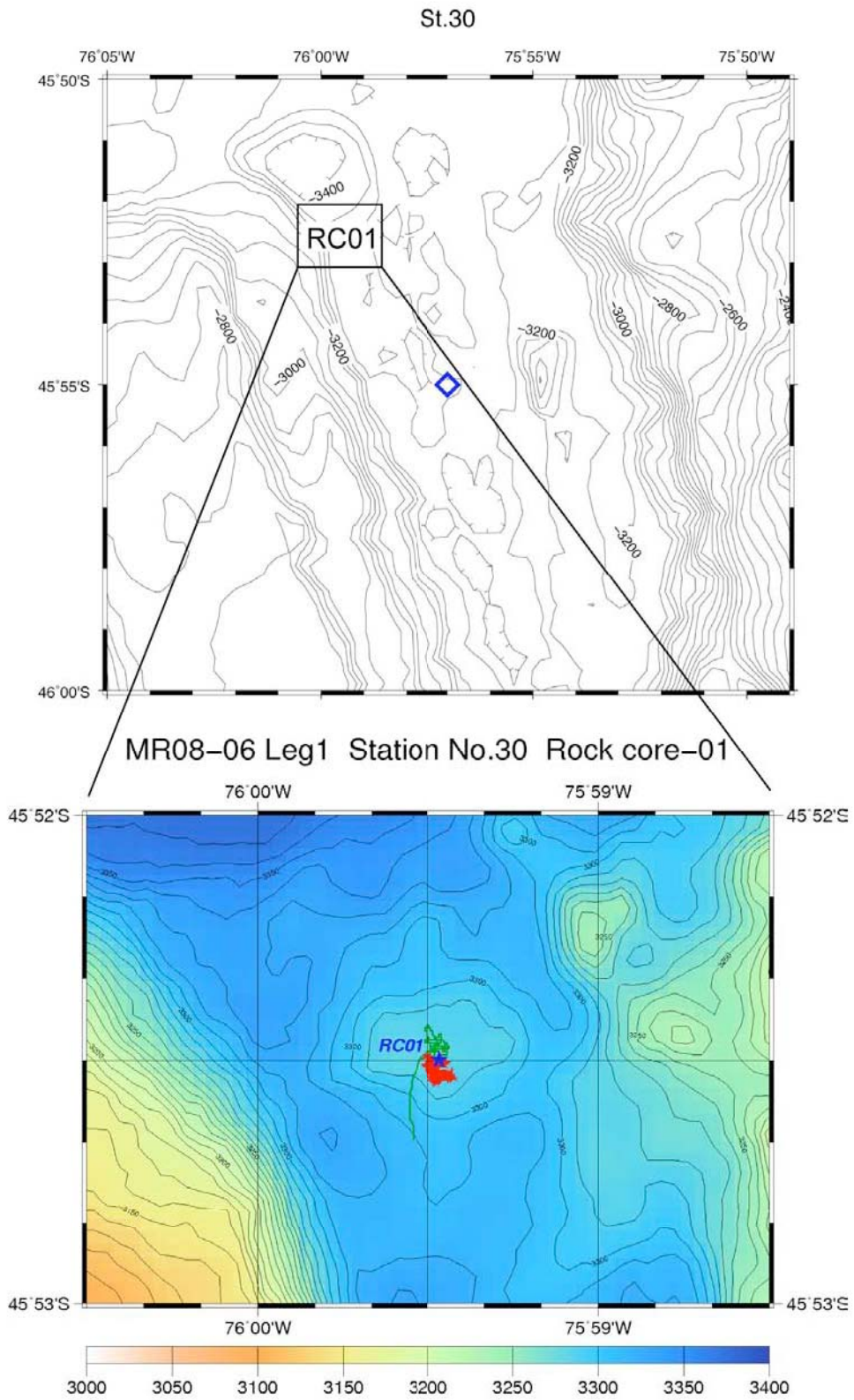


Figure 2-4-5-5: Bathymetric map around site RC01.

Rock core

1) Preparation



2) Recovered rock core



3) Recovered samples



Figure 2-4-5-6: Rock core operation during MR08-06 Leg.1b cruise.

2-4-5-2 Rock sampling at the Taitao area

Ryo Anma, Yuji Orihashi, Andres Veloso, Kiichiro Kawamura, Akihisa Motoki, Tiago Jalowitzki, Rodrigo de Souza, Christina Ortega, Sebastian Martini, Masamu Aniya and Natsue Abe

We conducted four dredge operations offshore of the Taitao peninsula, western-most promontory of the Chilean coastline (Figure 2-4-5-2). The study area underwent subduction of two segments of the Chile ridge system, that took place ~ 6 Ma and ~ 3 Ma ago and recent ridge subduction process is on-going in north (section 2-4-5). Nearby the study area, the ~ 6 Ma Taitao ophiolite and contemporaneous granite intrusions are exposed in the western tip of the Taitao peninsula. Overall aim of the four dredge operations is to map submarine extension of the Taitao ophiolite and to understand the fundamental processes involved in subduction of the Chile ridge. We were particularly interested in whether metamorphic sole exists at the base of the Taitao ophiolite, and in influence of the 3 Ma subduction event on rocks and sediments around the study area. Locations of the dredge sites are summarized in Table 2-4-5-1. Dredged rocks/sediments are listed in the “Supplementary material” TaitaoRockList.xls file.

Dredge D01 was operated at the basal part of northward slope of an EW-trending ridge (Figure 2-4-5-7 and Figure 2-4-5-8) located in southwest of the Taitao ophiolite. We refer to this ridge as the South Taitao ridge hereafter. We recovered tuff breccias, lapilli tuff and lapilli stones of dacitic composition with clasts/breccias of andestic to basaltic compositions (~ 54 kg), and consolidated sandstones and siltstones (~ 245 kg) from the South Taitao ridge. Recovered rocks are angular to sub-rounded in shapes. Pyroclastic rocks have no to sporadic Mn-coating, whereas thin Mn-coating was more commonly observed in sandstones and siltstones. Structures observed in sedimentary rocks include: thin alternation of sandstone and mudstone, graded bedding in sandstones, load cast, bioturbation in siltstones, micro-normal fault and vein structures. Thin alternation of sandstone and mudstone could be interpreted as distal turbidites. For detailed rock description, see “Supplementary material” D01SedSketch.pdf and D01VolSketch.pdf files, and also photographs in MR0806_D01_RockPhoto folder. Recovered pyroclastic and sedimentary rocks resemble to those of the Chile Margin Unit of the Taitao ophiolite (CMU in Figure 2-4-5-9) suggesting that the Chile margin Unit, supposedly a product due to subduction of a transform fault, is continuous to southwest swinging general NE-SW trend in the Taitao peninsula to EW.

Dredge D02 was conducted along the westward-facing slope beneath the Taitao ophiolite (Figure 2-4-5-10). D02 operation recovered granites (~ 6 kg), consolidated sandstones and siltstones (~ 46 kg) and a pyroclastic rock (0.12 kg). The pyroclastic rock includes breccias of

sparsely pyroxene-phyric basalt to basaltic andesite with thin altered glassy rim. Structures observed in the sedimentary rocks include: alternation of sandstone and mudstone, imbrication of clasts, bioturbation, black seams (layer-parallel coherent fault), vein structures and calcite veins (with and without slicken lines). Foraminifers were recognized in few specimens. The sedimentary rocks have thin Mn-coating. Granitic rocks resemble to those of the Cabo Raper intrusion (CR in Figure 2-4-5-9) based on mineral assemblage and texture. They are angular to sub-angular blocks and have no Mn-coating. We suggest that they are blocks fell off from a nearby exposure of the Cabo Raper pluton. No ultramafic rock from the base of the Taitao ophiolite, no rock of a metamorphic sole was recovered. For detailed rock description, see “Supplementary material” D02SedSketch.pdf file, and also photographs in MR0806_D02_RockPhoto folder.

Dredges D06 and D07 were conducted in the Taitao Ridge (Figure 2-4-5-11 and Figure 2-4-5-12) located northwest of the Taitao ophiolite (Figure 2-4-5-2). Dredge D06 operation recovered 194 kg of fine-grained sandstones, siltstones and claystones. Degree of consolidation is bimodal: one is weakly consolidated, and the others well consolidated. Consolidated sedimentary rocks are angular to sub-rounded blocks and have no to sporadic thin film of Mn-coating. Structures observed in consolidated sedimentary rocks include: thin lamina of sandstone, bioturbation, trace fossils, load cast and wavy depositional surface, vein structures, orthogonal brittle fractures, brecciation. They could be interpreted as distal turbidites. In contrast, weakly consolidated sediments are consist mainly of siltstones and claystones with no Mn-coating and significant deformation structures. For detailed rock description, see “Supplementary material” D06SedSketch.pdf file, and also photographs in MR0806_D06_RockPhoto folder. We suggest that the consolidated sedimentary rocks were deposited before ridge subduction, whereas the weakly consolidated sediments deposited after the ridge subduction. Further investigation is planned to confirm this idea.

Dredge D07 operation recovered 233 kg of fine-grained sandstones, siltstones and claystones. They are angular to sub-rounded blocks commonly without but in occasions with thin film of Mn-coating. Two angular and sub-rounded pebbles of pillow breccias of andestic to basaltic composition were also recovered. The pillow breccias have thin Mn-coating. Structures observed in consolidated sedimentary rocks include: thin layer of sandstones, grading, bioturbation, trace fossils, vein structures, orthogonal and en-echelon calcite veins, fractures with slicken line and pyritized burrows. A pebble of siltstone with bioturbation and vein structure was observed in a consolidated mudstone. Organic materials and foraminifers were

observed in places. For detailed rock description, see “Supplementary material” D07SedSketch.pdf file, and also photographs in MR0806_D07_RockPhoto folder.

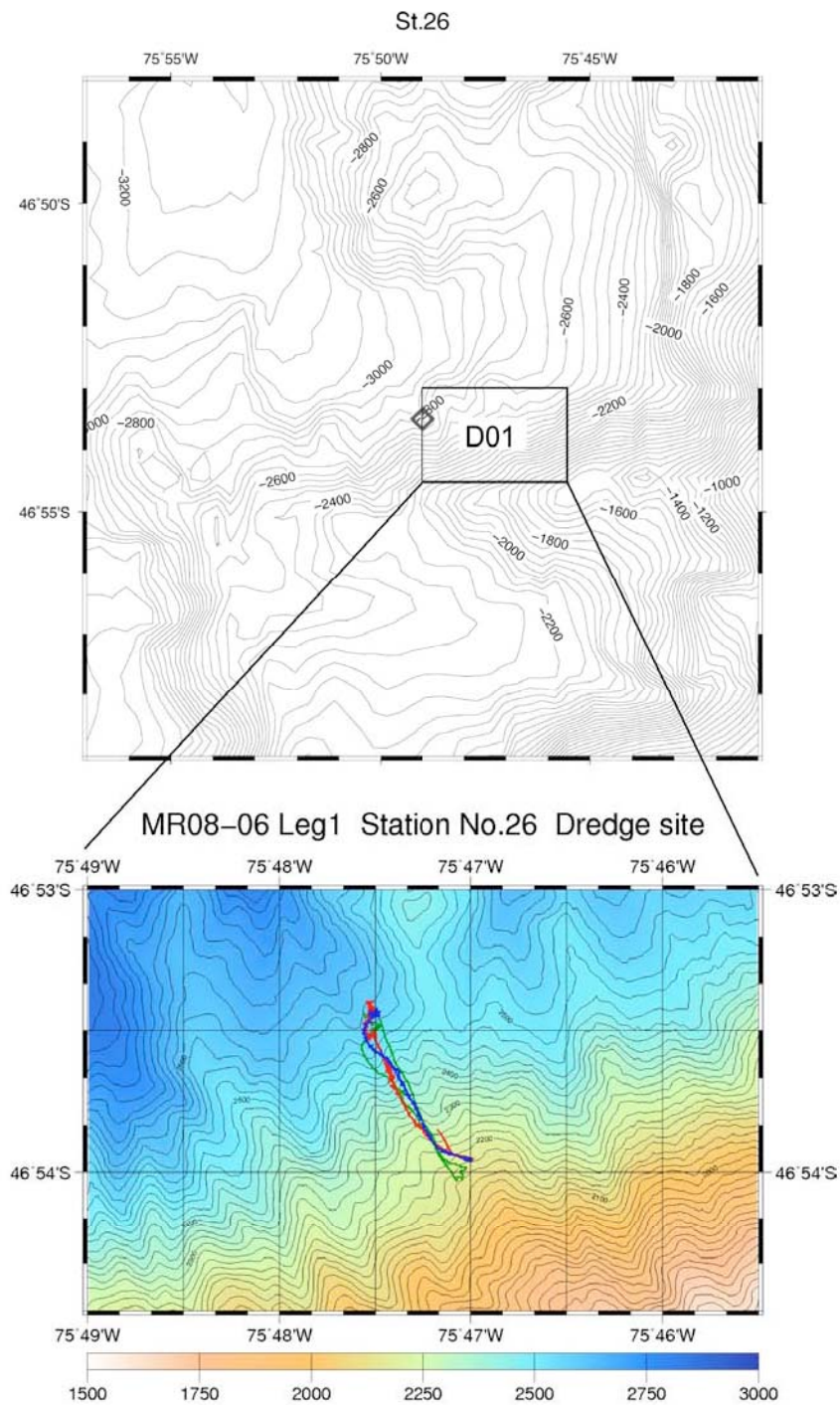


Figure 2-4-5-7: Bathymetric map around the South Taitao ridge and site D01.

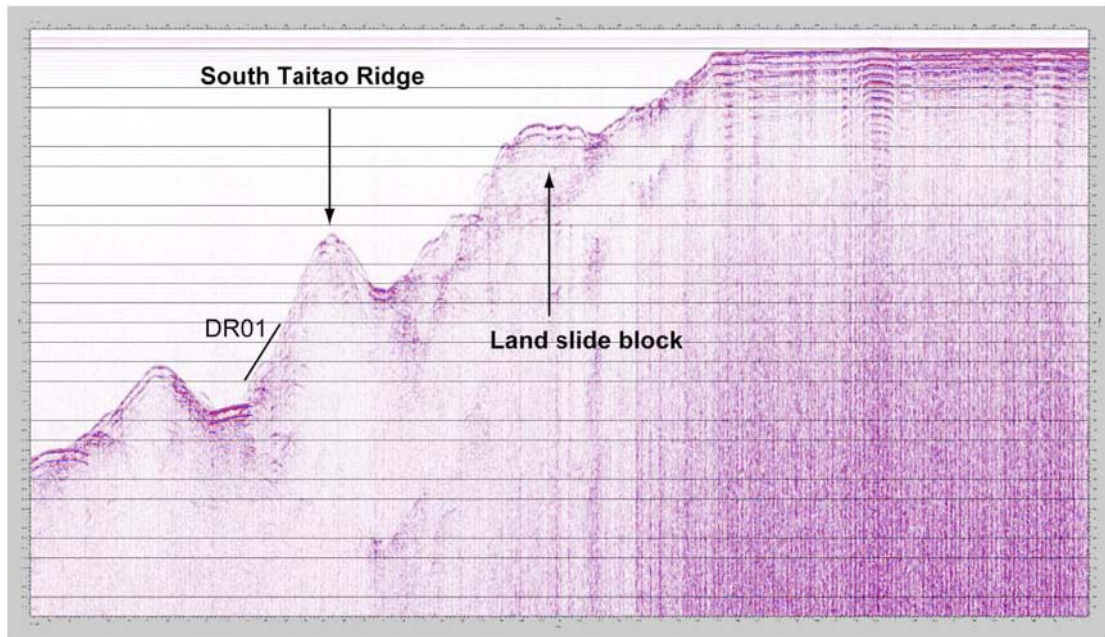


Figure 2-4-5-8: Dredge site DR01 indicated on SCS (st26) profile (position in Figure 2-4-5-2).

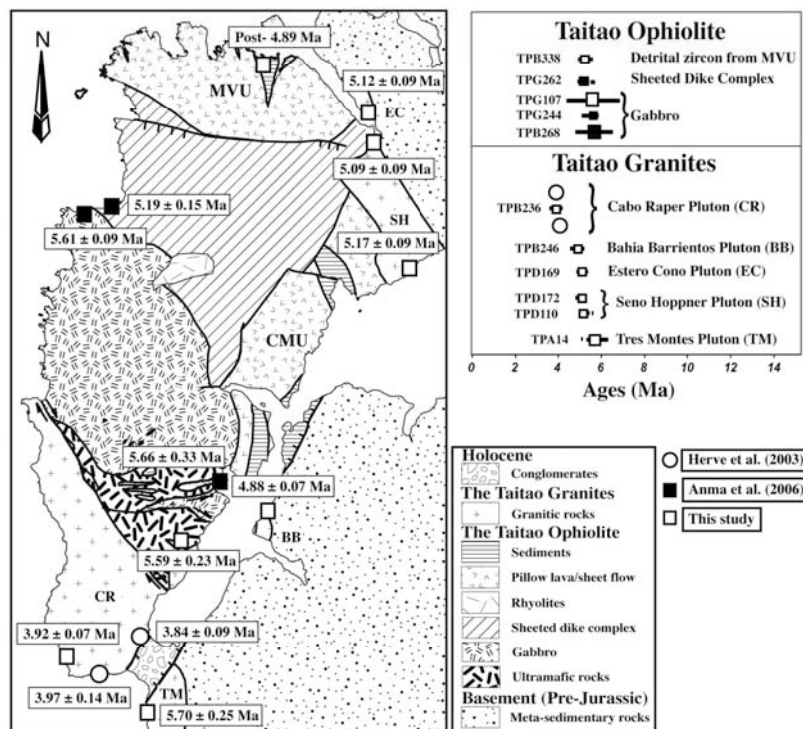


Figure 2-4-5-9: Lithological distribution and SHRIMP U-Pb ages of the Taitao ophiolite and related granites. Rocks resembling to the Chile Margin Unit (CMU) were dredged by D01 operation in the South Taitao ridge. D02 in the western slope by the Taitao ophiolite recovered granitic rocks (most probably fallen off blocks of the Cabo Raper (CR) pluton).

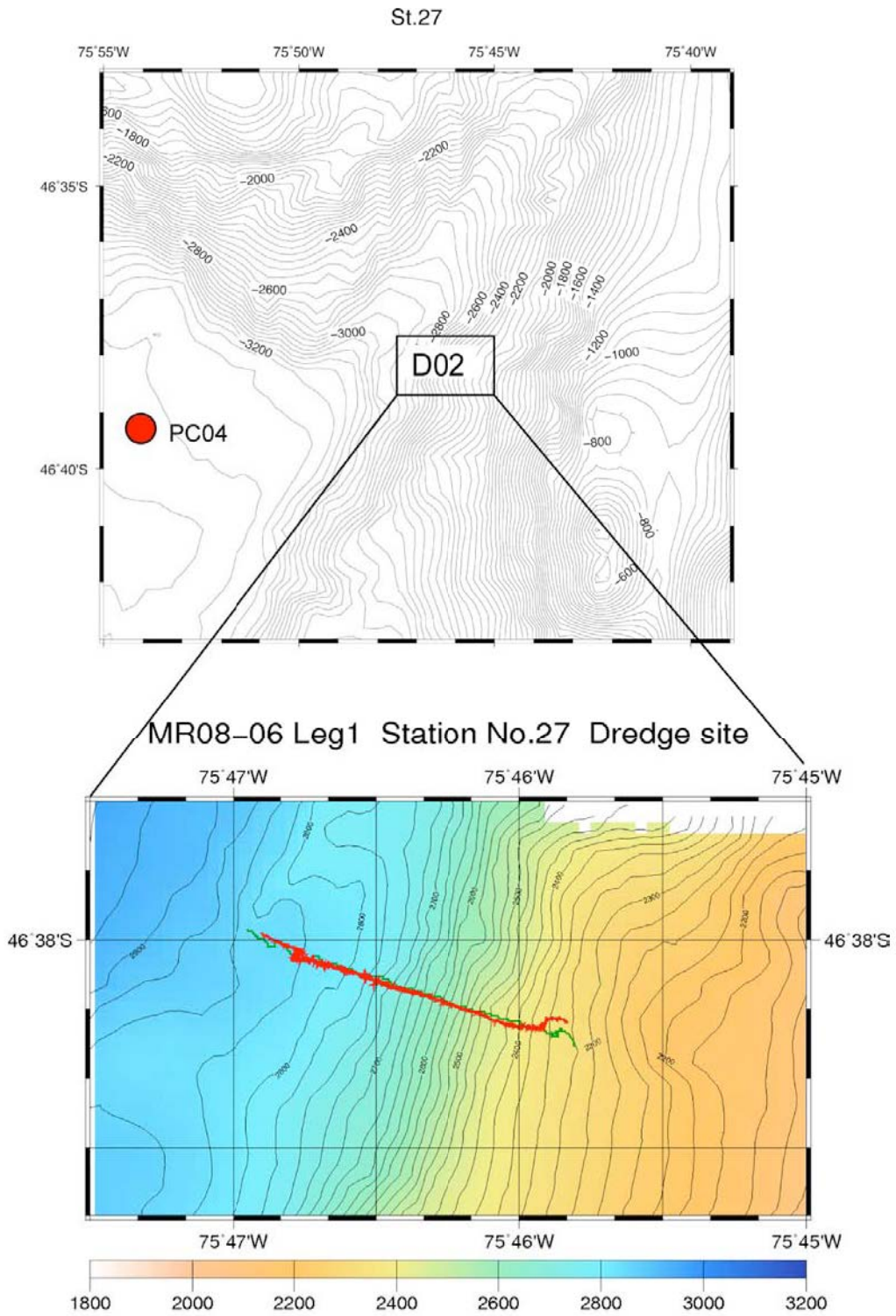


Figure 2-4-5-10: Bathymetric map of the western slope off Taitao peninsula and around site D02.

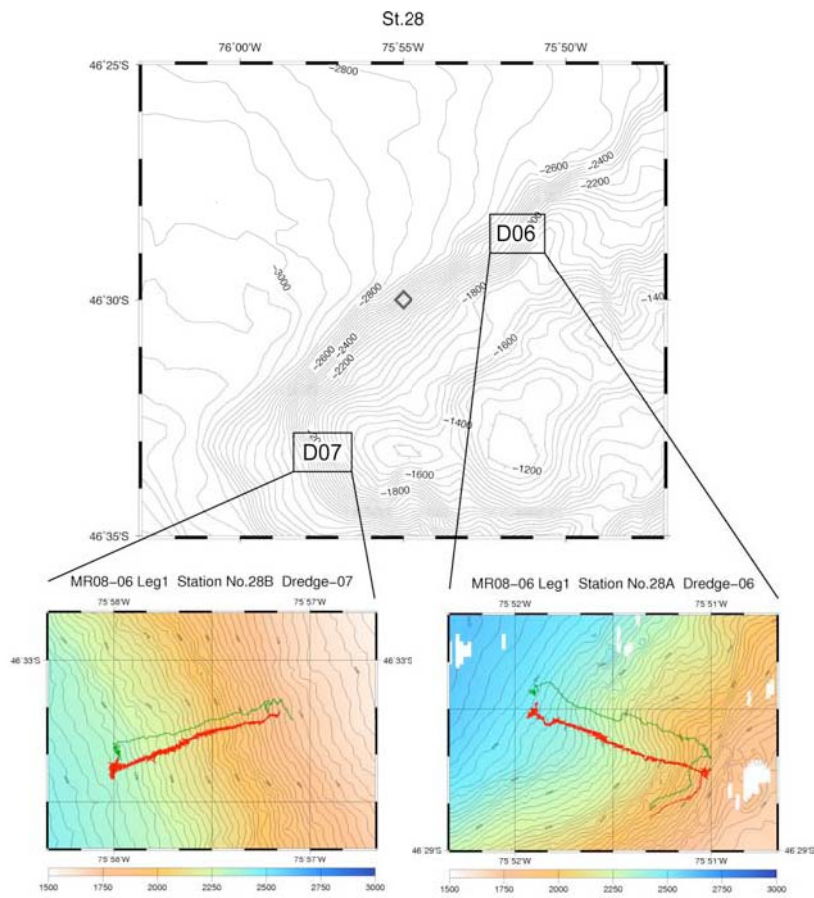


Figure 2-4-5-11: Bathymetric map around the Taitao ridge and sites D06 and D07.

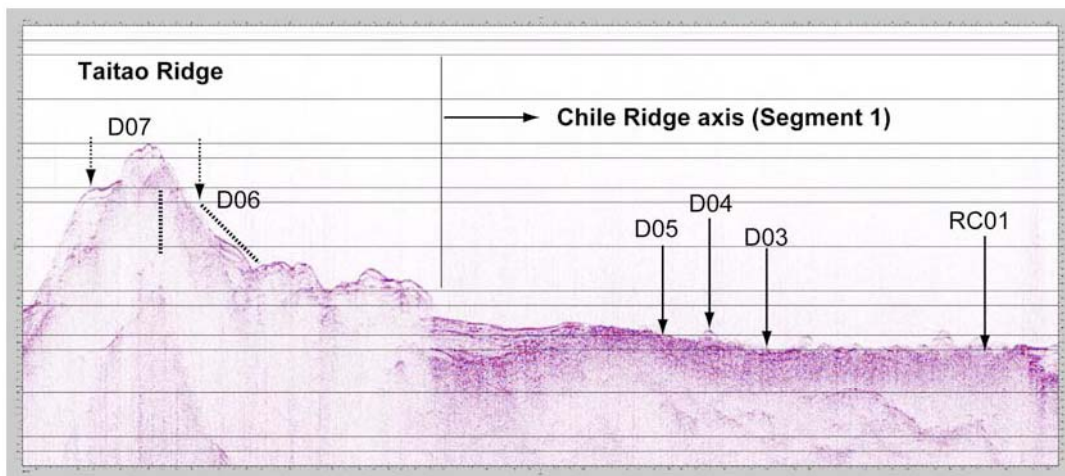


Figure 2-4-5-12: Dredge sites D06 and D07 indicated on the SCS (st27-st30) profile. Position of D06 and D07 is off profile from the NS-trending st27-st30 profile. Latitude of D06 and D07 is indicated by arrow with dashed line. When they are projected to the st27-st30 profile, the position of dredges D06 and D07 correspond to those indicated by oblique and vertical dashed lines, respectively.

6.8.4 Visual core description

Ryo Anma †, Kiichiro Kawamura ‡, Isao Motoyama † and Yasumi Yamada †

† University of Tsukuba, Japan

‡ Fukada Geological Institute, Japan

6-8-4-1 Methods

The sampling sites for multiple coring and piston coring are shown in Figure 6-8-4-1, together with grain components of the surface sediments.

Observation for visual core description (VCD) for core samples was made on split surface of working half sections. The split surface was scraped using a glass plate to expose fresh surface. Lithological and sedimentological features were described on a VCD spread sheet (see Appendix: VCD) for each section. Information in the VCD spread sheets was used to synthesize the stratigraphical column of PC-5 ~ PC-9 (Figure 6-8-4-2~ Figure 6-8-4-11). Symbols used for VCD is listed in Figure 6-8-4-12. Primary sediment lithology name was first described on core and then confirmed under a microscope (see Appendix: smear slide summary). We adopted the IODP-style nomenclature for lithological description (e.g., Mazzullo et al., 1988) with some modifications. Sediment classification scheme used here was the Shepard's ternary diagram for sand-silt-clay component system.

6-8-4-2 Results

Surface sediments

The components of surface sediments from Stations 37 to 46 are summarized in Figure 6-8-4-1. Station 38 corresponds to PC-05 site, Station 40 to PC-06 site, Station 43 to PC-07 site, Station 46 to PC-08 site and Station 44 to PC-09 site, respectively. Siliciclastic grains are predominant in sediments of the surface layers from northern latitudes between 43° S and 49° S, regardless inside or outside of the fjord. Nannofossils, diatoms and foraminifers were observed inside and offshore of the Golfo de Penas. In contrast, surface sediments in the southern latitudes (> 52° S) mainly consist of bioclasts, micro- and nannofossils, and contain only less than 30 % siliciclastic grains.

Piston cores

We used piston core with inner tube for PC-05 to PC-08 and without inner tube for PC-09. Length of the piston core was 20 m for PC-05, PC-06 and PC-08, and 10 m for PC-07 and PC-09. Lithology, photograph, detailed description, color reflectance, magnetic susceptibility and sediment composition of each core are summarized in Figures 6-8-4-2 through 6-8-4-11. The followings are brief description of each core.

PC-05: Total length of recovered core sample was 778.5 cm. Vertical structures due to flow-in were observed in section below 624.0 cm below sea floor (bsf) and hence, we do not describe this part of the core. Sediments of PC-05 consist of silt and clay (Figure 6-8-4-2) with siliciclastic grains and clay minerals more than 80 % throughout the core (Figure 6-8-4-3). Nannofossils, diatoms and foraminifers are present (few %) throughout the core. Neritic grains such as coarse-grained calcareous bioclasts and peloids are also present but less than 15 %. We therefore, used principal names applied for siliciclastic sediments (Mazzullo et al., 1988) for VCD in Figure 6-8-4-2.

Surface layer is composed of dark olive gray silty clay. The surface clay layer continues down to 70.5 cm bsf increasing degree of consolidation as sediments buried. Very dark gray to dark gray clayey silt composes sediments of the interval 70.5 - 271.3 cm bsf. This section is homogeneous and there was no visible evidence for bioturbation. H₂S smell was recognized in this section. Below this section, interval 271.3 - 624.0 cm bsf consists of semiconsolidated and heavily bioturbated, dark greenish gray silty clay to clayey silt. Laminated beds (472 - 491 cm and 601 - 624 cm bsf) or color banding (540 - 573 cm bsf) were observed in places. Shell fragments were distributed at interval 242 - 271 cm bsf, and at 384 cm bsf. Black patches defined by pyrite concentration were observed at interval 497 - 532 cm bsf.

PC-06: Total length of the recovered core was 1411.0 cm. Sediments of PC-06 consists of dark greenish gray to dark gray silty clay to clayey silt (Figure 6-8-4-4). Siliciclastic components increase downward from ~ 60 % to 80 %, except for smear slide at 203 cm bsf where nannofossils and pellets occupy approximately 35 % of the sediment (Figure 6-8-4-5). Nannofossils were frequently observed in the upper part of PC-06 and disappeared at ~ 670 cm bsf. Pellets were frequently observed (less than 10 %) throughout the core. Minor amount of diatoms and foraminifers were also observed throughout section. Hence, we used principal names applied for siliciclastic sediments with modifier (Mazzullo et al., 1988) for VCD of PC-06 (Figure 6-8-4-4).

Uppermost part of the PC-06 down to 198.3 cm bsf consists of homogeneous clayey silt and silty clay (50.0 - 97.3 cm bsf). There was no visible structure and visible evidence for bioturbation in this section. Interval between 198.3 - 694.7 cm bsf consists of dark gray silty clay with increasing degree of consolidation down section, from very soft (watery) to semiconsolidated. This section is homogeneous. Except for patches of dark greenish silty clay distributed in places (518 - 525 cm bsf), there was no visible evidence for bioturbation. Vertical fractures and voids with irregular shapes due to gas expansion were observed at intervals 265 - 298 cm bsf and below 342 cm bsf, respectively. Amount of gas caves increases below 342 cm bsf. Nannofossils disappeared at around 670 cm bsf in this section. The lowermost part of this section (680 - 695 cm bsf) was pyrite-rich. Below it, gas-free and bioturbated sediments of semiconsolidated dark gray silty clay were distributed at interval 694.7 - 797.2 cm bsf. This section is underlain by semiconsolidated olive gray silty clay (797.2 - 995 cm bsf) with thin horizontal cracks due to gas expansion, which increase both thickness and frequency below 880 cm bsf. Dark gray clayey silt (995.0 - 1195.0 cm bsf) with minor gas cracks and dark greenish gray silty clay (below 1195.0 cm bsf) with thicker and more frequently distributed gas cracks compose the lowermost part of the PC-06. Shell fragments and bioclasts were distributed throughout the core.

PC-07: Total length of the recovered core was 495.7 cm. Sediments of PC-07 consists mainly of siliciclastic grains of silty clay to very fine sand size (Figure 6-8-4-6) with minor amount of nannofossils, foraminifers, pellets and bioclasts less than 10 % in total (Figure 6-8-4-7). Below around 360 cm bsf, we did not observe any bioclasts or microfossils.

Bioturbated, dark gray to dark greenish gray silty clay comprises sediments in the uppermost part (0 - 45.0 cm bsf) of the PC-07 (Figure 6-8-4-6). This surface layer is underlain by semiconsolidated, dark gray silty clay interbedded with very fine sand and silt that continue to the bottom of the PC-07. This section typically develops few mm to cm thick fine layers of sand and silt throughout the section. Only minor influence of bioturbation was observed in places. Structures observed in the upper part of the section (interval 45.0 - 303.4 cm bsf) include: sharp or gradual boundaries between bedding planes, scoured boundaries (erosional and/or bioturbated), normal and anti-grading in sandy layer, color banding, patches or lenses of silt/sand. Structures observed in lower part of the section include: low-angle reverse and normal faults with few mm displacements, normal grading at the lowermost section (below 413 cm bsf), color banding and patches of dark silt. Ice rafted debris were distributed only at intervals 142 –

168 cm and 250 - 275 cm bsf. Pyrite enriched zones were observed in places.

PC-08: Total length of the recovered core was 749.7 cm. Bioclasts are more frequently observed in the PC-08 and are the predominant component at interval ~ 200 - 300 cm bsf (Figure 6-8-4-9). Smearslide at 208.8 cm bsf contains as much as 63 % bioclasts. Nevertheless, most sediments of PC-08 consist mainly of siliciclastic grains, and we used principal names applied for siliciclastic sediments with modifier for VCD of PC-08 (Figure 6-8-4-8). Except for minor facies at 520.3 cm bsf (a patch of very fine sand), all smearslide samples contain bioclasts and sponge spicules. Nannofossils and foraminifers were observed throughout the PC-08.

Thin layer (10 cm thick) of clayey silt comprises the uppermost surface layer of the PC-08 (Figure 6-8-4-8). Calcareous clayey sand observed in the pilot core (see Figure 6-8-4-1) was not preserved in the piston core. Homogeneous, olive gray to olive silty very fine sand to sandy silt comprise the upper part of the PC-08 sediments in interval 10.0 – 348.9 cm bsf. Mixed sediments with bioclasts are distributed in the middle of this section. There were few burrows in the upper part, but middle part was homogeneous and there was no visible evidence for bioturbation. The lowermost part of this section is heavily bioturbated. Minor gas caves were observed in places. Smell H₂S.

Interval 348.9 - 380.9 cm bsf is composed of fine to very fine sand with cross and parallel laminae. Below this sand layer, gas-rich dark gray to olive gray silt to very fine sand composes interval 380.9 - 686.4 cm bsf. Grain size coarsens downward. This section was less consolidated than above section. Horizontal fractures due to gas expansion were observed throughout this section with increasing frequency and thickness downward. Although, lenses and entrainment of very dark gray fine sand along the core wall were observed throughout, this section is structurally homogeneous and there was no visible evidence for bioturbation. The lowermost part of the PC-08 (686.4 - 749.7 cm bsf) is composed of olive gray to dark greenish gray fine sandy silt with horizontal gas cracks. Shell fragments were observed throughout the PC-08 sediments.

PC-09: Total length of the recovered core was 997.2 cm. The mixed sediments of 11 cm-thick surface layer (plus burrow-fill at 20 cm bsf) are foraminifer sand and calcareous sand, and are completely different from sediments in beneath (Figure 6-8-4-11). Below the surface layer, the sediments consist mainly of siliciclastic grains with clay to fine sand size. Thus, we used principal names applied for siliciclastic sediments with modifier for the summary of VCD in

Figure 6-8-4-10. Bioclasts, foraminifers, nannofossils and sponge spicules were observed throughout the core. Distribution of pellets is limited compared to the other cores.

The surface layer is 11 cm-thick light gray fine to medium foraminifer sand (Figure 6-8-4-10). This thin mixed sediment is underlain by thick layer of dark gray clayey silt with lenses and layers of fine sand (interval 11.0 - 760.0 cm bsf). This section is heavily bioturbated and frequently contains ice rafted debris throughout the section. Pyrite-rich zones were observed in places. Structures observed in this section include sandy layers with normal grading and parallel laminae. Below this section, very fine sand with parallel laminae is distributed at interval 760.0 – 786.2 cm bsf. Below this sand layer, no ice rafted debris was observed. Interval 786.2 – 997.2 cm bsf is composed of dark greenish gray silt and very fine sandy silty clay with bioturbation. Shell fragments were distributed throughout the core.

We observed siliciclastic sediments derived most likely from glacier through the Rio Baker in the surface sediments in the Golfo de Penas. There was only few, if any, ice rafted debris in the samples obtained by piston coring from the same sites (PC-05 and PC-06). Ice rafted debris were however, recognized offshore region in the same latitude (PC-07). In southern latitudes, on the contrary, the surface sediments were mostly composed of bioclasts and micro- and nannofossils, but ice rafted debris were more frequently distributed in the piston core samples (PC-08 and PC-09).

References:

Mazzullo, J., Meyer, A. and Kidd, R. (1988) New sediment classification scheme for the Ocean Drilling Program. Appendix I, In "Handbook for shipboard sedimentologists" eds. Mazzullo, J. and Graham, A. G., ODP Technical Note, 8, 44-63.

Preliminary results of smear slide observation: Grain components of surface layers in core sediments

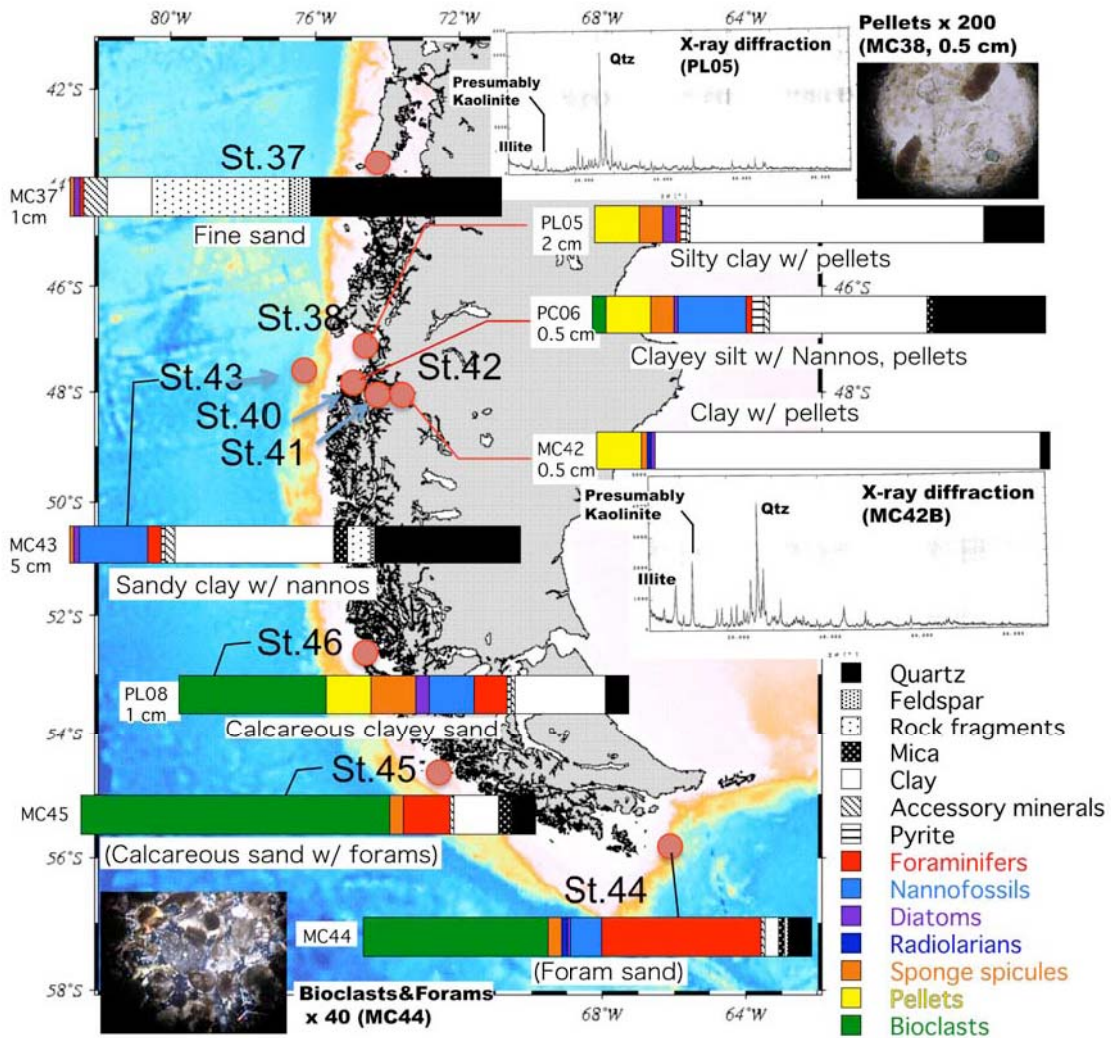


Figure 6-8-4-1: Sampling locations for sediments of the surface layers and their compositions.

MR08-06 Leg2 PC-05

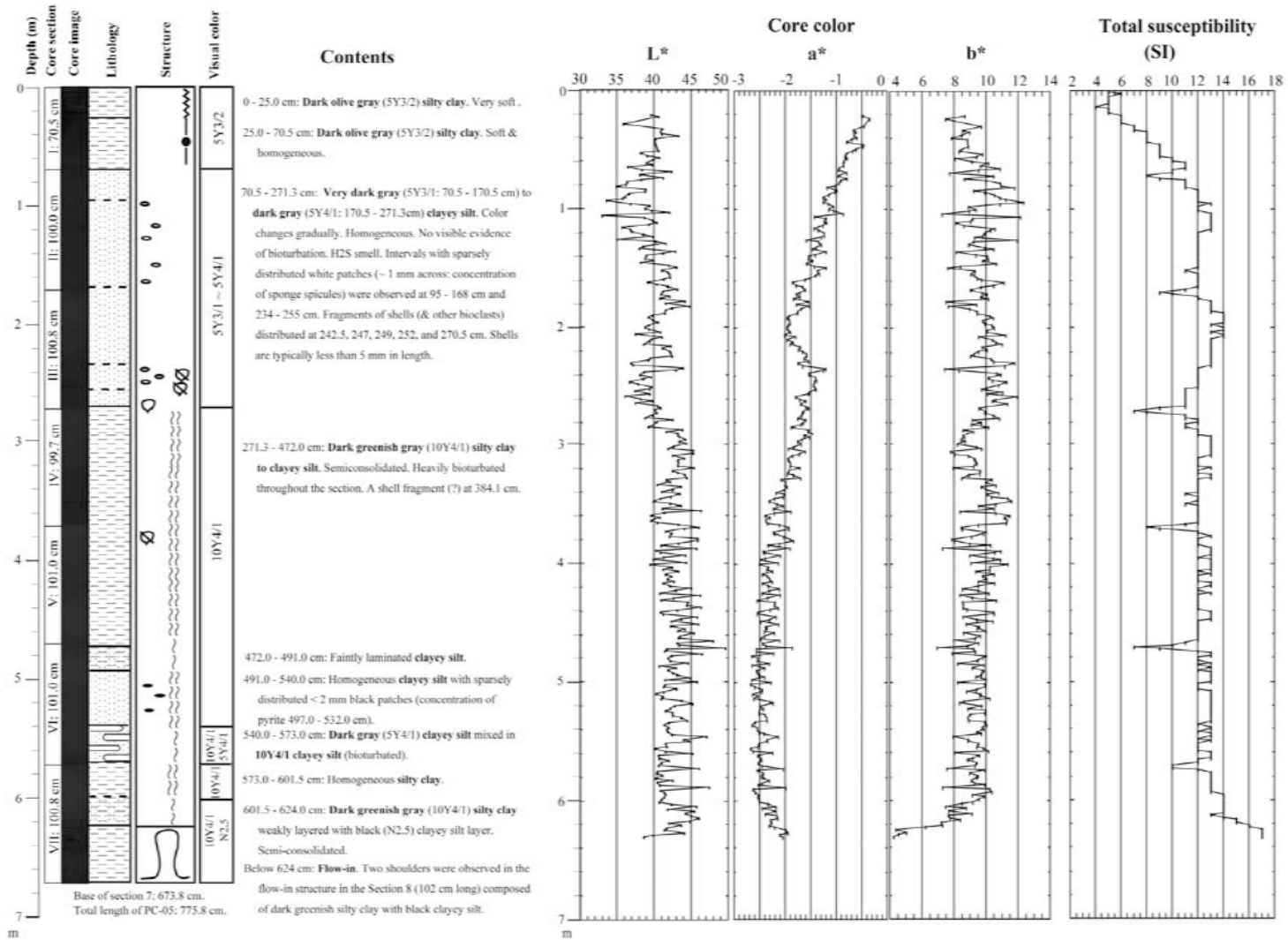


Figure 6-8-4-2: Visual core description for PC-05.

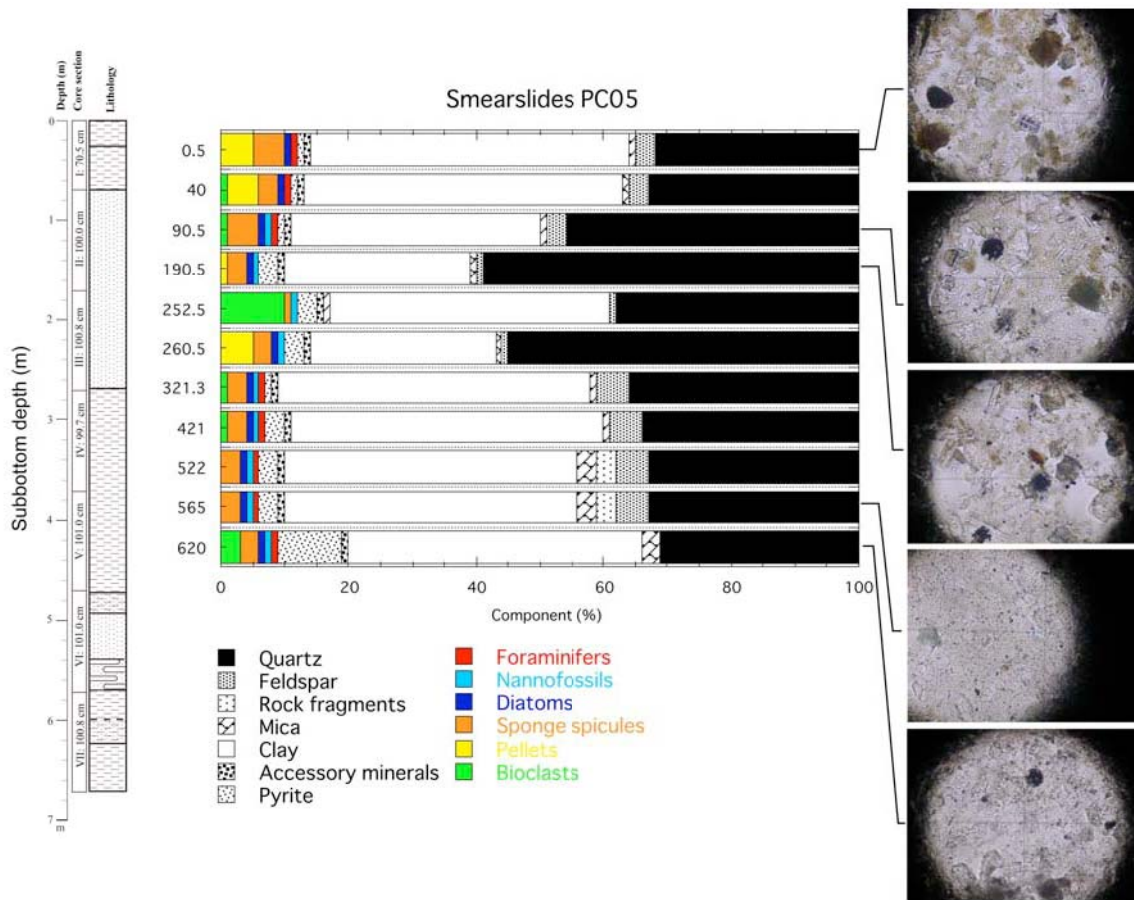
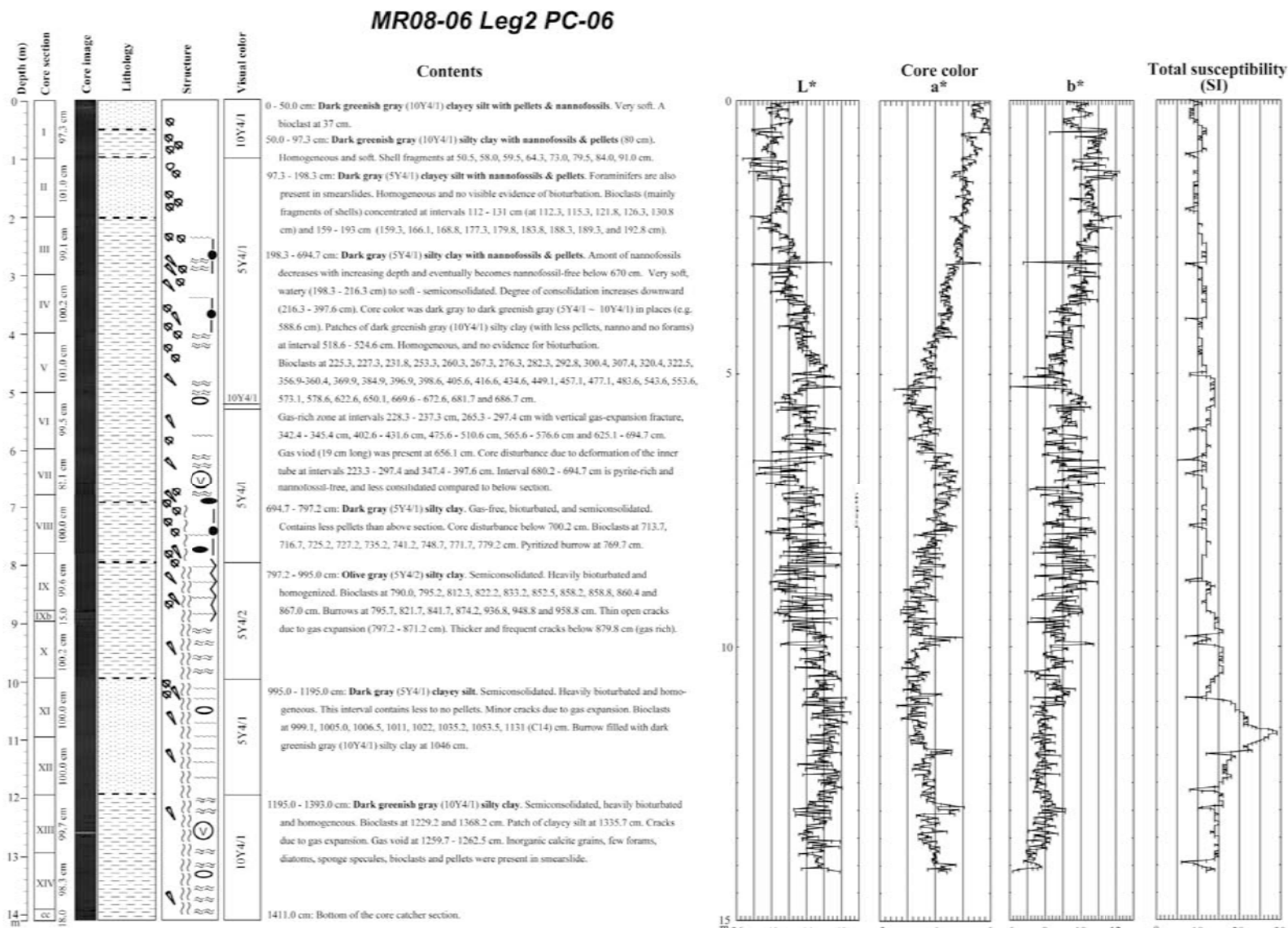


Figure 6-8-4-3: Composition of sediments of PC-05.

Figure 6-8-4-4: Visual core description for PC-06.



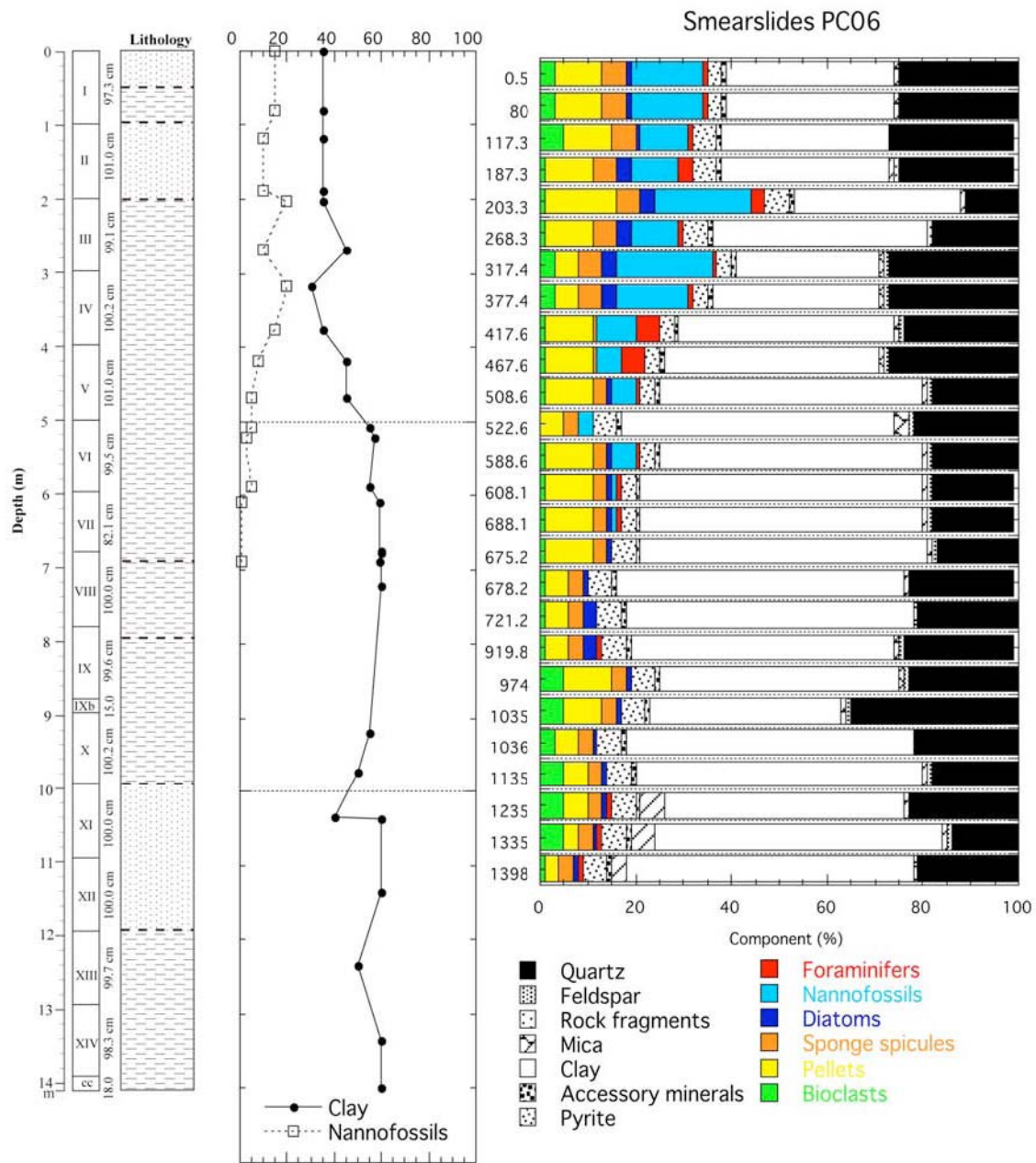


Figure 6-8-4-5: Composition of sediments of PC-06.

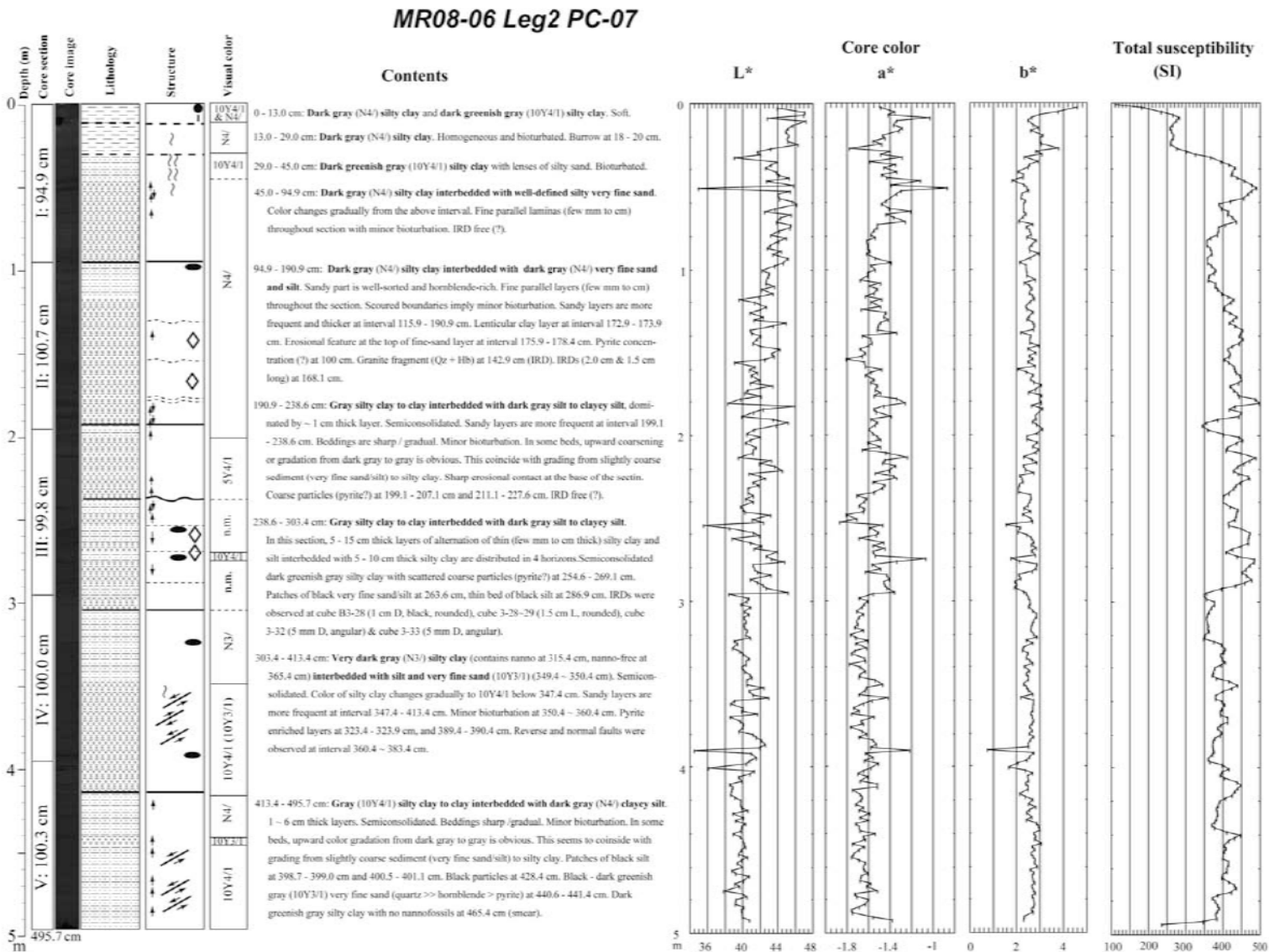


Figure 6-8-4-6: Visual core description for PC-07.

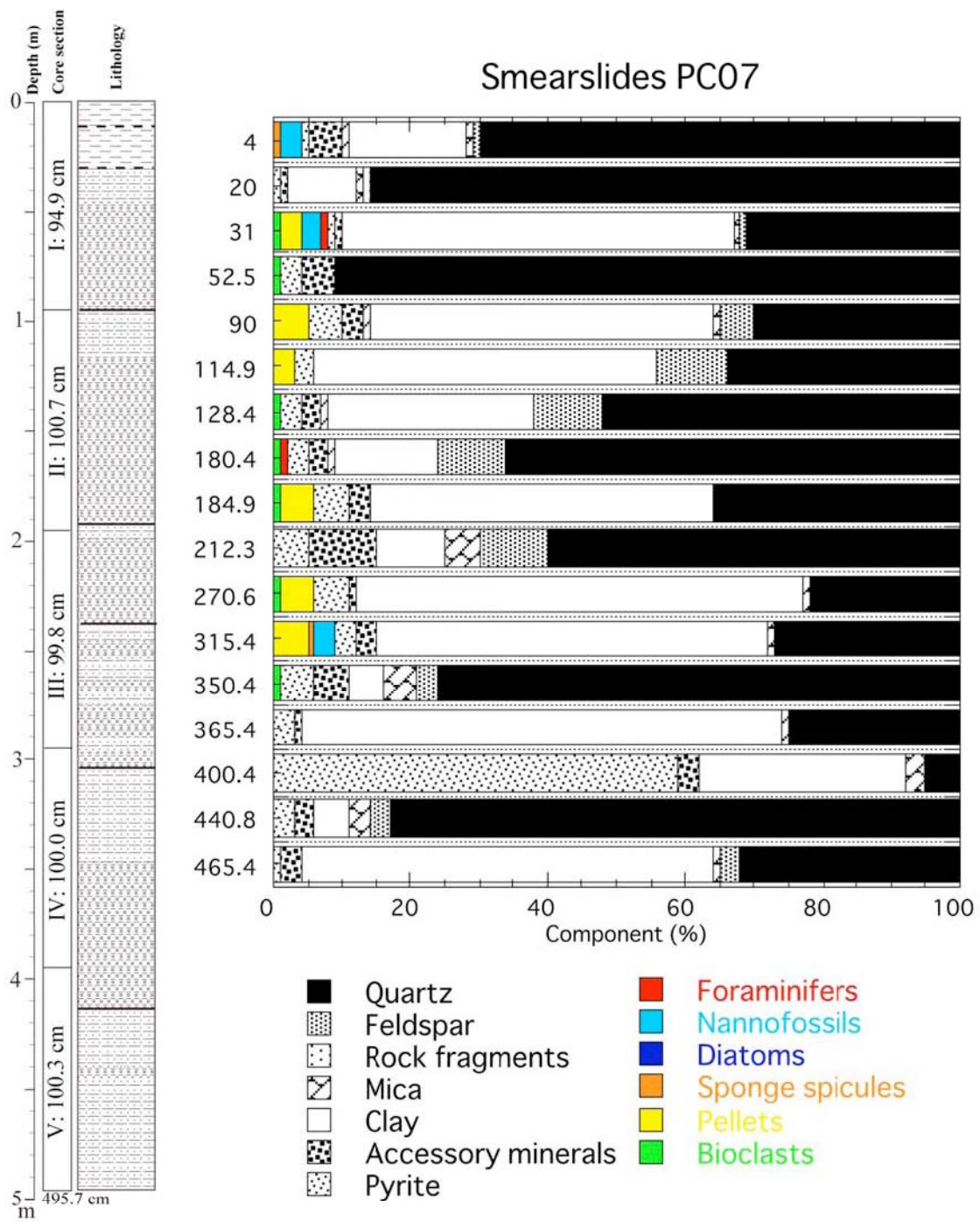
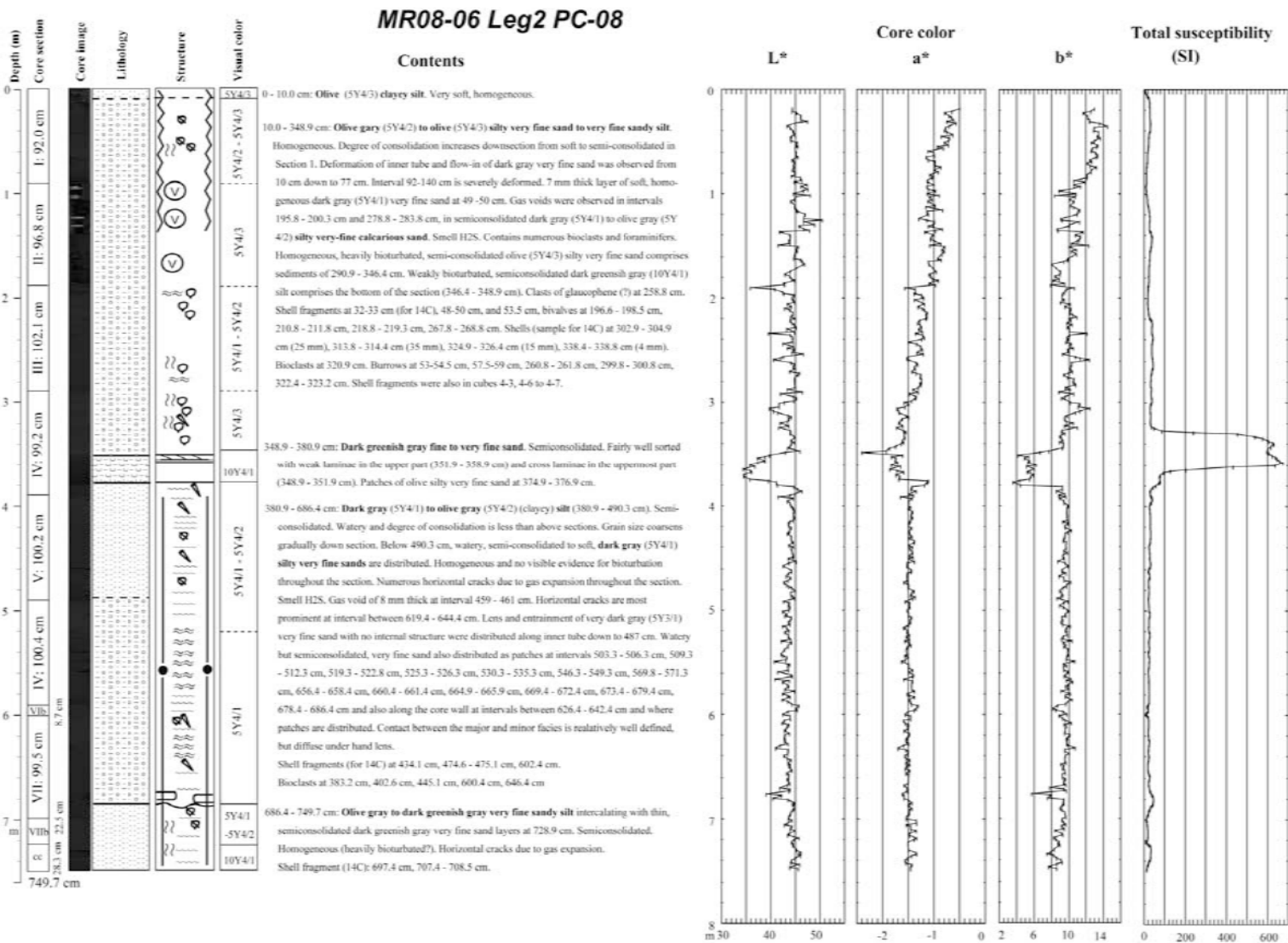


Figure 6-8-4-7: Composition of sediments of PC-07.

Figure 6-8-4-8: Visual core description for PC-08.



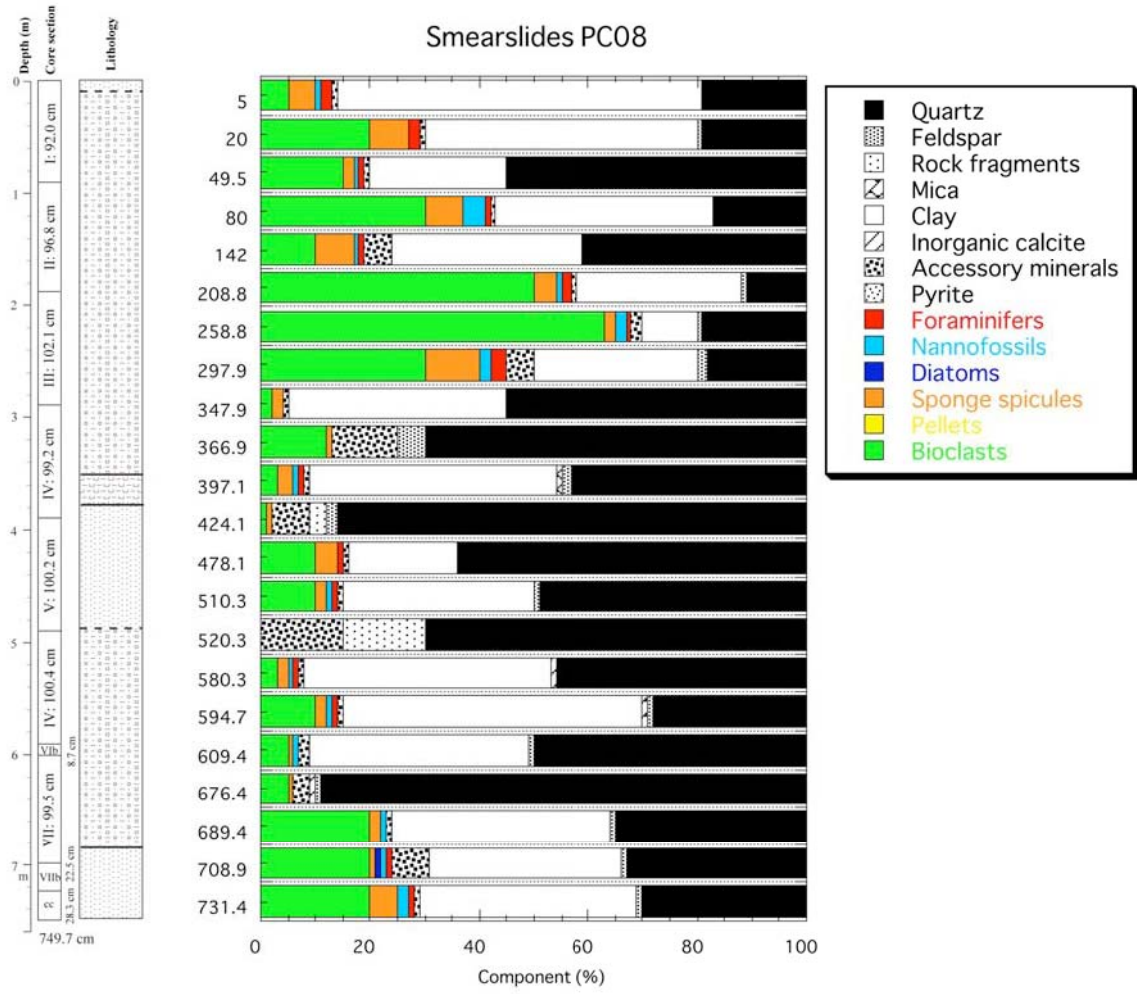
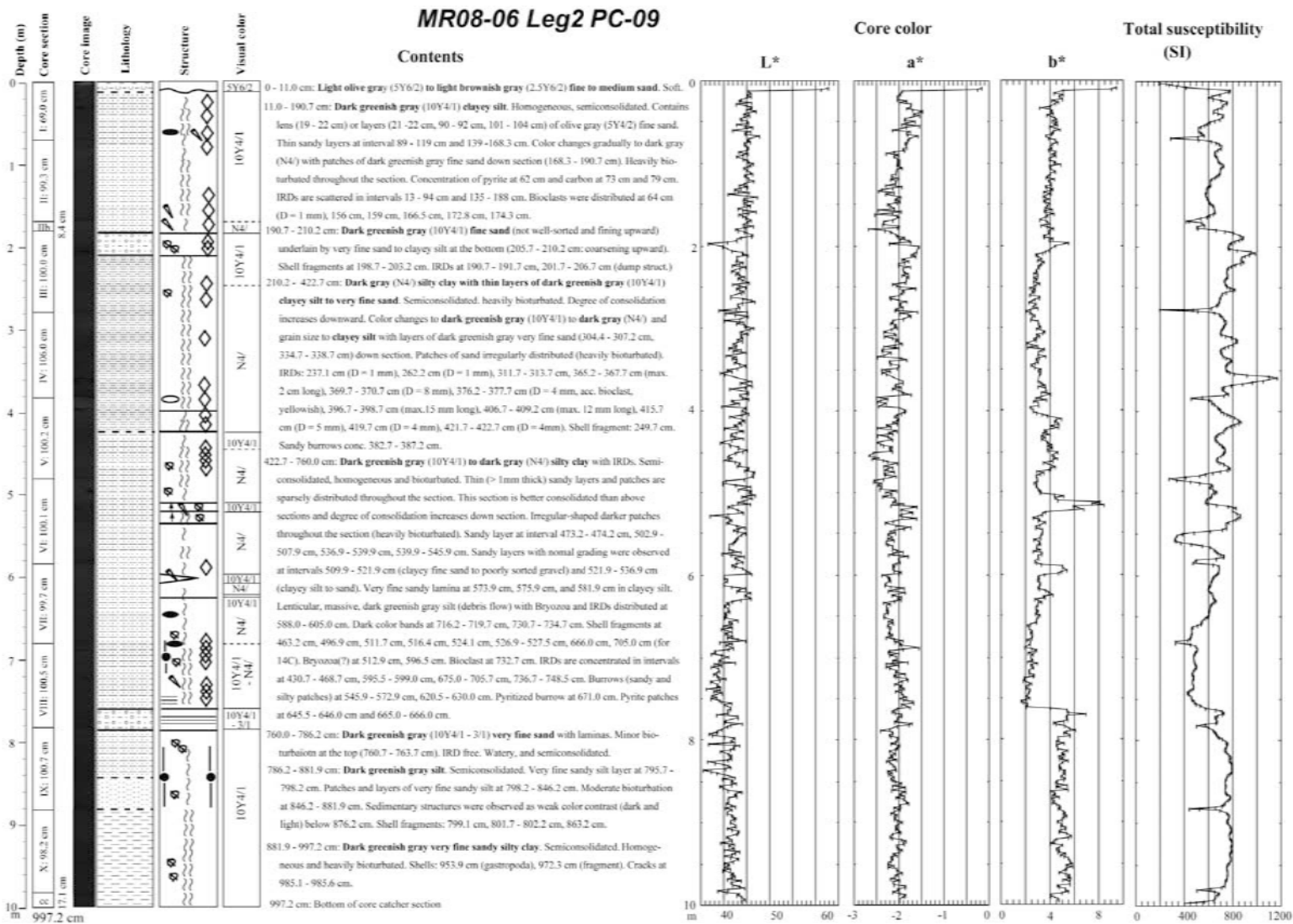


Figure 6-8-4-9: Composition of sediments of PC-08.

Figure 6-8-4-10: Visual core description for PC-09.



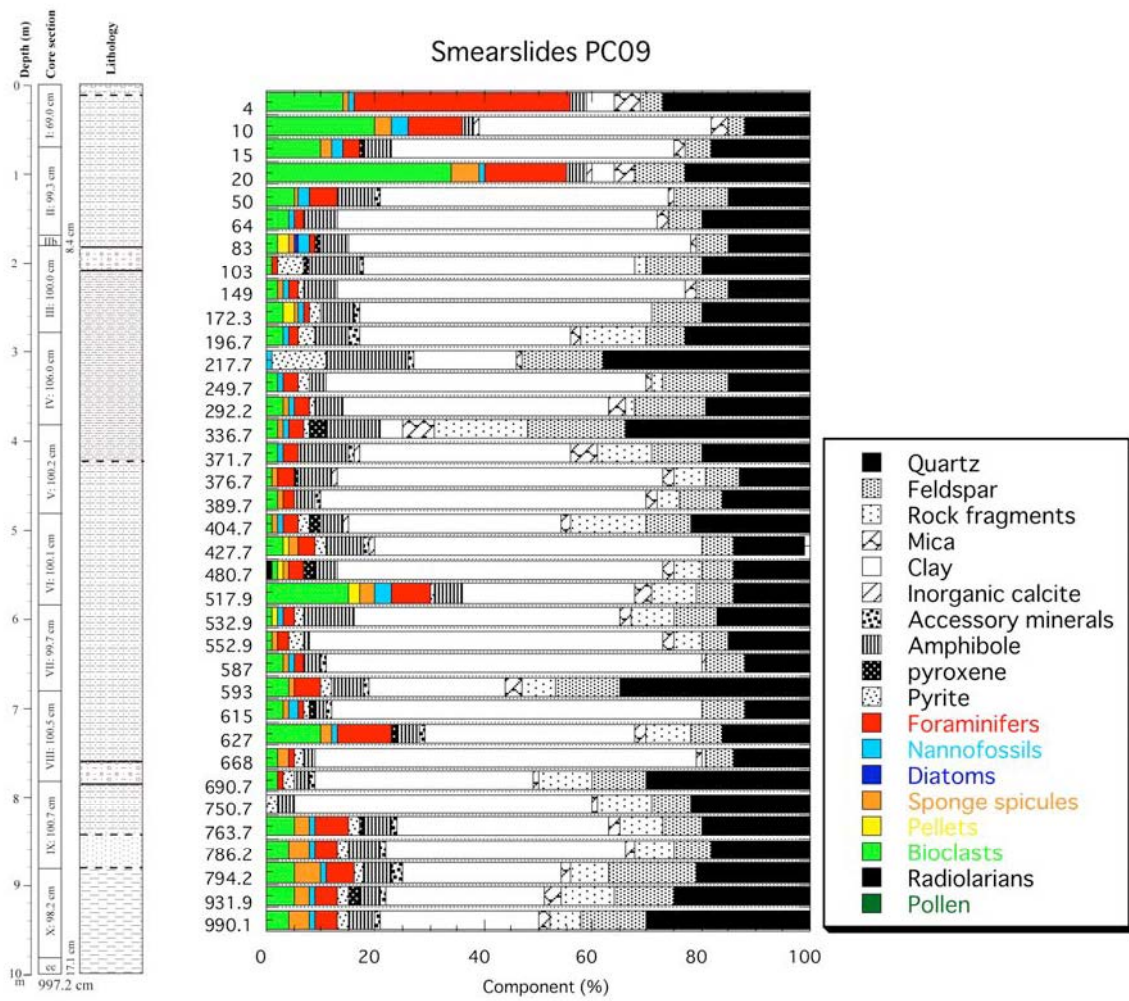
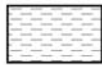


Figure 6-8-4-11: Composition of sediments of PC-09.

Lithology

	Clay/Silty clay
	Silt/Clayey silt
	Clay with lamina/patches
	Silt with lamina/patches
	Very fine sand
	Fine to medium sand

Boundary

	Lithological boundary
	Gradual boundary
	Irregular boundary

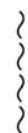
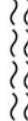
Structure

	Soopy
	Flow-in
	Lenticular lamina/bed
	Cross lamina
	Parallel lamina
	Isolated pebble (Ice rafted debris)
	Patches
	Gas void
	Gas crack (> 1 mm)
	Gas crack (< 1 mm)
	Shell (complete)
	Shell fragments
	Bioclasts

Core disturbance

	Slightly disturbed
	Moderately disturbed
	Very disturbed

Bioturbation

	Slightly bioturbated
	Heavily bioturbated

Symbols used for visual core description.

Figure 6-8-4-12: Legend for core description.

2-4-6 Sediment core sampling at the Chile triple junction area

by Ryo Anma, Kiichiro Kawamura, Yuji Orihashi and Masamu Aniya

Overall aim for the sediment core sampling offshore of the Taitao peninsula is to understand average composition of sediments flowing into the trench from Rio Baker through Golfo de Penas and its temporal changes. Because the Rio Baker has large watershed across the Andes, we expect to obtain average crust composition of this area. We also aim to estimate rate of sedimentation near the trench.

Site summary of PC04 is described in Table 2-4-6-1. Site PC04 (Figure 2-4-6-1) was selected because the site is located nearby the channel that connects to the mouth of the Golfo de Penas, located slightly off from the mid-axis of the channel to secure depositional environment, and located at the edge of submarine fan that deposited sediments from NE. A piston corer of 10m long with core liner was used for sampling.

Visual core description (VCD) was made on split surface of working half section, that was scraped using a glass plate to expose fresh surface. Lithological and sedimentological features were described on a VCD spreadsheet (see “Supplementary materials” PC04_VCD.pdf file) for each section. Principal sediment lithology name was first described on core and then confirmed under a microscope (see “Supplementary materials” Smearslides_PC04.xls). Information in the VCD spread sheets and smear slide summary were utilized to create the stratigraphical column of PC04 (Figure 2-4-6-3). We adopted the IODP-style nomenclature for lithological description of siliciclastic rocks (e.g., Mazzullo et al., 1988) observed in PC04.

Color reflectance was measured at 2 cm intervals using archive halves using a Minolta Photospectrometer CM-2002. Photographs were then taken using a digital camera (Nikon D1x). Figure 2-4-6-2 shows photographic image of PC04 with shutter speed adjusted at 1/20 to 1/10 and F value at 8 to 9. Results of color reflectance are summarized in Figures 2-4-6-4. The following is brief description of PC04 and interpretation based on visual core description. For detailed description, see “Supplementary materials” PC04_VCD.pdf file.

Core PC04 mainly consists of dark greenish gray to dark gray silty to sandy clay. Nannofossils were commonly observed throughout the PC04. Only three thin (less than 2 cm) layers of dark olive gray sand were observed in upper 111.5 cm interval. This interval does not contain ice rafted debris (IRD). In contrast, below 111.5 cm, thicker (usually 1 to 2 cm thick, max. 8 cm) sand layers are frequently distributed in 39 horizons in the lower part of the PC04 (interval 111.5 – 856.2 cm). IRDs were observed in the upper part of this interval implying

glacial advance. Sandy layers include grains of quartz, feldspars and mica, and are commonly graded. Normal grading and anti-grading were almost evenly observed (Figure 2-4-6-3). Boundaries between sand layer and overriding clay are usually irregular and wavy, suggesting strong current. We consider that each sand layer in the lower section recorded turbiditic flow event. Turbidite deposits are typically 7 to 20 cm thick. We tentatively interpreted as turbiditic current flowed along the mid axis of the main channel. Sediments in the upper interval could be deposited after the formation of submarine fan that dam up and cut off the sediment supply through the channel. Another possibility is that sediments derived from the Taitao ridge were continuously deposited through SW-ward channel that supplied sediments to the submarine fan system, but sediment supply was stopped at PC04 site because of change in flow direction. Thus, our future plan include detailed study of textures (+ anisotropy of magnetic susceptibility) and estimating paleo-current direction by combining textural data with paleomagnetic data.

Core ID	Date	Latitude	Longitude	Depth	Core length
PC04 (St.27)	2009.3.3	46°39.29' S	75°54.05' W	3319 m	856.2 cm

Table 2-4-6-1: Summary of piston core PC04 operation.

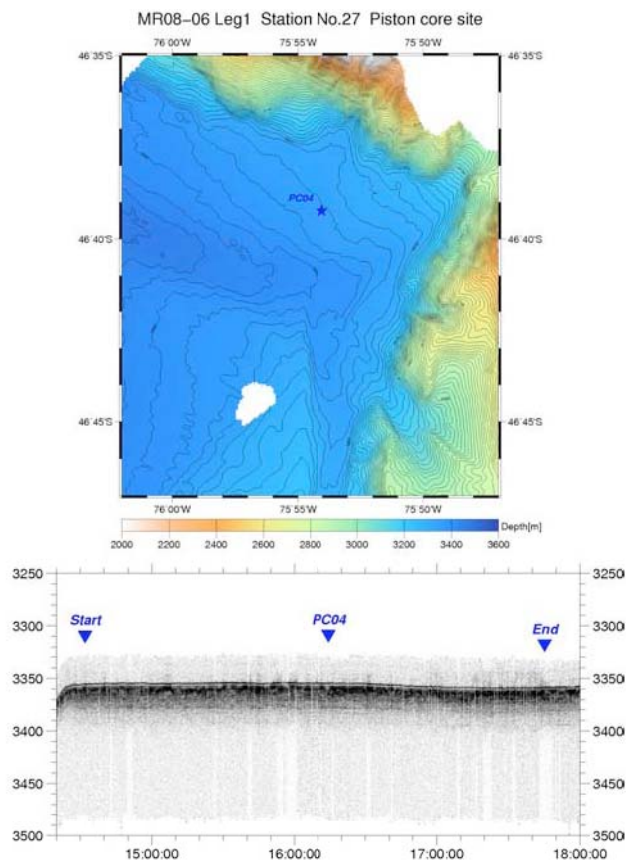
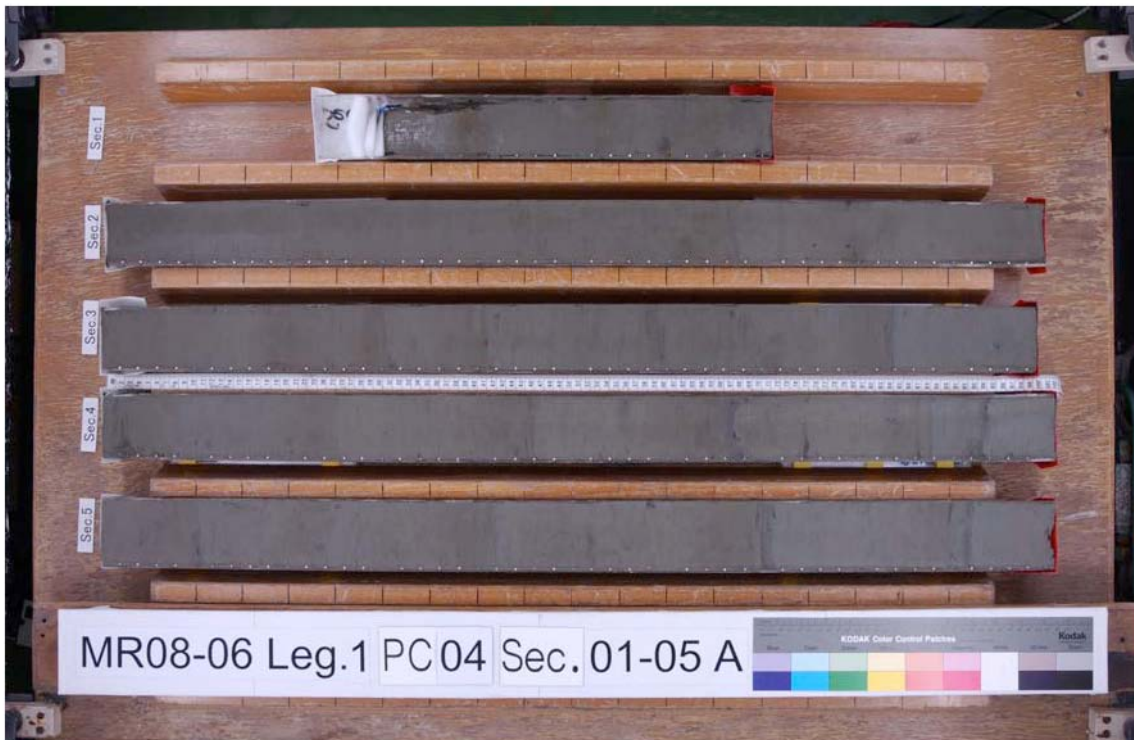


Figure 2-4-6-1: Bathymetric map around site PC04 and sub-bottom profiles during the coring.



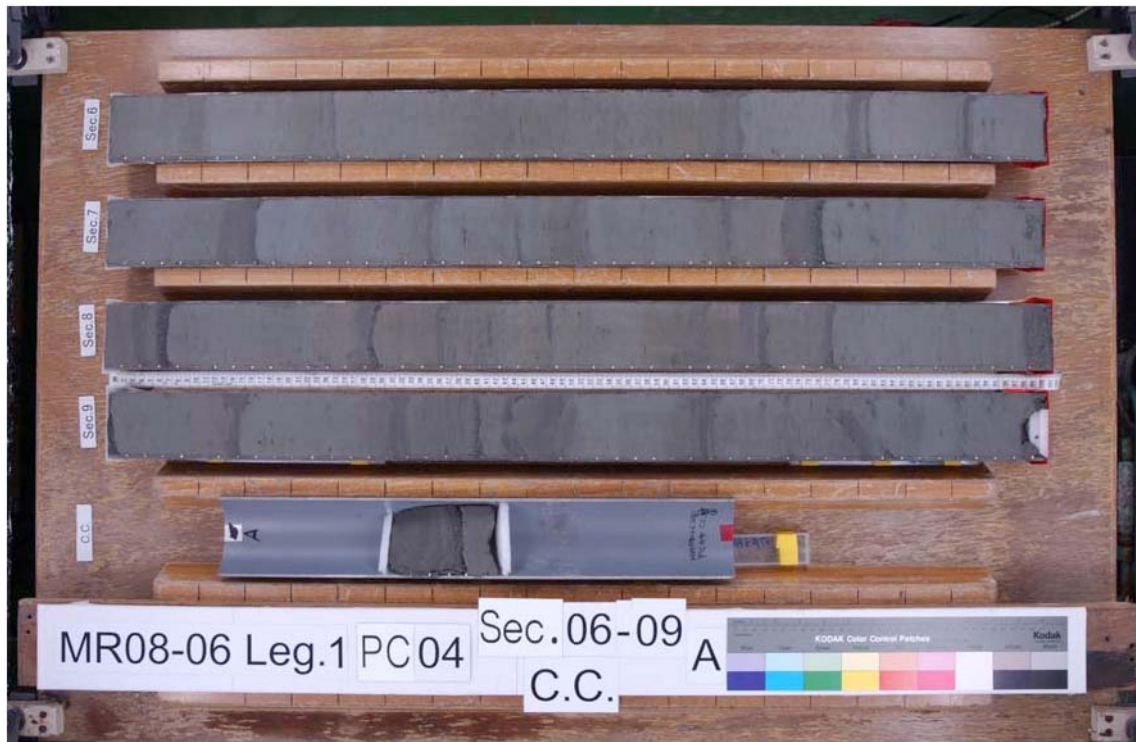


Figure 2-4-6-2: Photograph of the MR08-06 PC04.

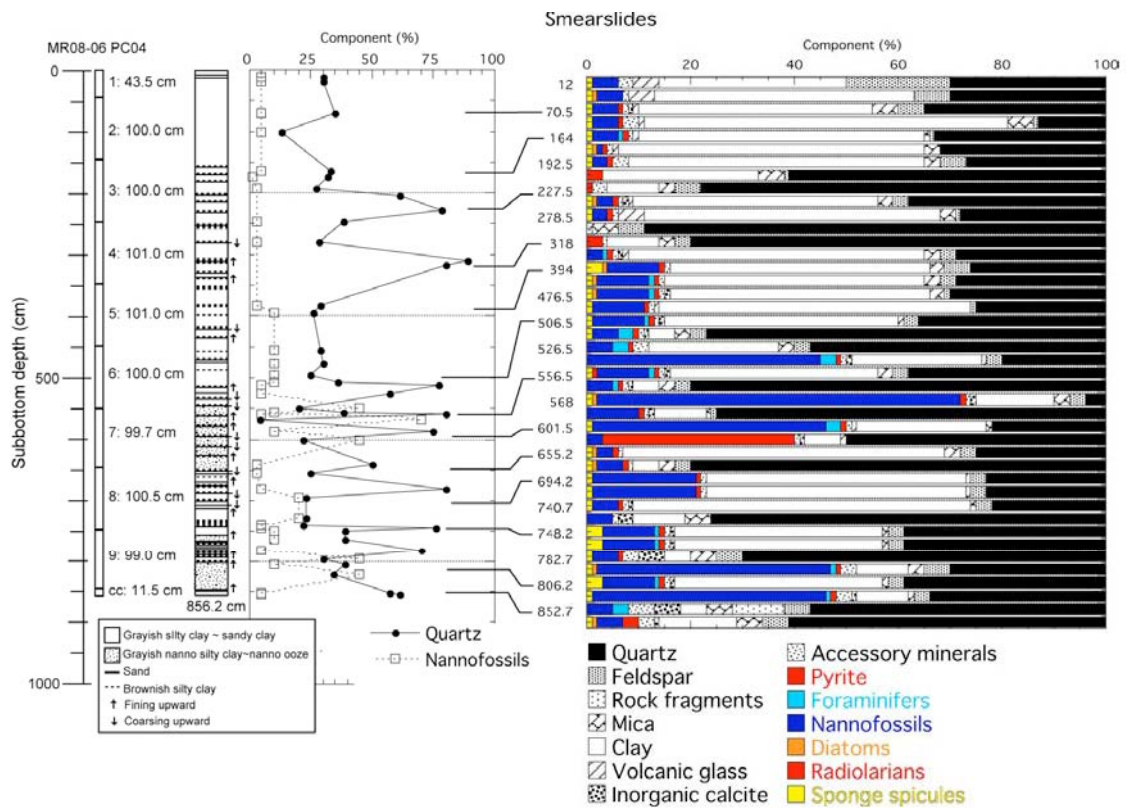


Figure 2-4-6-3: Summary of smear slide description for the MR08-06 PC04

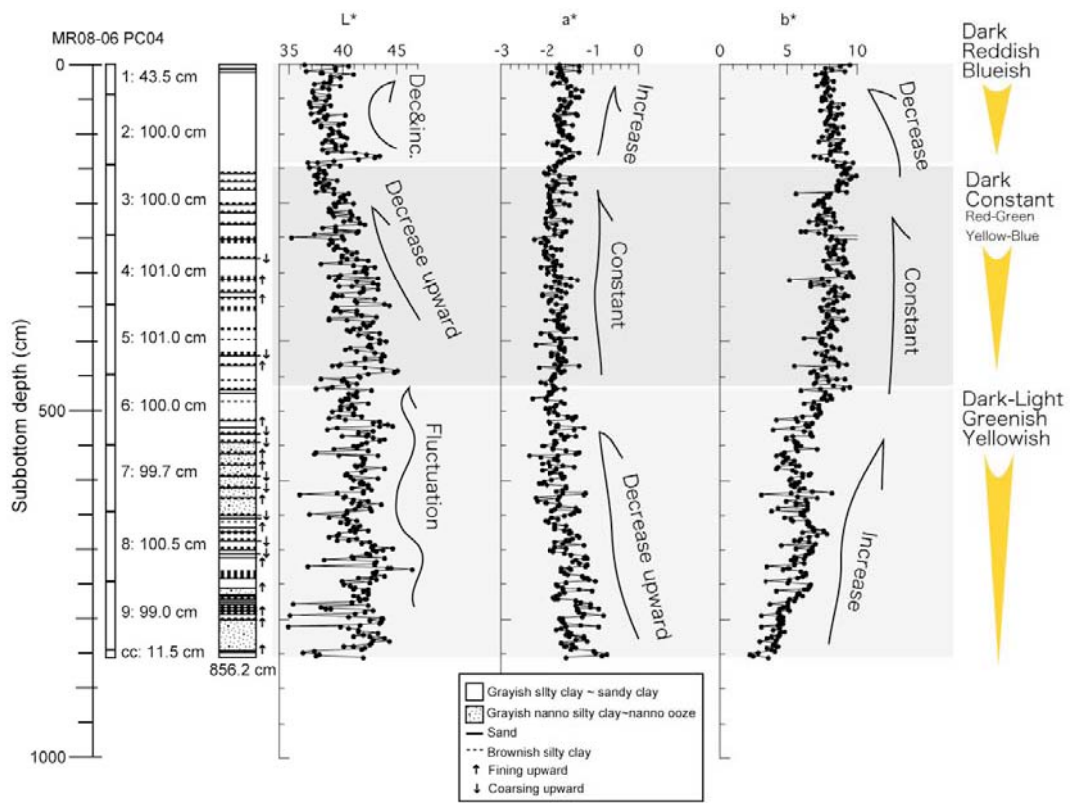


Figure 2-4-6-4: Color image of the MR08-06 PC04.

2-5. Petit-spot volcanoes, “Expedition of petit-spot VI”

by N. Hirano, N. Abe, S. Machida, MWJ, NME & GODI

Three times dredge operations were taken off-shore of Valparaiso during MR08-06 Leg1b. The positions and samples are listed in table 1-4-3. Single channel seismic surveys were also taken in this area (Fig. 2-5-1). Details of the single channel seismic survey are section 3-2. “Single channel seismic surveys of MR08-06 Leg1b” and Appendix data.

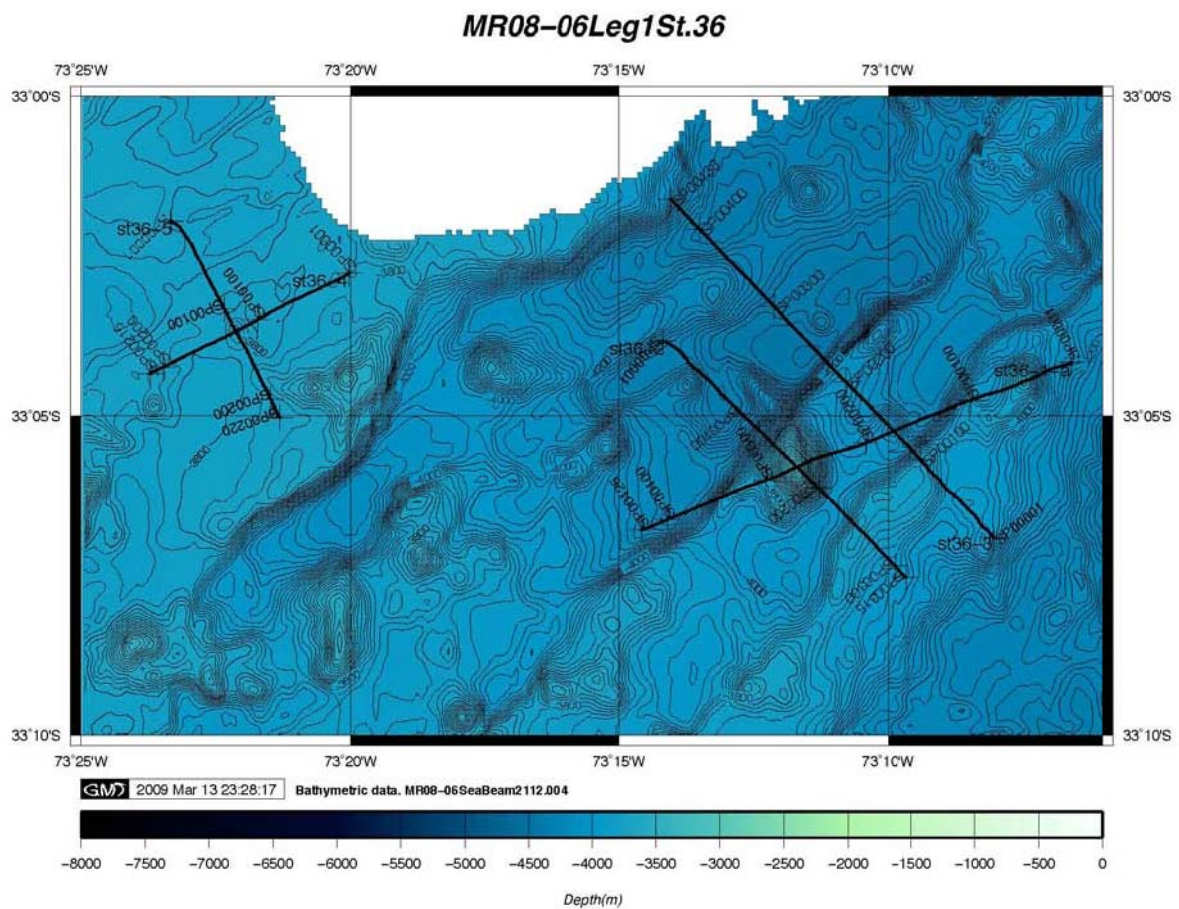


Fig. 2-5-1 Single channel seismic survey lines in the petit-spot VI research area.

2-6 Genetic diversity of planktonic foraminifera

(1) Personnel

Atsushi Kurasawa (Hokkaido University/JAMSTEC)

Masashi Tsuchiya (JAMSTEC)

Takashi Toyofuku (JAMSTEC)

Hiroshi Kitazato (JAMSTEC)

Hiroshi Nishi (Hokkaido University)

(2) Objectives

Marine planktonic species exhibit broad distributions and are assumed to form genetically continuous populations since they are considered to have high dispersal ability. However, recent molecular phylogenetic studies revealed that many marine planktonic groups show high intra-specific genetic diversity (i.e. Knowlton, 1993). Occasionally the distribution patterns show different trends among genotypes, which may reflect different environmental preferences. Furthermore, subtle morphological differences among genotypes are also recognized in various marine planktonic taxa (i.e. Huber *et al.*, 1997; Saez *et al.*, 2003; Mann *et al.*, 2004). These results suggest that the diversity of the marine planktonic organisms have been overlooked, and these genotypes may represent cryptic species.

Planktonic foraminifer is a single-celled calcite secret organism, which can be found in surface seawater around the world. Identification of planktonic foraminiferal species are based on morphological characters of test, however, molecular phylogenetic studies have revealed the presence of genetically discrete groups (genotypes) within many morphological species (i.e. Huber *et al.*, 1997; Darling *et al.*, 1999, 2000; Stewart *et al.*, 2001; de Vargas *et al.*, 1999). Some of the distribution patterns of these genotypes are correspond to oceanic provinces and oceanic current systems, which potentially reflect the distinct ecological features of each genotype. Revealing the biogeography of planktonic foraminiferal genotypes and its correlations to oceanic environments in the Pacific is essential to reconstruct the divergence and formation of genotype and the gene flow between the Northern and Southern hemisphere.

In order to reveal the genetic diversity of planktonic foraminifera, we have studied the molecular phylogenetic and biogeography of *Globigerina bulloides* in the Northwestern Pacific. Our previous study (Kurasawa, 2007MS) shows that the distribution patterns of the genotypes of *G. bulloides* exhibit good correlation with the water mass structures. However, the

genetic diversity in the South Pacific is largely unknown hence whether bipolarity of planktonic foraminiferal genotypes, which is reported for some genotypes in the Atlantic, also exists in the Pacific is not clarified. The Objective of this study is (i) to reveal the genetic diversity of *G. bulloides* and other planktonic foraminifera in the North and the South Pacific, (ii) to reveal the correlation between the biogeography of genotype and the oceanic environments, and (iii) to reconstruct the patterns of gene flow within the Pacific and gene flow between the Pacific and other oceans. In order to collect living planktonic foraminiferal specimens for molecular phylogenetic analysis, we conducted surface seawater filtration sampling (pump method) and plankton net sampling.

(3) Instruments and Method

a) Surface seawater filtration sampling (Pump method)

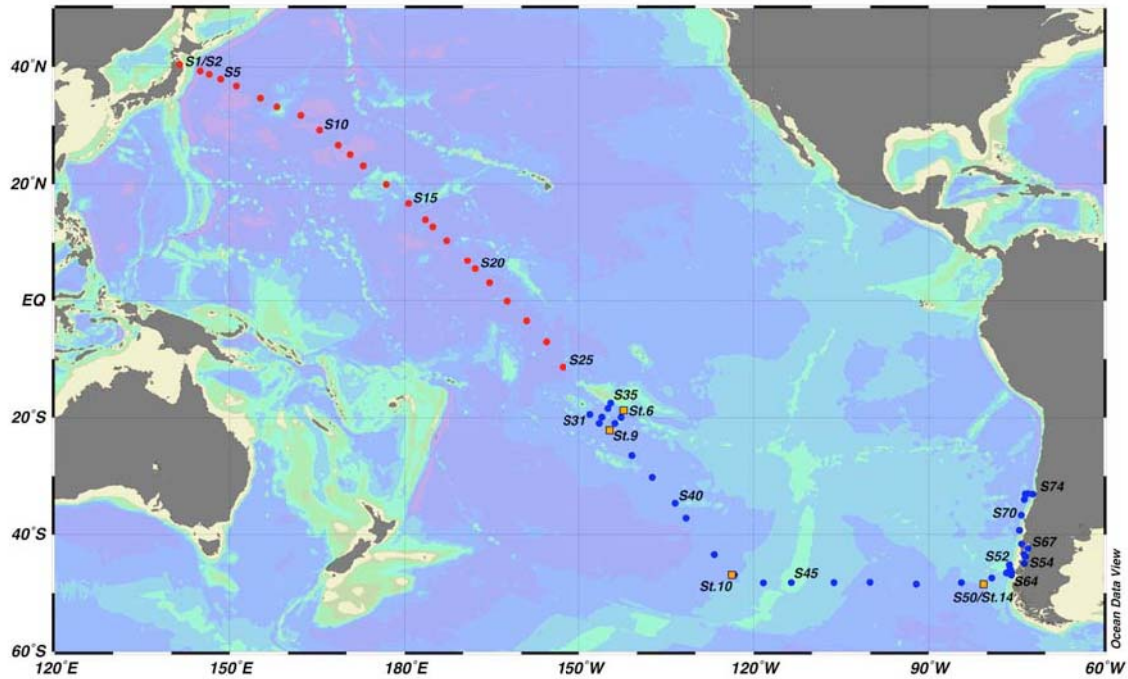
Sea surface Plankton samples were collected by filtering surface seawater in the laboratory during ship navigation. Sampling location, sampling time, water temperature, and number of sorted specimens were recorded. A Filtering apparatus (100 μm mesh) was used to filter planktonic foraminifera (2-6-fig1). The apparatus was connected to seawater supply tap and placed in a bucket. Surface seawater was filtrated for several hours at each sampling sites. Pumping methods were carried out for 66 times during navigation (2-6-fig2, 2-7-table1).



2-6-fig 1 Surface water filtration apparatus consists of 100 μm opening mesh and glass bottle.

2-7-table1. Surface seawater filtration sampling locations.

Sample Name	Start latitude			Start longitude			End latitude			End longitude			Starting Date (UTC)		DNA extraction and PCR
	degree	minute	N/S	degree	minute	E/W	degree	minute	N/S	degree	minute	E/W	Date	Time	
S1	40	26.95	N	141	26.95	E	40	11.61	N	142	37.75	E	2009.1.16	9:09	10
S2	40	26.95	N	141	26.95	E	40	11.61	N	142	37.75	E	2009.1.16	9:09	5
S3	39	18.82	N	144	55.83	E	39	07.51	N	145	27.34	E	2009.1.16	21:32	4
S4	38	44.52	N	146	30.56	E	38	31.42	N	147	00.00	E	2009.1.17	4:56	
S5	37	56.03	N	148	27.40	E	37	28.22	N	149	39.32	E	2009.1.17	14:01	
S6	36	46.41	N	151	10.38	E	36	01.54	N	152	33.37	E	2009.1.18	2:56	
S7	34	38.45	N	155	18.50	E	34	13.16	N	156	07.68	E	2009.1.18	22:33	3
S8	33	11.54	N	158	06.40	E	32	32.05	N	159	23.87	E	2009.1.19	11:58	2
S9	31	44.78	N	162	13.01	E	31	38.94	N	162	51.64	E	2009.1.20	10:09	
S10	29	14.18	N	165	23.79	E	28	39.46	N	166	06.43	E	2009.1.21	5:06	
S11	26	38.29	N	168	37.20	E	25	49.91	N	169	36.85	E	2009.1.22	1:05	
S12	25	02.22	N	170	39.69	E	23	57.94	N	171	05.87	E	2009.1.22	13:21	
S13	23	08.55	N	172	56.56	E	22	26.90	N	173	47.05	E	2009.1.23	2:30	
S14	19	57.23	N	176	51.03	E	19	08.07	N	177	51.13	E	2009.1.24	3:03	
S15	16	42.15	N	179	19.71	W	15	51.46	N	178	26.06	W	2009.1.25	3:31	
S16	13	55.85	N	176	26.07	W	13	02.46	N	175	29.91	W	2009.1.25	23:17	
S17	12	42.11	N	175	08.79	W	12	10.02	N	174	37.26	W	2009.1.26	8:13	
S18	10	21.82	N	172	45.31	W	9	27.01	N	171	49.79	W	2009.1.27	1:09	
S19	6	52.58	N	169	12.07	W	5	52.65	N	168	12.71	W	2009.1.28	1:15	
S20	5	28.97	N	167	51.69	W	4	56.44	N	167	18.41	W	2009.1.28	9:54	
S21	3	02.29	N	165	25.79	W	2	31.62	N	164	56.53	W	2009.1.29	2:32	
S22	0	03.36	S	162	24.03	W	0	42.13	S	161	46.55	W	2009.1.30	2:17	
S23	3	27.32	S	159	04.73	W	4	12.29	S	158	21.87	W	2009.1.31	2:17	1
S24	7	00.45	S	155	37.21	W	7	38.85	S	154	59.84	W	2009.2.1	2:12	
S25	11	21.94	S	152	49.23	W	15	09.55	S	150	51.57	W	2009.2.2	2:32	
S26	11	21.94	S	152	49.23	W	15	09.55	S	150	51.57	W	2009.2.3	1:38	
S31	19	27.77	S	148	02.90	W	20	45.56	S	146	44.39	W	2009.2.7	18:49	
S32	20	57.24	S	146	26.31	W	20	35.55	S	146	17.81	W	2009.2.8	8:16	
S33	19	55.62	S	146	01.41	W	19	55.20	S	146	01.48	W	2009.2.9	0:35	
S34	18	25.58	S	144	59.18	W	18	25.15	S	144	59.32	W	2009.2.9	17:26	
S35	17	29.90	S	144	30.41	W	17	43.35	S	144	08.44	W	2009.2.10	6:29	
S36	19	56.38	S	142	41.97	W	21	00.92	S	143	47.63	W	2009.2.11	17:50	
S37	20	57.14	S	143	45.30	W	20	57.56	S	143	50.21	W	2009.2.12	6:30	
S38	26	28.35	S	140	50.35	W	27	41.45	S	139	43.94	W	2009.2.14	0:34	
S39	30	12.81	S	137	22.26	W	31	57.47	S	135	58.82	W	2009.2.14	19:29	
S40	34	37.53	S	133	27.38	W	36	35.04	S	131	56.10	W	2009.2.15	19:27	
S41	37	09.59	S	131	32.23	W	38	34.28	S	130	29.54	W	2009.2.16	7:56	
S42	43	23.71	S	126	43.68	W	44	52.72	S	125	34.82	W	2009.2.17	18:46	
S43	46	49.89	S	123	40.29	W	46	49.22	S	123	40.30	W	2009.2.18	18:51	
S44	48	14.96	S	118	18.97	W	48	09.78	S	118	27.38	W	2009.2.20	17:15	
S45	48	09.85	S	113	30.62	W	48	10.42	S	111	37.45	W	2009.2.21	19:17	
S46	48	10.43	S	106	11.59	W	48	04.99	S	103	33.11	W	2009.2.22	17:40	
S47	48	08.68	S	100	03.04	W	48	11.79	S	98	49.58	W	2009.2.23	16:22	
S48	48	29.12	S	92	06.60	W	48	31.81	S	91	10.04	W	2009.2.24	16:57	
S49	48	12.47	S	84	21.39	W	48	14.03	S	81	55.20	W	2009.2.25	15:09	5
S50	48	25.01	S	80	28.41	W	48	20.65	S	80	24.67	W	2009.2.26	11:58	
S51	47	24.91	S	79	08.20	W	46	18.43	S	77	38.06	W	2009.2.27	4:43	
S52	45	08.96	S	76	07.80	W	44	27.64	S	75	14.88	W	2009.2.27	19:43	
S53	43	24.61	S	73	35.62	W	44	13.72	S	73	25.39	W	2009.2.28	11:20	
S54	44	55.19	S	73	33.38	W	45	26.12	S	73	57.84	W	2009.2.28	17:38	
S55	46	19.92	S	76	05.77	W	46	19.81	S	75	47.24	W	2009.3.1	13:51	
S56	46	19.81	S	75	45.57	W	46	17.09	S	75	28.53	W	2009.3.1	17:16	
S57	46	53.99	S	75	47.04	W	46	38.35	S	75	47.73	W	2009.3.2	15:25	
S58	46	39.32	S	75	53.99	W	46	38.76	S	75	53.79	W	2009.3.3	14:35	
S59	46	32.52	S	76	39.49	W	46	17.64	S	76	42.64	W	2009.3.3	22:23	3
S60	46	02.42	S	75	53.77	W	45	59.44	S	76	49.86	W	2009.3.4	18:15	
S61	46	04.29	S	75	54.10	W	46	05.71	S	75	53.35	W	2009.3.6	12:14	
S62	46	06.38	S	75	52.79	W	46	09.79	S	75	47.86	W	2009.3.6	18:14	
S63	46	28.41	S	75	51.84	W	46	29.47	S	75	52.25	W	2009.3.7	13:34	
S64	46	33.33	S	75	57.99	W	46	36.63	S	75	50.47	W	2009.3.7	18:31	
S65	45	52.46	S	75	59.48	W	45	55.42	S	75	36.39	W	2009.3.8	13:17	3
S66	43	46.47	S	73	21.39	W	42	43.57	S	72	53.41	W	2009.3.9	9:52	
S67	42	21.43	S	72	55.86	W	41	51.23	S	73	25.32	W	2009.3.9	15:32	
S68	41	35.83	S	74	02.54	W	40	34.42	S	74	17.02	W	2009.3.9	20:11	
S69	39	17.29	S	74	23.94	W	37	53.35	S	74	24.13	W	2009.3.10	5:24	
S70	36	40.69	S	74	06.58	W	35	39.98	S	73	53.67	W	2009.3.10	16:01	
S71	34	00.63	S	73	32.44	W	33	37.18	S	73	27.08	W	2009.3.11	3:16	5
S72	33	00.13	S	72	58.97	W	33	05.49	S	73	12.42	W	2009.3.11	11:55	
S73	33	03.72	S	73	22.03	W	33	04.41	S	73	19.35	W	2009.3.12	13:14	
S74	33	06.53	S	72	07.82	W	32	57.06	S	71	52.28	W	2009.3.13	9:15	4



2-6-fig 2 Locations of sampling sites. Red dots: surface seawater filtration sites (starting locations) during LEG 1a, blue dots: surface seawater filtration sites during LEG 1b, orange square: plankton net sampling sites.

2-7-table2 Plankton net sampling locations and numbers of picked foraminifera.

Station	Date	Sample Name	Latitude		Longitude		Depth (m)	Number of picked forams	DNA extraction and PCR		
			degree	minute	N/S	degree				minute	E/W
St. 6	2009.2.10	N06-1	18	48.25	S	142	17.61	W	0-200	114	
		N06-2	18	48.18	S	142	17.64	W	0-200	77	
St. 9	2009.2.12	N09-1	22	10.11	S	144	41.94	W	0-200	24	
		N09-2	22	10.13	S	144	41.37	W	0-200	12	
St. 10	2009.2.19	N10-1	46	52.34	S	123	19.02	W	0-200	44	5
		N10-2	46	52.35	S	123	19.06	W	0-200	83	
St. 14	2009.2.26	N14-1	48	25.62	S	80	29.16	W	0-200	48	
		N14-2*	48	25.70	S	80	29.28	W	0-200	-	
		N14-3	48	25.78	S	80	29.23	W	0-200	68	5

*Unsuccessful cast

b) Plankton net sampling

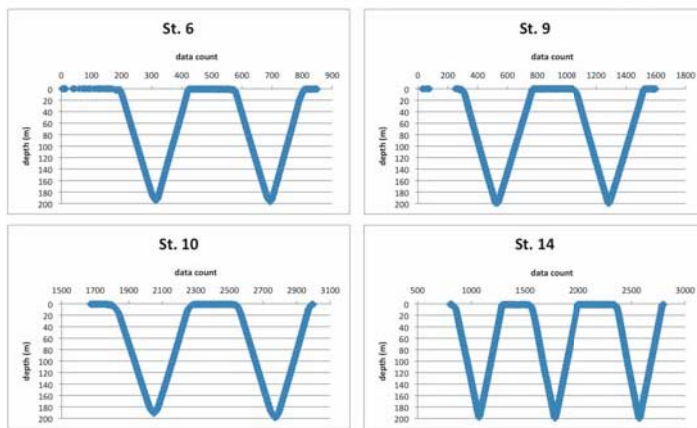
Samples were collected with NORPAC plankton net (45 cm diameter, 100 μ m opening mesh). The plankton net was towed vertically from 200 m in wire-out length to the sea surface. The net was washed with surface seawater and the recovered samples were collected in plastic bottles and kept at 4 °C until picking of specimens. A CTD logger (Star-Oddi Ltd., DST-CTD) was attached to the ring of the net to obtain the sampling depths, temperature and salinity profiles of the water column. Plankton net sampling was conducted at four sites during leg 1b and towing was conducted at least twice at each sampling sites (2-7-table2).

c) Onboard sample treatment

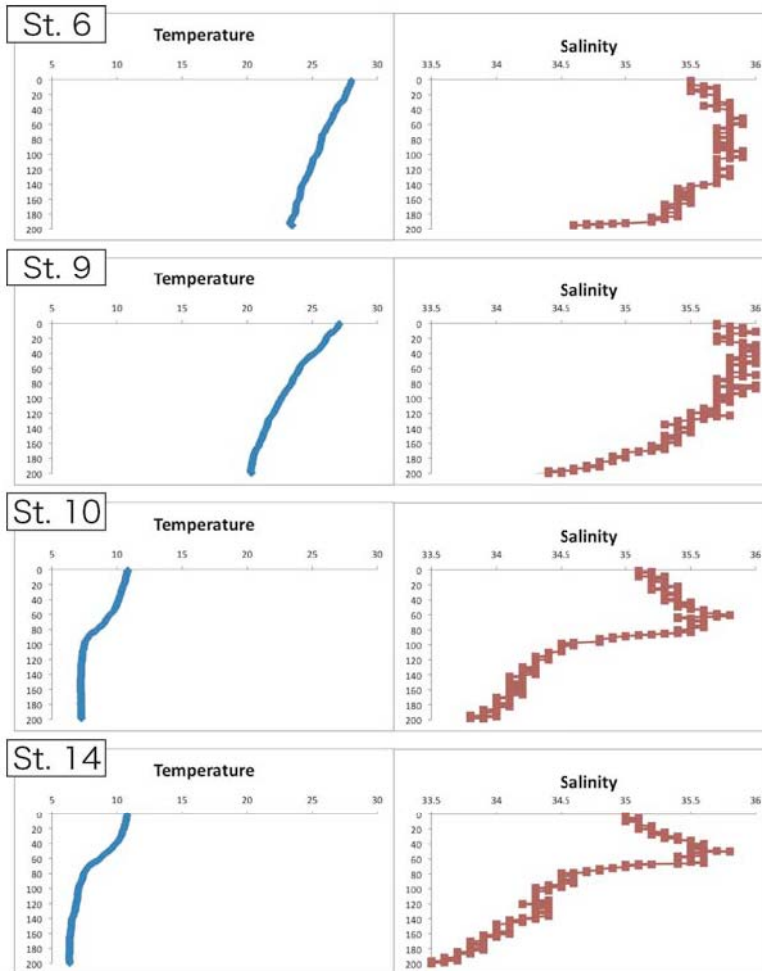
Living planktonic foraminifera were picked under stereomicroscope with needles and fine brushes and transferred on faunal slides. Specimens were air dried on the slides and stored at -80 °C. Residue of the samples were stored in plastic bags at -80 °C. DNA extraction and PCR amplification of small subunit ribosomal DNA (SSU rDNA) were carried out for some *G. bulloides* specimens (2-7-table1, 2-7-table2). Total DNA was extracted with Guanidine buffer (modified from Pawlowski, 2000). PCR amplification was carried out with TaKaRa *Ex Taq* (TaKaRa Bio inc., Japan). *G. bulloides* specific primer s14f1+40 (5'-ACGCGGAAAAGCTTATCTGGT-3') and universal primer sB-2A (5'-TTCTGCAGGTTACCTACGGATG-3') were used for amplifying approximately 1000 bp of 5'-terminal region of SSU rDNA. PCR condition consists of initial denature at 94°C for 5 minutes followed by 40 cycles of denature, annealing, and extension (94°C for 30 seconds, 55°C for 30 seconds, and 72°C for 1 minute, respectively) and final extension at 72°C for 5 minutes. Size of amplified products was confirmed by 1.5% agarose gel electrophoresis. Extracted DNA and PCR products were stored under -20 °C.

(4) Preliminary Results

The total numbers of picked foraminifera individuals from plankton net samples are listed in 2-7-table2. *G. bulloides* was found from S1, S2, S3, S7, and S8 in the North Pacific. In South Pacific, *G. bulloides* was found from high latitude sites (43°S and higher) and oceanic sites near Chile (S52-S74). *G. bulloides* was also found from low latitude area (S23, S32, S34). CTD logger data obtained during plankton net towing are shown in 2-6-fig3 and 2-6-fig4. CTD profiles at station 6 and 9 show similar properties, as well as station 10 and 14. As station 6 and 9 represent subtropical region while station 10 and 14 represent transitional region, different genotypes are expected from these two regions. The results of further molecular phylogenetic analysis will be significant data to understand the genetic diversity of planktonic foraminifera in the Pacific Ocean and the gene flow patterns between the Northern Pacific and Southern Pacific can be examined. Further molecular phylogenetic analysis and morphological observations will be carried out after cruise at JAMSTEC.



2-6-fig 3 Depth log of plankton net tows (data logging interval=2 seconds)..



2-6-fig 4 Vertical profiles temperature (left) and salinity (right) at plankton net sampling sites. Data was measured by the CTD logger during plankton net towing.

References

- Knowlton, N. (1993) Sibling species in the sea. *Annual Review of Ecology and Systematics* 24: 189-216.
- Huber, B., Bijma, J. and Darling, K. (1997) Cryptic speciation in the living planktonic foraminifer *Globigerinella siphonifera* (d'Orbigny). *Paleobiology* 23: 33-62.
- Saez, AG, Probert, I, Geisen, M, Quinn, P, Young, JR, Medlin, LK (2003) Pseudo-cryptic speciation in coccolithophores. *Proc Natl Acad Sci USA* 100:7163-7168.
- Mann, DG, McDonald, SM, Bayer, MM, Droop, SJM, Chepurnov, VA, Loke, RE, Ciobanu, A, du Buf, JMH (2004) The *Sellaphora pupula* species complex (Bacillariophyceae): morphometric analysis, ultrastructure and mating data provide evidence for five new species. *Phycologia* 43:459-482.
- Darling et al. (1999), The diversity and distribution of modern planktic foraminiferal SSU rRNA genotypes and their potential as tracers of present and past ocean circulations. *Paleoceanography* 14 (3), 3-12.
- Darling et al. (2000), Molecular evidence for genetic mixing of Arctic and Antarctic subpolar populations of planktonic foraminifers. *Nature* 404, 43-47.
- Huber et al. (1997), Cryptic speciation in the living planktonic foraminifer *Globigerinella siphonifera* (d'Orbigny). *Paleobiology* 23(1), 33-62.
- Stewart et al. (2001), Genotypic variability in subarctic Atlantic planktic foraminifera. *Marine Micropaleontology*. 43, 143-153.
- de Vargas et al. (1999), Molecular evidence of cryptic speciation in planktonic foraminifers and their relation to oceanic provinces. *Proc. Natl. Acad. Sci.* 96, 2864-2868.
- Kurasawa, A. (2007 MS) Genetic diversity of *Globigerina bulloides* d'Orbigny in the Western North Pacific inferred from ribosomal DNA sequences, and its correlation to test morphology and oceanographic environment. Master thesis, Hokkaido University.
- Pawlowski, J. (2000) Introduction to the molecular systematics of foraminifera. *Micropaleontology*. 46, supplement no. 1. 1-12.

2-7 Meteorological measurement

2-7-1 Surface Meteorological Observation

(1) Personnel

Kunio Yoneyama	(JAMSTEC) : Principal Investigator	Not on-board
Ryo Kimura	(Global Ocean Development Inc., GODI)	Leg1a,b
Asuka Doi	(GODI)	Leg1a,b
Satoshi Okumura	(GODI)	Leg1a
Wataru Tokunaga	(GODI)	Leg1b
Ryo Ohyama	(GODI)	Leg1b

(2) Objectives

Surface meteorological parameters are observed as a basic dataset of the meteorology. These parameters bring us the information about the temporal variation of the meteorological condition surrounding the ship.

(3) Methods

Surface meteorological parameters were observed throughout the MR08-06 cruise. During this cruise, we used two systems for the observation.

- i. MIRAI Surface Meteorological observation (SMET) system
- ii. Shipboard Oceanographic and Atmospheric Radiation (SOAR) system

i. MIRAI Surface Meteorological observation (SMET) system

Instruments of SMET system are listed in 2-8-1-table1 and measured parameters are listed in 2-8-1-table2. Data were collected and processed by KOAC-7800 weather data processor made by Koshin-Denki, Japan. The data set consists of 6-second averaged data.

ii. Shipboard Oceanographic and Atmospheric Radiation (SOAR) system

SOAR system designed by BNL (Brookhaven National Laboratory, USA) consists of major three parts.

- a) Portable Radiation Package (PRP) designed by BNL – short and long wave downward radiation.
- b) Zeno Meteorological (Zeno/Met) system designed by BNL – wind, air temperature, relative humidity, pressure, and rainfall measurement.
- c) Scientific Computer System (SCS) designed by NOAA (National Oceanic and Atmospheric Administration, USA) – centralized data acquisition and logging of all data sets.

SCS recorded PRP data every 6 seconds, Zeno/Met data every 10 seconds. Instruments and their locations are listed in 2-7-1-table3 and measured parameters are

listed in 2-8-1-table4.

We have checked the following sensors, before and after the cruise for the quality control as post processing.

i. Young Rain gauge (SMET and SOAR)

Inspect of the linearity of output value from the rain gauge sensor to change Input value by adding fixed quantity of test water.

ii. Barometer (SMET and SOAR)

Comparison with the portable barometer value, PTB220CASE, VAISALA.

iii. Thermometer (air temperature and relative humidity) (SMET and SOAR)

Comparison with the portable thermometer value, HMP41/45, VAISALA.

(4) Preliminary results

2-7-1-fig1 shows the time series of the following parameters;

Wind (SOAR)

Air temperature (SOAR)

Relative humidity (SOAR)

Precipitation (SOAR, Optical rain gauge)

Short/long wave radiation (SOAR)

Pressure (SOAR)

Sea surface temperature (SMET)

Significant wave height (SMET)

(5) Data archives

These meteorological data will be submitted to the Marine-Earth Data and Information Department (MEDID) of JAMSTEC just after the cruise. Corrected data sets will be available from K. Yoneyama of JAMSTEC.

(6) Remarks

i. SST (Sea Surface Temperature) data were available in the following periods.

07:45 16 Jan. 2009 – 01:56UTC 03 Feb. 2009

22:00 06 Feb. 2009 – 11:33UTC 13 Mar. 2009

2-7-1-Table1 Instruments and installations of MIRAI Surface Meteorological observation system

Sensors	Type	Manufacturer	Location (altitude from surface)
Anemometer	KE-500	Koshin Denki, Japan	foremast (24 m)
Tair/RH	HMP45A	Vaisala, Finland	
with 43408 Gill aspirated radiation shield		R.M. Young, USA	compass deck (21 m) starboard side and port side
Thermometer: SST	RFN1-0	Koshin Denki, Japan	4th deck (-1m, inlet -5m)
Barometer	AP370	Koshin Denki, Japan	captain deck (13 m) weather observation room
Rain gauge	50202	R. M. Young, USA	compass deck (19 m)
Optical rain gauge	ORG-115DR	Osi, USA	compass deck (19 m)
Radiometer (short wave)	MS-801	Eiko Seiki, Japan	radar mast (28 m)
Radiometer (long wave)	MS-202	Eiko Seiki, Japan	radar mast (28 m)
Wave height meter	MW-2	Tsurumi-seiki, Japan	bow (10 m)

2-7-1-Table2 Parameters of MIRAI Surface Meteorological observation system

Parameter	Units	Remarks
1 Latitude	degree	
2 Longitude	degree	
3 Ship's speed	knot	Mirai log, DS-30 Furuno
4 Ship's heading	degree	Mirai gyro, TG-6000, Tokimec
5 Relative wind speed	m/s	6sec./10min. averaged
6 Relative wind direction	degree	6sec./10min. averaged
7 True wind speed	m/s	6sec./10min. averaged
8 True wind direction	degree	6sec./10min. averaged
9 Barometric pressure	hPa	adjusted to sea surface level 6sec. averaged
10 Air temperature (starboard side)	degC	6sec. averaged
11 Air temperature (port side)	degC	6sec. averaged
12 Dewpoint temperature (starboard side)	degC	6sec. averaged
13 Dewpoint temperature (port side)	degC	6sec. averaged
14 Relative humidity (starboard side)	%	6sec. averaged
15 Relative humidity (port side)	%	6sec. averaged
16 Sea surface temperature	degC	6sec. averaged
17 Rain rate (optical rain gauge)	mm/hr	hourly accumulation
18 Rain rate (capacitive rain gauge)	mm/hr	hourly accumulation
19 Down welling shortwave radiation	W/m ²	6sec. averaged
20 Down welling infra-red radiation	W/m ²	6sec. averaged
21 Significant wave height (bow)	m	hourly

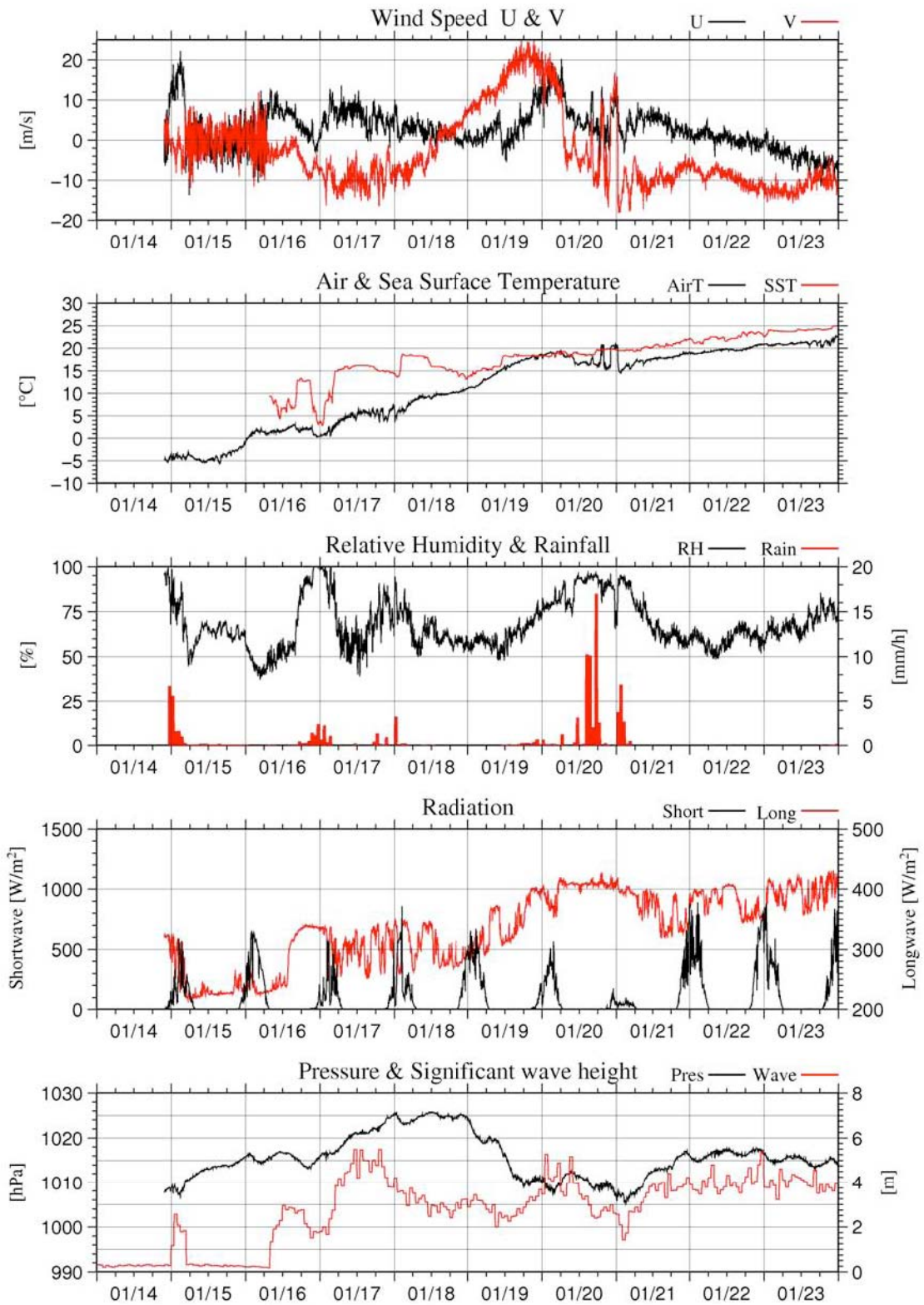
22 Significant wave height (aft)	m	hourly
23 Significant wave period (bow)	second	hourly
24 Significant wave period (aft)	second	hourly

2-7-1-Table3 Instruments and installation locations of SOAR system

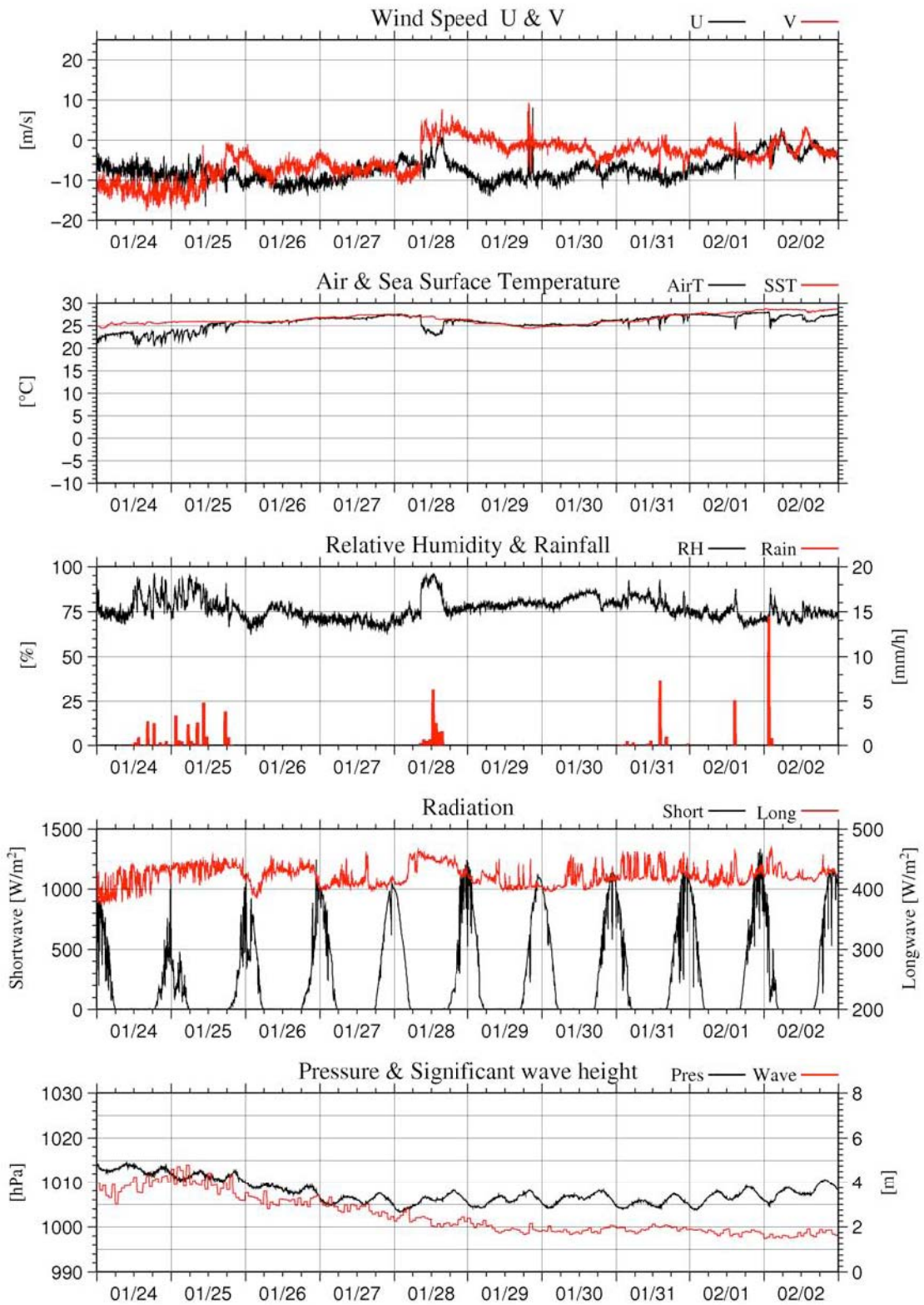
Sensors (Zeno/Met)	Type	Manufacturer	Location (altitude from surface)
Anemometer	05106	R.M. Young, USA	foremast (25 m)
Tair/RH	HMP45A	Vaisala, Finland	
with 43408 Gill aspirated radiation shield		R.M. Young, USA	foremast (23 m)
Barometer	61201	R.M. Young, USA	
with 61002 Gill pressure port		R.M. Young, USA	foremast (22 m)
Rain gauge	50202	R.M. Young, USA	foremast (24 m)
Optical rain gauge	ORG-115DA	Osi, USA	foremast (24 m)
Sensors (PRP)	Type	Manufacturer	Location (altitude from surface)
Radiometer (short wave)	PSP	Epply Labs, USA	foremast (24 m)
Radiometer (long wave)	PIR	Epply Labs, USA	foremast (24m)
Fast rotating shadowband radiometer		Yankee, USA	foremast (24 m)

2-7-1-Table4 Parameters of SOAR system

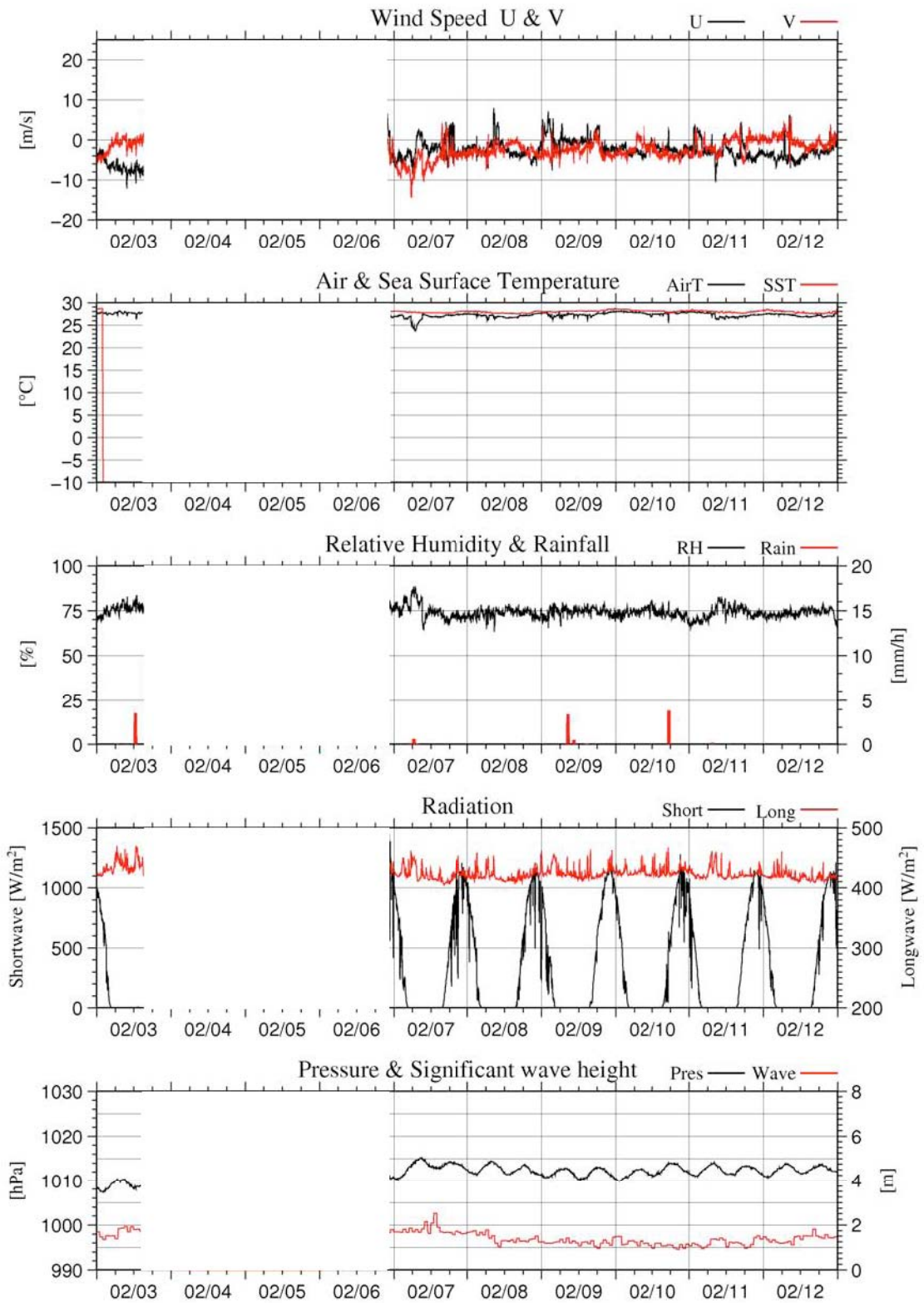
Parameter	Units	Remarks
1 Latitude	degree	
2 Longitude	degree	
3 SOG	knot	
4 COG	degree	
5 Relative wind speed	m/s	
6 Relative wind direction	degree	
7 Barometric pressure	hPa	
8 Air temperature	degC	
9 Relative humidity	%	
10 Rain rate (optical rain gauge)	mm/hr	
11 Precipitation (capacitive rain gauge)	mm	reset at 50 mm
12 Down welling shortwave radiation	W/m2	
13 Down welling infra-red radiation	W/m2	
14 Defuse irradiance	W/m2	



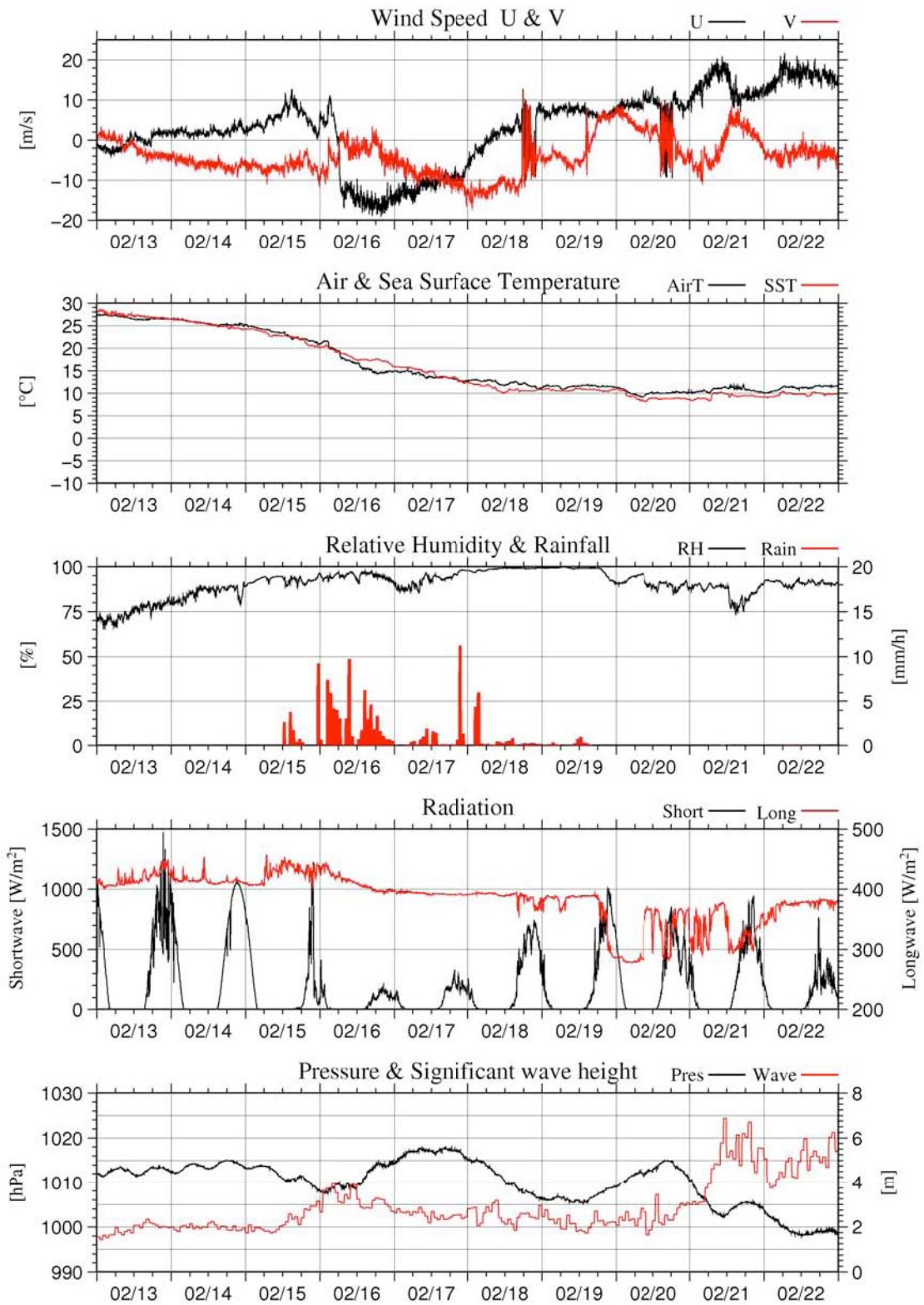
2-7-1-Fig1 Time series of surface meteorological parameters during the MR08-06 cruise



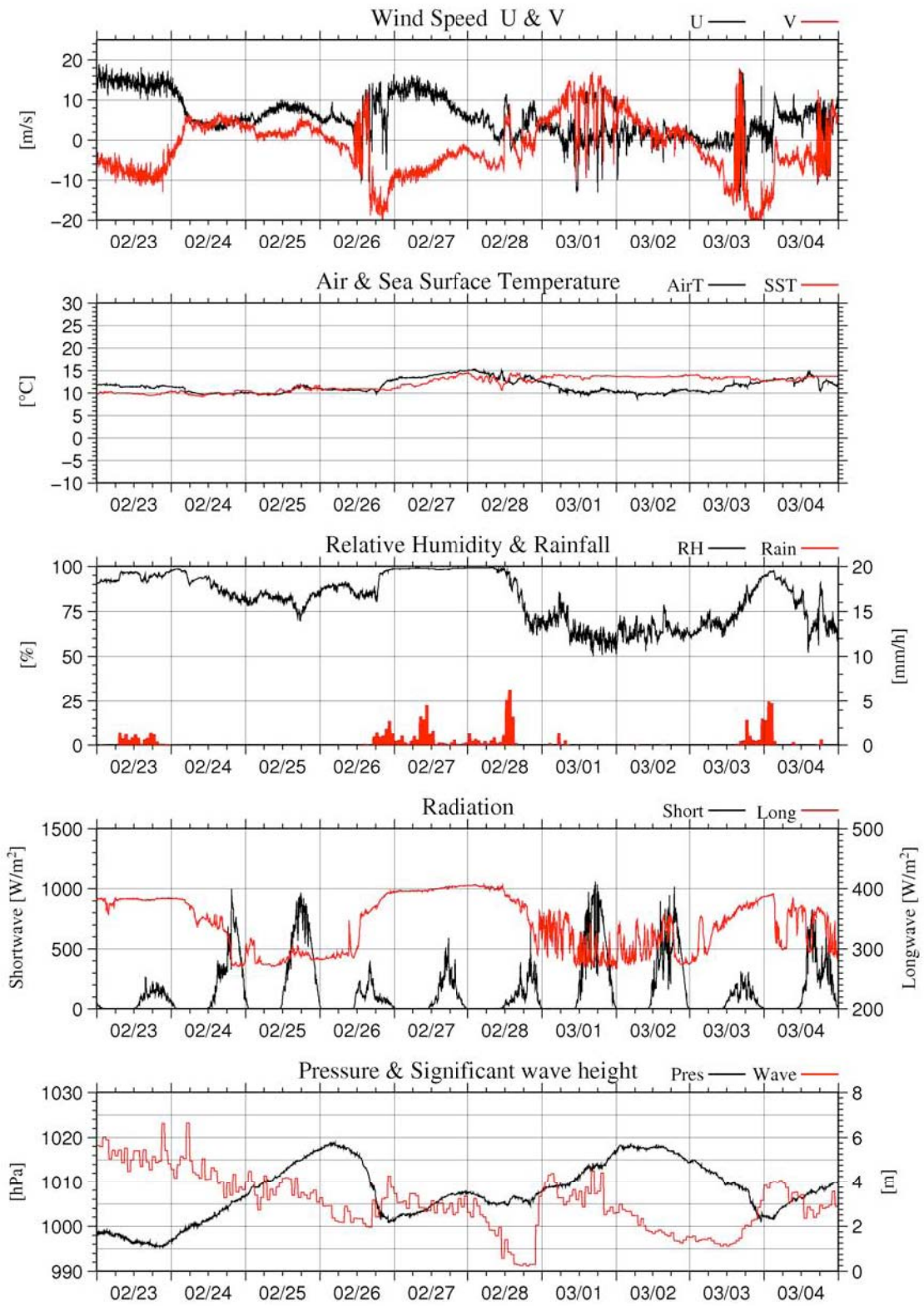
2-7-1-Fig1 (Continued)



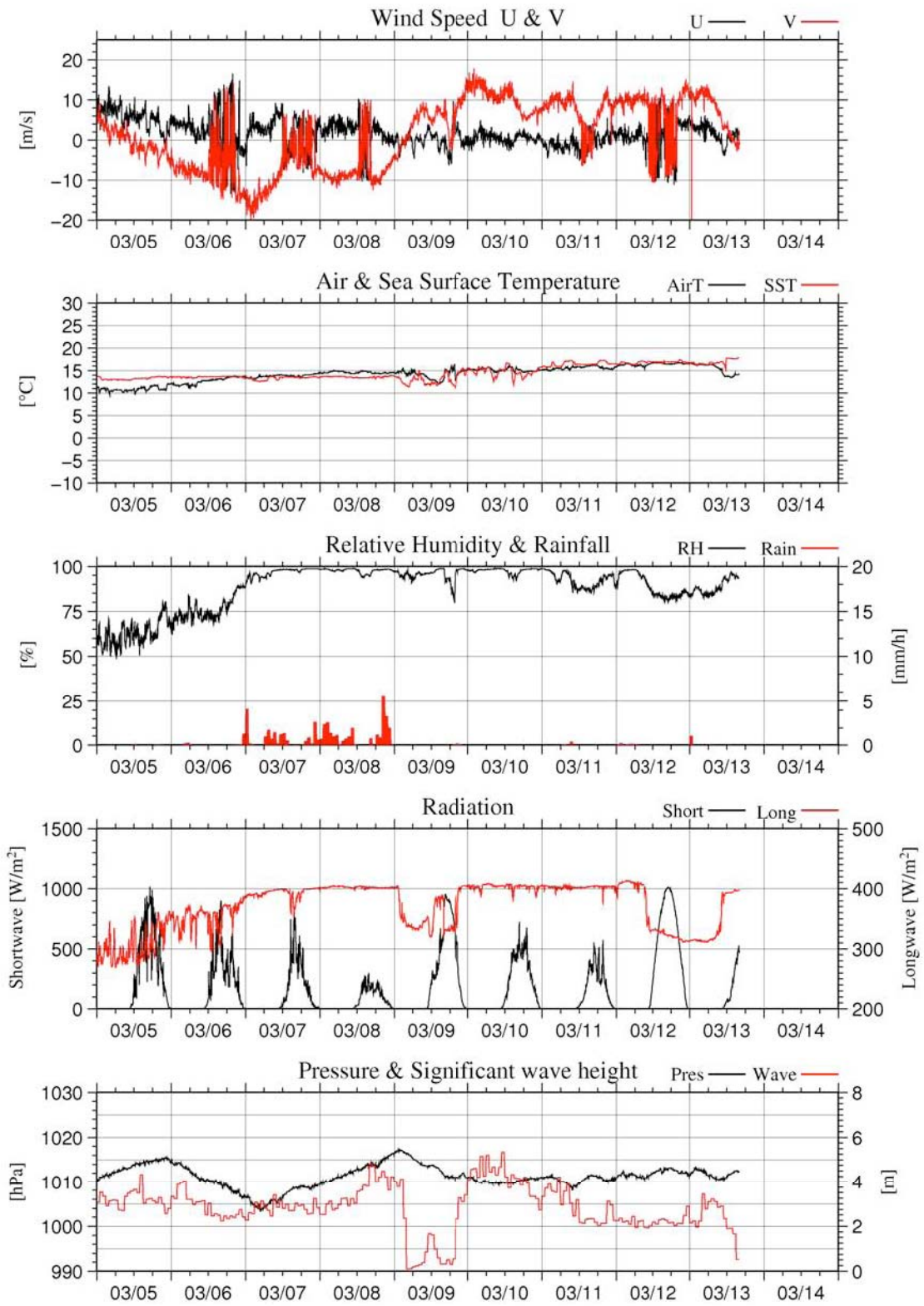
2-7-1-Fig1 (Continued)



2-7-1-Fig1 (Continued)



2-7-1-Fig1 (Continued)



2-7-1-Fig1 (Continued)

2-7-2 Ceilometer Observation

(1) Personnel

Kunio Yoneyama	(JAMSTEC) : Principal Investigator	Not on-board
Ryo Kimura	(Global Ocean Development Inc., GODI)	Leg1a,b
Asuka Doi	(GODI)	Leg1a,b
Satoshi Okumura	(GODI)	Leg1a
Wataru Tokunaga	(GODI)	Leg1b
Ryo Ohyama	(GODI)	Leg1b

(2) Objectives

The information of cloud base height and the liquid water amount around cloud base is important to understand the process on formation of the cloud. As one of the methods to measure them, the ceilometer observation was carried out.

(3) Parameters

1. Cloud base height [m].
2. Backscatter profile, sensitivity and range normalized at 30 m resolution.
3. Estimated cloud amount [oktas] and height [m]; Sky Condition Algorithm.

(4) Methods

We measured cloud base height and backscatter profile using ceilometer (CT-25K, VAISALA, Finland) throughout the MR08-06 cruise.

Major parameters for the measurement configuration are as follows;

Laser source:	Indium Gallium Arsenide (InGaAs) Diode
Transmitting wavelength:	905±5 nm at 25 degC
Transmitting average power:	8.9 mW
Repetition rate:	5.57 kHz
Detector:	Silicon avalanche photodiode (APD) Responsibility at 905 nm: 65 A/W
Measurement range:	0 ~ 7.5 km
Resolution:	50 ft in full range
Sampling rate:	60 sec
Sky Condition	0, 1, 3, 5, 7, 8 oktas (9: Vertical Visibility) (0: Sky Clear, 1:Few, 3:Scattered, 5-7: Broken, 8: Overcast)

On the archive dataset, cloud base height and backscatter profile are recorded with the resolution of 30 m (100 ft).

(5) Preliminary results

2-7-2-fig1 shows the time series of the lowest, second and third cloud base height during the cruise.

(6) Data archives

The raw data obtained during this cruise will be submitted to the Marine-Earth Data and Information Department (MEDID) in JAMSTEC.

(7) Remarks

1. Window cleaning;

07:50UTC 14 Jan. 2009

23:55UTC 15 Jan. 2009

20:59UTC 22 Jan. 2009

04:09UTC 28 Jan. 2009

18:26UTC 06 Feb. 2009

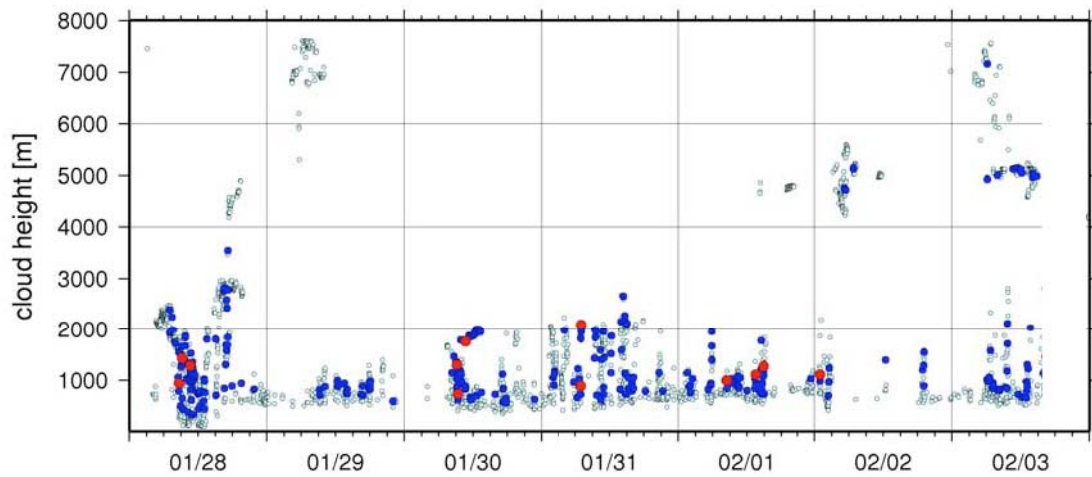
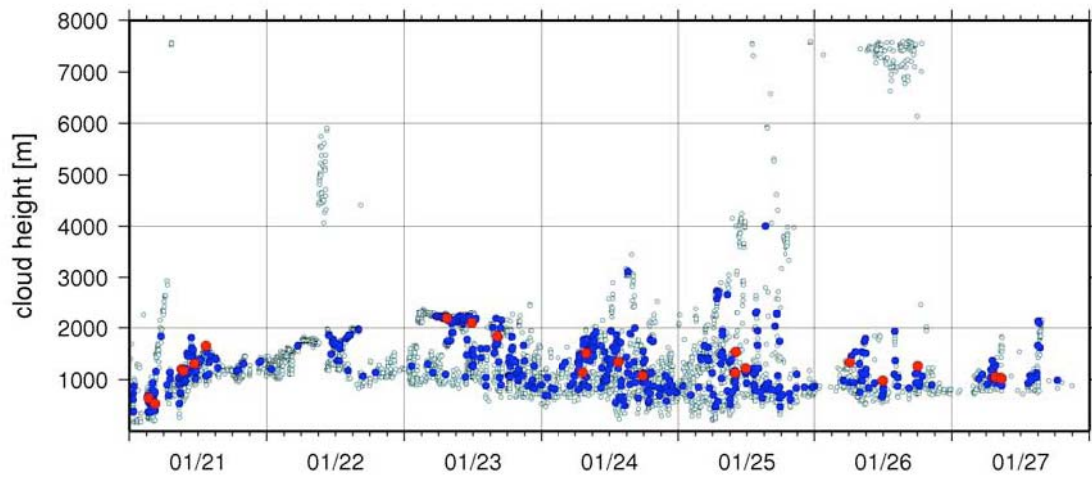
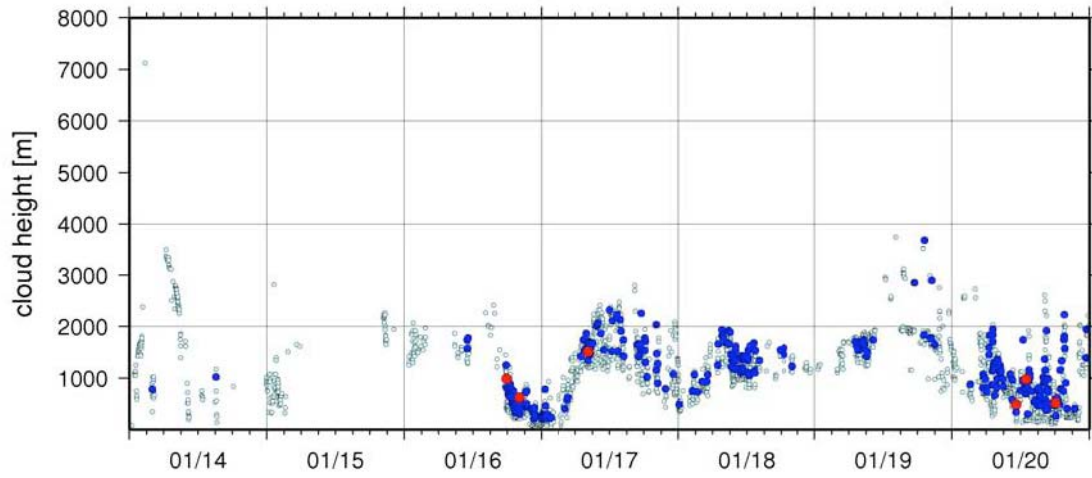
22:42UTC 07 Feb. 2009

13:58UTC 06 Mar. 2009

18:15UTC 13 Mar. 2009

Ceilometer

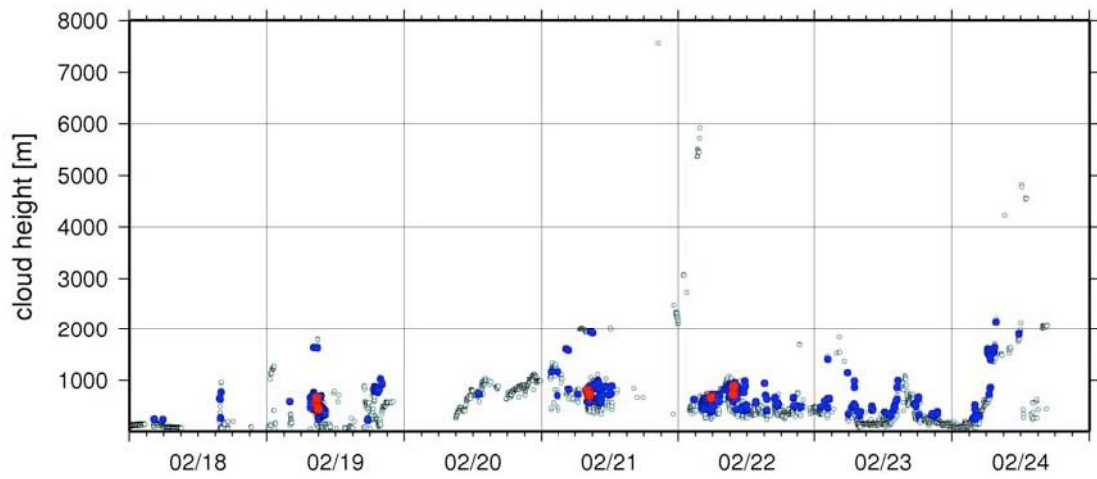
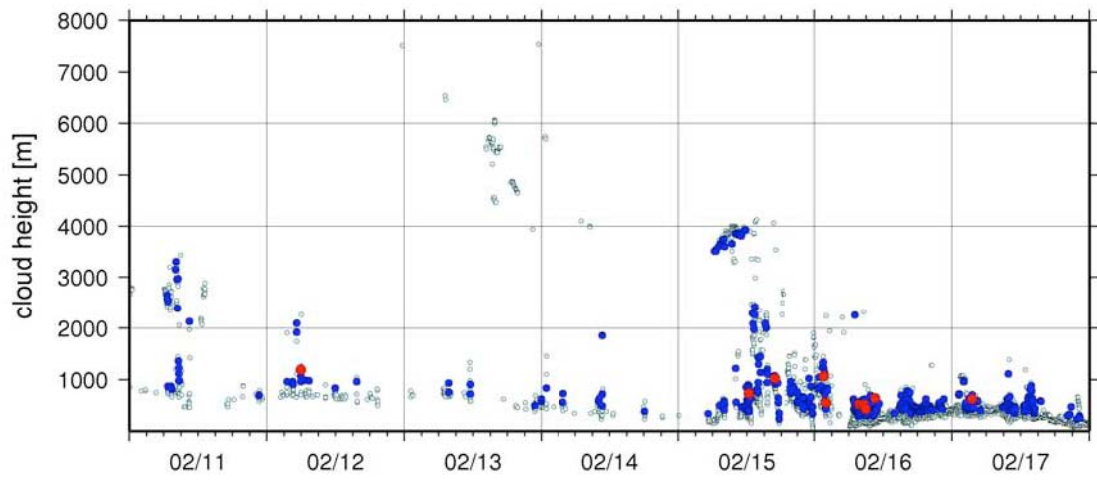
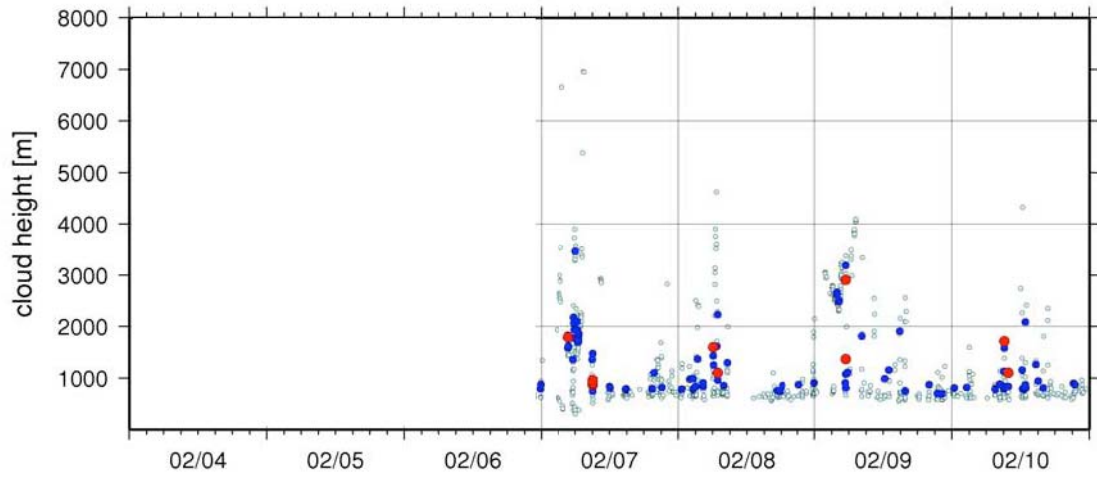
○: lowest, ●: 2nd, ●: 3rd



2-7-2-fig1 Lowest, 2nd and 3rd cloud base height during the cruise

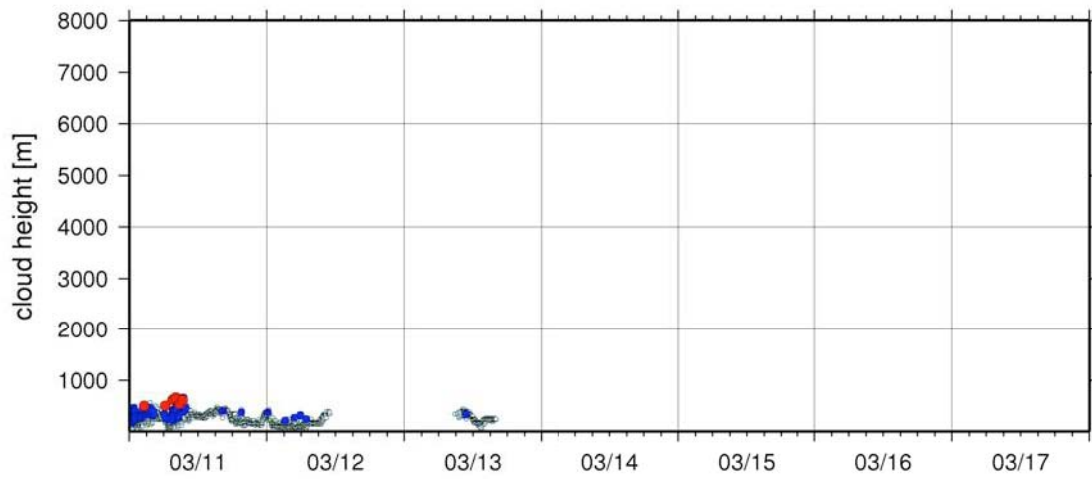
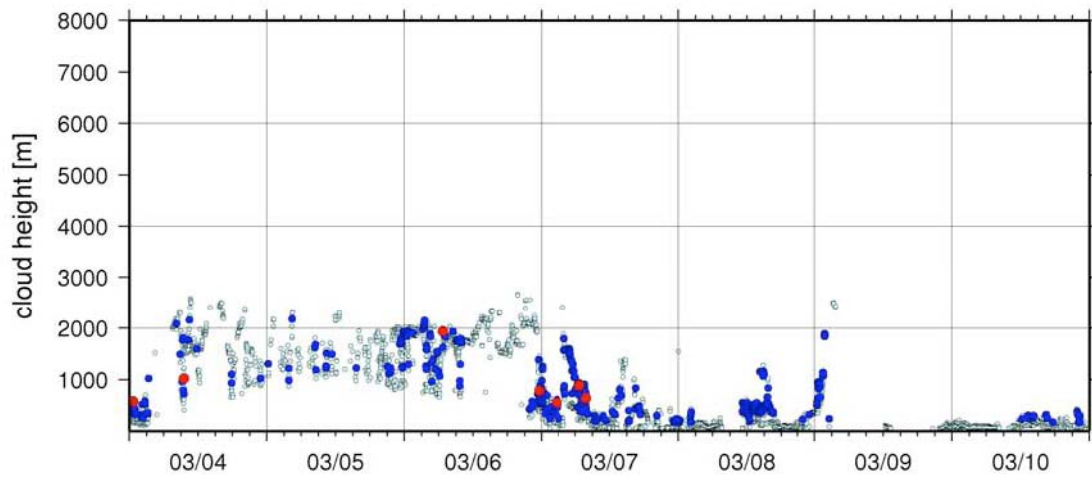
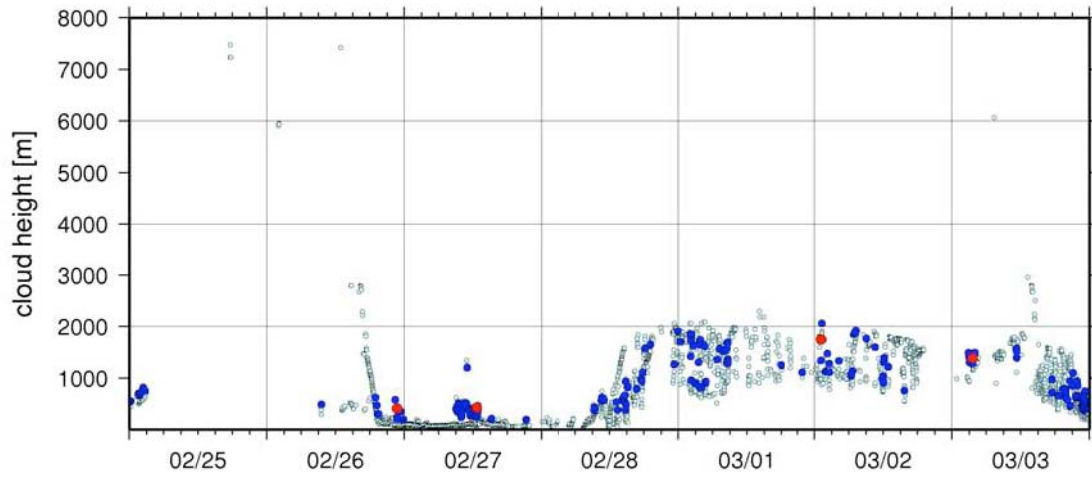
Ceilometer

○: lowest, ●: 2nd, ●: 3rd



2-7-2-fig1 (Continued)

Ceilometer



2-7-2-fig1 (Continued)

2-8 Shipboard ADCP

(1) Personnel

Ryo Kimura	Global Ocean Development Inc.	- Leg1a, b -
Asuka Doi	GODI	- Leg1a, b -
Satpshi Okumura	GODI	- Leg1a -
Wataru Tokunaga	GODI	- Leg1b -
Ryo Ohyama	GODI	- Leg1b -

(2) Objective

To obtain continuous measurement of the current profile along cruise track

(3) Methods

Upper ocean current measurements were made throughout MR08-04 cruise, using the hull mounted Acoustic Doppler Current Profiler (ADCP) system. For most of its operation, the instrument was configured for water-tracking mode recording. Bottom-tracking mode, interleaved bottom-ping with water-ping, was made in shallower water region to get the calibration data for evaluating transducer misalignment angle.

The system consists of following components;

- 1) R/V MIRAI has installed the Ocean Surveyor for vessel-mount (acoustic frequency 75 kHz; Teledyne RD Instruments). It has a phased-array transducer with single ceramic assembly and creates 4 acoustic beams electronically. We mounted the transducer head rotated to a ship-relative angle of 45 degrees azimuth from the keel.
- 2) For heading source, we use ship's gyro compass (Tokimec, Japan), continuously providing heading to the ADCP system directory. Additionally, we have Inertial Navigation System (INS) which provide high-precision heading, attitude information, pitch and roll, are stored in ".N2R" data files with a time stamp.
- 3) GPS navigation receiver (Trimble DS4000) provides position fixes.
- 4) We used VmDas version 1.4.2 (TRD Instruments) for data acquisition.
- 5) To synchronize time stamp of ping with GPS time, the clock of the logging computer is adjusted to GPS time every 1 minute.
- 6) We have placed ethylene glycol into the fresh water to prevent freezing in the sea chest.
- 7) The sound speed at the transducer does affect the vertical bin mapping and vertical velocity measurement, is calculated from temperature, salinity (constant value; 35.0 psu) and depth (6.5 m; transducer depth) by equation in Medwin (1975).

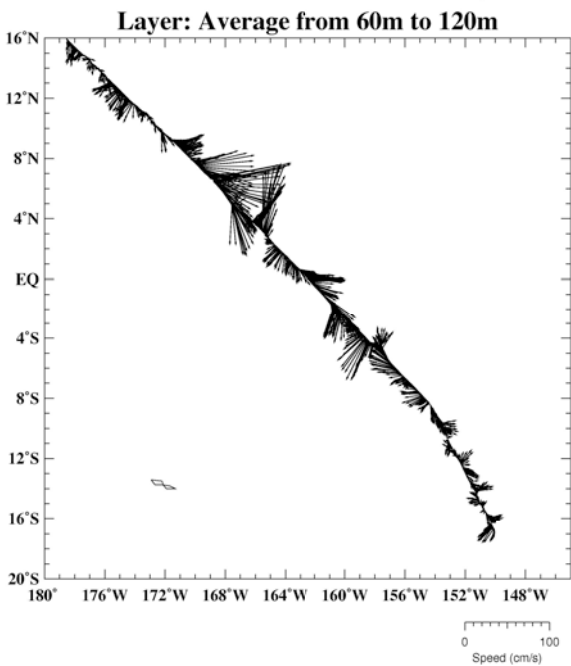
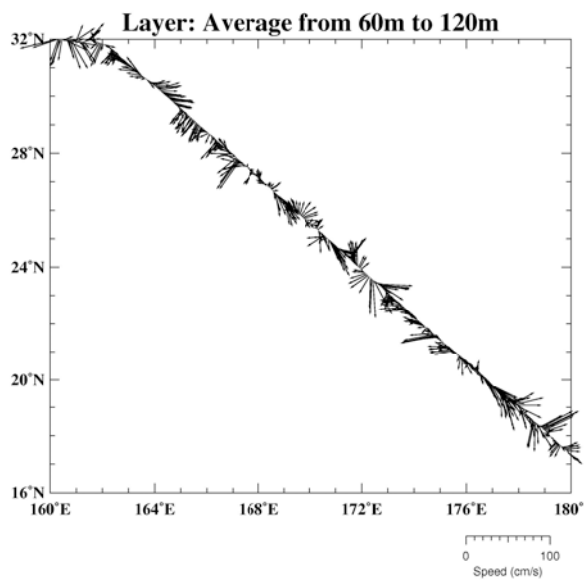
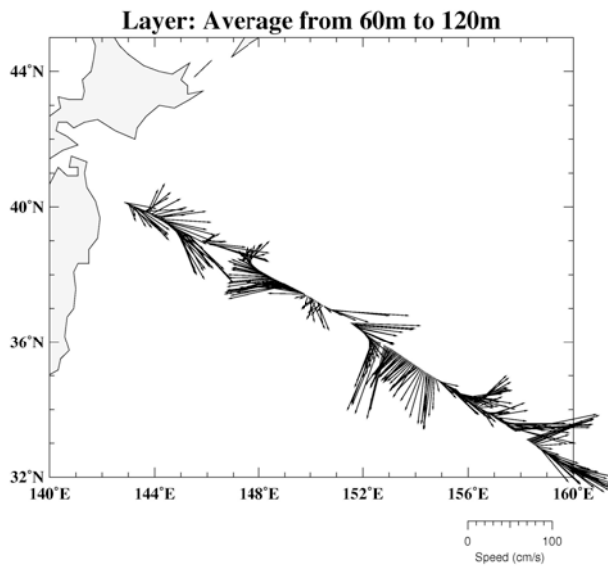
The data was configured for 16 m processing bin, 8 m intervals and starting 22.5m below the surface. Every ping was recorded as raw ensemble data (.ENR). Also, 60 seconds and 300 seconds averaged data were recorded as short term average (.STA) and long term average (.LTA) data, respectively.

(3) Preliminary results

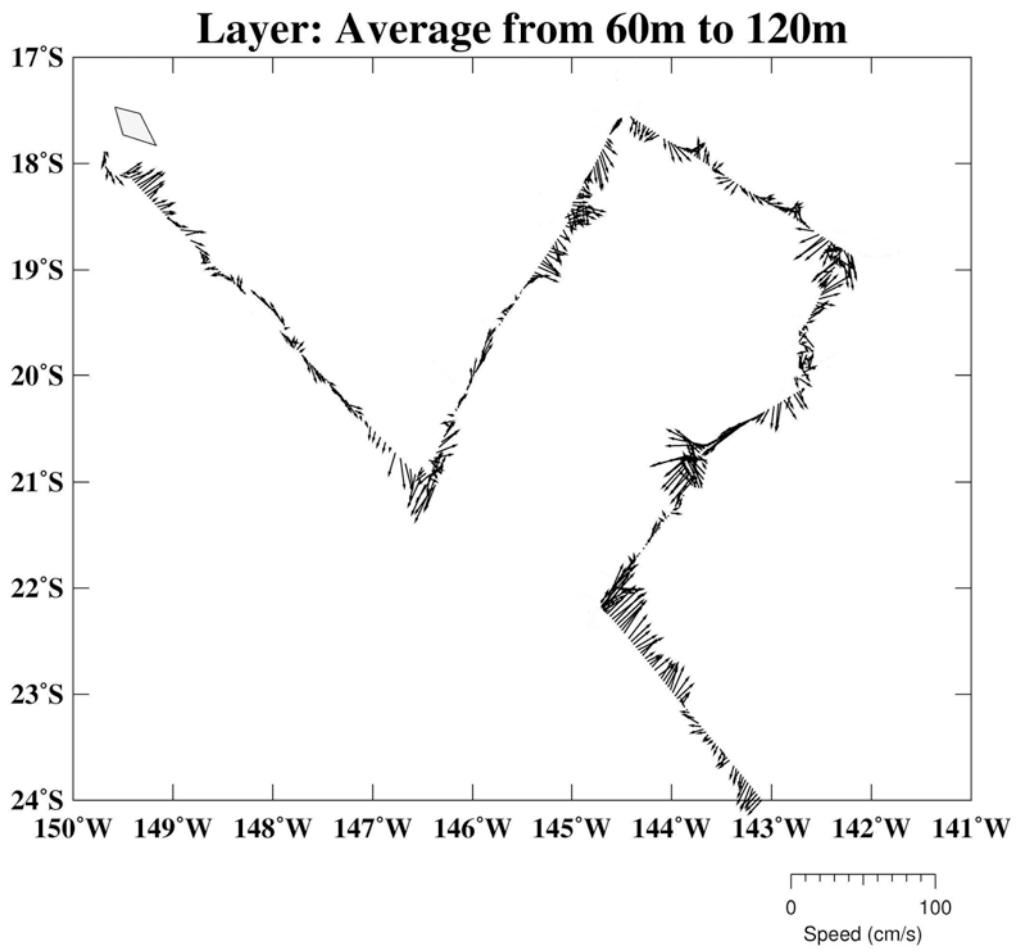
2-8-fig1 to 2-8-fig4 show current vector along the ship track in the observed station. The data was processed STA data using CODAS (Common Oceanographic Data Access System) software, developed at the University of Hawaii.

(4) Data archive

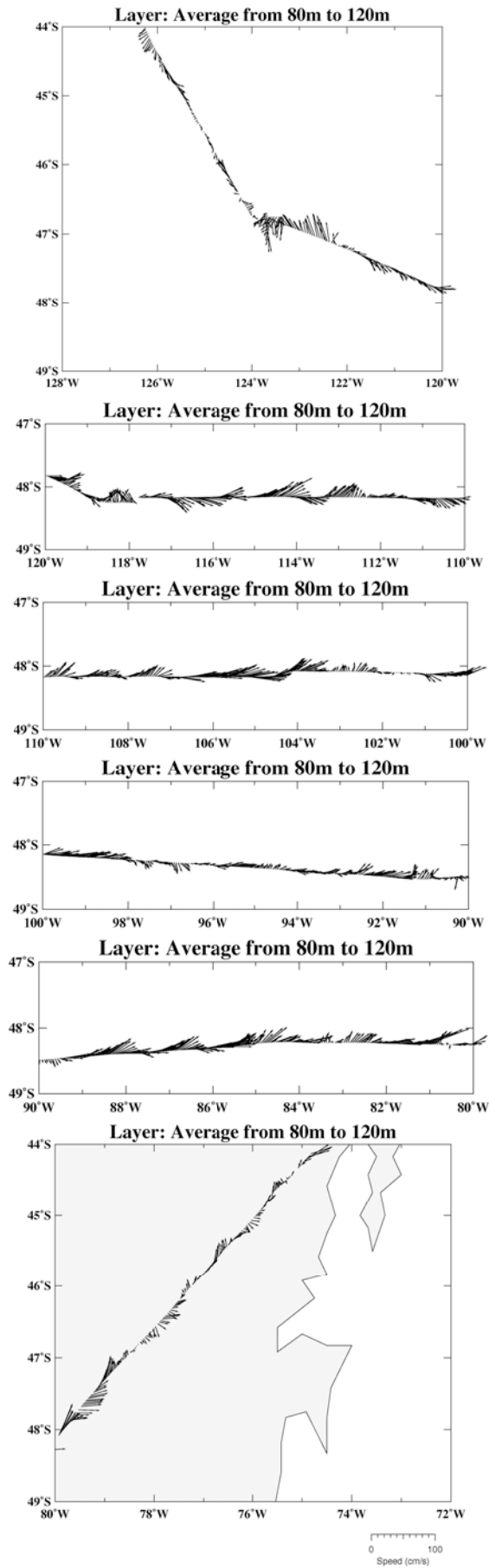
These data obtained in this cruise will be submitted to the Marine-Earth Data and Information Department (MEDID) of JAMSTEC, and will be opened to the public via "R/V Mirai Data Web Page" in JAMSTEC home page.



2-8-fig1 Current vector. Leg1a

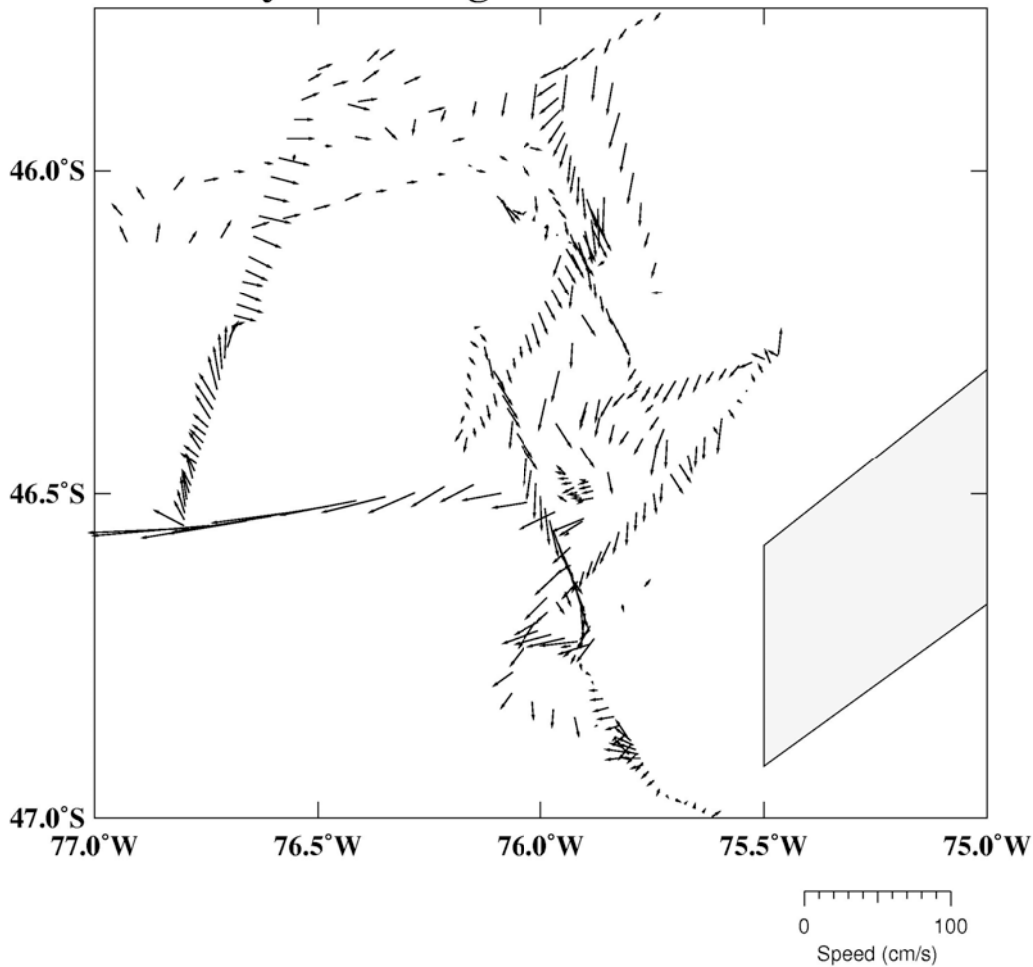


2-8-fig2 Current vector. Leg1b St01 - St.09



2-8-fig3 Current vector. Leg1b 48S LINE

Layer: Average from 80m to 120m



2-8-fig4 Current vector. Leg1b Area of Titao

2-9 Satellite observation

Natsue Abe	JAMSTEC: Principal Investigator	- Leg1a, b -
Ryo Kimura	Global Ocean Development Inc.	- Leg1a, b -
Aska Doi	GODI	- Leg1a, b -
Satoshi Okumura	GODI	- Leg1a -
Wataru Tokunaga	GODI	- Leg1b -
Ryo Ohyama	GODI	- Leg1b -

(1) Objectives

It is our objectives to collect data of sea surface temperature in a high spatial resolution mode from the Advance Very High Resolution Radiometer (AVHRR) on the NOAA polar orbiting satellites and to build a time and depth resolved primary productivity model.

(2) Method

We receive the down link High Resolution Picture Transmission (HRPT) signal from NOAA satellites by the same way as the signal of OrbView-2. We processed the HRPT signal with the inflight calibration and computed the sea surface temperature by the multi-channel sea surface temperature (MCSST) method. A daily composite map of MCSST data is processed for each day on the R/V MIRAI for the area, where the R/V MIRAI located.

We received and processed NOAA data throughout MR08-06 Leg1 cruise from the departure of Sekinehama on 14 January 2009 to the arrival of Valparaiso on 13 March 2009.

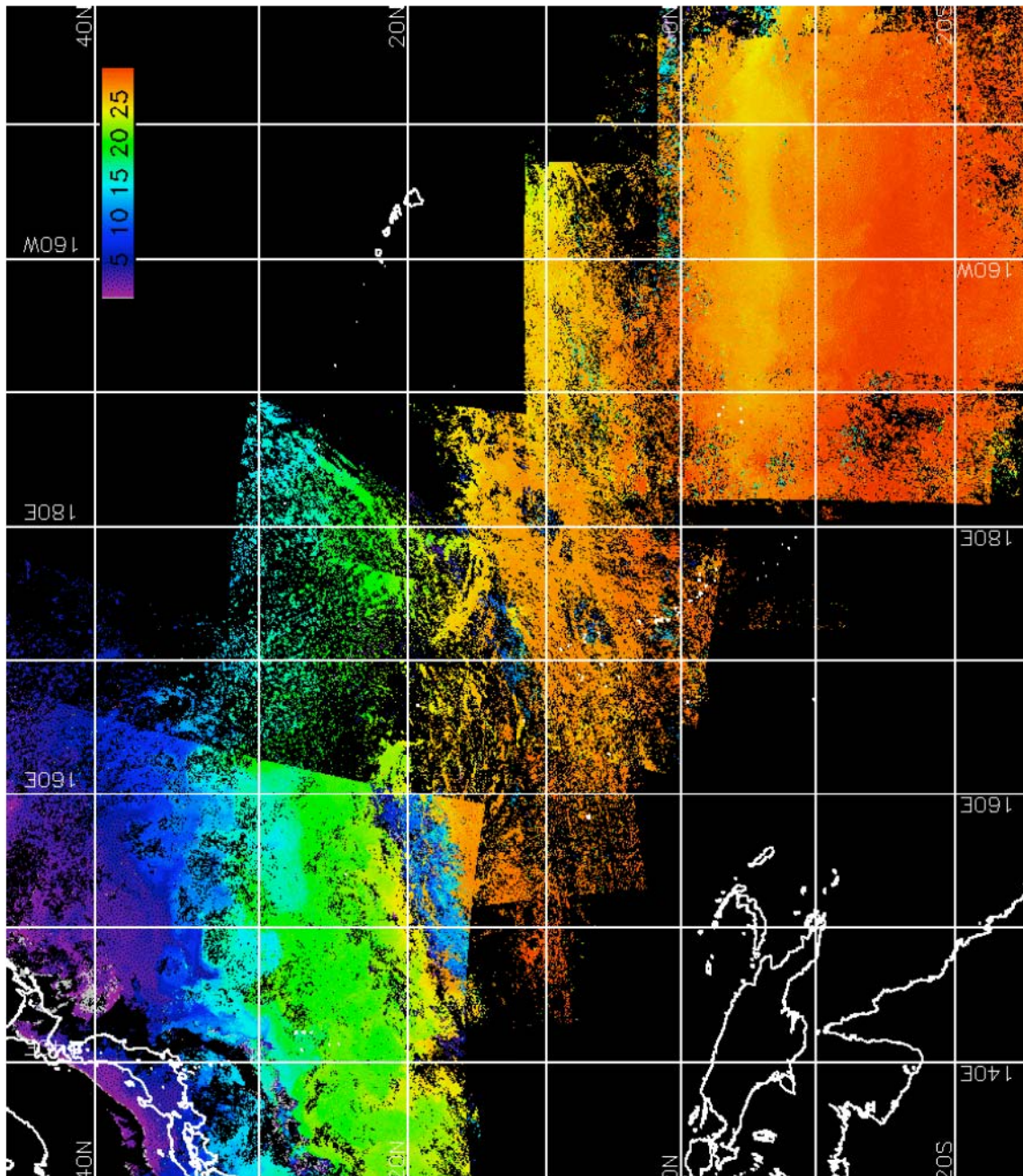
The sea surface temperature data will be applied for the time and depth resolved primary productivity model to determine a temperature field for the model.

(3) Preliminary results

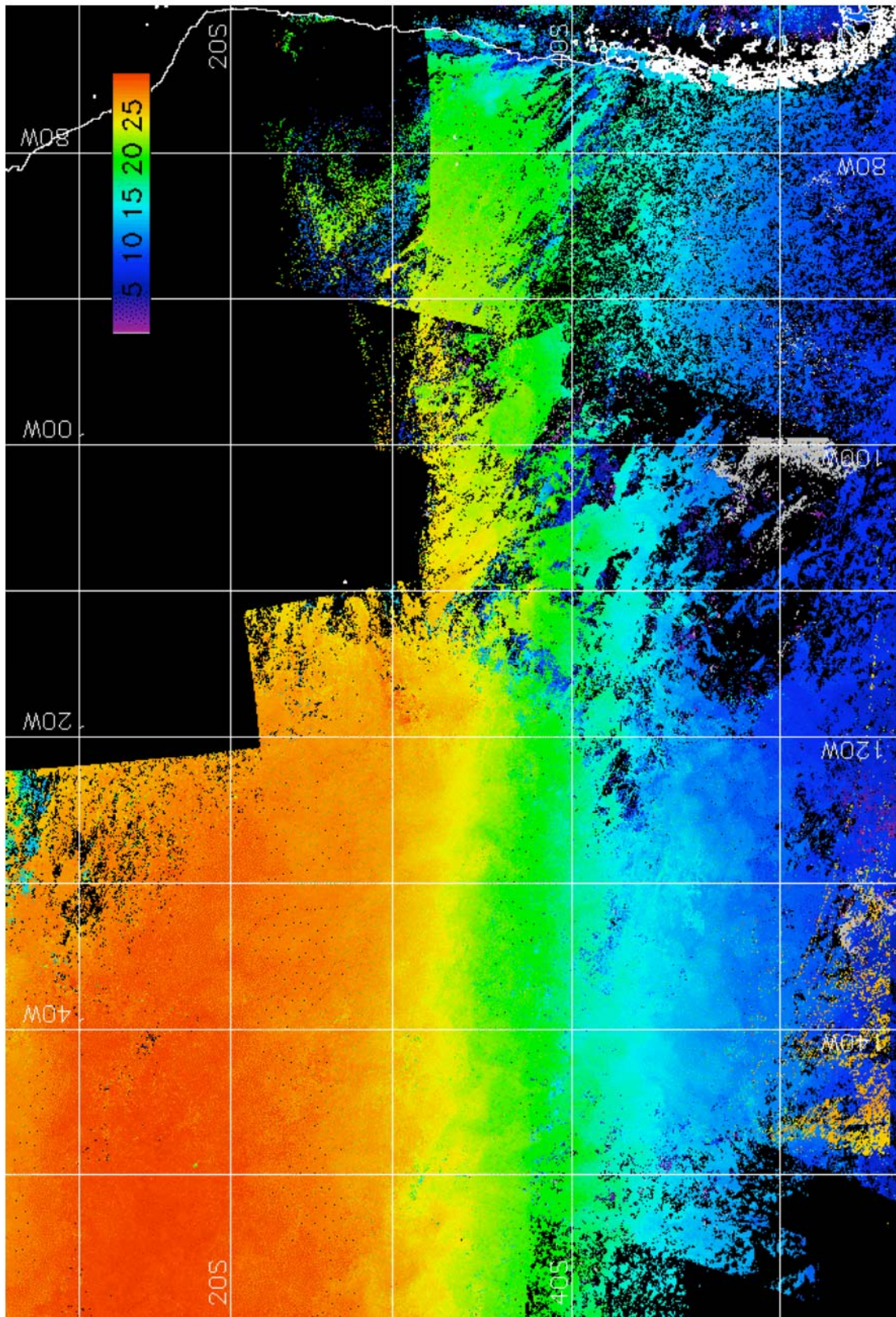
2-9-fig1 to 2-19-fig3 showed MCSST composite image three part of this cruise.

(4) Data archives

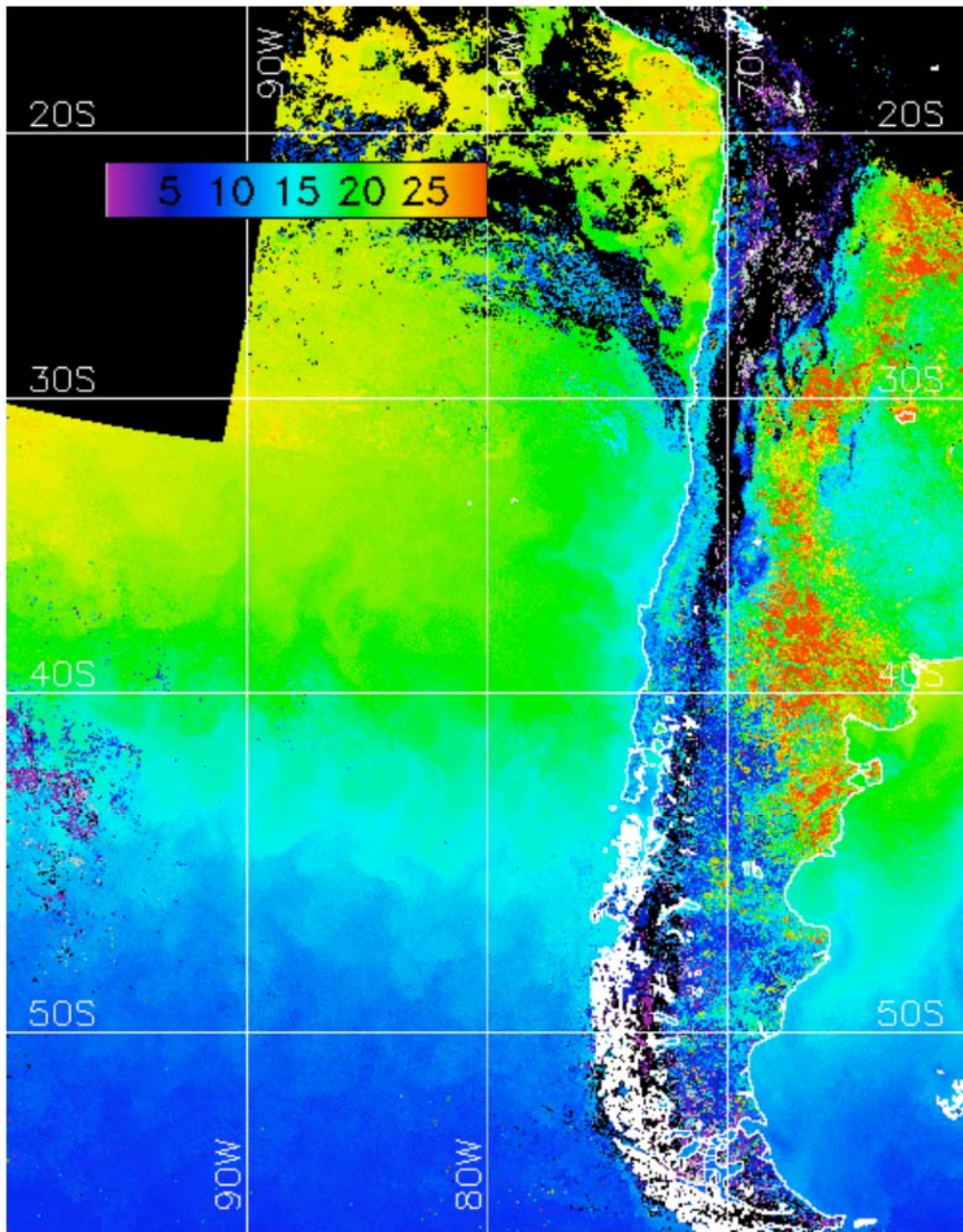
The raw data obtained during this cruise will be submitted to the Marine-Earth Data and Information Department (MEDID) in JAMSTEC, and will be archived there.



2-9-fig1 MCSST composite image
 Sekinehama to Papete: 14 January to 04 February, 2009



2-9-fig2 MCSST composite image
 Papeete to the Triple junction: 05 February to 01 March, 2009



2-9-fig3 MCSST composite image
The Triple junction to Valparaiso: 02 March to 13 March, 2009

3-1. Operation details of the geological sampling

Piston corer system (PC)

Y. Matsuura, K. Yoshida, Y. Taketomo, Y. Hashimoto, S. Oshitani.
(Marine Works Japan, Ltd.)

The piston corer system is a device that collects sediments from the seafloor. It is composed of the head of the corer, barrels, piston, catcher, bit, trigger and pilot core sampler. The duralumin pipes are used for the barrel, so that measurements of magnetic properties are available. A total of 10 or 20m-long duralumin pipe is composed of four 5m segments which are combined one another by stainless joint sleeves. We used a Ewing type corer for a pilot core sampler. For PC01, PC02 and PC03, we didn't use inner liners (Outer type). For PC04, we used inner liners: polycarbonate liner tubes (Inner type). A compass with inclinometer was attached above the weight of the corer to examine performance of the corer.

In the Outer type piston corer, after cutting duralumin pipes to the 1 m length with the band saw, the sediment is extruded into half round PVC lining using the hydraulic piston. It cuts the sediment section that put on another half round PVC lining longitudinal by a stainless wire, and it divides it into working and archive halves. After splitting, both cores are putted white pins at interval of 2cm and blue pins at interval of 10cm.

In the Inner type piston corer, it pulls out inner tubes only from the duralumin pipes and the sediment can be collected. The inner tubes filled by sediments are cut with the handy cutter every 1m after taking out from the barrel. The sediment sections are longitudinally cut into working and archive halves by a splitting devise and a stainless wire. After that, it marks with the white and blue pins in the 2 cm interval as same as the Outer type piston corer.

Specification of the piston corer system is shown below.

Head of the corer Main unit (Stainless, Lead):

Weight; 1.3ton

Barrel (Duralumin):

Length; 5m

Inner diameter; 80mm

Outer diameter; 92mm

Inner tube (Polycarbonate):

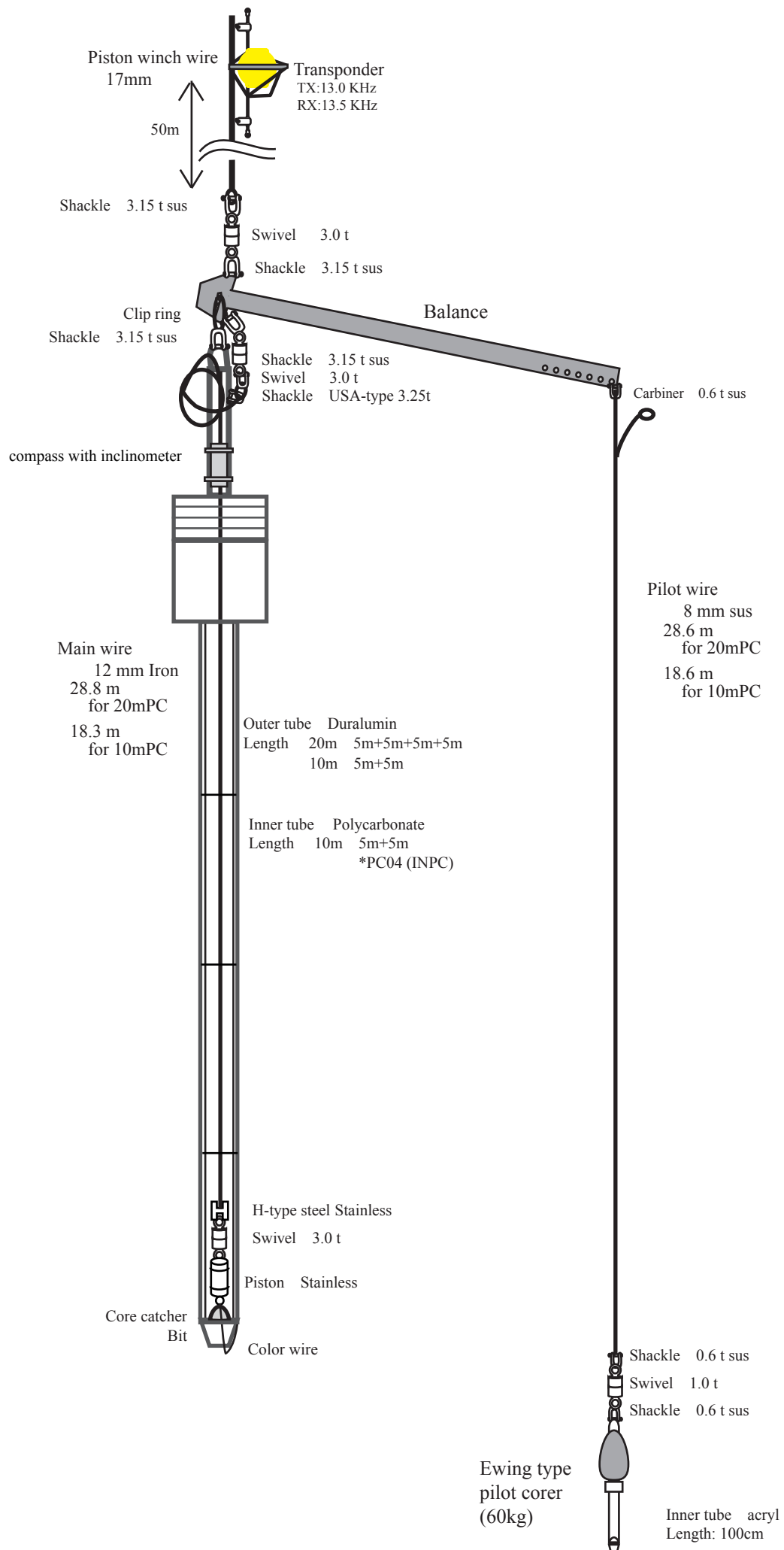
Length; 5m

Inner diameter; 74mm

Outer diameter; 78mm

Winch operation

When we started lowering, a speed of wire out was set to be 0.2 m/s., and then gradually increased to the maximum of 1.0 m/s. The corers were stopped at a depth about 100 m above the sea floor for 3-5 minutes to reduce any pendulum motion of the system. After the corers were stabilized, the wire was stored out at a speed of 0.3 m/s., and we carefully watched a tension meter. When the corers touched the bottom, wire tension abruptly decreases by the loss of the corer weight. Immediately after confirmation that the corers hit the bottom, wire out was stopped and rewinding of the wire was started at a dead slow speed (~0.3m/s.), until the tension gauge indicates that the corers were lifted off the bottom. After leaving the bottom, winch wire was wound in at the maximum speed.



Piston corer system

Sediment color

Y. Matsuura, K. Yoshida, Y. Taketomo, Y. Hashimoto, S. Oshitani.
(Marine Works Japan, Ltd.)

(1) Objectives

Split cores were measured color reflectance because of observe characteristics of the sediments such as lithology, oxidation rate, concentrations of carbonates, organic matter and certain inorganic compounds. It is also frequently used to different cores.

(2) Measured parameters

There are different systems to quantify the color reflectance for soil and sediment measurements, the most common is the $L^*a^*b^*$ system, also referred to as the CIE (Commission International d'Eclairage) LAB system. It can be visualized as a cylindrical coordinate system in which the axis of the cylinder is the lightness variable L^* , ranging from 0% to 100%, and the radii are the chromaticity variables a^* and b^* . Variable a^* is the green (negative) to red (positive) axis, and variable b^* is the blue (negative) to yellow (positive) axis. Spectral data can be used to estimate the abundance of certain components of sediments.

(3) Instruments and methods

Core color reflectance was measured by using the Minolta CM-2002 reflectance photospectrometer using 400 to 700nm in wavelengths. This is a compact and hand-held instrument, and can measure spectral reflectance of sediment surface with a scope of 8mm diameter. To ensure accuracy, the CM-2002 was used with a double-beam feedback system, monitoring the illumination on the specimen at the time of measurement and automatically compensating for any changes in the intensity or spectral distribution of the light. The Minolta CM-2002 has a switch that allows the specular component to be include (SCI) or excluded (SCE). Including the specular component (SCI) essentially includes glare and provides a better estimate of color as seen by the human eye. However, glare does not contribute to the spectrum reflected from the sediments. We recommend setting the switch to SCE. The SCE setting is the recommended mode of operation for sediments in which the light reflected at a certain angle (angle of specular reflection) is trapped and absorbed at the light trap position on the integration sphere.

Calibration was carried out using the zero and white calibration piece (Minolta CM-2002 standard accessories) without crystal clear polyethylene wrap before the measurement of core samples. The color of the sediment surface of split working half core was measured on

every 2-cm through crystal clear polyethylene wrap.

Measurement parameters are displayed Table-1.

Table-1. Measurement parameters.

Instrument	Minolta Photospectrometer CM-2002
Illuminant	d/8 (SCE)
Light source	D ₆₅
Viewing angle	10 degree
Color system	L*a*b* system

X-Ray Diffract meter (XRD)

Y. Matsuura, K. Yoshida, Y. Taketomo, Y. Hashimoto, S. Oshitani.
(Marine Works Japan, Ltd.)

RIGAKU RINT 2200 X-ray diffract meter was used for the XRD analysis of mineral phases. Ni filtered Cu K radiation generated at 40kV and 50mA was used. The Peaks were scanned from 3° to $90^{\circ} 2\theta$, with a step size of 0.02° and a counting time of 4s per minute. The Bulk samples were dried, ground, and mounted in random orientation in glass sample holders. Then the powder was pressed into the glass sample holders for analysis.

Core Photographs

Y. Matsuura, K. Yoshida, Y. Taketomo, Y. Hashimoto, S. Oshitani.
(Marine Works Japan, Ltd.)

After splitting each section of piston and pilot cores into working and archive halves, sectional photographs of archive halves were taken using a Nikon single-lens reflex digital camera (Nikon D1x). When using the digital camera, shutter speed was between 1/8 and 1/30, F value was between 8 and 11, Exposure value was 0.7, 0 and -0.7, sensitivity ISO 125 was used. Details for settings were included on property of each file.

Winch wire: Diameter of winch wire is 17mm. It is 0.983kg weight per one meter in water (i.e. about 983kg for 1,000m in the sea water) and having a 24.2t breaking force.

Lead wire: This wire is prepared for protection against damage to the winch wire, jointed by shackles (3.15t SUS) and a swivel (5t). It is iron wire of 12mm diameter (in case of more than 4,000m, 10mm diameter has to be used), 200m long and a 7.24t (10mm diameter: 5.03t) breaking force.

Chain: Chain (19mm diameter, 5m long) is used to stabilize the dredge sampler and was jointed to the lead wire with a swivel (5t) and shackles (ϕ 19).

Weight(50kg per each): The weight is used to assure the dredge sampler is on the bottom as can be observed by the tension meter in the operation room, and linked by shackles (ϕ 16) to the chain together with a swivel (1t), fuse wire (6 or 8mm diameter, 0.25m long) and life wire (8 or 10mm diameter, 1.0m and 1.7m long).

Pipe dredge: Pipe dredge assumes the function as the backup of the main chain-bag dredge. This is linked as same as the weight. (life wire is 1m long)

Life wire (chain-bag): End of the life wire (8 or 10mm diameter, 7 m long) is connected parallel with fuse wire, and the other end is connected with the middle part of the chain-bag. In the case of fuse wire is broken by a big bite or anchoring, life wire works to prevent the dredge from lost, and keeps the samples in the box type bucket.

Fuse wire: Fuse wire (6 or 8mm diameter, 0.25m long) is prepared to release the dredge from big bites that might damage the winch wire. It is jointed to the chain with a swivel (1t or 3t) and shackles in the main chain-bag dredge.

Chain-bag dredge: The square type dredge consists of box type jaw (60*45 cm mouth, 60*27 cm throat), handle (26mm diameter, 85cm long) and steel chain-bag (6 mm diameter, 100cm long) with box type bucket (27*60*50cm) made from stainless steel (5mm thick). The bucket can recover all kinds of sediments on seafloor, it was jointed with shackles to the 0.25 m fuse wire.

In case of wire out length are more than 4,000m, JAMSTEC decided that fuse/life/lead wire should be used 6/8/10mm in diameter respectively, in order to protect the winch wire from own weight. Otherwise, wire out length are less than 4000 m, fuse/life/lead wire should be use 8/10/12mm in diameter respectively.

About details of wire diameter and breaking force are written in below.

Diameter	Breaking Force
6mm	1.81t
8mm	3.22t
10mm	5.03t
12mm	7.24t

MR08-06_Leg1 Cruise Dredge summary

Date (mmddy)	Dredge number	Location	On the bottom				Off the bottom				Depth (m)		Tension max. (t)	Survey time
			Lat. (SOQ)	Lon. (SOQ)	Lat. (SOJ)	Lon. (SOJ)	Lat. (SOQ)	Lon. (SOQ)	Lat. (SOJ)	Lon. (SOJ)	On the bottom	Off the Bottom		
2009.3.2	D01	Off Chile	46°53.4604' S	75°47.5284' W	46°53.5501' S	75°47.5701' W	46°53.9750' S	75°47.0734' W	46°53.9947' S	75°47.0481' W	2,535	2,160	4.0	1h 49min.
2009.3.2	D02	Off Chile	46°38.0472' S	75°46.7522' W	46°38.0564' S	75°46.6576' W	46°38.2124' S	75°45.9950' W	46°38.2213' S	75°45.8765' W	2,810	2,338	2.9	1h 43min.
2009.3.4	D03	Off Chile	46°02.4567' S	75°53.7736' W	46°02.3955' S	75°53.8244' W	46°02.2395' S	75°53.8420' W	46°02.1471' S	75°53.9954' W	3,289	3,293	3.2	1h 23min.
2009.3.6	D04	Off Chile	46°04.2374' S	75°54.3587' W	46°04.1988' S	75°54.3793' W	46°04.2416' S	75°54.5826' W	46°04.2118' S	75°54.8161' W	3,000	2,968	4.8	54min.
2009.3.6	D05	Off Chile	46°06.4253' S	75°52.8063' W	46°06.3784' S	75°52.8386' W	46°06.4664' S	75°53.2284' W	46°06.4200' S	75°53.2557' W	3,177	3,047	4.6	46min.
2009.3.7	D06	Off Chile	46°28.5177' S	75°51.9178' W	46°28.4443' S	75°51.8990' W	46°28.7198' S	75°51.0565' W	46°28.6712' S	75°51.0053' W	2,487	1,857	3.7	2h 8min.
2009.3.7	D07	Off Chile	46°33.3914' S	75°57.9993' W	46°33.3009' S	75°57.9977' W	46°33.2254' S	75°57.3002' W	46°33.1554' S	75°57.2041' W	2,330	1,783	3.8	1h 45min.
2009.3.11	D08	Off Chile	33°05.1826' S	73°09.6847' W	33°05.1908' S	73°09.7598' W	33°05.2278' S	73°09.7887' W	33°05.2183' S	73°09.8528' W	4,113	3,981	5.2	1h 45min.
2009.3.12	D09	Off Chile	33°03.6648' S	73°22.2874' W	33°03.7031' S	73°22.2990' W	33°03.7045' S	73°22.0696' W	33°03.7186' S	73°22.0341' W	3,790	3,737	4.0	1h 41min.
2009.3.12	D10	Off Chile	33°04.6612' S	73°19.2248' W	33°04.6673' S	73°19.2825' W	33°04.5025' S	73°19.4036' W	33°04.4783' S	73°19.5021' W	3,849	3,646	6.0	59min.

MR08-06_Leg1 Cruise Coring summary (Piston Corer)

Date (mmddyy)	Core ID	Location	Lat. (SOQ)	Lon. (SOQ)	Lat. (SOJ)	Lon. (SOJ)	Depth (m)	Corebarrel length (m)	Tension max. (t)	Core length (cm)	PC type
2009.2.18	PC01	Southeast Pacific	46°49.9321'S	123°40.2990'W	46°49.8635'S	123°40.3031'W	3,983	20	6.5	1,066.5	Outer type PC
2009.2.20	PC02	Southeast Pacific	48°15.0153'S	118°18.7154'W	48°14.9917'S	118°18.8352'W	3,358	20	7.5	625.5	Outer type PC
2009.2.26	PC03	Southeast Pacific	48°24.9530'S	80°28.4289'W	48°24.9532'S	80°28.4295'W	4,094	20	6.1	1,966.0	Outer type PC
2009.3.3	PC04	Off Chile	46°39.2866'S	75°54.0455'W	46°39.2326'S	75°54.0391'W	3,345	10	5.1	856.2	Inner type PC

MR08-06_Leg1 Cruise Coring summary (Pilot Corer)

Date (mmddy)	Core ID	Corer type	Location	Lat. (SOQ)	Lon. (SOQ)	Lat. (SOJ)	Lon. (SOJ)	Depth (m)	HAND No.	Core length(cm)
2009.2.18	PL01	Ewing	Southeast Pacific	46°49.9321'S	123°40.2990'W	46°49.8635'S	123°40.3031'W	3,983		11.5
2009.2.20	PL02	Ewing	Southeast Pacific	48°15.0153'S	118°18.7154'W	48°14.9917'S	118°18.8352'W	3,358		0.0
2009.2.26	PL03	Ewing	Southeast Pacific	48°24.9530'S	80°28.4289'W	48°24.9532'S	80°28.4295'W	4,094		65.0
2009.3.3	PL04	Ewing	Off Chile	46°39.2866'S	75°54.0455'W	46°39.2326'S	75°54.0391'W	3,345		54.5

MR08-06_Leg1 Cruise Coring summary (Rock Corer)

Date (mmddy)	Core ID	Location	Lat. (SOQ)	Lon. (SOQ)	Lat. (SOJ)	Lon. (SOJ)	Depth (m)	core sample
2009.3.8	RC01	Off Chile	45°52.5177' S	75°59.4908' W	45°52.4588' S	75°59.4641' W	3,285	Basaltic glass

Cruise No.: MR08-06_Leg1

Core No.: PC01

Date: 2009.2.18

Cut method	Section	1m cut (cm)	MSCL	Pinprick (cm)		CCR	Core description	Core top (cmbsf)	Core bottom (cmbsf)	Remarks
			length (cm)	W	A	length (cm)	length (cm)			
Band Saw>	Sec.1	64.5	-	60.8	60.7	60.7	60.5	0.0	60.5	
Band Saw>	Sec.2	99.8	-	103.2	102.5	102.5	103.0	60.5	163.5	
Band Saw>	Sec.3	100.4	-	102.5	102.4	102.4	102.0	163.5	265.5	
Band Saw>	Sec.4	100.0	-	101.1	102.1	102.1	100.5	265.5	366.0	
Spatula>	Sec.5	99.9	-	100.0	100.5	100.5	100.0	366.0	466.0	
Band Saw>	Sec.6	100.0	-	100.5	100.2	100.2	100.5	466.0	566.5	
Band Saw>	Sec.7	100.2	-	97.9	97.9	97.9	98.0	566.5	664.5	
Band Saw>	Sec.8	99.8	-	99.9	99.7	99.7	100.0	664.5	764.5	
Band Saw>	Sec.9	100.3	-	101.7	101.8	101.8	101.5	764.5	866.0	
Spatula>	Sec.10	100.2	-	100.5	100.4	100.4	100.0	866.0	966.0	
Band Saw>	Sec.11	100.7	-	100.6	101.5	101.5	100.5	966.0	1066.5	Bottom 28cm is flow in.
Band Saw>	Sec.12	99.6	-	98.6	98.9	-	-	-	-	flow in
Band Saw>	Sec.13	99.2	-	99.4	99.1	-	-	-	-	flow in
Band Saw>	Sec.14	100.7	-	100.7	100.0	-	-	-	-	flow in
Spatula>	Sec.15	99.5	-	99.2	98.4	-	-	-	-	flow in
Band Saw>	Sec.16	100.1	-	100.3	100.1	-	-	-	-	flow in
Band Saw>	Sec.17	100.4	-	98.1	98.2	-	-	-	-	flow in
Band Saw>	Sec.18	100.0	-	99.2	98.7	-	-	-	-	flow in
Band Saw>	Sec.19	99.5	-	99.3	99.0	-	-	-	-	flow in
Spatula>	Sec.20	100.1	-	94.8	97.0	-	-	-	-	flow in
	Sec.cc	-	-	21.0	19.6	-	-	-	-	flow in

Total length: 1066.5 (cm)

Cruise No.: MR08-06_Leg1

Core No.: PC02

Date: 2009.2.20

Cut method	Section	1m cut (cm)	MSCL	Pinprick (cm)		CCR	Core description	Core top (cmbsf)	Core bottom (cmbsf)	Remarks
			length (cm)	W	A	length (cm)	length (cm)			
Band Saw>	Sec.1	29.0	-	27.4	27.0	27.0	28.0	0.0	28.0	
Band Saw>	Sec.2	99.7	-	96.9	97.1	97.4	97.0	28.0	125.0	
Band Saw>	Sec.3	100.1	-	101.3	101.2	101.2	101.5	125.0	226.5	
Spatula>	Sec.4	99.9	-	98.8	98.8	98.8	98.5	226.5	325.0	
Band Saw>	Sec.5	100.4	-	101.6	102.3	102.3	101.5	325.0	426.5	
Band Saw>	Sec.6	100.1	-	95.7	93.4	93.4	95.0	426.5	521.5	
Band Saw>	Sec.7	99.7	-	104.0	104.1	104.1	104.0	521.5	625.5	flow in
Band Saw>	Sec.8	100.2	-	98.0	98.5	-	-	-	-	flow in
Spatula>	Sec.9	100.0	-	102.8	102.2	-	-	-	-	flow in
Band Saw>	Sec.10	100.0	-	98.4	97.8	-	-	-	-	flow in
Band Saw>	Sec.11	99.8	-	99.8	98.0	-	-	-	-	flow in
Band Saw>	Sec.12	100.4	-	98.1	97.1	-	-	-	-	flow in
Band Saw>	Sec.13	100.0	-	97.8	97.5	-	-	-	-	flow in
Spatula>	Sec.14	100.0	-	106.0	105.8	-	-	-	-	flow in
	Sec.cc	-	-	-	-	-	-	-	-	flow in

Total length: 625.5 (cm)

Cruise No.: MR08-06_Leg1

Core No.: PC03

Date: 2009.2.26

Cut method	Section	1m cut (cm)	MSCL	Pinprick (cm)		CCR	Core description	Core top (cmbsf)	Core bottom (cmbsf)	Remarks
			length (cm)	W	A	length (cm)	length (cm)			
Band Saw>	Sec.1	68.9	-	71.3	70.2	70.2	71.0	0.0	71.0	
Band Saw>	Sec.2	100.7	-	101.7	101.7	101.7	101.5	71.0	172.5	
Band Saw>	Sec.3	100.1	-	100.9	100.0	100.0	101.0	172.5	273.5	
Band Saw>	Sec.4	99.7	-	99.0	98.7	98.7	99.0	273.5	372.5	
Spatula>	Sec.5	100.1	-	96.9	97.0	97.0	97.0	372.5	469.5	
Band Saw>	Sec.6	100.2	-	100.9	100.8	100.8	100.5	469.5	570.0	
Band Saw>	Sec.7	100.1	-	97.4	97.4	97.4	97.0	570.0	667.0	
Band Saw>	Sec.8	99.7	-	98.4	98.5	98.5	98.5	667.0	765.5	
Band Saw>	Sec.9	100.0	-	99.2	99.2	99.2	99.0	765.5	864.5	
Spatula>	Sec.10	100.0	-	100.4	100.9	100.9	100.0	864.5	964.5	
Band Saw>	Sec.11	99.8	-	101.8	101.8	101.8	102.0	964.5	1066.5	
Band Saw>	Sec.12	99.4	-	100.4	100.0	100.0	100.0	1066.5	1166.5	
Band Saw>	Sec.13	100.2	-	100.4	100.3	100.3	100.0	1166.5	1266.5	
Band Saw>	Sec.14	100.2	-	101.7	101.8	101.8	101.5	1266.5	1368.0	
Spatula>	Sec.15	100.0	-	100.6	100.6	100.6	100.5	1368.0	1468.5	
Band Saw>	Sec.16	99.8	-	101.3	101.5	101.5	101.0	1468.5	1569.5	
Band Saw>	Sec.17	99.9	-	101.6	101.4	101.4	101.5	1569.5	1671.0	
Band Saw>	Sec.18	100.2	-	100.5	101.0	101.0	100.5	1671.0	1771.5	
Band Saw>	Sec.19	99.9	-	100.5	101.1	101.1	100.5	1771.5	1872.0	
Band Saw>	Sec.20	99.7	-	79.9	79.1	79.1	79.0	1872.0	1951.0	flow in
Spatula>	Sec.cc	18.0	-	15.2	14.2	14.2	15.0	1951.0	1966.0	flow in

Total length: 1966.0 (cm)

Cruise No.: MR08-06_Leg1

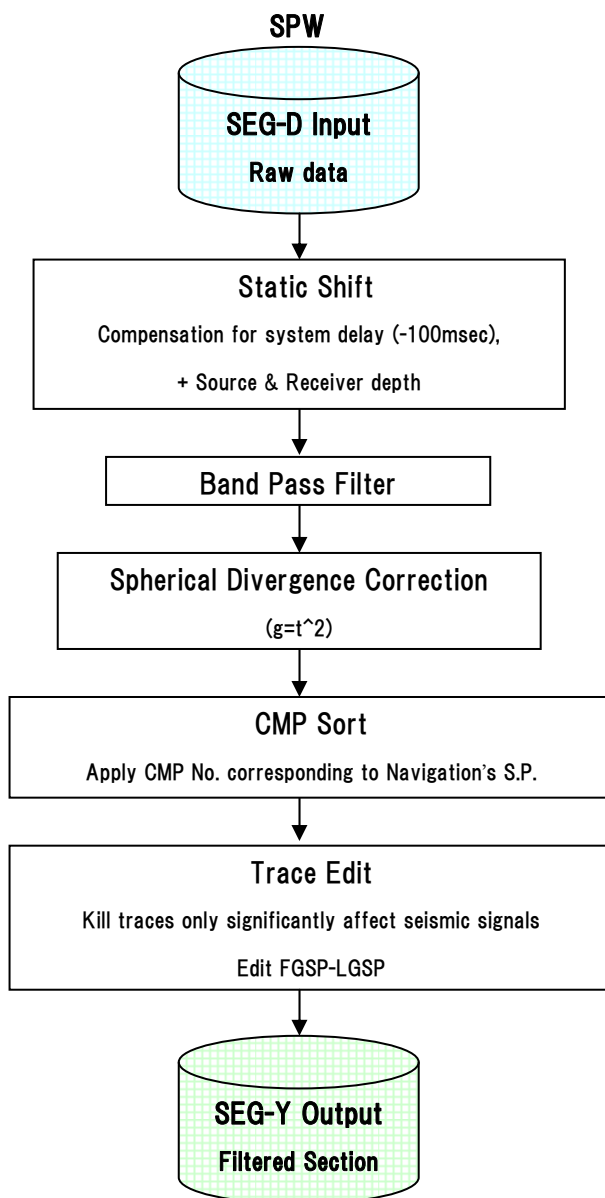
Core No.: PC04

Date: 2009.3.3

Cut method	Section	1m cut (cm)	MSCL	Pinprick (cm)		CCR	Core description	Core top (cmbsf)	Core bottom (cmbsf)	Remarks
			length (cm)	W	A	length (cm)	length (cm)			
Tube cutter>	Sec.1	41.8	-	43.0	41.3	41.3	43.5	0.0	43.5	
Tube cutter>	Sec.2	100.5	-	100.5	100.1	100.3	100.0	43.5	143.5	
Tube cutter>	Sec.3	99.6	-	99.8	99.4	99.4	100.0	143.5	243.5	
Spatula>	Sec.4	101.0	-	101.2	101.2	101.2	101.0	243.5	344.5	
Tube cutter>	Sec.5	101.2	-	100.8	100.8	100.8	101.0	344.5	445.5	
Tube cutter>	Sec.6	100.4	-	100.1	100.2	100.2	100.0	445.5	545.5	
Tube cutter>	Sec.7	100.2	-	100.1	99.9	99.9	99.7	545.5	645.2	
Tube cutter>	Sec.8	100.7	-	100.6	100.5	100.5	100.5	645.2	745.7	
Spatula>	Sec.9	100.0	-	99.0	99.0	99.0	99.0	745.7	844.7	
	Sec.cc	-	-	11.1	10.3	10.1	11.5	844.7	856.2	

Total length: 645.2 (cm)

Seismic Data Processing Flow to Filtered Section





NME SINGLE CHANNEL SEISMIC SURVEY LINE LIST MR08-06 (Leg.1b)

Line No.	Date (UTC)	Time (UTC)	Passing Point	Shot No.	Vessel Position			Length [m]	Direction [deg]	Remarks	
					Lat.	Lon.					
St10-1	2009/2/19	0:49:36	F.G.S.P	1	46-57.97119	S	123-40.32440	W	29620.8	359.5	
	2009/2/19	4:52:21	L.G.S.P	607	46-41.76842	S	123-40.30426	W			
St10-2	2009/2/19	8:38:12	F.G.S.P	1	46-49.95232	S	123-52.25464	W	29621.7	89.5	Direction : 89.5 (SP No.1-580), 111.0 (SP No.581-778)
	2009/2/19	13:49:30	L.G.S.P	778	46-52.04727	S	123-20.03723	W		111.0	
St11-1	2009/2/20	20:40:48	F.G.S.P	1	48-20.26291	S	118-18.75229	W	18527.3	359.0	
	2009/2/20	23:12:17	L.G.S.P	379	48-09.86092	S	118-18.72162	W			
St11-2	2009/2/21	1:08:24	F.G.S.P	13	48-15.01099	S	118-11.26007	W	18514.9	269.0	SP No.1 - 12 : Lost shot (gun did'nt fire)
	2009/2/21	3:38:17	L.G.S.P	387	48-15.02014	S	118-26.39008	W			
St14-1	2009/2/26	17:37:48	F.G.S.P	1	48-24.99939	S	80-18.33618	W	22215.3	270.4	SP No. 28 : Recording error (lost seismic data)
	2009/2/26	19:47:11	L.G.S.P	324	48-25.04608	S	80-31.07300	W			
St14-2	2009/2/26	20:16:48	F.G.S.P	1	48-26.68694	S	80-28.44818	W	22970.6	0.4	
	2009/2/26	21:18:02	L.G.S.P	154	48-23.48305	S	80-28.38959	W			
St26-1	2009/3/3	0:18:42	F.G.S.P	1	46-47.13020	S	75-53.30978	W	66358.8	147.4	Direction : 147.4(SP No.1-829), 114.6(SP No.830-1806), 115.2(SP No.1807-2151) SP No.368 : Recording error (lost seismic data)
	2009/3/3	8:41:54	L.G.S.P	2151	47-06.21780	S	75-17.06360	W		114.6 115.2	
LC4-LC5	2009/3/4	13:09:34	F.G.S.P	1	46-04.04434	S	76-02.28561	W	59331.1	119.5	
	2009/3/4	15:31:50	L.G.S.P	295	46-09.84718	S	75-47.48978	W			
LC4-LC2	2009/3/4	23:12:58	F.G.S.P	1	46-01.73126	S	75-50.86578	W	47439.2	209.0	
	2009/3/5	4:34:45	L.G.S.P	666	46-24.64050	S	76-09.73709	W			
LC2-LC1	2009/3/5	6:46:44	F.G.S.P	1	46-14.67430	S	76-08.37204	W	56527.0	158.4	
	2009/3/5	13:08:30	L.G.S.P	790	46-43.43376	S	75-52.73575	W			
LC1-LC5	2009/3/5	14:32:27	F.G.S.P	1	46-42.23122	S	76-00.83908	W	72419.8	41.3	
	2009/3/5	22:44:06	L.G.S.P	1017	46-13.09044	S	75-23.03925	W			
LC5-LC3	2009/3/5	23:35:58	F.G.S.P	1	46-16.14189	S	75-20.99121	W	43459.0	255.9	
	2009/3/6	4:23:25	L.G.S.P	595	46-21.45859	S	75-53.79639	W			



NME SINGLE CHANNEL SEISMIC SURVEY GENERAL INFORMATION MR08-06(Leg.1b) St11-1

GENERAL			RECEIVER		REMARKS
CLIENT	JAMSTEC		RECEIVER TYPE	S.I.G. Streamer	
CRUISE	MR08-06(Leg.1b)		HYDROPHONE	S.I.G.16	
AREA	South east pacific		NUMBER OF CHANNEL	1	
LINE	St11-1		NO. OF HYD./GROUP	48	
DIRECTION (deg.)	359.0		SENSITIVITY	90.0 +/- 1 dB ref 1V/ubar	
DATE (UTC)	2009/2/20		CABLE DEPTH	10m	
WEATHER	Fine but cloudy		ACTIVE SECTION	47m	
WIND	Fresh breeze(WNW)		LEAD-IN SECTION	135m	
SEA CONDITION	Sea rough				
FIRST SHOT POINT	SP No.	1			
FIRST GOOD SHOT POINT	SP No.	1			
	S	48-20.26291	RECORDING		
	W	118-18.75229	RECORDING SYSTEM	Geode	
	Time (UTC)	20:40:48	SAMPLE FREQUENCY	1,000 Hz	
	Water Depth (m)	3426.0	RECORDING LENGTH	10,000 msec	
LAST SHOT POINT	SP No.	379	WATER DELAY	0 msec	
LAST GOOD SHOT POINT	SP No.	379	RECORDING FORMAT	SEG-D Rev.1	
	S	48-09.86092	ANALOG PREAMP	39dB	
	W	118-18.72162	HICUT FILTER	None	
	Time (UTC)	23:12:17	LOWCUT FILTER	None	
	Water Depth (m)	3455.0	SYSTEM DELAY	100msec (from start recording to gun firing)	
			GPS SYSTEM	SkyFix DGPS	
			NAVIGATION SYSTEM	Navlog	
SOURCE					
GUN TYPE	Sercel GI-Gun		DATA		
SHOT TYPE	Harmonic GI Mode (46msec G-I delay)		SEISMIC DATA	1.sgd -379.sgd	
SHOT MODE	Time			(Folder name : St11-1)	
SHOT INTERVAL	24sec		NAVIGATION DATA	st11-1_Shot.csv	
NUMBER OF STRINGS	1				
TOTAL VOLUME	355 cu.in				
CONFIGURATION	250(G) + 105(I) cu.in				
GUN DEPTH	8m		OBSERVER		
AIR PRESSURE	14MPa				
GUN CONTROLLER	Hotshot				
GUN TOWING WIRE LENGTH	30m			S.Shimizu, S.Hosoya, S.Machida	
				PROCESSING	
			BAND PASS FILTER	5-10-75-90	
			STATIC CORRECTION	88msec	
			SPHERICAL DIVERGENCE CORR T^2		
			Kill Traces	None	



NME SINGLE CHANNEL SEISMIC SURVEY GENERAL INFORMATION MR08-06(Leg.1b) St14-1

GENERAL		RECEIVER		REMARKS
CLIENT	JAMSTEC	RECEIVER TYPE	S.I.G. Streamer	
CRUISE	MR08-06(Leg.1b)	HYDROPHONE	S.I.G.16	Ave. ship speed against ground 3.92knot
AREA	South east pacific	NUMBER OF CHANNEL	1	Ave. ship speed against water 3.96knot
LINE	St14-1	NO. OF HYD./GROUP	48	
DIRECTION (deg.)	270.4	SENSITIVITY	90.0 +/- 1 dB ref 1V/ubar	The survey stoped on the way because of the rough weather.
DATE (UTC)	2009/2/26	CABLE DEPTH	10m	SP No. 28 : Recoding error (lost seismic data)
WEATHER	Rain	ACTIVE SECTION	47m	SP No.198 - 205 : The vessel position was drifted
WIND	Gale (N) → Gale (NNW)	LEAD-IN SECTION	135m	because of the DGPS status degradation.
SEA CONDITION	Sea high → Sea very high			
FIRST SHOT POINT	SP No. 1			The outset data of the line is very noisy.
FIRST GOOD SHOT POINT	SP No. 1			
		RECORDING		
	S 48-24.99939	RECORDING SYSTEM	Geode	
	W 80-18.33618	SAMPLE FREQUENCY	1,000 Hz	
	Time (UTC) 17:37:48	RECORDING LENGTH	10,000 msec	
	Water Depth (m) 4056.0	WATER DELAY	0 msec	
LAST SHOT POINT	SP No. 324	RECORDING FORMAT	SEG-D Rev.1	
LAST GOOD SHOT POINT	SP No. 324	ANALOG PREAMP	39dB	
	S 48-25.04608	HICUT FILTER	None	
	W 80-31.07300	LOWCUT FILTER	None	
	Time (UTC) 19:47:11	SYSTEM DELAY	100msec (from start recording to gun firing)	
	Water Depth (m) 4102.0	GPS SYSTEM	SkyFix DGPS	
		NAVIGATION SYSTEM	Navlog	
SOURCE		DATA		PROCESSING
GUN TYPE	Sercel GI-Gun	SEISMIC DATA	1.sgd -323.sgd	BAND PASS FILTER 7-12-75-90
SHOT TYPE	Harmonic GI Mode (46msec G-I delay)		(Folder name : St14-1)	STATIC CORRECTION 88msec
SHOT MODE	Time	NAVIGATION DATA	st14-1_Shot.csv	SPHERICAL DIVERGENCE CORR T^2
SHOT INTERVAL	24sec			Kill Traces Yes
NUMBER OF STRINGS	1			
TOTAL VOLUME	355 cu.in			
CONFIGURATION	250(G) + 105(I) cu.in			
GUN DEPTH	8m			
AIR PRESSURE	14MPa			
GUN CONTROLLER	Hotshot			
GUN TOWING WIRE LENGTH	30m			
OBSERVER				
S.Shimizu, S.Hosoya, S.Machida				



NME SINGLE CHANNEL SEISMIC SURVEY GENERAL INFORMATION MR08-06(Leg.1b) LC4-LC5

GENERAL		RECEIVER		REMARKS
CLIENT	JAMSTEC	RECEIVER TYPE	S.I.G. Streamer	
CRUISE	MR08-06(Leg.1b)	HYDROPHONE	S.I.G.16	Ave. ship speed against ground 4.98knot
AREA	Off Chile	NUMBER OF CHANNEL	1	Ave. ship speed against water 4.90knot
LINE	LC4-LC5	NO. OF HYD./GROUP	48	
DIRECTION (deg.)	119.5	SENSITIVITY	90.0 +/- 1 dB ref 1V/ubar	
DATE (UTC)	2009/3/4	CABLE DEPTH	10m	The survey was stoped on the way.
WEATHER	Overcast → Cloudy	ACTIVE SECTION	47m	
WIND	Moderate breeze (NW)	LEAD-IN SECTION	135m	
SEA CONDITION	Sea moderate → Sea rough			
FIRST SHOT POINT	SP No. 1	RECORDING		
FIRST GOOD SHOT POINT	SP No. 1	RECORDING SYSTEM	Geode	
	S 46-04.04434	SAMPLE FREQUENCY	1,000 Hz	
	W 76-02.28561	RECORDING LENGTH	10,000 msec	
	Time (UTC) 13:09:34	WATER DELAY	0 msec	
	Water Depth (m) 2569.0	RECORDING FORMAT	SEG-D Rev.1	
LAST SHOT POINT	SP No. 295	ANALOG PREAMP	39dB	
LAST GOOD SHOT POINT	SP No. 295	HICUT FILTER	None	
	S 46-09.84718	LOWCUT FILTER	None	
	W 75-47.48978	SYSTEM DELAY	100msec (from start recording to gun firing)	
	Time (UTC) 15:31:50	GPS SYSTEM	SkyFix DGPS	
	Water Depth (m) 2254.0	NAVIGATION SYSTEM	Navlog	
SOURCE		DATA		PROCESSING
GUN TYPE	Sercel GI-Gun	SEISMIC DATA	1.sgd - 295.sgd	BAND PASS FILTER 5-10-60-75
SHOT TYPE	GI-simultaneous		(Folder name : LC4-LC5)	STATIC CORRECTION 86msec
SHOT MODE	Time	NAVIGATION DATA	lc4-lc5_Shot.csv	SPHERICAL DIVERGENCE CORR T^2
SHOT INTERVAL	29sec			Kill Traces None
NUMBER OF STRINGS	1			
TOTAL VOLUME	210 cu.in	OBSERVER		
CONFIGURATION	105(G) + 105(I) cu.in	S.Shimizu, S.Hosoya, S.Machida		
GUN DEPTH	11m			
AIR PRESSURE	14MPa			
GUN CONTROLLER	Hotshot			
GUN TOWING WIRE LENGTH	30m			



NME SINGLE CHANNEL SEISMIC SURVEY GENERAL INFORMATION MR08-06(Leg.1b) LC2-LC1

GENERAL		RECEIVER		REMARKS
CLIENT	JAMSTEC	RECEIVER TYPE	S.I.G. Streamer	
CRUISE	MR08-06(Leg.1b)	HYDROPHONE	S.I.G.16	Ave. ship speed against ground 4.82knot
AREA	Off Chile	NUMBER OF CHANNEL	1	Ave. ship speed against water 4.20knot
LINE	LC2-LC1	NO. OF HYD./GROUP	48	
DIRECTION (deg.)	158.4	SENSITIVITY	90.0 +/- 1 dB ref 1V/ubar	SP No.1 - 55 : The vessel traveled away from the survey line. (Offset 200m)
DATE (UTC)	2009/3/5	CABLE DEPTH	10m	
WEATHER	Fine but cloudy	ACTIVE SECTION	47m	
WIND	Moderate breeze (WSW) → Moderate breeze (NW)	LEAD-IN SECTION	135m	
SEA CONDITION	Sea rough → Sea moderate			
FIRST SHOT POINT	SP No. 1			
FIRST GOOD SHOT POINT	SP No. 1			
	S 46-14.67430	RECORDING		
	W 76-08.37204	RECORDING SYSTEM	Geode	
	Time (UTC) 6:46:44	SAMPLE FREQUENCY	1,000 Hz	
	Water Depth (m) 2544.0	RECORDING LENGTH	10,000 msec	
LAST SHOT POINT	SP No. 790	WATER DELAY	0 msec	
LAST GOOD SHOT POINT	SP No. 790	RECORDING FORMAT	SEG-D Rev.1	
	S 46-43.43376	ANALOG PREAMP	39dB	
	W 75-52.73575	HICUT FILTER	None	
	Time (UTC) 13:08:30	LOWCUT FILTER	None	
	Water Depth (m) 3318.0	SYSTEM DELAY	100msec (from start recording to gun firing)	
		GPS SYSTEM	SkyFix DGPS	
		NAVIGATION SYSTEM	Navlog	
SOURCE				
GUN TYPE	Sercel GI-Gun	DATA		
SHOT TYPE	GI-simultaneous	SEISMIC DATA	1.sgd - 790.sgd (Folder name : LC2-LC1)	BAND PASS FILTER 5-10-60-70
SHOT MODE	Time			STATIC CORRECTION 86msec
SHOT INTERVAL	29sec	NAVIGATION DATA	lc2-lc1_Shot.csv	SPHERICAL DIVERGENCE CORR T^2
NUMBER OF STRINGS	1			Kill Traces Yes
TOTAL VOLUME	210 cu.in			
CONFIGURATION	105(G) + 105(I) cu.in			
GUN DEPTH	11m	OBSERVER		
AIR PRESSURE	14MPa	S.Shimizu, S.Hosoya, S.Machida		
GUN CONTROLLER	Hotshot			
GUN TOWING WIRE LENGTH	30m			



NME SINGLE CHANNEL SEISMIC SURVEY GENERAL INFORMATION MR08-06(Leg.1b) St27-St30

GENERAL			RECEIVER		REMARKS
CLIENT	JAMSTEC		RECEIVER TYPE	S.I.G. Streamer	
CRUISE	MR08-06(Leg.1b)		HYDROPHONE	S.I.G.16	
AREA	Off Chile		NUMBER OF CHANNEL	1	
LINE	St27-St30		NO. OF HYD./GROUP	48	
DIRECTION (deg.)	359.4、344.4		SENSITIVITY	90.0 +/- 1 dB ref 1V/ubar	
DATE (UTC)	2009/3/7 → 2009/3/8		CABLE DEPTH	8m → 10m	
WEATHER	Drizzling rain/Fog → Drizzling rain		ACTIVE SECTION	47m	
WIND	Fresh breeze (NNW) → Fresh breeze (N)		LEAD-IN SECTION	135m	
SEA CONDITION	Sea rough				
FIRST SHOT POINT	SP No.	1			
FIRST GOOD SHOT POINT	SP No.	1			
	S	46-36.82594	RECORDING		
	W	75-47.01050	RECORDING SYSTEM	Geode	
	Time (UTC)	23:14:00	SAMPLE FREQUENCY	1,000 Hz	
	Water Depth (m)	2858.0	RECORDING LENGTH	10,000 msec	
LAST SHOT POINT	SP No.	2950	WATER DELAY	0 msec	
LAST GOOD SHOT POINT	SP No.	2950	RECORDING FORMAT	SEG-D Rev.1	
	S	45-48.45337	ANALOG PREAMP	39dB	
	W	76-00.33234	HICUT FILTER	None	
	Time (UTC)	11:32:43	LOWCUT FILTER	None	
	Water Depth (m)	3218.0	SYSTEM DELAY	100msec (from start recording to gun firing)	
			GPS SYSTEM	SkyFix DGPS	
			NAVIGATION SYSTEM	Navlog	
SOURCE					
GUN TYPE	Sercel GI-Gun		DATA		
SHOT TYPE	GI-simultaneous		SEISMIC DATA	1.sgd - 2950.sgd	
SHOT MODE	Time			(Folder name : St27-St30)	
SHOT INTERVAL	15sec		NAVIGATION DATA	st27-st30_Shot.csv	
NUMBER OF STRINGS	1				
TOTAL VOLUME	210 cu.in				
CONFIGURATION	105(G) + 105(I) cu.in				
GUN DEPTH	11m		OBSERVER		
AIR PRESSURE	14MPa				
GUN CONTROLLER	Hotshot				
GUN TOWING WIRE LENGTH	30m			S.Shimizu, S.Hosoya, S.Machida	
				PROCESSING	
			BAND PASS FILTER	5-8-65-80	
			STATIC CORRECTION	86msec	
			SPHERICAL DIVERGENCE CORR T^2		
			Kill Traces	None	

MR08-06 Leg1a (2009/1/15 Sekinehama - 2009/2/4 Papeete)



MR08-06 Leg1b (2009/2/6 Papeete - 2009/3/14 Valparaiso)